

An Examination of the Role of IFI16 in Detecting Viral DNA in Human Immortalised Keratinocytes

Faculty of Health and Medicine,
Division of Biomedical and Life Science Laboratories,
Lancaster University.

2017



Author: Craig O'Hare (BA. Mod) (31900855)
Supervisor: Dr Leonie Unterholzner (PhD)

A thesis submitted for the degree of Doctor of Philosophy,
Lancaster University, August 2017.

**I declare that this thesis is my own work and has not
been previously submitted in part, or as whole, for
the award of a higher degree or qualification at this
university or elsewhere**

Table of Contents

List of Figures	5
List of Tables	7
List of Abbreviations	8
Acknowledgements	14
Abstract	15
Publications	16
Chapter One; <i>An Overview of Innate Immune Signalling in Response to Nucleic Acids</i>	17
1.1. The Immune System.....	18
1.2. Anti-viral immunity.....	19
1.2.1 Interferons:	20
1.2.2 Type I Interferon Receptor Signalling	21
1.3. Inflammation	25
1.3.1 The Inflammasome.....	26
1.4. Nucleic Acid Sensing Pathogen Recognition Receptors.....	26
1.4.1 Endolysosomal detection of nucleic acids is mediated by TLRs 3, 7-9 and 13	27
1.4.2 Cytosolic Nucleic Acid Sensing.....	30
1.4.2.1 RNA Sensing in the Cytosol by RLRs.....	31
1.4.2.2.1 Inflammatory DNA Sensing in the Cytosol by AIM2	35
1.4.2.2.2 NLRP3, Another Inflammasome for DNA?	36
1.4.2.2.3 Sox2.....	37
1.5. STING is an adapter protein for DNA-induced interferon production	37
1.5.1 STING is a receptor for Cyclic Di-Nucleotides	38
1.5.2 STING mediated RNA sensing.....	40
1.5.3 STING trafficking and signalling via TBK1	41
1.5.4 STING Post-Translational Modifications	41
1.6. STING-Dependent IFN Production.....	46
1.6.1 cGAS and the Second Messenger cGAMP	46
1.6.3 DDX41	51
1.6.4 DAI.....	52
1.6.5 DNA-PK.....	52
1.6.6 Mre11	53
1.6.7 LSm14A	54
1.7. STING-Independent Mechanisms of DNA-induced IFN Production	56
1.7.1 RNA polymerase III.....	56
1.7.2 LRRFIP1	56
1.7.3 HMGB1	57
1.8. Which Receptors are Required for the STING-mediated IFN response?	57
1.9. What defines a DNA sensor?	57
1.10 IFI16's Candidacy as a DNA sensor; Perspectives from Virus-Host Interactions.....	63
1.11 Aims and Objectives of Investigation	64
Chapter Two: <i>Methods and Materials</i>	66
2.1 Materials	67
2.2 Solutions	67
SDS-PAGE and Western Blot Buffers.....	67
Cell Lysis Buffers	68
Bacterial Growth Media	69

DNA/Agarose Gel Reagents	69
Enzyme Reaction Buffers	70
cGAMP Infusion	70
Real Time PCR Solutions	70
cGAMP Extraction Reagents	71
2.3 Antibodies:	72
2.4 Methods:	73
2.4.1 Cell Culture	73
2.4.1.1 Generation of IFI16 Knockout Cell Lines	73
2.4.2 Nucleic Acid Transfection Conditions	73
2.4.3 cGAMP Stimulation Conditions	74
2.4.4 Overexpression Transfection Conditions	74
2.4.4.1 Plasmids	75
2.4.5 SDS-PAGE and Western Blotting	75
2.4.6 Viral Infections	76
2.4.7 Cell Lysis	76
2.4.8 Immunoprecipitations	77
2.4.9 Real-Time PCR	77
2.4.10 Confocal Microscopy	78
2.4.11 ELISA	79
2.4.12 DNA Sequencing	79
2.4.13 cGAMP Quantification	81
2.4.14 Snake Venom Phosphodiesterase Treatment	82
2.5 Statistical Analysis	82
2.6 Data Visualisation	82
Chapter Three Part One: <i>IFI16 is required for the induction of innate immune responses to DNA in human immortalised keratinocytes</i>	83
3.1.1 Human Immortalised Keratinocytes (HaCaT) cells express IFI16 and the cGAS-STING pathway and produce anti-viral cytokines in response to DNA transfection.	84
3.1.2 Human Immortalised Keratinocytes (HaCaT) cell lines without IFI16 still possess the other components of the DNA sensing pathway	89
3.1.3 IFI16 is required for HaCaT cells to produce IFN- β , cytokine and chemokine mRNA in response to DNA	89
3.1.4 IFI16 is required for HaCaT cells to produce CCL5 protein in response to transfected DNA and infection with DNA Viruses	92
3.1.5 Cells without IFI16 do not efficiently activate the STING pathway	98
3.1.6 Discussion	102
Chapter Three Part Two: <i>IFI16 does not influence production of cGAMP in human immortalised keratinocytes</i>	105
3.2.1 IFI16 and cGAS associate via DNA when initiating an immune response	106
3.2.2 Overview of method to extract cGAMP for quantification using LC-MS/MS	109
3.2.3 Detection of Cyclic Di-Nucleotides by LC-MS/MS	110
3.2.4 Optimisation and refinement steps for cGAMP extraction method:	113
a) Optimisation of solid phase extraction step:	113
b) Optimisation of cell lysis conditions:	114
c) Optimisation of endogenous cGAMP production and detection conditions:	114
3.2.5 IFI16 does not influence production of cGAMP in HaCaT cells	120
3.2.6 Discussion:	122
Chapter Three Results Part Three: <i>IFI16 facilitates activation of STING during DNA sensing in human immortalised keratinocytes</i>	124
3.3.1 IFI16 ^(-/-) HaCaT cells display impaired responses to cGAMP stimulation	125

3.3.2	STING and IFI16 associate during DNA stimulation	125
3.3.3	Discussion.....	129
Chapter Three Results Part Four: <i>IFI16 promotes STING palmitoylation during DNA sensing in human immortalised keratinocytes</i>		
3.4.1	Palmitoylation regulates protein trafficking and ligand binding	132
3.4.2	Overview of acyl-RAC method of studying palmitoylation.....	132
3.4.3	Optimisation of conditions for detecting STING palmitoylation	132
3.4.4	STING palmitoylation is required for immune responses to DNA in HaCaT cells	135
3.4.5	STING Palmitoylation is dependent on IFI16	143
3.4.6	Discussion	145
Chapter Four <i>Discussion: IFI16 and cGAS co-operate to detect exogenous DNA in human keratinocytes</i>		
4.1	IFI16 and cGAS are both required for DNA sensing in keratinocytes.....	147
4.2	IFI16 does not influence cGAS activity in keratinocytes.....	148
4.3	IFI16 facilitates STING activation in keratinocytes.....	151
4.4	IFI16 promotes STING phosphorylation, translocation palmitoylation in Keratinocytes.....	152
4.5	Outlook: IFI16 is required for DNA sensing with specific functions that vary with cell type	154
4.6	Outlook: IFI16 as a DNA Sensor, challenges with experimental models.....	155
4.7	Outlook: Clinical Importance of IFI16 to Immunity; Lessons from Infection and Auto-immunity	158
4.8	What are the benefits to the host of having more than one receptor for viral DNA?	159
4.9	Conclusion.....	160
Bibliography		161
Appendix.....		192

List of Figures

Introduction:

Fig 1.1	Induction of Interferon and Activation of the Interferon-stimulated Response Element.....	23
Fig 1.2	Endosomal TLR Signalling.....	29
Fig 1.3	Overview of RLR and MAVS Signalling.....	34
Fig 1.4	Overview of STING Activation.....	39
Fig 1.5	Summary of STING Post-Translational Modifications.....	44
Fig 1.6	cGAS-STING Signalling and Proposed STING-dependent DNA Sensors.....	55

Results:

Fig 3.1.1	Human Immortalised Keratinocyte (HaCaT) cell lines express IFI16, cGAS and STING and activate the STING pathway in response to transfected DNA.....	86
Fig 3.1.2	HaCaT cell lines express IFN- β and anti-viral cytokines in response to DNA transfection.....	87
Fig 3.1.3	HaCaT cell lines secrete the chemokines CCL5 and CXCL10 in response to DNA.....	88
Fig 3.1.4	HaCaT cell lines without IFI16 still possess the cGAS-STING Pathway.....	90
Fig 3.1.5	HaCaT Cell lines without IFI16 produce less IFN, ISGs and pro-inflammatory cytokines in response to DNA transfection.....	93
Fig 3.1.6	HaCaT Cell lines without IFI16 fail to produce IFN- β and anti-viral cytokines in response to DNA but maintain responses to double stranded RNA.....	94
Fig 3.1.7	HaCaT Cell lines do not require IFI16 to produce IFN- β in response to single stranded RNA.....	95
Fig 3.1.8	IFI16 is required to produce CCL5 in response to Immunogenic DNA but is dispensable for responses to RNA.....	96
Fig 3.1.9	IFI16 is required for CCL5 production in response to HSV-1 infection in HaCaT cell lines.....	97
Fig 3.1.10	DNA induced STING trafficking is decreased in IFI16 ^(-/-) cell Lines.....	100
Fig 3.1.11	IFI16 ^(-/-) HaCaT cell lines do not efficiently activate the cGAS -STING pathway.....	101
Fig 3.2.1	IFI16 and cGAS associate following DNA stimulation.....	107
Fig 3.2.2	IFI16 and cGAS associate via DNA.....	108
Fig 3.2.3	Schematic of cGAMP extraction protocol.....	111
Fig 3.2.4	Detection of cGAMP and ci-di-AMP standards by Liquid Chromatography-Mass Spectrometry.....	112
Fig 3.2.5	cGAMP from neat lysates elutes early from the liquid chromatography graphitised carbon column.....	116
Fig 3.2.6	Comparison of Solid Phase Extraction Columns.....	117

Fig 3.2.7	Optimisation of lysis conditions for cGAMP quantification.....	118
Fig 3.2.8	Verification of endogenous cGAMP production in HaCaT cell lines.....	119
Fig 3.2.9	IFI16 does not influence cGAMP production in HaCaT Cell Lines.....	121
Fig 3.3.1	IFI16 ^(-/-) HaCaT cell lines display impaired responses to cGAMP stimulation.....	127
Fig 3.3.2	IFI16 and STING association increases following DNA Stimulation.....	128
Fig 3.4.1	Schematic of Palmitoylation Pulldown Technique (Acyl-Resin Assisted Capture).....	133
Fig 3.4.2	STING is Palmitoylated.....	134
Fig 3.4.3	STING Palmitoylation is inducible with serum starvation.....	136
Fig 3.4.4	STING Palmitoylation is DNA Dependent.....	137
Fig 3.4.5	2-Bromopalmitate inhibits STING Phosphorylation.....	140
Fig 3.4.6	2-Bromopalmitate suppresses cytosolic nucleic acid sensing....	141
Fig 3.4.7	DNA induced STING trafficking is decreased following 2-Bromoplamate treatment.....	142
Fig 3.4.8	STING Palmitoylation is decreased in the absence of IFI16.....	144
Fig 4.1	Summary of the Roles of IFI16 According to Knockout Studies	156

List of Tables

Chapter One: An Overview of Innate Immune Signalling in Response to Nucleic Acids

Table 1.1:	IFNs, IFN Receptors, their ligands, and functions (Adapted from Pestka et al., 2004).....	20
Table 1.2:	Cell Autonomously Immunity by Interferon Stimulated Genes...	24
Table 1.3:	Incidences where proposed STING-Dependent Receptors have been implicated to immunity to pathogen DNA.....	58-61

Chapter Two: Materials and Methods

Table 2.1:	Reagents used in developing a method to extract and quantify cGAMP (v/v)%	71
Table 2.2:	Primary Antibodies and supplier information.....	72
Table 2.3:	Secondary Antibodies and supplier information.....	72
Table 2.4:	Immunofluorescence Secondary Antibodies and supplier Information.....	72
Table 2.5:	Sequences of DNA Oligomers used to stimulate cell lines...	74
Table 2.6:	Primer Sequences for House Keeping Gene and Cytokines..	78
Table 2.7:	Sequences of Primers used in Sequencing Reactions.....	80

List of Abbreviations

(-/-)	Knockout
ADAR1	Adenosine Deaminase, RNA-specific 1
AIDS	Acquired Immunodeficiency Syndrome
AIM2	Absent in Melanoma
APOBEC3G	Apolipoprotein B mRNA editing enzyme, catalytic polypeptide-like 3
APC	Antigen Presentation Cell
ASC	Apoptosis associated speck like protein containing a caspase activation and recruitment domain
ATM	Ataxia telangiectasia
ATP	Adenosine Tri-Phosphate
BMDM	Bone Marrow Derived Macrophage
BRCA-1	BReast CAncer gene 1
c-di-AMP	Cyclic di-adenosine monophosphate
c-di-GMP	Cyclic di-guanylate
C₂H₃NO₄	Acetyl-Nitrate
CaCl₂	Calcium Chloride
Cardif	CARD adaptor inducing IFN- β
CARD	Caspase Activation and Recruitment Domains
CCP	Cytosolic Carboxyl Peptidase
CD	Cluster of Differentiation
cGAMP	Cyclic Guanosine Monophosphate-Adenosine Monophosphate
cGAS	cGAMP synthase
CpG	Cytosine-phosphate-Guanosine
CSV	Coxsackievirus group B serotype 3
DAI	DNA-dependent activator of IFN-regulatory factors
DAMPs	Damage Associated Molecular Patterns
DEPC	Diethyl Dicarbonate
dH₂O	Deionised Water
DDX	DEAD-Box Helicase
DNA	Deoxyribonucleic acid
DNA-PKcs	DNA dependent Protein Kinase

Ds	Double Stranded
DTT	Dithiothreitol
EBV	Epstein-Barr Virus
ECL	Enhanced Chemiluminescence
EDTA	Ethylenediaminetetraacetic acid
ELISAs	Enzyme-Linked Immunosorbent Assays
EMCV	Encephalomyocarditis virus
ENPP1	Ectonucleotide pyrophosphatase/phosphodiesterase 1
ER	Endoplasmic Reticulum
ERGIC	Endoplasmic reticulum-golgi intermediate Compartments
ERIS	Endoplasmic Reticulum Interferon Stimulator
FCS	Foetal Calf Serum
GAS	Interferon gamma-activated sequences
GTP	Guanosine Tri-Phosphate
HaCaT	Human Immortalised Keratinocyte
HCl	Hydrochloric Acid
hCMV	Human Cytomegalovirus
HCV	Hepatitis C Virus
HEK293T	Human Embryonic Kidney Cells
HEPES	4-(2-hydroxyethyl)-1-piperazineethanesulfonic acid
HIN	Hematopoietic expression, IFN-inducible nature and Nuclear localization
HIV	Human Immunodeficiency Virus
HEK	Human Embryonic Kidney
HFF	Human Foreskin Fibroblasts
HMBG	High Mobility Box Group
HMVE	Human Vascular Endothelial
HSV-1	Herpes Simplex-Virus 1
HSV-2	Herpes Simplex-Virus 2
HT-	Herring Testis
IAV	Influenza A Virus
IFI16	Interferon Gamma Inducible Protein 16
IFIT	Interferon Induced Protein with Tetratricopeptide Repeats

IFITM	Interferon-induced transmembrane protein
IFN	Interferons
IFNAR	Type I Interferon Receptor
IKK	IκB kinase
IL	Interleukin
IPS-1	IFN-β promoter stimulator 1
IRAK	Interleukin-1 receptor-associated kinase
IRF	Interferon Regulatory Factor
ISD	Immune Stimulated DNA
ISG	Interferon Stimulated Gene
ISRE	Interferon Stimulated Response Element
JAK1	Janus-Activated Kinase 1
K₂HPO₄	Dipotassium phosphate
KCl	Potassium Chloride
KSHV	Kaposi Sarcoma-associated Herpesvirus
LB	Lysogeny broth
LCV	Lymphocytic Choriomeningitis virus
LGP2	Laboratory of Genetics and Physiology 2
LLR	Leucine Rich Repeats
LRRFIP1	Leucine rich repeat (in FLII) interacting protein 1
LPS	Lipopolysaccharide
MAFFT	Multiple Alignment using Fast Fourier Transform
MAVS	Mitochondrial antiviral-signaling protein
mCMV	Murine Cytomegalovirus
MDA5	Melanoma Differentiation-Associated protein 5
MEF	Murine Endothelial Fibroblasts
MNDA	Myeloid cell nuclear differentiation antigen
MHC	Major Histocompatibility Complex
MKK	Mitogen-activated protein kinase kinase
MLU-1	Mitochondrial E3 ubiquitin protein ligase 1
Mre11	Meiotic recombination factor 11
MyD88	Myeloid differentiation primary response gene 88

MPYS	Membrane tetraspanning protein
MVA	Modified Vaccinia Ankara
MxA	Human myxovirus resistance protein 1
NaH₂PO₄	Sodium phosphate (Monobasic)
NaCl	Sodium Chloride
NaF	Sodium Fluoride
NaOH	Sodium Hydroxide
Na₃VO₄	Sodium Orthovanadate
NH₄CH₃CO₂	Ammonium Acetate
NH₄OH	Ammonium Hydroxide
NAPL3	NACHT, LRR and PYD domain containing protein 3
NADPH	Nicotinamide Adenine Dinucleotide Phosphate
NEMO	NFκB essential modulator
NDV	Newcastle Disease Virus
NFκB	Nuclear Factor Kappa-light-chain-enhancer of Activated B Cells
NK	Natural Killer
NLR	Nucleotide-binding oligomerization domain-like receptors
NP40	nonyl-phenoxypolyethoxyethanol
OAS1	2'-5'-oligoadenylate synthetase 1
PAMPs	Pathogen Associated Molecular Patterns
PBS	Phosphate Buffered Saline
PKR	Protein Kinase R
PMSF	Phenylmethane Sulfonyl Fluoride
Poly I:C	Polyinosinic:polycytidylic
POP3	Pyrin only Protein 3
PQBP1	Polyglutamine binding protein 1
PRRs	Pattern Recognition Receptors
PVDF	Polyvinylidene Difluoride
PYD	Pyrin Domain
PYHIN1	Pyrin and HIN domain family member 1
RAD50	DNA repair protein RAD50
RAP55	RNA Associated Protein 55

RIG-I	Retinoic acid-inducible gene I
RIP	Receptor-interacting protein kinases
RLR	RIG-I Like Receptor
RNA	Ribonucleic acid
RNF	Ring Finger
RT	Real-Time
SAMHD1	SAM and HD domain-containing protein 1
SDS	Sodium Dodecyl Sulfate
SDS-PAGE	SDS-polyacrylamide gel electrophoresis
SeV	Sendai Virus
SENP	SUMO-specific protease
siRNA	Small Interfering RNA
SOC	Super Optimal Broth w/Catabolite Repression
SOX2	SRY (sex determining region Y)-box 2
Ss	Single Stranded
STAT	Signal Transducer and Activator
STING	Stimulator of Interferon Genes
TAB2	TGF-Beta Activated Kinase 1/MAP3K7 Binding Protein 2
TAE	Tris Acetate-EDTA
TALENs	Transcription activator-like effector nucleases
TAK1	Transforming growth factor beta-activated kinase 1
TBK1	TANK Binding Kinase 1
TBS	Tris-Buffered Saline
TIR	Toll/Interleukin-1 receptor
TLR	Toll Like Receptor
TMEM173	Transmembrane protein 173
TNFα	Tumour Necrosis Factor-Alpha
TPS	Thiopropyl Sepharose 6b
TRAF	TNF receptor associated factor
TRIF	TIR domain-containing adaptor inducing IFN- β
TRIM	Tripartite motif-containing protein
Tyr2	Tyrosine Kinase 2

ULK1	Unc-51 like autophagy activating kinase 1
USP	Ubiquitin Specific Protease
UNC93B1	Unc-93 homolog B1
UV	Ultra-Violet
VACV	Vaccinia Virus
Viperin	Virus inhibitory protein, ER-associated, IFN-inducible
VISA	Virus-induced signalling adaptor
VSV	Vesicular Somatis Virus
WNV	West Nile Virus
ZBP1	Z-DNA binding protein 1
ZDHCC1	Zinc Finger DHHC-Type Containing 1

Acknowledgements

I would like to thank my supervisor Leonie Unterholzner for the opportunity to undertake my PhD and for choosing me as her first PhD student. Without her guidance, support and relentless optimism, I would not have been able to finish this project.

I would like to extend my thanks to previous members of the Unterholzner group; Ian and Rangeetha, for their support and advice during their time in the lab, and for making it a nice place to work. I would like to specifically acknowledge Gillian and Jessica for their friendship and support throughout the entirety of PhD. In addition, personal and technical advice from other PhD students, post-docs, support staff and PIs from the University of Dundee and Lancaster University was invaluable.

I'd like to acknowledge the support of my friends; Conor, Grace, Liam, Hugh and Dan, and my boyfriend Bentley for being excellent people, and assuring me that it will all be ok in the end.

Finally, I'd like to thank my family for their support and faith in me during the last four years, and for pretending to understand what I do.

Abstract

The presence of exogenous DNA in the cytosol results in the activation of the DNA sensor cyclic GMP-AMP synthase (cGAS). cGAS produces the second messenger cyclic GMP-AMP (cGAMP) which binds to and activates the endoplasmic reticulum adapter STimulator of INterferon Genes (STING). Activated STING initiates transcription of the anti-viral cytokine interferon- β , and by extension, induces activation of the anti-viral immune response. Other DNA sensors have been proposed to recognise exogenous DNA via STING but their relevance to the cGAS-STING pathway is unclear. Interferon- γ inducible protein 16 (IFI16) is a putative DNA sensor that has also been proposed to induce interferon- β transcription via STING. This thesis demonstrates that both IFI16 and cGAS are required for full activation of immune responses to DNA and DNA virus infection in human immortalised keratinocytes (HaCaT).

The cGAS-STING pathway was examined in IFI16^(-/-) HaCaT cell lines to conclusively determine the contribution of IFI16 to DNA sensing. IFI16^(-/-) HaCaT cell lines produced drastically reduced levels of interferon- β , interferon-stimulated genes and pro-inflammatory cytokine mRNAs following stimulation with exogenous DNA due to reduced activation of the STING pathway. IFI16 was observed not influence cGAS activity as DNA-induced cGAMP levels were comparable between Wild type and IFI16^(-/-) cell lines. IFI16 was required for STING signalling following cGAMP stimulation. IFI16 was found to interact with STING promoting STING phosphorylation and translocation to peri-nuclear foci. Additionally, in preliminary experiments we observe that IFI16 may be required for STING palmitoylation. Thus, we propose that IFI16 and cGAS co-operate for the full activation of DNA sensing in HaCaT cells.

Publications

Almine, J.F., O'Hare, C.A., Dunphy, G., Haga, I.R., Naik, R.J., Atrih, A., Connolly, D.J., Taylor, J., Kelsall, I.R., Bowie, A.G., *et al.* (2017). IFI16 and cGAS cooperate in the activation of STING during DNA sensing in human keratinocytes. *Nat Commun* 8, 14392.

Chapter One

An Overview of Innate Immune Signalling in Response to Nucleic Acids

1.1. The Immune System

The immune system is composed of a collection of cells, organs and tissues that function in concert to defend an organism against infection from pathogens (Reviewed by Janeway, 2001). In higher organisms, the immune system is composed of two distinct arms that differ by means of pathogen recognition, kinetics and cells; termed the innate and adaptive immune system, that work together to protect the host from infection.

The innate immune system depends on a series of germline-encoded pattern recognition receptors (PRRs) to distinguish between pathogen and host (Reviewed by Wu and Chen, 2014). PRRs recognise evolutionarily conserved molecular signatures from pathogens known as pathogen associated molecular patterns (PAMPs) such as bacterial cell wall components e.g. bacterial lipopolysaccharide (LPS) or features of viral RNAs such as an exposed 5'-triphosphate. Additionally, PRRs may recognise damaged or mislocalised self-material known as damage associated molecular patterns (DAMPs) (Reviewed by Lotze et al., 2007). PRRs facilitate pathogen detection by initiating the production and secretion of pro-inflammatory cytokines, chemokines, and anti-viral interferons (IFN) to co-ordinate an immune response against a pathogen before infection can be established. Activation of PRR signalling culminates in the recruitment and activation innate immune cells such as macrophages and dendritic cells, which attempt to eliminate the pathogen by phagocytosis. Macrophages and dendritic cells are also referred to as antigen presenting cells (APCs) (Reviewed by Janeway, 2001). Engagement of APC PRRs results in APC activation and maturation, and induces the expression of cell surface co-stimulatory molecules, cluster of differentiation (CD)80 and CD86. Many pathogens cannot be eliminated by the innate immune system alone and require activation of the adaptive immune system. Following maturation, dendritic cells migrate to lymph nodes where they induce activation of the adaptive immune system.

The adaptive immune system is composed of B and T lymphocytes. Unlike the evolutionary conserved PAMPs of the innate immune system, the adaptive system mounts an immune response to a specific soluble protein antigen (Reviewed by Janeway, 2001). T cells recognise peptides from phagocytosed pathogens presented on major histocompatibility complex

(MHC) molecules by APCs. The cell surface markers CD80 and CD86 on activated APCs interact with the T cell co-receptor CD28. CD80/86:CD28 interactions break T cell anergy and enable T cell activation. T cells are comprised of two lineages; CD8⁺ cytotoxic T Cells and CD4⁺ helper T cells. CD8⁺ T cells contain the cytolytic proteins perforin and granzyme B. CD8⁺ T cells recognise peptides presented on MHC I molecules by infected cells or tumour cells. Upon engagement of MHC class I by the T Cell receptor, CD8⁺ T cells degranulate, inducing apoptosis in their target cells. CD4⁺ T cells recognise peptides presented on MHC II molecules by activated APCs. CD4⁺ helper T cells produce cytokines which can promote either the secretion of soluble protein antibodies by B cells or the cytotoxic functions of CD8⁺ T cells and intracellular killing mechanisms of phagocytes. The cytokine profile of a CD4⁺ T cell is determined by the local cellular environment and is subject to regulation by pathogens and host cells alike (Reviewed by Zhu and Paul, 2008). B cells produce antibodies that bind to pathogens, restricting their movement, and promoting their killing by phagocytes and Natural Killer (NK) cells through opsonisation. Additionally, virus-neutralising antibodies can prevent viral infection by inhibiting virus-cellular entry. Induction of a CD8⁺ cytotoxic T cell response is required to clear infections with intracellular pathogens and viruses.

Cytokines produced in the innate immune response up-regulate co-stimulatory molecules on adaptive immune cells, priming their activation. The inflammatory response initiated by the innate immune response aids recruitment of adaptive immune cells to the site of infection. Thus, the innate immune system enables and augments the functions of the adaptive immune system. The specificity of a PRR for a unique PAMP and distinct downstream PRR signalling, ensures that an appropriate immune response against a pathogen is produced (Reviewed by Kawai and Akira, 2011; Sparrer and Gack, 2015).

1.2 Anti-viral immunity

The clearance of viral infection requires the recognition of viral peptides and viral nucleic acids by the immune system (Reviewed by Stetson and Medzhitov, 2006b). Viral infection is detected by infected cells presenting viral peptides on MHCI. APCs can additionally detect viral infection *in-trans* by phagocytosing infected cells resulting in the presentation of viral peptides on MHCI and MHCII molecules. Presentation of viral peptides on both MHC

molecules enables induction of a CD4+ T cell response which promotes the cytotoxic functions of CD8+ T cells. Activation of both CD4+ and CD8+ T cells enables effective clearance of viral infection. Recognition of viral nucleic acids by PRRs induces transcription of IFNs (Reviewed by Wu and Chen, 2014).

1.2.1 Interferons:

IFNs are a family of anti-viral cytokines which induce transcription of anti-viral genes to limit viral replication (Reviewed by Pestka et al., 2004). Additionally, IFNs support the functions of the adaptive immune response by up-regulating MHC molecules on APCs and virally infected cells. IFNs are designated as three classes based on the variety of receptor that they signal through; grouped as type I, type II and type III IFNs (**Table 1.1**).

IFN- γ is the sole Type II IFN. IFN- γ is primarily produced by activated CD4+ T cells and NK cells. IFN- γ supports adaptive immune responses by upregulating expression of co-stim-

Class	Receptor	Chains	Ligand	Function
Type I	IFNAR	IFN- α R1 IFN- α R2	IFN- β IFN- α subtype 1-13 IFN- ϵ , IFN- κ IFN- ω	Induction of genes with anti-viral activity (Global distribution, vital importance)
Type II	IFN γ Receptor	IFN- γ R1 IFN- γ R2	IFN γ	<u>Upregulation of:</u> CD80/86 co-stimulatory molecules on antigen presenting cells for lymphocyte activation MHC molecules Reactive Oxygen Species generating enzymes in Phagocytes
Type III	Type III IFN Receptor	IL10R2 IL28AR	IL29 (IFN- λ 1) IL28A (IFN- λ 2) IL28B (IFN- λ 3)	Induction of genes with anti-viral activity (Localised distribution and importance)

Table 1.1 IFNs, IFN Receptors, their ligands, and functions (Adapted from Pestka et al., 2004).

-ulatory molecules on APCs, promoting the activation of T cells (Reviewed by Pestka et al., 2004). IFN- γ also upregulates MHC class I molecules thus facilitating recognition of virally infected cells by T cells. Additionally IFN- γ improves the phagocytic activity of APCs by promoting expression of nitric oxide synthase (Xie et al., 1993).

Type I and type III IFNs are produced by most somatic cells following viral infection (Reviewed by McNab et al., 2015). Type I and type III IFNs signal in an autocrine and paracrine manner to induce activation of genes which impede viral replication; collectively referred to as IFN-stimulated genes (ISGs) (Reviewed by Pestka et al., 2004). While Type I and Type III IFNs have overlapping functions, the expression of the Type III IFN receptor is restricted to largely to the liver and mucosal sites such as the lung and gastrointestinal tract (Reviewed by Kotenko and Durbin, 2017). Mice lacking the type III IFN receptor, IL28AR, displayed no change in the ability to clear viruses but IL28AR signalling was found to synergise with Toll Like Receptor (TLR) signalling for anti-viral cytokine production in certain tissues (Ank et al., 2008). In contrast, the Type I IFN receptor (IFNAR) is expressed more globally and is vital to anti-viral immunity. Mice and patients without functional Type I IFN receptor (IFNAR) signalling succumb to lethal viral infections with significantly higher viral loads observed in viral replicative niches (Ank et al., 2008; Dupuis et al., 2003; Hwang et al., 1995; Müller et al., 1994).

1.2.2 Type I Interferon Receptor Signalling

5 forms of type I IFNs have been described in humans; IFN- α , IFN- β , IFN- ϵ , IFN- κ , and IFN- ω (Reviewed by Pestka et al., 2004). The IFNAR is unique among cytokine receptors for the number of ligands it may bind as the 13 IFN- α subtypes, and the other type I IFNs all signal via the IFNAR. The IFNAR is structurally composed of two subunits designated IFNAR1 and IFNAR2.

IFN- β is the first type I IFN produced during viral infection. IFN- β is produced following activation of the transcription factor IFN regulatory factor (IRF)-3 by PRR signalling (**Fig.1.1**) (Lin et al., 1998; Schafer et al., 1998). PRR signalling also typically culminates in activation of Nuclear Factor Kappa-light-chain-enhancer of Activated B Cells (NF κ B)

resulting in the transcription of pro-inflammatory cytokines (Reviewed by Kawai and Akira, 2011; Reviewed by Sparrer and Gack, 2015). NF κ B activation supports transcription of IFN- β as the RelA subunit of NF κ B forms a transcriptional complex with IRF3 known as the IFN- β enhanceosome (Schafer et al., 1998). IRF-3 also promotes the transcription of a subset of other ISGs such the chemokine CCL5/RANTES (Génin et al., 2000; Grandvaux et al., 2002). IFN- β signals in an autocrine and paracrine manner via the IFNAR to induce transcription of the ISG, IRF7 (Marié et al., 1998; Sato et al., 1998). IRF7 is then activated by PRR signalling and initiates IFN- α transcription. Cells then switch to a pre-dominantly IFN- α mediated response and continue to induce more ISGs via the IFNAR receptor.

Ligand binding to the IFNAR induces receptor clustering and activates the Janus-associated kinases (JAK) associated with each subunit of the IFNAR; JAK1 which is associated with IFNAR2, and tyrosine kinase 2 (Tyr2) which is associated with IFNAR1. Receptor clustering results in JAK1 and Tyr2 activation by auto-phosphorylation (Reviewed by Ivashkiv and Donlin, 2014). JAK1 and Tyr2 phosphorylate the IFNAR, facilitating the recruitment and activation of signal transducer and activator (STAT) 1 and 2. JAK1 and Tyr2 then phosphorylate STAT1 and STAT2 enabling their dimerisation and nuclear translocation.

STAT1/2 heterodimers form a complex with IRF9 in the cytoplasm known as IFN-stimulated gene factor 3 (ISGF3) and translocate to the nucleus (Fu et al., 1990). ISGF3 then initiates transcription of the IFN-Stimulated Response elements (ISRE) (Reviewed by Plataniias, 2005). The ISRE is present in the promoters of hundreds of anti-viral genes with deleterious effects on viral replication resulting in the induction of an anti-viral state (Schoggins et al., 2011). Many of these ISGs promote what is described as a cell intrinsic anti-viral response and antagonise viral replication at several stages of the virus life cycle (Examples in **Table 1.2**). STAT1 homodimers or STAT1/3 heterodimers bind and activate IFN gamma-activated sequences (GAS) to transcribe pro-inflammatory genes such as nicotinamide adenine dinucleotide phosphate (NADPH) oxidase and Dual oxidase 1 which aid in the production of reactive oxygen species (Reviewed by Plataniias, 2005).

Most cells possess the capacity to induce IFN- α and IFN- β via PRR signalling, albeit through differing stimuli determined by PRR expression (Reviewed by Kawai and Akira, 2011; Rev-

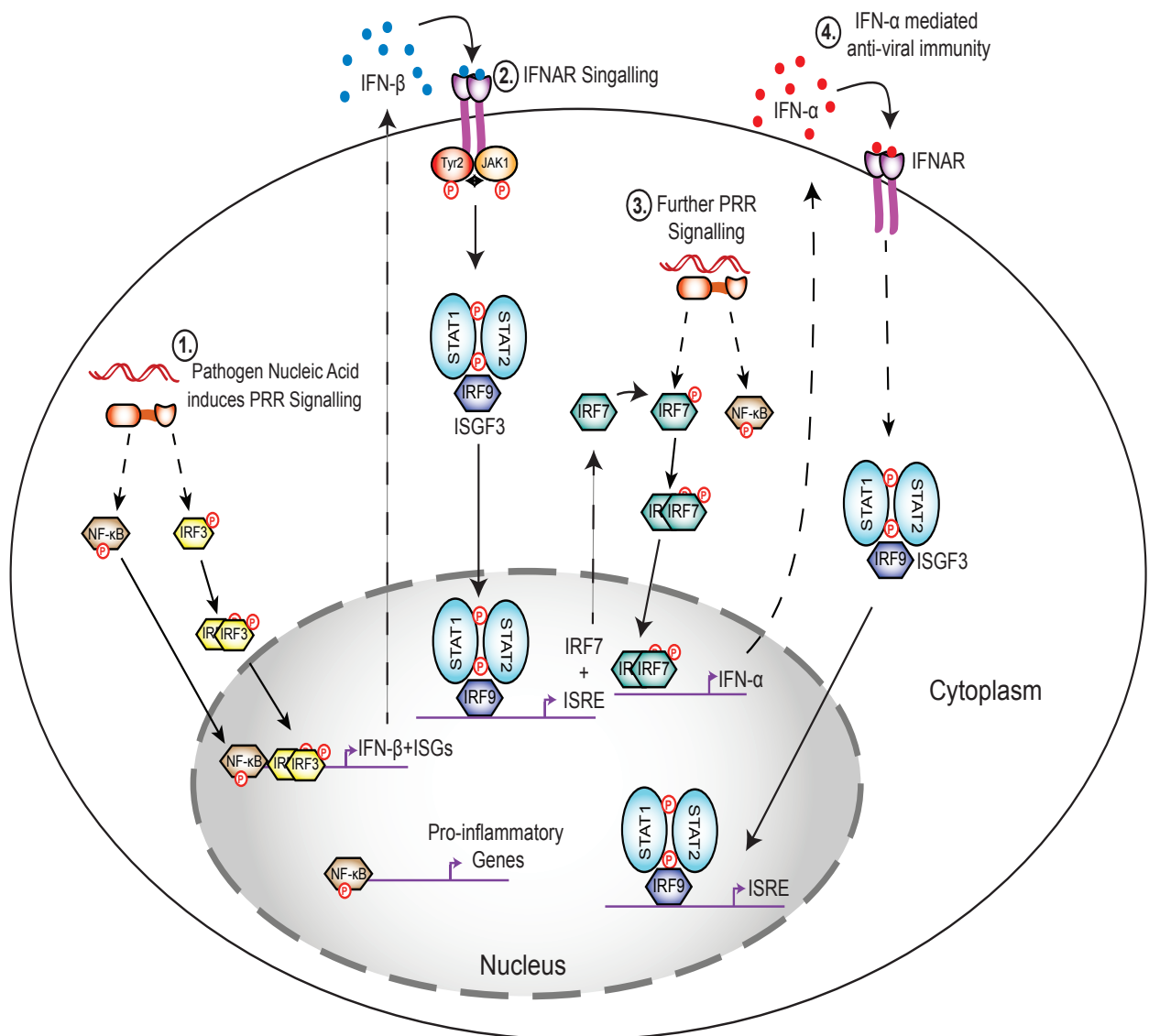


Fig 1.1 Induction of Interferon and Activation of the Interferon-stimulated Response Element

(1) The presence of a virus or pathogen nucleic acid stimulates PRR signalling, promoting the phosphorylation and activation of the transcription factor IRF3. Phospho-IRF3 then dimerises and translocates to the nucleus. Phospho-IRF3 and the Rel-A subunit of NF-κB, form the IFN-β enhanceosome and initiate IFN-β transcription. (2) IFN-β signals in an autocrine and paracrine manner through the IFNAR. IFN-β binding to the IFNAR receptor promotes IFNAR clustering, leading to the activation of Tyk2 and JAK1 by reciprocal auto-phosphorylation. Activated-Tyk2 and JAK1 then phosphorylate STAT1/2, enabling the formation of STAT1 and STAT2 dimers. STAT1/2 dimers associate with IRF9 in the cytoplasm forming the ISGF3 complex. ISGF3 translocates to the nucleus to initiate transcription of IRF7 and anti-viral genes via the ISRE. (3) IRF7 is activated by PRR signalling, where it initiates the transcription of IFN-α. (4) Cells then switch to a predominately IFN-α mediated response leading further transcription of ISRE genes. NF-κB is typically activated alongside IFN in many PRR pathways. NF-κB promotes the transcription of pro-inflammatory genes which complement the anti-viral functions of many ISRE genes.

IFN Stimulated Gene	Function	Ref
<i>Inhibition of Cytoplasmic Entry</i>		
TRIM 5 α (Tripartite motif-containing protein 5 α)	Binds to viral capsid upon entry into cytoplasm and prevents uncoating, inhibits release of genetic material	(Stremlau et al., 2004)
IFITM Proteins (Interferon-induced transmembrane protein 1)	Inhibit cytosolic entry by inhibiting virus-membrane fusions	(Brass et al., 2009)
<i>Inhibition of Viral Replication</i>		
ADAR-1 (Adenosine Deaminase, RNA-specific 1)	RNA specific Adenosine deaminase; converts Adenosine to Inosine resulting in mutations in target RNA	(Herbert et al., 1997)
APOBEC3G (Apolipoprotein B mRNA editing enzyme, catalytic polypeptide-like 3)	DNA specific Cytidine deaminase; Converts Cytosine to Uracil resulting in mutations in negative strand of cDNA in target retroviruses	(Bishop et al., 2004)
SAMHD1 (SAM and HD domain-containing protein 1)	GTP-activated deoxynucleoside triphosphate triphosphohydrolase; depletes host nucleotide pool preventing synthesis of new virus genomes	(Goldstone et al., 2011)
OAS1 (2'-5'-oligoadenylate synthetase 1)	Synthesises (2',5')-oligoadenylates; small molecules which activate RNaseL promoting virus and host RNA degradation	(Kristiansen et al., 2010)
<i>Inhibition of Transcription and Translation</i>		
PKR (Protein Kinase R)	Phosphorylates translation initiation factor eIF2 α , inhibiting mRNA synthesis	(Davies et al., 1993)
IFIT Family (Interferon Induced Protein with Tetratricopeptide Repeats)	Recognises 5' Triphosphate and lack of 2' O-methylation on viral RNAs and binds to them inhibiting their translation	(Daffis et al., 2010; Pichlmair et al., 2011)
MxA (Human myxovirus resistance protein 1)	Suppresses transcription of viral RNAs	(Pavlovic et al., 1992)
<i>Prevention of Assembly and Release of New Virions</i>		
Tetherin	Prevents release of new virions from infected cells	(Neil et al., 2008)
Viperin (Virus inhibitory protein, endoplasmic reticulum-associated, interferon-inducible)	Downregulates expression of virus structural proteins, alters composition of membrane by inhibiting farnesyl diphosphate synthase activity, preventing lipid raft formation and virion release	(Chin and Cresswell, 2001; Wang et al., 2007)

Table 1.2 Cell Autonomous Immunity by Interferon Stimulated Genes

iewed by Sparrer and Gack, 2015). IFN- α possesses 13 subtypes in humans with different affinities for IFNAR binding that have been observed to induce different subsets of ISGs *in-vitro* (Reviewed by Gibbert et al., 2013; Hillyer et al., 2012). The activity of the other type I IFNs are restricted to particular tissues or cell types; IFN- ϵ is expressed in the female reproductive tract and is regulated by local oestrogen levels (Fung et al., 2013), IFN- κ is only expressed in keratinocytes and is upregulated upon infection or IFN- β treatment (LaFleur et al., 2001) and IFN- ω has only been described in lymphoma cells infected with EBV (Hauptmann and Swetly, 1985).

1.3 Inflammation

Inflammation describes a localised physiological state characterised by redness, swelling, fever and pain at the site of insult (Reviewed by Netea et al., 2017). Inflammation is mediated by pro-inflammatory cytokines such as Tumour Necrosis Factor alpha (TNF α), Interleukin(IL)-1 β and IL-6. Pro-inflammatory cytokines act in an autocrine and paracrine manner to activate endothelial cells promoting vascular permeability and aids immune cell infiltration to the site of infection by chemokines (Reviewed by Melchjorsen et al., 2003). At high concentrations, these cytokines exert an endocrine effect on the host. These endocrine effects include inducing production of the acute phase protein response in the liver increasing the concentration of coagulation factors and components of the complement cascade in the bloodstream (Reviewed by Gabay and Kushner, 1999). Additionally, pro-inflammatory cytokines promote the activation of localised macrophages and neutrophils; prompting the release of prostaglandins which act on the hypothalamus to induce fever and sickness behaviours (Reviewed by Netea et al., 2017).

TNF α , IL-1 β and IL-6 are transcribed by NF κ B following PRR signalling (Collart et al., 1990; Hiscott et al., 1993; Reviewed by Kawai and Akira, 2011; Matsusaka et al., 1993). IL-1 β is transcribed in a pro-form by NF κ B and requires processing by the cysteine-aspartate protease caspase-1 for its biological activity (Thornberry et al., 1992). Caspase-1 is activated by a multiprotein complex known as the inflammasome.

1.3.1 The Inflammasome

The inflammasome describes a cytosolic multiprotein complex composed of a PRR containing a pyrin (PYD) domain and the adapter molecule ASC (apoptosis associated speck like protein containing a caspase activation and recruitment domain) (Martinon et al., 2002). Several varieties of inflammasome complexes exist, each with unique PAMP ligands (Reviewed by Broz and Dixit, 2016). Inflammasome activation promotes the assembly of ASC filaments aided by homotypic interactions between receptor and ASC PYD domains (Lu et al., 2014; Martinon et al., 2002). The nucleation of receptor and ASC in turn, promotes the recruitment, cleavage and activation of Caspase 1. Active caspase 1 cleaves the pro-forms of the cytokines IL-1 β and IL-18 into their pro-inflammatory active forms. Inflammasome activation also results in the formation of large super-molecular complex of ASC dimers known as the pyroptosome (Fernandes-Alnemri et al., 2007; Lu et al., 2014). Large-scale Caspase 1 activation in the pyroptosome leads to cleavage of gasdermin D (Kayagaki et al., 2015; Shi et al., 2015). Cleaved gasdermin D binds to phosphatidylinositol phosphates and phosphatidylserine present in the cell membrane leading to the formation of pores, resulting in a form of osmotic cell death known as pyroptosis (Liu et al., 2016). Pyroptosis results in the release of PAMPs, DAMPs and the mature IL1 β and IL18 produced during inflammasome activation from the cell.

1.4 Nucleic Acid Sensing Pathogen Recognition Receptors

Engagement of unique PRR signalling pathways by specific PAMPs enables the activation of an appropriate immune response (i.e. humoral vs cell mediated) to prevent the establishment of infection (Reviewed by Kawai and Akira, 2011; Sparrer and Gack, 2015). Unlike bacteria or fungi, viruses lack conserved cell wall components (e.g. LPS), thus the main PAMPs for viral detection are typically nucleic acids. Deoxyribonucleic acid (DNA) and Ribonucleic acid (RNA) can be detected in the endolysosome following phagocytosis or accumulate in the cytoplasm during infection and be recognised as a PAMP (Sparrer and Gack, 2015). In recent years, there have been great advances in our understanding of the mechanisms of how nucleic acids are detected by PRRs (Reviewed by Sparrer and Gack, 2015; Reviewed by Wu and Chen, 2014). These will be discussed based on cellular location.

1.4.1 Endolysosomal detection of nucleic acids is mediated by TLRs 3, 7-9 and 13

Toll Like Receptors (TLRs) are a family of membrane associated PRRs (Reviewed by Kawai and Akira, 2011). TLRs are comprised of an N-terminus of multiple regions of leucine rich repeats (LRRs) that mediate ligand binding and a C-terminus containing a Toll/Interleukin-1 receptor (TIR) domain which mediates downstream signalling. TLRs form dimers upon engaging with their ligands for subsequent signalling (Reviewed by Shimizu, 2017). Intracellular pathogens enter the cell through endocytic or phagocytic routes and release nucleic acids following their degradation in the endolysosome which are detected by TLRs 3, 7-9 and 13 (Reviewed by Barton and Kagan, 2009; Wu and Chen, 2014). The forms of nucleic acids sensed in the endolysosome are single stranded(ss) (TLR 7 and TLR 8) and double stranded (ds) RNAs (TLR 3), 23S ribosomal RNA (TLR 13) and dsDNA (TLR 9). TLRs involved in the recognition of nucleic acids are trafficked to the endolysosomal compartment by the chaperone protein Unc-93 homolog B1 (UNC93B1) (Kim et al., 2008; Lee et al., 2013). Mice and patients possessing UNC93B1 mutations present with defects in endosomal TLR signalling and an increased susceptibility to viral infection, emphasising the importance of UNC93B1 to this process (Casrouge et al., 2006; Tabeta et al., 2006).

1.4.1.1 TLR 3

TLR 3 was first identified as a receptor for dsRNA in a screen for activators of an NF κ B reporter in Human Embryonic Kidney (HEK293T) cells (Alexopoulou et al., 2001). TLR 3 also recognises the synthetic dsRNA mimic Polyinosinic:polycytidylic acid, Poly(I:C) (Alexopoulou et al., 2001; Marshall-Clarke et al., 2007). dsRNA forms as a replication intermediate during positive strand ssRNA virus replication and is a product of DNA virus replication due to suspected convergent transcription and long ssRNA self-association (Weber et al., 2006). TLR 3 detects dsRNA in the endolysosome like compartments in phagocytes, however in cell lines and tumours, TLR 3 is often expressed on the extracellular surface (Matsumoto et al., 2003). TLR 3 initiates IFN- β and pro-inflammatory cytokine production via the TIR adapter TIR domain-containing adaptor inducing IFN- β (TRIF) (**Fig 1.2**) (Yamamoto et al., 2003). Structural studies have revealed that TLR 3 achieves sequence-independent recognition of RNA through amino acids within the LRRs interacting with the RNA sugar phosphate backbone (Bell et al., 2006). Specifically, mutation of His539 and

Asn541 within LRR20 (Bell et al., 2006) and Arg64, Phe84, Ser86 and Glu110 within LRR-NT to LRR3 region (Leonard et al., 2008) impeded TLR 3 signalling by reducing interactions with the RNA backbone.

The contribution of TLR 3 to immunity *in vivo* is unclear as TLR 3 knockout (^{-/-}) mice were found to have normal immune responses to Vesicular Stomatitis Virus (VSV), Murine Cytomegalovirus (mCMV), Lymphocytic Choriomeningitis Virus (LCV) and Reovirus (RV) infections (Edelmann et al., 2004). However another study by (Negishi et al., 2008), reported that TLR 3 conferred resistance in mice against Coxsackievirus group B serotype 3 (CSV). Furthermore, IFNAR(^{-/-}) mice expressing a transgenic TLR 3 were found to display increased resistance to VSV and Herpes Simplex Virus 1(HSV-1) infections, implying that TLR 3 has functions beyond IFN induction. Further studies are needed to elucidate the precise contribution of TLR 3 to anti-viral immunity.

1.4.1.2 TLR 7 and TLR 8

TLR 7 and TLR 8 are expressed in the endolysosomes of phagocytic APCs and recognise ssRNAs, imidazoquinolines and synthetic small molecule nucleotides (Diebold et al., 2004; Heil et al., 2004; Lund et al., 2004). TLRs 7 and 8 initiate IFN- α and pro-inflammatory cytokine production via Myeloid differentiation primary response gene 88 (MyD88) signalling following activation. The crystal structure of TLR 8 reveals that TLR 8 recognises the RNA degradation products; uridine and short oligo-nucleotides of 20bp (Tanji et al., 2015). Similarly, TLR 7 structural studies revealed a preference of short ssRNAs, guanidine and guanidine derivatives such as 7-methylguanosine and 8-hydroxyguanosine that occur during DNA damage (Shibata et al., 2015; Zhang et al., 2016). However, TLR 7's recognition of ssRNAs relies on amino acid residues which specifically interact with uridine moieties in RNA affording it the capacity to recognise a broader range of ssRNA ligands than TLR 8 (Zhang et al., 2016). TLR 7 has been observed to detect VSV and Influenza A (IAV) in mice (Lund et al., 2004).

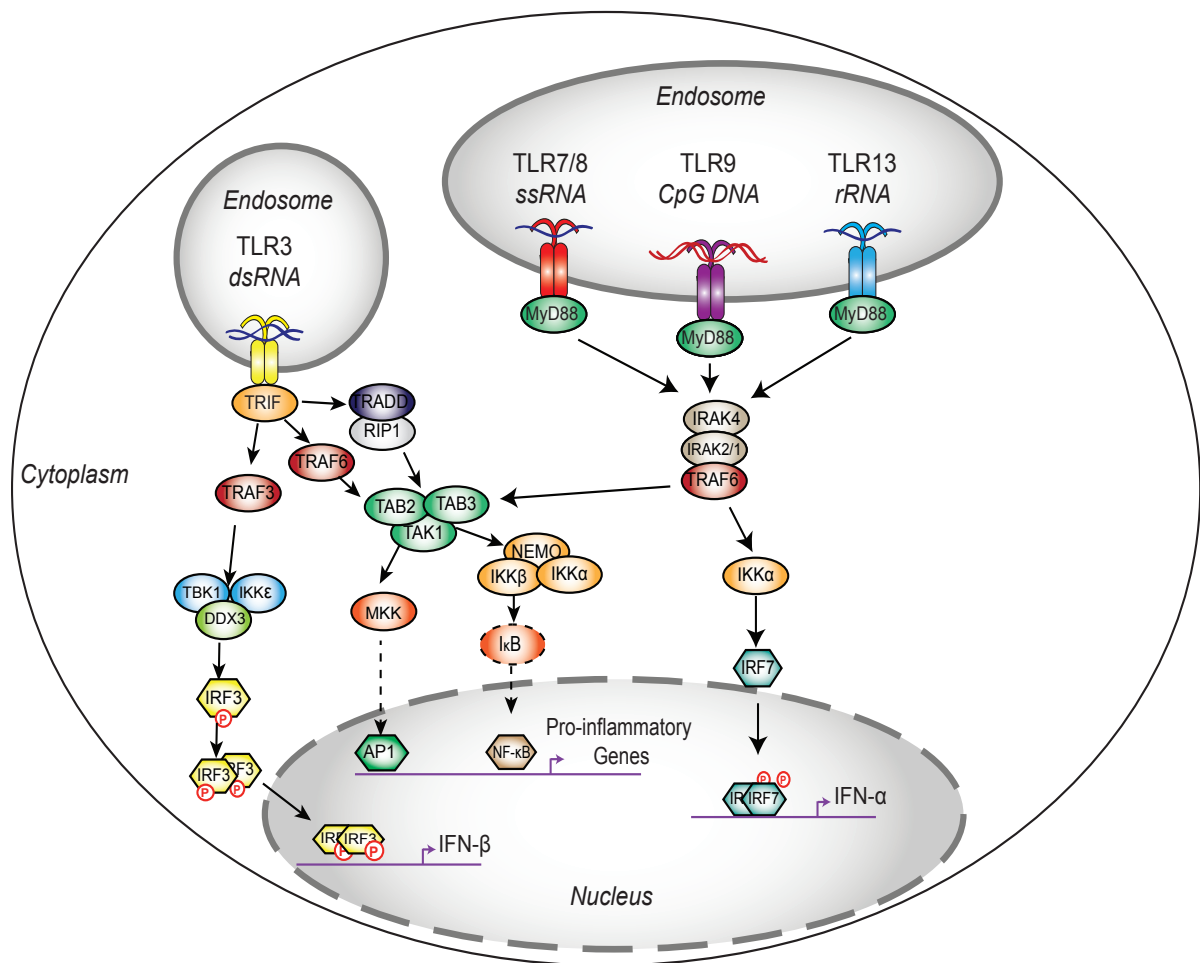


Figure 1.2 Endosomal TLR Signalling

Upon ligand binding TLRs dimerise to initiate signalling. TLR3 signals via TRIF. TRIF signalling diverges to initiate the production of IFN- β and pro-inflammatory cytokines. TRIF induces IFN- β by activating the ubiquitin E3 ligase TRAF3, which in turn enables TBK1 and IKK ϵ to activate IRF3 and initiate IFN- β transcription. The other arm of TRIF signalling is mediated by TRAF6 and RIP1. It is believed that the K63 ubiquitin chains on RIP1 and TRAF6 recruit and activate the TAB2/3-TAK1 complex, leading activation of MKK signalling culminating in the activation of AP1. The TAB2/3-TAK1 complex also activates NEMO, which enables the IKKs to phosphorylate I κ B prompting its degradation, leading to transcription of pro-inflammatory genes by NF- κ B. TLRs7-9 and 13 signal via MyD88. MyD88 signalling results in the formation of a complex between IRAK4 and IRAK2 or IRAK1 known as the MyDDosome which recruits TRAF6. TRAF6 then activates the TAB2/3-TAK1 and NEMO complexes to induce activation of pro-inflammatory genes. TRAF6 also induces IFN- α via IKK α mediated phosphorylation of IRF7.

1.4.1.3 TLR 13

TLR 13 has been reported to recognise a specific 13 nucleotide sequence of bacterial 23S ribosomal RNA in the endosomes of dendritic cells and monocytes (Li and Chen, 2012; Oldenburg et al., 2012). TLR 13 has been implicated in the immune response against *Streptococcus pyogenes* (Fieber et al., 2013). TLR13 is understood to signal via MyD88 (Fieber et al., 2013).

1.4.1.4 TLR 9

TLR 9 recognises unmethylated Cytosine-phosphate-Guanosine(CpG) regions of DNA in the endosomes of B cells and dendritic cells (Bauer et al., 2001; Hemmi et al., 2000). These unmethylated CpG regions are 20 times more prevalent in microbial DNA than in mammalian DNA, and have been confirmed to confer immunogenicity using oligonucleotides. Similar to TLRs 7 and 8, TLR 9 signals via MyD88 and induces IFN α and following activation (Reviewed by Kawai and Akira, 2011). TLR 9 binds DNA in a 2:2 complex with the N terminal groove of the TLR 9 LRR recognising the CpG region of DNA and the C-terminus primarily interacting with the sugar-phosphate backbone (Ohto et al., 2015). TLR 9 has been implicated in the immune response to HSV-2 as plasmatoid dendritic cells from TLR 9^(-/-) mice were unable to produce IFN- α upon infection (Lund et al., 2003). TLR 9 has also been observed to recognise viral RNA:DNA hybrids that form as replication intermediates during retroviral infection in human and murine dendritic cells (Rigby et al., 2014). Further *in vitro* analysis of TLR 9's binding capabilities revealed that TLR 9 binds RNA:DNA hybrids with a greater affinity than reported for dsDNA.

1.4.2 Cytosolic Nucleic Acid Sensing

The expression of endolysosomal TLRs is restricted to phagocytic APCs. Although APCs can detect viruses released from infected or apoptotic cells, the cytoplasm and/or nucleus is the major replicative niche of a virus, and thus is outside the jurisdiction of the endolysosomal nucleic acid sensing TLRs. Cells that do not express the endolysosomal TLRs such as epithelial cells and fibroblasts mount effective immune responses to viral infection due to the presence of cell-intrinsic nucleic acid sensors in the cytosol (Stetson and Medzhitov, 2006a).

1.4.2.1 RNA Sensing in the Cytosol by RLRs

Detection of cytoplasmic RNA is mediated by the RIG-I like Receptor (RLR) family and the adapter protein Mitochondrial Antiviral-Signaling protein (MAVS) (also known as CARD Adaptor Inducing IFN- β (Cardif), Virus-Induced Signalling Adaptor (VISA) and IFN- β Promoter Stimulator 1 (IPS-1)) (Kawai et al., 2005; Meylan et al., 2005; Seth et al., 2005; Reviewed by Wu and Chen, 2014; Xu et al., 2005). The RLR family contains three members; Retinoic acid-Inducible gene I (RIG-I), Melanoma Differentiation-Associated protein 5 (MDA5) and Laboratory of Genetics and Physiology 2 (LGP2) (Kato et al., 2006; Yoneyama et al., 2005; Yoneyama et al., 2004).

The RLRs are DExD/H box RNA helicases which function as PRRs for different features of pathogen RNA (Reviewed by Loo and Gale, 2011). Structurally, RLRs are comprised of three domains; a DExD/H box RNA helicase domain which contains RNA binding and unwinding capabilities and functions as an Adenosine Tri-Phosphate (ATP) hydrolase, a C-terminal repressor domain, and an N-terminus consisting of two caspase activation and recruitment domains (CARDs). LGP2 is distinct from RIG-I and MDA5 in that it does not possess the N-terminal CARD domains (Yoneyama et al., 2005).

RIG-I was first proposed to be a receptor for dsRNA by (Yoneyama et al., 2004). While (Kato et al., 2008) demonstrated that RIG-I recognises short Poly(I:C) fragments, it has been shown that RIG-I preferentially recognises RNAs with exposed 5' triphosphate ends enabling RIG-I to distinguish from cellular RNA species (Hornung V et al., 2006). Further studies using IAV genomic RNA revealed that at least one 5' phosphate was required for RIG-I mediated immunity (Pichlmair et al., 2006). RIG-I has also been demonstrated to recognise 5' diphosphates ends of RNA. In an investigation by Goubau et al., (2014), RIG-I was found to associate with base-paired 5'pp-RNAs made by in vitro transcription. RIG-I was also essential for controlling reovirus infection (i.e a dsRNA virus with a free 5'pp terminus on its negative strand due to triphosphate processing by a viral phosphohydrolase) in MEFs and in mouse models of infection. Studies using next generation sequencing of RIG-I:RNA complexes also demonstrated that RIG-I binds short RNA transcripts containing 5' triphosphates (Baum et al., 2010). Synthetic 5' triphosphate oligoribonucleotides were

utilised to determine that ssRNAs must form blunt dsRNA panhandle regions from self-pairing to be recognised by RIG-I (Schlee et al., 2009). Additionally, (Rehwinkel et al., 2010) demonstrated using a viral reconstitution system with segments of the IAV genome that the full length of genome of IAV and Sendai virus (SeV) which contain exposed 5'triphosphates confer stimulatory RIG-I activity. Replication intermediates of these viruses lack 5'triphosphates and thus do not substantially contribute to RIG-I immunity (Rehwinkel et al., 2010).

Other features have also been observed to enhance the immunogenicity of RNA by RIG-I such as poly uridine motifs found in the Hepatitis C virus (HCV) genome (Saito et al., 2008). RIG-I was also found to detect the short self RNAs produced by RNase L during viral infection to enhance IFN production (Malathi et al., 2007). MDA5 has been proposed to recognise longer RNAs molecules over 4000 nucleotides in length that form higher secondary structures such as branches and webs (Kato et al., 2008; Pichlmair et al., 2009). Perhaps because of this preference for viral genome length, RIG-I and MDA5 have been observed to mediate immunity to distinct families of RNA virus; RIG-I mediates immunity to Paramyxoviruses, Rhabdoviruses, Orthomyxoviruses and Flaviviruses among others, while MDA5 mediates the detection of picornaviruses (Kato et al., 2006; Loo et al., 2008; Rehwinkel et al., 2010; Yoneyama et al., 2005).

The specific contributions of LGP2 to the detection of viral RNA have been challenging to elucidate. Initially it was proposed that LGP2 was a negative regulator for RIG-I signalling as L929 cells overexpressing LGP2 presented with increased titres of encephalomyocarditis virus (EMCV) following infection (Yoneyama et al., 2005). Consistent with this observation, an investigation by (Venkataraman et al., 2007) highlighted that *lgp2*^(-/-) MEFs were greatly sensitised to poly(I:C) stimulation and resistant to lethal VSV infection (i.e. a virus which is sensed by RIG-I during replication). Conversely, (Sato et al., 2010) used *lgp2*^(-/-) mice to propose that LGP2 acts upstream of RIG-I and MDA5 as a positive regulator of RLR signalling. In this study *lgp2*^(-/-) mice were compromised in their ability to produce IFN- β in response to RNA virus infection. Similar results were observed in dendritic cells containing a functionally compromised LGP2 mutant without ATPase activity. This study also highlighted that LGP2 had no role in the recognition of *in vitro* transcribed RNAs and that

LGP2 synergised with MDA5 to drive an IFN- β reporter construct suggesting that LGP2 may sense RNA through MDA5 (Sato et al., 2010). While the authors of this study were unable to provide a clear explanation for the contradictory observations of Venkataraman et al., (2007), they were able to demonstrate that restoring LGP2 expression in *lgp2*^(-/-) MEFs rescued defects in IFN- β in response to EMCV infection. This confusing finding was partially explained by a later investigation by (Suthar et al., 2012). Unlike Sato et al., (2010) and Venkataraman et al., (2007), the authors in this study used *lgp2*^(-/-) mice generated on a pure C57BL/6 background with complete disruption of *lgp2* transcription. Suthar et al., (2012) demonstrated that IFN- β production was attenuated in response to SeV and DENV infection in BMDMs but not MEFs, suggesting that LGP2 may only function as a positive regulator of RLR signalling in certain cell types. Analysis of LGP2/RNA complexes purified from cells has revealed that LGP2 has a high affinity for specific sequences within the L region of the EMCV antisense RNA strand and the nucleoprotein-coding region of Measles virus, whether LGP2 recognises other specific regions of RNA virus genomes is presently unclear (Deddouche et al., 2014; Sanchez David et al., 2016) Thus, further studies are required to fully elucidate the precise contribution of LGP2 to RNA sensing.

The RLRs signal through the adapter protein MAVS at the mitochondria to initiate IFN- β and pro-inflammatory cytokine transcription (**Fig 1.3**) (Kawai et al., 2005; Meylan et al., 2005; Seth et al., 2005). RIG-I and MDA5 were anticipated to activate MAVS via their CARD domains as overexpression of the RIG-I CARD drives an IFN- β reporter construct (Yoneyama et al., 2004). Structural studies of MDA5 bound to RNA reveals that it recognises the internal duplex of the RNA structure unlike RIG-I which preferentially binds to the RNA ends (Wu et al., 2013a). Prior to RNA binding, RIG-I exists in an auto-inhibited state with CARD1 interacting with the Hel-2i domain within the DExD box (Kolakofsky et al., 2012; Luo et al., 2011). RNA binding and ATP hydrolysis releases the CARD from Hel-2i domain and this results in a conformational change permitting subsequent signalling by exposing the CARDS for K63 polyubiquitination by tripartite motif protein (TRIM) 25 and riplet/Ring Finger (RNF) 135 (Gack et al., 2007; Oshiumi et al., 2009; Oshiumi et al., 2010). TRIM25 binding to RIG-I and RIG-I translocation from the cytosol to MAVS, is mediated by 14-3-3 ϵ (Liu et al., 2012). Additionally, unanchored polyubiquitin chains bind to RIG-I and potently activate RIG-I signalling (Zeng et al., 2010). MDA5 stacks along the dsRNA filament in a

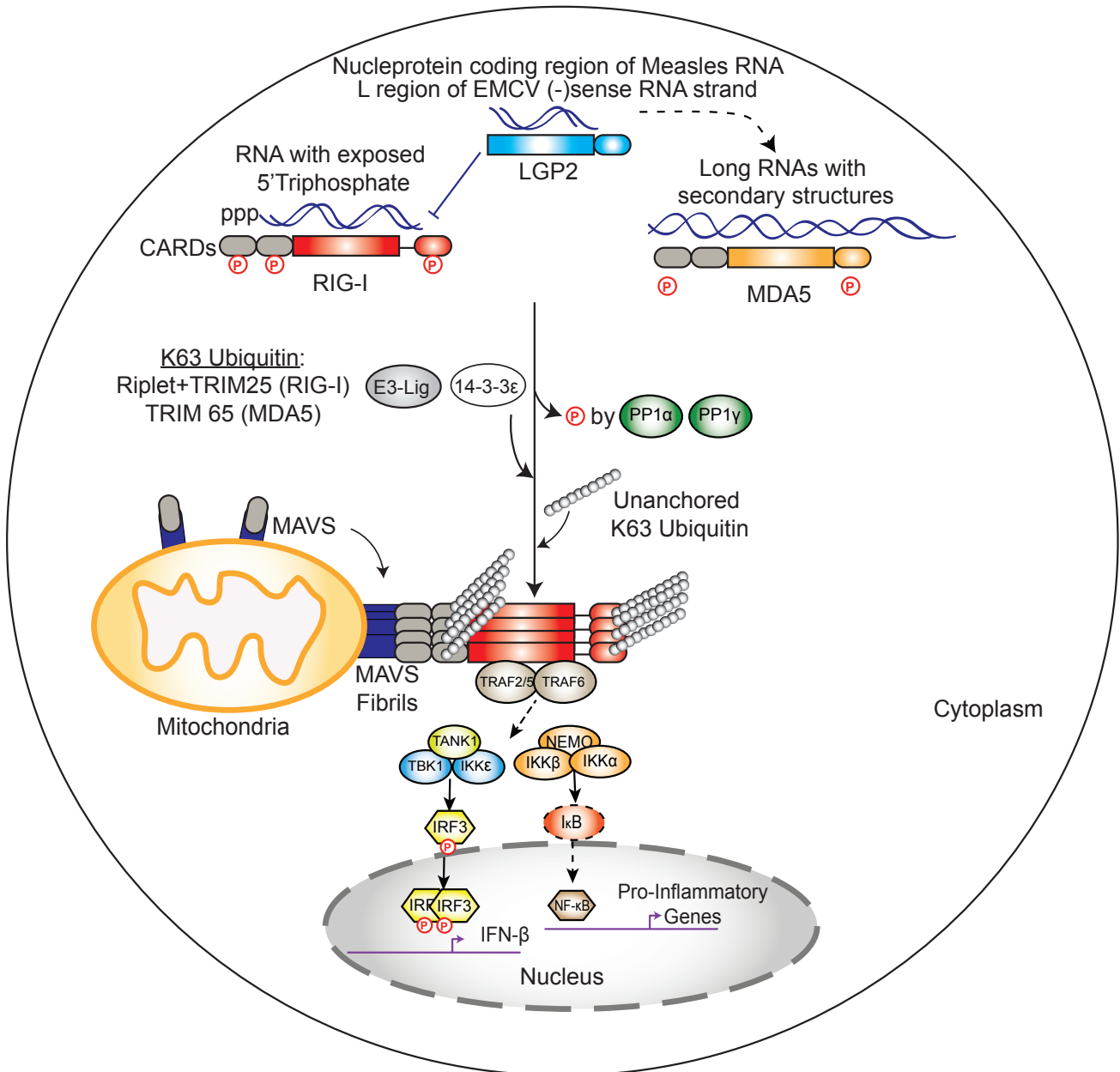


Fig 1.3 Overview of RLR and MAVS Signalling

The RLRs recognise RNA ligands. RIG-I preferentially binds to short dsRNAs with exposed 5'-triphosphates. MDA5 recognises longer dsRNAs based on secondary structures such as branches and webs. The precise features of RNA that LGP2 binds have been difficult to characterise but LGP2 has been observed to directly bind the L region of the EMCV virus anti-sense RNA strand, and nucleoprotein coding region of the Measles virus RNA. Upon binding RNA, RLRs undergo a conformational change. RLRs are licensed for activation by dephosphorylated by PP1α and PP1γ and SUMOylation by TRIM38. RLRs bind to MAVS as tetramers. RLR binding to MAVS results in MAVS nucleation and the formation of MAVS fibril structures. MAVS nucleation is promoted by K63 ubiquitination of the RLRs and the binding of unanchored K63 ubiquitin chains. RLR translocation and ubiquitination is promoted by binding of the chaperone protein 14-3-3ε. MAVS nucleation attracts TRAFs 2, 5 and 6 which induce activation of IFN and pro-inflammatory genes by the TANK/TBK/IKK and NEMO complexes.

head-to-tail arrangement, resulting in oligomerisation of the CARDS of MDA5 and MAVS activation. MDA5 is also K63 polyubiquitinated by TRIM65 and binds unanchored polyubiquitin chains prior to activating MAVS (Jiang et al., 2012; Lang et al., 2016). RIG-I and MDA5 are licensed for activation by SUMOylation by TRIM38 and dephosphorylation of the CARDS (RIG-I (K96/K888 and S8/T170) and MDA5 (K43/K865 and S88)) by the phosphatases PP1 α and PP1 γ (Hu et al., 2017)

MAVS signalling (**Fig 1.3**) results in the IRF3 and NF κ B transcription (Kawai et al., 2005; Meylan et al., 2005; Seth et al., 2005) The current model of MAVS signalling is that MAVS filament formation recruits the ubiquitin E3 ligases TNF receptor associated factor (TRAF)2, TRAF5 and TRAF6 (Liu et al., 2013). It is expected that bringing the TRAFs in close proximity to one another promotes their activation, resulting in the production of K63 polyubiquitin chains, and enables recruitment of NF- κ B essential modulator (NEMO) to the MAVS signalling complex. NEMO then activates TANK-binding kinase 1 (TBK1) and I κ B kinase ϵ (IKK ϵ) to activate IRF3 transcription, and IKK α/β to NF κ B transcription resulting in IFN- β and pro-inflammatory gene expression. Following filament formation and TRAF recruitment, MAVS is phosphorylated on Ser442 by IKK and TBK1, forming a platform for IRF3 recruitment and activation by TBK1 and IKK ϵ (Liu et al., 2015a).

RLRs are important for defence against viruses in mouse models. With the exception of plasmatiod dendritic cells, cells from MAVS^(-/-) mice were unable to produce immune responses to infections with VSV, ECMV, Newcastle disease virus (NDV), and SeV (Kumar et al., 2006; Sun et al., 2006). MAVS^(-/-) mice also succumbed to VSV infection. The N-terminal CARD domain of MAVS is crucial for its interactions with RIG-I and MDA5. Interactions between tetramers of activated RLRs bound to unanchored polyubiquitin chains and MAVS induce the formation of prion-like supramolecular MAVS filaments which activate MAVS signalling (Hou et al., 2011; Jiang et al., 2012).

1.4.2.2.1 Inflammatory DNA Sensing in the Cytosol by AIM2

Absent in melanoma 2 (AIM2) is a cytosolic PYHIN protein (Fernandes-Alnemri et al., 2009; Hornung et al., 2009). PYHIN proteins contain a pyrin domain (PYD) and a hematopoietic

expression, interferon-inducible nature, and nuclear localization (HIN) domain. AIM2 forms an inflammasome upon detecting DNA in the cytoplasm. AIM2 was first identified by examining the functions of other PYD proteins that could potentially interact with DNA, following an observation that NACHT, LRR and PYD domain containing protein 3 (NLPR3)^(-/-) THP1 cells could still produce IL1 β during adenovirus infection in an ASC dependent manner (Bürckstümmer et al., 2009; Fernandes-Alnemri et al., 2009; Hornung et al., 2009; Muruve et al., 2008). AIM2 was found to co-immunoprecipitate and co-localise with ASC following DNA stimulation in THP1 cells. Additionally, AIM2 overexpression in HEK293T cells promoted the cleavage of Caspase1 and release of IL-1 β (Hornung et al., 2009). Transfection of plasmid DNA into NLRP3^(-/-) THP1 cells also resulted in the formation of AIM2 oligomers and the ASC pyroptosome (Fernandes-Alnemri et al., 2009). Structural studies of AIM2 and another PYHIN protein interferon-gamma inducible protein 16 (IFI16), revealed that PYHIN proteins recognise DNA independent of its sequence through binding the sugar phosphate backbone via the HIN200 domain (Jin et al., 2012).

Sustained IFN signalling during viral infection has also been shown to increase expression of pyrin only protein 3 (POP3) in BMDMs (Khare et al., 2014). POP3 has also been shown to bind to AIM2 and inhibit cleavage of pro-caspase 1 when overexpressed in transgenic mice BMDMs, suggesting that it may form part of a negative feedback loop to prevent sustained AIM2 signalling and excessive pyroptosis (Khare et al., 2014). In mice, AIM2 inhibition is mediated by another PYHIN protein, p202 (Yin et al., 2011a). p202 is believed to inhibit AIM2 signalling by preventing the nucleation and formation of AIM2 filaments, thus reducing the capability of AIM2 to form an inflammasome.

1.4.2.2.2 NLRP3, Another Inflammasome for DNA?

NLRP3 is the most widely studied inflammasome and has been demonstrated to form an inflammasome in response to a wide range of stimuli e.g. uric acid crystals, extracellular ATP, reactive oxygen species and bacterial pore forming toxins (Reviewed by Broz and Dixit, 2016). Due to the number and diversity of ligands for NLRP3, it is unlikely that it recognises its ligands through direct binding. The ability of NLRP3 to form an inflammasome in response to cytosolic DNA is poorly understood. For example, in a study by (Muruve et al., 2008), NLRP3^(-/-) peritoneal macrophages were shown to respond to adenovirus infection.

However, enzyme-linked immunosorbent assays (ELISAs) performed on spleens taken from adenovirus infected NLRP3^(-/-) mice demonstrated a significant reduction in IL1 β and IL1 associated cytokines. Another study using *Listeria monocytogenes* infected macrophages demonstrated that IL1 β production was lost only when both AIM2 and NLRP3 were absent (Kim et al., 2010). Thus, it appeared that NLRP3 contributes to DNA sensing *in vivo* and was potentially redundant with AIM2 in certain cell types. Recently a report by (Gaidt et al., 2017) demonstrated that AIM2 was dispensable for inflammasome activation in human monocytes. Using Aim2^(-/-) and pharmacological inhibitors of NLRP3 the authors show that inflammasome activation was mediated by NLRP3 following K⁺ efflux due to activation of the cGAS-STING (Section 1.5 and 1.6.1) lysosomal cell death pathway.

1.4.2.2.3 Sox2

SRY (sex determining region Y)-box 2 (Sox2) is a transcription factor responsible for the formation of endodermal and ectodermal tissues during foetal development (Reviewed by Sarkar and & Hochedlinger, 2013). However, in neutrophils, Sox2 has been observed to function as a cytosolic DNA sensor and induce expression of pro-inflammatory genes upon challenge with *Listeria Monocytogenes*, *Bartonella*, *Staphylococci* and *Salmonella* (Xia et al., 2015). Sox2^(-/-) mice exhibited more severe bacterial loads and reduced pro-inflammatory cytokine production during infection. Sox2 was observed to bind conserved bacterial DNA sequences through its High Mobility Group (HMG) domain consistent with its role as a transcription factor. Sox2 induced activation of NF- κ B via TGF- β Activated Kinase 1/MAP3K7 Binding Protein 2 (TAB2) and Transforming Growth Factor- β Activated Kinase 1 (TAK1) induced activation of IKK and Mitogen-activated protein kinase kinase (MKK) signalling.

1.5 STING is an adapter protein for DNA-induced interferon production

The specific cellular signalling cascades that control IFN β transcription during DNA sensing have been difficult to characterise, but are understood to require the endoplasmic reticulum (ER) adapter molecule stimulator of interferon genes (STING), also known as Membrane tetraspanning protein (MPYS), transmembrane protein 173 (TMEM173), MITA and endoplasmic reticulum interferon stimulator (ERIS) (Ishikawa, 2008; Ishikawa et al., 2009;

Jin et al., 2008; Sun et al., 2009; Zhong et al., 2008). The importance of STING was verified as antigen presenting cells taken from *Sting*^(-/-) mice were demonstrated to be incapable of producing IFN in response to DNA transfection and infections with the intracellular pathogens *Listeria monocytogenes* and HSV1 (Ishikawa et al., 2009). Additionally, *Sting*^(-/-) mice used in this study succumbed to lethal HSV1 infection. STING expression has been observed across numerous cell types (Zhong et al., 2008). Due to the importance of IFN- β in co-ordinating effective anti-viral immunity, STING has been the centre of intense research focus over the last decade (Reviewed by Barber, 2015).

1.5.1 STING is a receptor for Cyclic Di-Nucleotides

Until recently it was unclear how STING detected the presence of cytoplasmic DNA. While STING has been reported to directly bind DNA by (Abe et al., 2013), it is unlikely that it functions as a DNA sensing PRR itself as HEK293T cells stably expressing STING remained unresponsive to DNA transfection (Burdette et al., 2011). Instead, STING was found to be a receptor for the cyclic di-nucleotides that are produced by bacteria that leak into the cytosol during infection; cyclic di-adenosine monophosphate (c-di-AMP) and cyclic di-guanylate monophosphate (c-di-GMP) (Jin et al., 2011; McWhirter et al., 2009). Further structural studies revealed the crystal structure of STING in complex with c-di-GMP and demonstrated that STING is functionally active as a dimer, with a cyclic di-nucleotide binding cleft at the dimer interface (Huang et al., 2012; Ouyang et al., 2012; Shu et al., 2012).

While these observations explained the mechanism of IFN induction by certain species of intracellular bacteria the mechanism by which DNA activated STING remained elusive until the discovery of the novel mammalian second messenger cyclic guanosine monophosphate-adenosine monophosphate (cGAMP) which is produced by the cytosolic enzyme cGAMP synthase (cGAS) upon binding DNA (Sun et al., 2013a; Wu et al., 2013b). cGAMP is capable of directly binding to and activating STING, resulting in a conformational change in STING structure now believed to be required for STING activation and subsequent signalling (Diner et al., 2013; Zhang et al., 2013). Additional proteins were also proposed to recognise DNA and signal through STING to induce IFN- β , however their mechanism of STING activation is now unclear (Reviewed by Unterholzner, 2013).

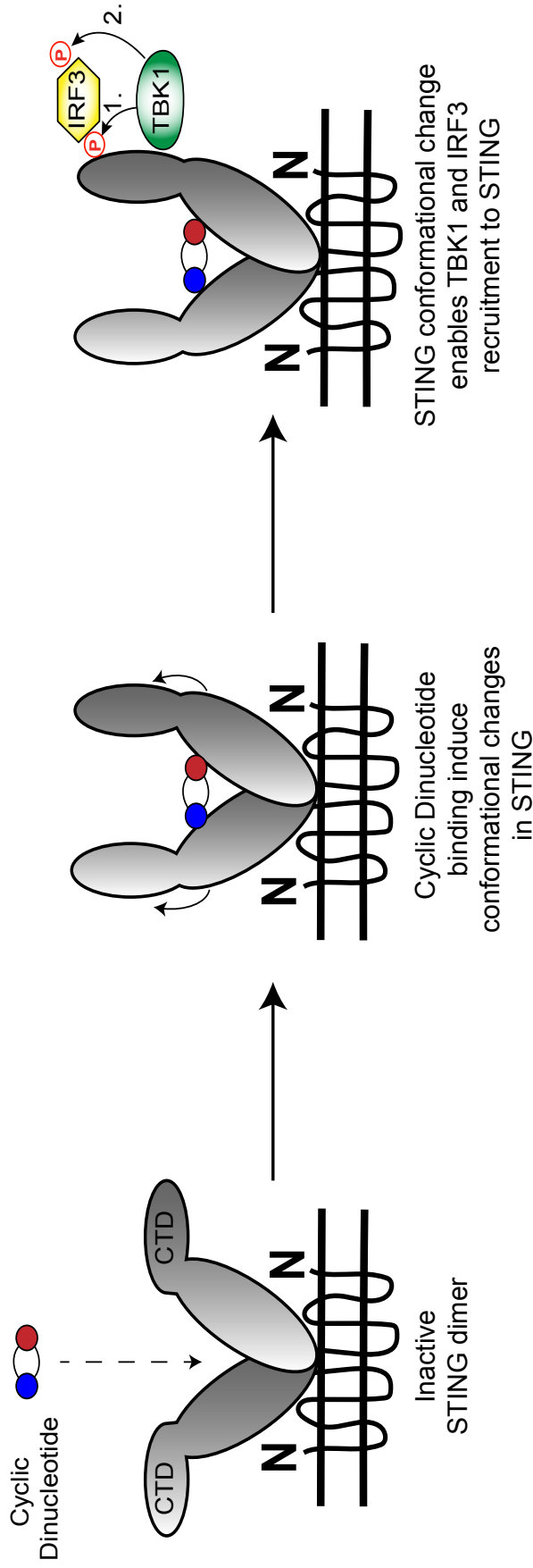


Fig 1.4 Overview of STING Activation

Cyclic dinucleotides accumulate in the cytoplasm during infection. Cyclic di-AMP and Cyclic-di-GMP are produced as signalling molecules by bacteria and leak into the cytoplasm from phagosomes and endolysosomes. cGAMP is produced by the cytosolic enzyme cGAS upon detecting DNA in the cytoplasm. Cyclic dinucleotides bind to the ER adapter protein STING, promoting its activation. Cyclic dinucleotide binding triggers conformational changes in the STING C-terminus. This conformational change facilitates the recruitment of the kinase TBK1, which is activated by auto-phosphorylation. STING is phosphorylated by activated-TBK1 on S366, creating a scaffold for the recruitment of the transcription factor IRF3. IRF3 is recruited to STING S366 where it is also phosphorylated by TBK1. Phosphorylated IRF3 then dimerises and translocates to the nucleus to initiate IFN- β transcription.

1.5.2 STING mediated RNA sensing

The involvement of STING in RNA sensing is contentious. Several early studies suggested that STING was involved in RNA sensing pathways (Ishikawa, 2008; Sun et al., 2009; Zhang, 2012; Zhong et al., 2008; Zhong et al., 2009). However, others have also shown that STING is dispensable for detection of SeV (Chen et al., 2011; Tanaka, 2012). Furthermore, many RNA viruses such as Dengue virus, HCV and Coronaviruses block STING function during infection suggesting inhibition of STING aids their survival (Aguirre et al., 2012; Ding et al., 2013; Nitta et al., 2013; Sun et al., 2012). It is important to note that as Dengue virus mediated activation of STING is due to host cell mitochondrial DNA leaking into the cytosol and that other RNA viruses may induce STING activation by similar mechanisms of host cell damage (Aguirre et al., 2017; Sun et al., 2017). STING may still possess cell type specific or virus specific roles for RNA sensing. However, considering the evidence that STING is a receptor for cyclic-di-nucleotides, the mechanism by which STING could sense RNA is ambiguous. A possible mechanism by which STING could regulate detection of RNA is through what Gough et al., (2002) describe as tonic signalling. Tonic signalling describes a homeostatic role of constitutive low level IFN production in the absence of infection. As MAVS and the RLRs are ISGs, it is possible that deletion of STING alters constitutive IFN levels by perturbing tonic signalling, and thus has knock-on consequences for the homeostatic regulation of ISGs.

A study by (Holm et al., 2016) has demonstrated a cGAS-independent mechanism of STING activation during infection with IAV. Although IAV is an RNA virus, the authors demonstrate that virus particles and liposomes could induce STING activation in the absence of RNA, therefore it is unlikely that the viral RNA is being sensed through STING itself. The authors identify Arg169 to be a region of functional importance for STING mediated immunity in response to enveloped RNA viruses and liposomes. Arg169 sits outside the cGAMP binding cleft and is exposed to the cytosol for interactions with currently unknown additional factors. This study also demonstrated that the hemagglutinin fusion peptide of IAV was also found to bind to this region of STING, inhibiting STING dimerisation and the recruitment of TBK1 upon stimulation with virus particles and liposomes but not DNA or cGAMP (Holm et al., 2016).

1.5.3 STING trafficking and signalling via TBK1

STING activation results in STING trafficking from the endoplasmic reticulum to endoplasmic reticulum-golgi intermediate compartments (ERGIC) in an autophagy-like process controlled by autophagy-related protein 9a (Atg9a) (Dobbs et al., 2015; Saitoh et al., 2009). Trafficking from the ER to the ERGIC is an essential hallmark of STING activation, as inhibition of the process by the *Shigella flexneri* and *Yersinia pestis* effector proteins IpaJ and YopJ abrogated STING induced IFN production (Cao et al., 2016b; Dobbs et al., 2015). Activated STING at the ERGIC then acts as a scaffold protein for the recruitment of the non-canonical IKK kinase TBK1 and transcription factor IRF3 (Liu et al., 2015a; Tanaka, 2012). After being recruited to STING, TBK1 then undergoes auto-phosphorylation and phosphorylates IRF3 and STING (Shu et al., 2013). IRF3 subsequently dissociates from STING, dimerises and translocates to the nucleus to initiate IFN β transcription.

While STING signalling is understood to require TBK1 and IRF3, many of the other aspects controlling STING behaviour and signalling remain nebulous such as the nature of the punctuate structures that STING forms at ERGICs. Although the formation of similar nucleated structures is also observed during formation of MAVS fibrils, it is presently unknown if STING forms such a supramolecular complex upon activation (Hou et al., 2011). NF κ B activation is another hallmark of STING signalling; (Abe and Barber, 2014) have proposed that this is mediated by TBK1 activation of the IKK complex and also propose the involvement of additional factors such as TRAF6 with unpublished data. Thus, many aspects of this arm of STING signalling remain elusive. Although autophagy has been implicated in STING regulation and trafficking (Saitoh et al., 2009), the precise mechanism by which it specifically turnover after signalling has yet to be elucidated.

1.5.4 STING Post-Translational Modifications

STING is subjected to extensive post-translational modification during infection (Summarised in Fig 1.4).

1.5.4.1 STING Phosphorylation

STING phosphorylation has been described on S358 and has been reported as a requirement for STING activation, albeit in an RNA sensing context (Zhong et al., 2008). STING phosphorylation has also been described in cells and in *in vitro* cell free assays on S366 by TBK1 and is reported as an essential requirement for STING signalling, permitting the recruitment IRF3 (Liu et al., 2015a). Conversely, S366 phosphorylation has also been proposed to represent inactivated STING following phosphorylation by unc-51 like autophagy activating kinase 1 (ULK1) during a negative feedback loop induced by sustained cGAMP signalling by (Konno et al., 2013). STING also possesses additional serines in its C-terminus that have also been observed to undergo phosphorylation however their functional consequences are presently unknown (Zhong et al., 2008).

1.5.4.2 STING Ubiquitination and SUMOylation

Ubiquitination of STING has also been reported in numerous studies. Ubiquitin contains several lysines in its structure allowing for the conjugation of additional ubiquitin molecules to ubiquitin leading to the formation of either Met1, K6, K11, K27, K29, K33, K48 and K63 polyubiquitin chains (Reviewed by Akutsu et al., 2016). Different forms of polyubiquitin chains mediate different cellular functions; K48 chains mediate proteasomal degradation while the other forms of ubiquitin chains mediate unique signalling functions. The addition of K11, K27, K48 and K63 chains to STING have all been reported as essential steps in the activation and regulation of STING signalling (Qin et al., 2014; Tsuchida et al., 2010; Wang et al., 2014; Zhang, 2012; Zhong et al., 2009). Intriguingly, every E3 ligase reported in these studies has been found to ubiquitinate the same lysine on STING, K150. While (Wang et al., 2014) demonstrate using a stringent two-step immunoprecipitation experiment that K27 ubiquitin chains are the only ubiquitin chains directly bound to STING, they also suggest that the K63 and K11 chains that were lost could have been bound to another protein or cofactor in a STING signalling complex. K48 chains were still present on STING in this report, suggesting that various E3 ligases could potentially compete for K150 over time during STING signalling to promote the differential regulation of the pathway. This study also demonstrated that TBK1 directly binds to K27 ubiquitin chains, which presently have no widely understood function.

K63 ubiquitination on K224 of STING has recently been demonstrated to aid in the recruitment of IRF3 to the STING signalling complex (Ni et al., 2017). A small interfering RNA (siRNA) screen identified mitochondrial E3 ubiquitin protein ligase 1 (MLU-1) as the E3 ligase responsible for this modification. STING is also modified with small ubiquitin like modifier (SUMO) on K337 during viral infection by TRIM38 promoting STING activation and stability (Hu et al., 2016)

One caveat of these studies is their reliance on over-expression experiments, which are occasionally prone to artefacts, or may neglect additional regulatory pathways or co-factors that may be cell type specific. For example, Hepatitis B virus and *Yersinia pestis* have been shown to block STING signalling by preventing K63 ubiquitination, affirming the importance of K63 chains to STING activation (Cao et al., 2016b; Liu et al., 2015b). This suggests that more rigorous and refined approaches using endogenous STING are required to appreciate how ubiquitin regulates this pathway.

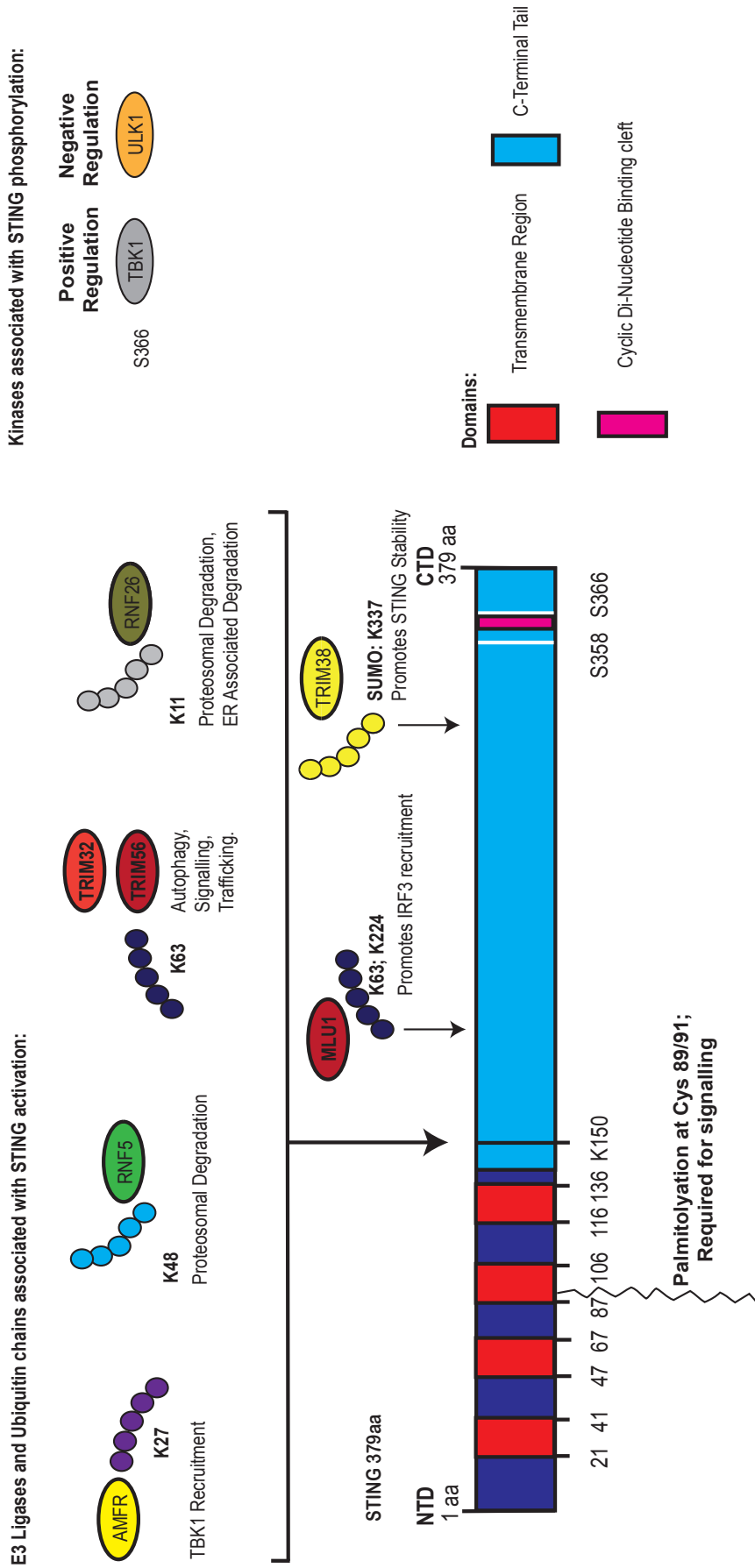


Fig 1.5 Summary of STING Post-Translational Modifications

STING is subject to a range of post translational modifications during its activation. Many E3 ubiquitin ligases have been proposed to ubiquitinate STING on K150, each with a unique ubiquitin chain and function that promotes an aspect of STING behaviour. K63 ubiquitination on K224 promotes IRF3 recruitment to STING. SUMOylation on K337 has been described to promote STING stability. STING is phosphorylated on S358 by an unknown kinase. STING is also phosphorylated on S366 however the functional consequences of this event are disputed. TBK1 mediated phosphorylation by on S366 is believed to enable recruitment of IRF3. Meanwhile, ULK1 mediated phosphorylation of S366 has been proposed to be part of a negative feedback loop following sustained cGAMP signalling. STING palmitoylation has recently been described on Cys89/81 as an essential requirement for STING activation and subsequent signalling.

1.5.4.3 STING Palmitoylation

Palmitoylation has recently been described as an essential modulator of STING activation (Mukai et al., 2016). Palmitoylation describes the reversible transfer of palmitic acid to membrane proximal cysteines on proteins by palmitoyl transferases and their subsequent removal by palmitoyl protein thioesterases (Reviewed by Linder and Deschenes, 2006). Palmitoylation influences the ability of membrane associated proteins to traffic into cholesterol rich lipid rafts wherein signal transduction is initiated. Palmitoylation can also alter the steric conformation of a protein in a membrane, thus influencing the ability of a receptor to bind a ligand (Reviewed by Goddard and Watts, 2012). (Mukai et al., 2016) identify that STING is palmitoylated on Cys88 and 91. Using a Cys88/91 Ser mutant or the palmitoyl transferase inhibitor, 2-Bromopalmitate, the authors demonstrate that inhibition or loss of palmitoylation abrogates STING signalling. Additionally, defects in intra-cellular responses to RNA sensing were observed with 2-Bromopalmitate suggesting that palmitoylation may also influence the RLR-MAVS pathway (Mukai et al., 2016).

While the study by (Mukai et al., 2016) was the first to demonstrate STING palmitoylation, a palmitoyl transferase had previously been reported to positively regulate the STING pathway. The ER associated protein Zinc Finger DHHC-Type Containing 1 (ZDHHC1) is a palmitoyl transferase which has been observed to constitutively associate with STING and promote STING dimerisation and signalling (Zhou et al., 2014). Mice and murine embryonic fibroblasts (MEFs) lacking ZDHCC1 were impaired in their ability to mount an innate immune response to DNA and succumbed to HSV-1 infection. While ZDHHC1 was found to augment poly(I:C) responses during overexpression experiments in HeLa cells, *Zdhhc1*^(-/-) mice and MEFs responded normally to infections with vesicular stomatitis virus and poly(I:C) stimulation (Zhou et al., 2014), suggesting that another a palmitoyl transferase may mediate the effects over RLRs as reported by (Mukai et al., 2016). The palmitoyl transferase activity of ZDHHC1 was considered not to be required for STING function as overexpression of a catalytically dead mutants of ZDHHC1 potentiated the activation of an IFN- β reporter during HSV-1 and SeV infection in HeLa cells (Zhou et al., 2014). However, whether ZDHHC1 palmitoylates STING has not been examined. Thus, further studies are needed.

1.6 STING-Dependent IFN Production

In recent years, several receptors have been proposed to detect cytoplasmic DNA and signal through STING (Reviewed by Unterholzner, 2013). However, of all receptors studied only cGAS has a well-defined mechanism of STING activation thus the role of other receptors is contentious (**Fig 1.5**).

1.6.1 cGAS and the Second Messenger cGAMP

The importance of cGAS to DNA sensing was demonstrated by the inability of cGAS^(-/-) cell lines and mice to produce IFN- β in response to DNA transfection, DNA vaccinations and infections with DNA and retroviruses (Gao et al., 2013a; Li et al., 2013b; Sun et al., 2013a). The crystal structure of cGAS revealed that cGAS possess a highly conserved Mab21 nucleotidyl transferase domain and possessed a similar overall structure to the cytosolic dsRNA sensor 2'-5' oligoadenylate synthetase (OAS1) (Civril et al., 2013). Unlike OAS1, cGAS possesses a zinc thumb that affords cGAS sequence-independent recognition of DNA. DNA binding of cGAS to its zinc thumb induced as a conformational change to the cGAS active site (Civril et al., 2013). Further structural studies of cGAS revealed the presence of an activation loop adjacent to the DNA binding zinc thumb (Zhang et al., 2014b). DNA binding is believed to create a steric clash with this activation loop inducing major “switch-like” conformational changes in the DNA binding region and active site of cGAS. Other structural studies have also suggested that cGAS could initially form 2:2 dimers upon binding DNA and may show a steric preference for binding the ends of DNA (Li et al., 2013a; Zhang et al., 2014b). Structural studies of cGAS:DNA complexes demonstrate that cGAS dimers assemble as ladder-like structures on U-turns and bends in DNA structure in the spaces induced by bacterial and mitochondrial nucleoid proteins; HU and mitochondrial transcription factor A, and high-mobility group box 1 protein (HMGB1) (Andreeva et al., 2017). The positively charged N-terminus of cGAS has been reported to undergo structural changes upon DNA binding which have been observed to increase cGAS activity and promote the formation of 1:1 DNA cGAS complexes following DNA binding (Lee et al., 2017; Tao et al., 2017). Recently, Luecke et al., (2017) have demonstrated that cGAS is capable of length-dependent DNA recognition. The authors of this study demonstrate using *in vitro* transcribed DNA oligomers that cGAS is sensitised to respond to DNA of <2000 base

pairs in length and that DNA of this length is immunestimulatory at concentrations low as 0.0167 μ g/ml.

cGAS DNA binding and activity are subject to regulation by a growing number of post-translational modifications. cGAS DNA binding and nucleotidyl-transferase activity is promoted by K27 ubiquitination on K173 and K384 mediated by RNF185 (Wang et al., 2017). Removal of K48 ubiquitin on K414 by Ubiquitin Specific Protease (USP)14 was identified as a stabilising modification by preventing p62 mediated autophagic turnover (Chen et al., 2016). Similarly, removal of SUMO from K335, 372 and 382 by sentrin/SUMO-specific protease 7 (SENP7), and polyglutamate on Q272 and monoglutamate on Q302 by the cytosolic carboxypeptidases (CCPs) CCP5 and CCP6, improved cGAS' DNA binding and nucleotidyl-transferase activity (Cui et al., 2017; Xia et al., 2016a) .

The discovery of the mammalian second messenger, cGAMP, afforded significant mechanistic insights into the recognition of intracellular DNA by the innate immune system. cGAMP is produced following DNA transfection and infection with viruses (Gao et al., 2013a; Wu et al., 2013b). cGAMP then directly binds to STING, inducing a conformational change in STING (Diner et al., 2013; Zhang et al., 2013), activating STING trafficking (Dobbs et al., 2015) and enabling the recruitment of TBK1 to STING for the activation of IRF3 (Liu et al., 2015a; Shu et al., 2013). cGAMP is likely to be important in priming immune responses in adjacent uninfected cells as it has been demonstrated to induce STING activation in bystander cells through gap junctions (Ablasser et al., 2013b), and is packaged into viral particles in cells with an active cGAS response (Bridgeman et al., 2015; Gentili et al., 2015).

cGAMP is understood to bind STING with a greater affinity than other cyclic dinucleotides, inducing a more significant conformational change in STING (Zhang et al., 2013). It is suggested that c-di-GMP is also capable of inducing a similar STING conformational change, albeit to a lesser extent than the change induced by cGAMP (Huang et al., 2012). This was later explained by (Zhang et al., 2013), who highlight that the crystal structures of c-di-GMP bound to STING used in the studies that do not report a conformational change (Ouyang et al., 2012; Shu et al., 2012), use a single nucleotide polymorphism of STING (STING R232H),

that has been observed to be less effective at binding to c-di-GMP and c-di-AMP (Yi et al., 2013).

Upon binding DNA, cGAS produces 2'-3' cGAMP from cytosolic molecules of ATP and GTP (Ablasser et al., 2013a; Sun et al., 2013a). This reaction is permitted by conformational changes upon DNA binding that allow ATP and GTP to enter the catalytic pocket (Gao et al., 2013b). Following the entry of ATP and GTP into the active site, cGAMP is proposed to be generated in a two-step process; GTP is first linearized to pppGp, which then attacks ATP to form a pppGpA(2'-5') reaction intermediate, this is then followed by the formation of the (3'5') adenosine-guanosine bond to form cGAMP (Ablasser et al., 2013a; Gao et al., 2013b). A distinct feature of cGAMP is its 2'-5' guanosine-adenosine bond which has been speculated to promote stability and efficient transduction as a second messenger as many nucleases are unable to hydrolyse such a linkage (Gao et al., 2013b).

Currently ectonucleotide pyrophosphatase/phosphodiesterase 1 (ENPP1) is the only known endogenous phosphodiesterase with the ability to hydrolyse cGAMP (Li, 2014). Snake venom phosphodiesterase from *Crotalus adamanteus* has been used to degrade cGAMP to confirm its identity by Liquid Chromatography-Mass spectrometry (Ablasser et al., 2013a). *Mycobacterium tuberculosis* evades the immune system by producing its own phosphodiesterase CdnP. Loss of CdnP from *M.tb.*, or ENPP1 from mice, was observed to attenuate *Mycobacterium tuberculosis* infection (Dey et al., 2017).

While cGAS has been predominately studied as a DNA sensor, a screen of the activity of IFN stimulated genes revealed that cGAS possesses additional undefined roles in the immune response against RNA viruses (Schoggins et al., 2014). Additionally *cGas*^(-/-) mice succumbed to lethal infection with West Nile Virus (WNV) and possessed higher viral titres than *cGas*^(+/+) mice, suggesting that cGAS may have a greater ligand specificity that previously anticipated (Schoggins et al., 2014). This hypothesis was verified with the discovery that cGAS can directly sense RNA:DNA hybrids (Mankan et al., 2014), however further studies are required to observe if this is a mechanism by which cGAS can detect RNA viruses. Alternatively, *cGas*^(-/-) mice may respond differently to RNA virus infection because

of altered RLR regulation as a result of differences in tonic signalling in the absence of low level IFN production by cGAS (Reviewed by Gough et al., 2002)

1.6.2 IFI16/p204

Interferon Gamma Inducible Protein 16 (IFI16) is a nuclear PYHIN protein composed of an N-terminal pyrin domain (PYD) and two C-terminal HIN domains. PYHIN proteins bind to DNA in a sequence independent manner via an electrostatic charge between the HIN domain and the DNA sugar-phosphate backbone (Jin et al., 2012). The PYD has been observed to mediate PYHIN oligomerisation in *in vitro* studies, which is believed to be a pre-requisite for subsequent signalling (Morrone et al., 2014).

In humans, the PYHIN protein family consists of five members; IFI16, Myeloid cell nuclear differentiation antigen (MNDAA), Pyrin and HIN domain family member 1 (PYHIN1/IFIX), AIM2, and the AIM2 regulator POP3 (Fernandes-Alnemri et al., 2009; Hornung et al., 2009; Khare et al., 2014). IFI16, MNDAA and PYHIN1/IFIX reside in the nucleus while AIM2 and POP3 reside in the cytosol. In mice, the PYHIN protein family is comprised of thirteen family members and AIM2 is the only obvious PYHIN orthologue present in both species (Cridland et al., 2012). p204 is believed to function as the murine orthologue of IFI16 as it also possesses two HIN domains and resides in the nucleus (Unterholzner et al., 2010).

IFI16 is capable of inducing IFN- β transcription via STING upon detecting intracellular DNA (Unterholzner et al., 2010). IFI16 was first identified as a DNA sensor through a mass spectrometry screen on cytosolic THP-1 proteins that bound to a biotinylated 70mer motif from the Vaccinia virus (VACV) genome (Unterholzner et al., 2010). IFI16's role as a DNA sensor was first confirmed using siRNA knockdown for IFI16 and p204, in DNA transfection experiments and HSV-1 infections in human and murine monocytes (Unterholzner et al., 2010) and has since been observed in dendritic cells (Kis-Toth et al., 2011), neutrophils (Tamassia, 2012), human foreskin fibroblasts (Orzalli et al., 2012), vascular endothelial cells (Iqbal et al., 2016) and human primary macrophages (Horan et al., 2013; Soby et al., 2012).

IFI16 is predominately nuclear at steady state. IFI16 has been observed to shuttle between the nucleus and cytoplasm in response to the presence of foreign DNA (Li et al., 2012a), and is capable of detecting foreign DNA in both locations (Horan et al., 2013; Li et al., 2012a; Orzalli et al., 2012; Unterholzner et al., 2010). Proteomic analysis of IFI16 revealed that the ability of IFI16 to shuttle between nucleus and cytoplasm, is regulated by acetylation of K99 and K128 within the multipartite nuclear localization signal by the p300 acyltransferase (Li et al., 2012a). (Ansari et al., 2015) demonstrated that acetylation of IFI16 by the p300 histone acetyltransferase increases following association with Kaposi Sarcoma-associated Herpesvirus (KSHV) and HSV-1 genomes using proximity ligation microscopy assays. Inhibition of IFI16 acetylation did not influence its ability to bind the genomes of either virus but impeded its cytoplasmic translocation. (Dutta et al., 2015) observe an interaction between Breast Cancer gene 1 (BRCA1) and IFI16 that increases during KSHV, HSV-1 and Epstein-Barr Virus (EBV) infection that promotes IFI16 acetylation. Vascular endothelial cells lacking BRCA1 displayed reduced IFI16 acetylation, reduced inflammasome activation and reduced activation of the STING pathway suggesting that BRCA1 enables IFI16 to function as a DNA sensor. (Iqbal et al., 2016) demonstrate that an association between Histone H2B in addition to BRCA1 promotes IFI16 function. Using the nuclear export inhibitor Leptomycin B, the authors demonstrate that Histone H2B-IFI16-BRCA1 complexes recognise viruses in the nucleus and translocate to the cytoplasm to activate the STING pathway. Histone H2B depletion by siRNA produced comparable decreases in IFN- β production to cGAS, IFI16 and STING depletion during HSV-1 and KSHV infections.

It is currently unknown how IFI16 recognises pathogen DNA as “foreign DNA” and why IFI16 does not recognise host DNA in the nucleus. *In vitro* experiments have revealed that IFI16 forms cooperative filaments along DNA and suggest that IFI16 may discriminate between self and non-self DNA using filament length (Morrone et al., 2014). Further structural studies highlight how the presence of nucleosomes hinder the assembly of IFI16 filaments, suggesting that chromatinization of host DNA is sufficient to prevent it from being recognised by IFI16 (Stratmann et al., 2015). This hypothesis is supported by an observation by (Orzalli et al., 2013), where IFI16 restricted expression of a large T antigen encoded on a plasmid containing the Simian vacuolating virus 40 but did not restrict T antigen expression from transfected chromatinized Simian vacuolating virus 40 DNA.

AIM2 is understood to form an inflammasome upon binding DNA in the cytoplasm (Fernandes-Alnemri et al., 2009; Hornung et al., 2009). Following oligomerisation, the PYD of AIM2 associates with the PYD of ASC, inducing ASC nucleation and resulting in the activation of Caspase-1 (Yin et al., 2011b). Conversely, IFI16 has only been shown to form a nuclear inflammasome during infection with particular viruses, namely Kaposi Sarcoma-associated Herpesvirus (KSHV) (Kerur et al., 2011; Singh et al., 2013), Epstein Barr virus (EBV) (Ansari et al., 2013) and HSV-1 (Johnson et al., 2013). IFI16 was found to induce cell death via pyroptosis in CD4+ T cells during Human Immunodeficiency Virus (HIV) infection and is speculated to be a major contributor to the progression of HIV-1 infection to Acquired Immunodeficiency Syndrome (AIDS) (Monroe et al., 2014).

The other PYHIN proteins Myeloid cell nuclear differentiation antigen (MNDA) and Pyrin and HIN domain family member 1 (PYHIN1/IFIX) have been shown to interact with proteins governing RNA processing and chromatin remodelling in a functional interactome composed by (Diner et al., 2015). IFIX was also shown to have functions as a STING-dependent DNA sensor in this study during overexpression experiments in HEK293Ts (Diner et al., 2015).

1.6.3 DDX41

DExD/H box helicases (DDX) are a family of nucleic acid binding proteins; which include the RLRs (Reviewed by Loo and Gale, 2011). DDX41 was first identified as a DNA sensor through an RNAi screen of 59 DExD/H box helicases (Zhang et al., 2011b). DDX41 knockdown experiments in murine immortalised dendritic cells, bone marrow derived dendritic cells and human monocytic THP1 cell lines revealed a reduction in IFN- β transcription. DDX41 was later found to be able to bind the bacterial cyclic dinucleotides c-di-AMP and c-di-GMP also using its DEAD/c domain (Parvatiyar et al., 2012). DDX41 has been proposed to work upstream of STING and enhance STING recognition of cyclic dinucleotides (Parvatiyar et al., 2012), as siRNA against STING and DDX41 was found to reduce IFN- β transcription during *L.monocytogenes* infection and upon c-di-AMP and c-di-GMP stimulations. It is presently unknown if DDX41 can recognise the novel second messenger and mammalian cyclic dinucleotide, cGAMP (Wu et al., 2013b).

1.6.4 DAI

DNA-dependent activator of IFN-regulatory factors (DAI), also known as DLM-1/Z-DNA binding protein 1 (ZBP1), was the first receptor for cytosolic DNA to be identified (Takaoka et al., 2007). Experiments in murine L929 cells and murine embryonic fibroblasts (MEF) cells demonstrated that DAI is encoded by an IFN stimulated gene and co-localised with DNA upon transfection and associated with TBK1 and IRF3 to induce IFN β transcription. Further studies elucidated that DAI also interacted with receptor-interacting protein kinases (RIP)1 and RIP3 to activate the NF κ B pathway and suggested that DAI, like STING, also undergoes dimerisation and is regulated by TBK1 phosphorylation upon activation (Kaiser et al., 2008; Rebsamen, 2009; Wang et al., 2008). However, the generation of DAI^(-/-) mice and human cell lines revealed that DAI is redundant for DNA sensing as these mice and cell lines lacking DAI displayed normal responses to DNA stimulation and DNA based vaccinations (Ishii et al., 2008; Lippmann, 2008). DAI was shown to be linked to virus-induced necrosis in a study using mCMV infection (Upton et al., 2012). Recently, another study focusing on DAI necroptosis by (Maelfait et al., 2017) demonstrated that the DAI Z DNA binding domain induced necrosis through recognising Z-RNA. DAI-mediated necrosis was reduced when transcription was ablated as seen with infections with inactivated mCMV virus and reduced necrosis upon treatment with transcription blocker actinomycin D. Inhibition of DNA polymerases did not alter necrosis, while RNA labelling experiments demonstrated that DAI bound newly synthesised endogenous RNAs (Maelfait et al., 2017; Sridharan et al., 2017).

1.6.5 DNA-PK

DNA damage from environmental stress and DNA damaging chemotherapy drugs results in the production of IFN- β (Ahn et al., 2014; Kim et al., 1999; Kim et al., 2000). Many DNA viruses in turn have been observed to induce and manipulate the DNA damage response to aid their replication suggesting that these pathways may overlap and many receptors for DNA damage could also function as DNA sensing PRRs (Reviewed by Turnell and Grand, 2012). While the DNA binding catalytic subunits of the DNA-dependent protein kinase (DNA-PKcs), Ku70/80 and the DNA damage protein kinase Ataxia telangiectasia (ATM) were

found to be dispensable for IFN- β induction in murine bone marrow derived macrophages (BMDMs) by (Stetson and Medzhitov, 2006a), evidence has emerged to suggest that DNA-PKcs and ATM may contribute to DNA sensing in other cell types.

DNA-PKcs orchestrates the repair of double strand breaks through the process of non-homologous end joining. The Ku subunits of DNA PKcs bind to the double stranded break, stabilising the interactions between DNA-PKcs and its substrate. DNA-PKcs then recruits the DNA ligase IV-XRCC4 to repair the broken DNA ends. Ku70 has been implicated in the production of IFN- λ after immune stimulatory DNA (ISD) stimulation with in HEK293 cells (Zhang et al., 2011a) and both Ku70 and Ku80 have been shown to be required for IFN- β responses to transfected DNA in murine and human fibroblasts (Ferguson et al., 2012). An *in vivo* requirement for DNA-PKcs and its Ku subunits was demonstrated during HSV-1 and Modified Vaccinia Ankara (MVA) infections in mouse embryonic fibroblasts and in mouse intradermal infection models (Ferguson et al., 2012). Finally, using an inducible expression system in HEK293T cells DNA-PKcs was demonstrated to detect DNA in a STING dependent manner (Ferguson et al., 2012).

1.6.6 Mre11

Meiotic recombination factor 11 (Mre11) is recruited to double strand breaks following activation of ATM, along with Nibrin/NSB1 and RAD50 (collectively known as the MRN complex) (Reviewed by Lavin et al., 2015). Recently, Mre11 has been demonstrated to bind and mediate responses to transfected ISD in bone marrow derived dendritic cells (Kondo et al., 2013). Treatment of these cells with the Mre11 inhibitor Mirin also decreased IFN β transcription upon transfection with ISD. Further experiments in an Mre11^(-/-) cell line also revealed that Mre11 mediated IFN production was ablated with STING siRNA knockdown and that the other components of the MRN complex were not required for Mre11's functions as a DNA sensor. Curiously, Mre11 knockdown did not impair IFN β production during *Listeria monocytogenes* infection suggesting that Mre11 may only function as a DNA sensor in cases of sterile inflammation.

1.6.7 LSm14A

LSm14A (also known as RNA Associated Protein 55 (RAP55)) is a constituent of RNA processing bodies (P bodies), which are sites of cytoplasmic mRNA degradation. An investigation by (Li et al., 2012b) revealed that LSm14A was capable of detecting nucleic acids in a manner that was dependent on MAVS, RIG-I and STING suggesting that LSm14A could potentially sample nucleic acids in P bodies and deliver them to nucleic acid sensing PRRs during infections.

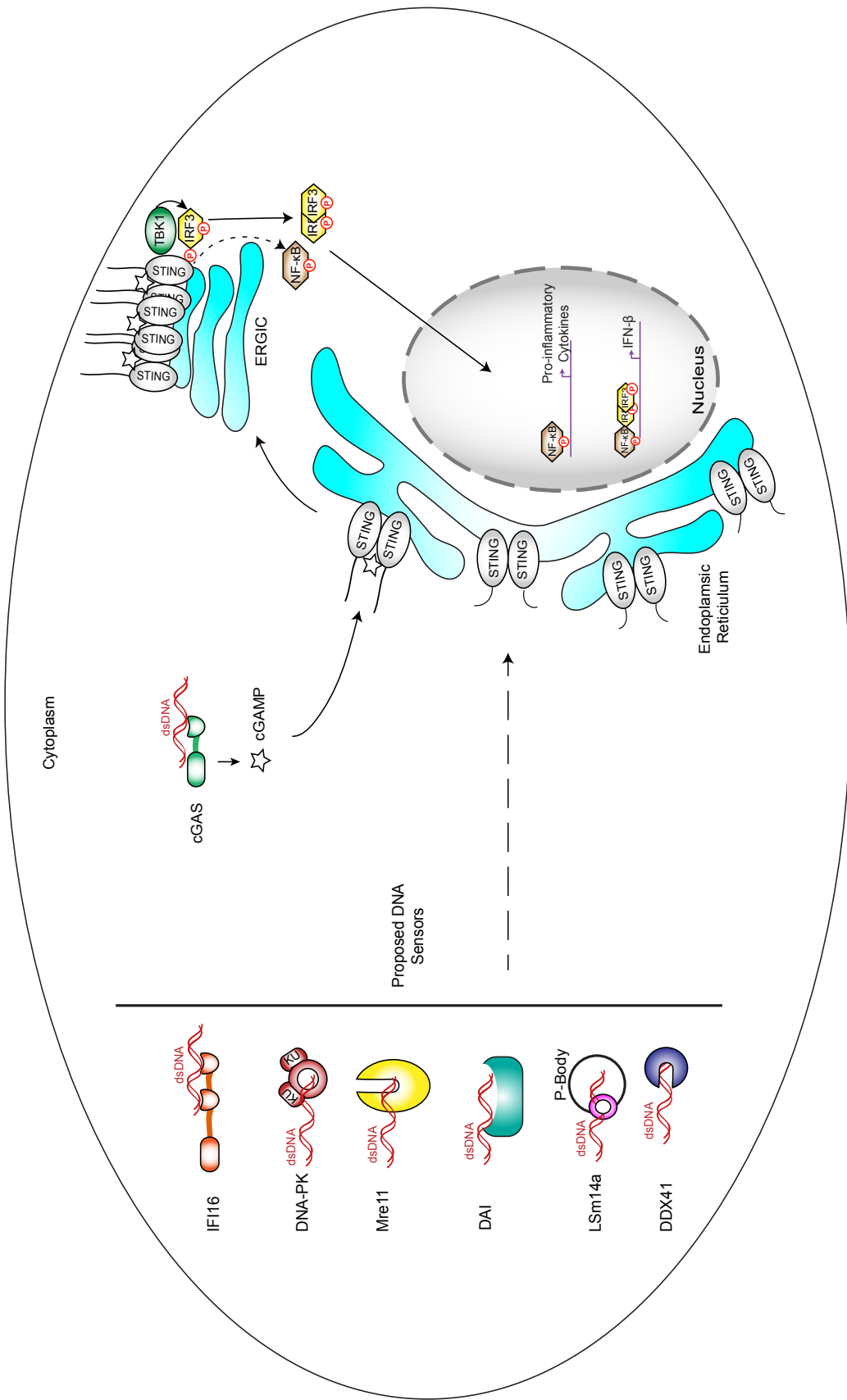


Fig 1.6 Proposed DNA sensors and cGAS-STING Signalling

Upon binding DNA, cGAS produces the second messenger cGAMP. cGAMP binds to STING, inducing a STING conformational change. STING then trafficks to the ERGIC where it recruits TBK1. TBK1 phosphorylates STING, enabling the recruitment of IRF3. TBK1 then phosphorylates IRF3 enabling its activation and IFN- β transcription. NF- κ B is also activated by STING but the precise mechanism remains elusive. Several other receptors have been proposed to induce IFN- β transcription via STING. However their precise contributions have been obscured by the discovery that cGAS(-/-) mice and cells are unable to respond to DNA.

1.7 STING-Independent Mechanisms of DNA-induced IFN Production

While many DNA sensors have been proposed to signal in a STING-dependent manner, several receptors have been observed to induce IFN production in a STING-independent manner after detection of intracellular DNA.

1.7.1 RNA polymerase III

RNA polymerase III is responsible for the synthesis of a range small RNA molecules such as 5S ribosomal RNA, transfer RNAs, non-coding and micro-RNAs, and RNA molecules that function in RNA splicing and quality control (e.g. the spliceosome component U6 and RNaseP), in all eukaryotic cells (Reviewed by White, 2011). Investigations by (Ablasser et al., 2009; Chiu et al., 2009) revealed that RNA Pol III could also function as a DNA sensor for the synthetic DNA mimic, Poly(dA:dT). RNA pol III was found to transcribe Poly(dA:dT) into dsRNA which in turn induced IFN- β transcription via the RIG-I pathway. This method of DNA sensing is seemingly unique to Poly(dA:dT) as other forms of DNA do not induce dsRNA production (Ablasser et al., 2009; Unterholzner et al., 2010). Additionally, HEK293 cells which possess the RNA pol III and RIG-I pathways are unable to respond to DNA of microbial or mammalian origin (Unterholzner et al., 2010). Because these observations suggest that RNA Pol III may only recognise Poly(dA:dT) rich DNA it has been difficult to verify if RNA Pol III plays an active role in infections with pathogens. The best-characterised examples of Pol III activity during infection are found within studies using EBV. However in these studies, the virus has been found to use RNA Pol III to encode Epstein Barr virus small RNAs, which are then recognised by the RIG-I pathway and not function as a DNA sensor (Ablasser et al., 2009; Chiu et al., 2009; Samanta et al., 2006)

1.7.2 LRRFIP1

Leucine rich repeat (in FLII) interacting protein 1 (LRRFIP1) is a cytosolic nucleic acid binding protein that has been observed to bind RNA during vesicular stomatitis virus infections and DNA from *Listeria monocytogenes* infections in macrophages (Yang et al., 2010). Unlike STING-dependent DNA sensors, LRRFIP1 promotes IFN- β transcription through a unique pathway by binding to the transcriptional co-activator β -catenin. β -catenin

then binds to the C-terminus of IRF3 and recruits the acetyltransferase p300 to the IFN- β promoter to promote assembly of the IFN- β enhanceosome (Yang et al., 2010).

1.7.3 HMGB1

High mobility group box (HMBG) proteins are strongly expressed in the nucleus where they are believed to regulate chromatin structure and transcription. HMGB1 is a ubiquitously expressed protein that has previously been implicated in DAMP associated activation of Toll-like receptor pathways (Tian, 2007). In addition to Toll-like receptors, HMGB1 has been observed to bind nucleic acids and potentiate activation of RIG-I and intracellular DNA sensing pathways (Yanai et al., 2009). The precise mechanism by which HMGB1 improves the efficiency of nucleic acid recognition by these PRRs is presently unknown.

1.8 Which Receptors are Required for the STING-mediated IFN response?

One striking feature of the innate immune response to DNA is the number of receptors proposed to signal through STING. (**Table 1.3**) details studies where a STING-dependent receptor has been implicated in the immune response to a pathogen. These studies typically describe the role of a proposed DNA sensor using siRNA depletion complemented with overexpression experiments in HEK293T cells. The discovery that cGAS^(-/-) cells and mice are unable to respond to DNA transfection and viral infection has questioned the validity of the other proposed DNA sensors (Gao et al., 2013a; Li et al., 2013b). Further knockout studies will be required to conclusively confirm the precise contribution of other receptors, and to determine if there is redundancy or co-operation with cGAS, or cell type specificities.

1.9 What defines a DNA sensor?

When discussing the candidacy of the putative DNA sensors it is necessary to develop an operational definition of what defines a DNA sensor. Using the features of the verified DNA sensors AIM2 (Bürckstümmer et al., 2009; Fernandes-Alnemri et al., 2009; Hornung et al., 2009), TLR 9 (Bauer et al., 2001; Hemmi et al., 2000) and cGAS (Sun et al., 2013a) as examples, a DNA sensor should possess the following features;

Pathogen	Species	DNA Receptor	Cell Type/Infection Model	Reference
DNA Virus	Herpes Simplex Virus 1	IFI16	THP1 cells, peripheral blood mononuclear cells, human foreskin fibroblasts, U2OS cells, RAW264.7 cells	(Horan et al., 2013; Johnson et al., 2013; Orzalli et al., 2012; Unterholzner et al., 2010)
		cGAS	THP1 cells, cGAS ^(-/-) murine embryonic fibroblasts, cGAS ^(-/-) bone marrow derived-macrophages, cGAS ^(-/-) dendritic cells, murine embryonic fibroblasts, microglia	(Gao et al., 2013a; Li et al., 2013b; Reinert et al., 2017; West et al., 2015)
		DAI	L929 cells	(Takaoka et al., 2007)
		DDX41	murine dendritic cells	(Zhang et al., 2011b)
		DNA-PK	murine embryonic fibroblasts	(Ferguson et al., 2012)
		LSm14a	THP1 Ccells	(Li et al., 2012b)
	Cytomegalovirus	IFI16	human embryonic lung fibroblasts, human foreskin fibroblasts	(Dell'Oste et al., 2014; Diner et al., 2016; Gariano et al., 2012)
		cGAS	murine plasmacytoid dendritic cells, monocyte derived DCs and macrophages, human foreskin fibroblasts, primary human endothelial cells	(Bridgeman et al., 2015; Diner et al., 2016; Lio et al., 2016; Paijo et al., 2016)

DNA Virus	Kaposi-Sarcoma Herpes virus	IFI16	human dermal microvascular endothelial cells	(Iqbal et al., 2016; Kerur et al., 2011; Roy et al., 2016; Singh et al., 2013)
	Epstein-Barr Virus	IFI16	primary human B cells, lymphoblastoid Cell lines	(Ansari et al., 2013)
	Vaccinia Ankara Virus	cGAS	dendritic cells, murine cancer models	(Dai et al., 2014; Dai et al., 2017; Lin et al., 1998)
		DNA-PK	murine embryonic fibroblasts	(Ferguson et al., 2012)(Peters et al., 2013)
	Adenovirus	cGAS	RAW 264.7 cells, murine MS1 endothelial cells	(Lam et al., 2014)
		DDX41	murine dendritic cells	(Zhang et al., 2011b)
	Human Papillomavirus 16	IFI16	HPV-induced tumour biopsy	(Reinholz et al., 2013)
Retrovirus	Endogenous Retroviruses	cGAS	TREX ^(-/-) murine embryonic fibroblasts, TREX ^(-/-) bone marrow derived macrophages	(Ablasser et al., 2014)
	Human Immunodeficiency Virus	IFI16	THP1 cell lines, HIV+ patient peripheral blood mononuclear cells, primary CD4+ T cells	(Berg et al., 2014; Jakobsen et al., 2013; Monroe et al., 2014; Nissen et al., 2014)
		cGAS	THP1 cell lines, L929 cell lines, HIV+ patient peripheral blood mononuclear cells, dendritic cells.	(Gao et al., 2013a; Lahaye et al., 2013b; Nissen et al., 2014)

RNA Viruses	West Nile Virus	cGAS	cGAS ^(-/-) mice succumb to infection	(Schoggins et al., 2014)
	Dengue Virus	cGAS	cGAS detects mitochondrial DNA leakage during dengue infection in THP1s and A549s	(Aguirre et al., 2017; Sun et al., 2017)
Intracellular Bacteria	<i>Listeria monocytogenes</i>	cGAS	bone marrow derived macrophages, THP1 cells, human primary monocyte derived macrophages, U937 Cells	(Hansen et al., 2014)
		IFI16		
		DDX41	murine dendritic cells, bone marrow derived macrophages	(Parvatiyar et al., 2012; Zhang et al., 2011b)
	<i>Chlamydia trachomatis</i>	cGAS	murine embryonic fibroblasts	(Zhang, 2014)
	<i>Francisella novicida</i>	cGAS	cGAS ^(-/-) and p204 ^(-/-) RAW264.7 cells	(Storek et al., 2015)
		IFI16(p204)		
	<i>Mycobacterium tuberculosis</i>	STING-Dependent IFN (ci-di-AMP)	STING ^(-/-) RAW 264.7 Cells	(Dey et al., 2015)
		cGAS	cGAS ^(-/-) THP1, bone marrow derived macrophages	(Collins et al., 2015; Majlessi and Brosch, 2015; McNab et al., 2015)
<i>Streptococcus pneumoniae</i>	DAI	DAI ^(-/-) mice	(Parker et al., 2011)	

	<i>Streptococcus pneumoniae</i>	STING-Dependent IFN (Unknown DNA Receptor)	murine alveolar macrophages, bone marrow derived macrophages, alveolar epithelial cells, Sting ^(-/-) Mice	(Koppe et al., 2012; Parker et al., 2011)
Extracellular Bacteria	<i>Neisseria gonorrhoeae</i> (Following internalisation)	cGAS	cGAS ^(-/-) THP1s and bone marrow derived macrophages	(Andrade et al., 2016)
Protozoan Parasites	<i>Plasmodium yoelii</i>	cGAS	plasmatioid dendritic cells	(Yu et al., 2016)
	<i>Plasmodium falciparum</i>	STING-dependent IFN response (Unknown Receptor)	STING ^(-/-) bone marrow derived macrophages	(Sharma et al., 2011)

Table 1.3 Incidences where proposed STING-Dependent Receptors have been implicated to immunity to pathogen DNA

1) Sequence-independent recognition of DNA:

A candidate DNA sensor should be able to recognise non-self DNA irrespective of its origin. Additionally, a potential DNA sensor should be capable of recognising DNA independent of a particular sequence or circumstantial structural motifs such as double stranded breaks. cGAS and AIM2 achieve sequence independent recognition by binding the sugar phosphate backbone of DNA, enabling them to recognise DNA from a range of sources (Civril et al., 2013; Jin et al., 2012). TLR 9 also utilises the sugar phosphate backbone for its DNA recognition capabilities (Ohto et al., 2015). Although TLR 9 activation is potentiated by CpG motifs in pathogen DNA, there is a substantial body of evidence to suggest TLR 9 binds indiscriminately to a broad range of DNAs (Reviewed by Lamphier et al., 2006).

2) Bind DNA and Induce transcription of an Immune Response via Signalling Cascades:

A candidate DNA sensor should indirectly mediate the induction of an immune response following DNA binding. cGAS induces activation of the STING pathway through production of cGAMP (Sun et al., 2013a; Wu et al., 2013b), AIM2 forms an inflammasome complex to induce IL-1 β and IL-18 activation following DNA binding (Bürckstümmer et al., 2009; Fernandes-Alnemri et al., 2009; Hornung et al., 2009), while TLR 9 signals via MyD88 to induce transcription of IFN and pro-inflammatory genes (Bauer et al., 2001; Hemmi et al., 2000). This is an important operational caveat in defining a putative DNA sensor as it is necessary to distinguish between potential DNA sensing PRRs and transcription factors that directly bind DNA and induce activation of immune genes such as IRF3 (Lin et al., 1998; Schafer et al., 1998)

3) Validation by a Knockout Study

The function of a putative DNA sensor must be determined by a knockout study to conclusively confirm its contribution to immunity. *cGAS*^(-/-) mice are unable to respond to DNA transfection or infection with DNA viruses or retroviruses (Li et al., 2013b). Similarly, *aim2*^(-/-) mice are vulnerable to infection with intracellular bacteria and DNA viruses (Rathinam et al., 2010) and plasmacytoid dendritic cells from *tlr9*^(-/-) mice are impaired in their responses to HSV-2 infection (Lund et al., 2003).

1.10 IFI16's Candidacy as a DNA sensor; Perspectives from Virus-Host Interactions

IFI16 is one of more widely studied proposed DNA sensors and has been implicated in the immune response to an array of intracellular pathogens in a variety of cell types (**Table 1.3**). Further evidence of the importance of IFI16 to DNA sensing can be observed from a perspective of virus-host interactions. Viruses typically subvert the immune response by disabling essential components of immune signalling pathways to enable their continued replication (Reviewed by Bowie and Unterholzner, 2008; Chan and Gack, 2016b). Viruses have been previously used to identify essential components of innate immune signalling and anti-viral immunity such as PKR (Davies et al., 1993), 14-3-3 ϵ (Chan and Gack, 2016a) and IRAK2 (Keating et al., 2007). cGAS is also inhibited during KSHV and HIV-1 infections (Lahaye et al., 2013a; Li et al., 2016).

The importance of IFI16 to *Herpesviridae* immunity is emphasised by the diversity of ways this family can interact with IFI16 function. For example, IFI16 is antagonised and degraded by the HSV-1 proteins ICP0 and UL46 (Deschamps and Kalamvoki, 2017; Orzalli et al., 2012) and by hCMV protein pUL83 (Biolatti et al., 2016). IFI16 is packaged into HCMV virions and exported from the infected cell to prevent it detecting viral DNA (Biolatti et al., 2016; Dell'Oste et al., 2014). During latent KSHV infections, IFI16 inflammasomes are exported from infected endothelial cells in exosomes in what has been speculated to be a form of viral immune evasion (Singh et al., 2013). IFI16 degradation is also required for lytic reactivation of KSHV (Roy et al., 2016). Additionally, IFI16 also functions as a transcriptional repressor for HSV-1, HPV-18 and hCMV during infection (Gariano et al., 2012; Johnson et al., 2014; Lo Cigno et al., 2015).

To conclusively assess the function of IFI16, our lab has used transcription activator-like effector nucleases (TALENs) to generate an immortalised human keratinocyte cell line lacking IFI16. This cell line is a valuable tool, as it will allow us to examine the role of IFI16 in DNA sensing in human cells. Keratinocytes constitute the outermost layer of skin and are frequently the initial point of contact for pathogens. Additionally, keratinocytes are the natural host for many DNA viruses such as HSV. As DNA sensing has been predominately studied in monocytes, using viruses that initially infect keratinocytes, we wished to study the

contribution of these receptors to innate immunity in skin cells. We propose that our observations in this model system can be extrapolated to the initial key events that shape the innate and adaptive immune responses to viral infections.

1.11 Aims and Objectives of Investigation

The principle aim of this investigation was to establish what function IFI16 has in the recognition of intracellular DNA. This was addressed through answering the following questions:

1. *Are HaCaT keratinocytes able to sense foreign DNA?*

Keratinocytes constitute a physical barrier between host and environment, and as such are the first point of contact for many pathogens and environmental insults. We aimed to investigate if human immortalised keratinocytes (HaCaTs) expressed components of a functional DNA sensing pathway and could mount an anti-viral innate immune response to foreign DNA.

2. *Is the DNA sensor IFI16 essential for the interferon response to DNA?*

As several DNA sensors have been implicated in the innate immune response to DNA, the contribution of IFI16 to intracellular DNA sensing is at present unclear. To conclusively determine the function of IFI16, our lab has used TALENs to generate IFI16 knockout HaCaT cells. We will determine if IFI16 is required for DNA sensing by assessing the ability of the IFI16 knockout HaCaT cell line to respond to DNA.

3. *Does IFI16 affect the cGAS-cGAMP-STING pathway of DNA sensing?*

How IFI16 interacts with the cGAS-STING pathway will be investigated in two phases:

I. Does IFI16 influence the activity of cGAS and facilitate the production of cGAMP?

cGAS has not been studied in the context of another DNA sensor since its discovery. We will assess whether cGAS and IFI16 cooperate to sense pathogen DNA through examining whether IFI16 and cGAS form a complex during DNA sensing and by developing a quantitative Liquid

Chromatography–Mass Spectrometry method to measure cGAMP production to infer if IFI16 influences cGAS activity.

II. Does IFI16 influence the ability of STING to recognise cGAMP?

If cGAS functions are not influenced by IFI16, we will examine whether IFI16 influences STING function. This will be addressed by examining if IFI16 and STING form a complex upon DNA stimulation and monitoring if cGAMP-induced STING signalling or STING post-translational modifications are altered in the absence of IFI16.

Chapter Two

Methods and Materials

2.1 Materials

General lab chemicals were purchased from Sigma Aldrich or VWR chemicals unless otherwise stated. All solutions were prepared using de-ionised water from a Milli-Q system (Millipore).

2.2 Solutions

SDS-PAGE and Western Blot Buffers

10X Running Buffer:	0.25M Tris-Cl, 1.92M Glycine, 1%(w/v) sodium dodecyl sulfate (SDS)
10X Transfer Buffer:	0.25M Tris-Cl, 1.92M Glycine
1X Transfer Buffer:	100 mL 10x Transfer Buffer, 200 mL Methanol, made up to 1L with deionized water (dH ₂ O).
1.5M Tris (pH 8.8):	0.75M Tris-Cl dissolved in 420mL dH ₂ O. Adjust to pH 8.8 using Sodium Hydroxide (NaOH) + Hydrochloric acid (HCl). Bring to 500 mL using dH ₂ O
0.5M Tris (pH 6.8):	0.25M Tris-Cl, dissolved in 420mL dH ₂ O. Adjust to pH 6.8 using NaOH+HCl Bring to 500 mL using dH ₂ O
3x Sample Buffer:	62.5mM Tris-Cl pH 6.8, 10%(v/v) Glycerol, 2%(w/v) SDS, 0.1%(w/v) Bromophenol blue, <i>Add 150µL 1M Dithiothreitol(DTT) per 1 mL of 3xSample Buffer before use.</i>
2x Native Gel Sample Buffer:	125mM Tris-Cl pH6.8, 30%(v/v) Glycerol, 0.2%(v/v) Bromophenol Blue

Native Gel

Running Buffer: 1x Transfer buffer without methanol.

10xPhosphate Buffered

Saline (PBS): 1.37M Sodium Chloride (NaCl), 100mM Sodium phosphate (NaH₂PO₄), 18mM Dipotassium phosphate (K₂HPO₄), 27mM Potassium Chloride (KCl).

PBS/Tween: 0.1%(v/v) Tween per Litre of 1xPBS.

10xTris-Buffered

Saline (TBS): 200mM Tris-HCl, 1.5M NaCl.

TBS/Tween: 0.1%(v/v) Tween per Litre of 1xTBS.

Cell Lysis Buffers

Note: All lysis buffers require the addition of 10µL/mL protease inhibitors; 0.7mM Aprotinin, 1mM phenylmethane sulfonyl fluoride (PMSF) and 1 mM sodium orthovanadate (Na₃VO₄) prior to use.

Cell Lysis Buffer: 50mM Tris-HCl pH 7.4, 150mM NaCl, 30mM Sodium Fluoride (NaF), 5mM Ethylenediaminetetraacetic acid (EDTA), 40mM Beta-glycerophosphate, 10%(v/v) Glycerol, 1%(v/v) Triton X-100

Thermo IP Lysis Buffer: 25mM Tris-HCl pH 7.4, 150mM NaCl, 1mM EDTA, 50mM NaF, 5%(v/v) Glycerol, 1%(v/v) nonyl phenoxyethoxyethanol (NP-40)

2xPalmitoylation Lysis

Buffer: 200mM Tris-HCl pH 7.2, 300mM NaCl, 10mM EDTA, 2.5%(w/v) SDS.

Palmitoylation Wash

Buffer: 1x Palmitoylation Lysis Buffer with 6M Urea.

Bacterial Growth Media

Note: Must be at pH 7.0 to facilitate bacterial growth

Super Optimal Broth w/ Catabolite Repression

(SOC Media): 10mM NaCl, 2.5 mM KCl, 10mM MgCl₂, 20mM Glucose,
2% (w/v) Tryptone, 0.5%(w/v) yeast extract.

Lysogeny broth (LB): 170mM NaCl, 1%(w/v) Tryptone, 0.5%(w/v) yeast extract

Add 15g/L of agar to LB broth to produce agar plates upon cooling. Ampicillin resistance requires a final concentration of 100µg/mL of antibiotic. Kanamycin resistance requires a final concentration of 50µg/mL antibiotic.

DNA/Agarose Gel Reagents

50xTris-acetate-EDTA

(TAE) Buffer: 2M Tris-Cl, 5.7%(v/v) Gacial Acetic Acid,
50mM EDTA pH 8.0

6xDNA Loading Dye: 30%(v/v) Glycerol, 0.025%(w/v) Bromophenol Blue,
0.025%(w/v) Xylene Cyanol

Enzyme Reaction Buffers

Note: All enzyme reaction buffers described in this subsection are at a concentration of 1x

Benzonase: 50mM Tris-HCl, pH 8.0, 2mM MgCl₂, 150mM NaCl

λ Phosphatase: 50mM 4-(2-hydroxyethyl)-1-piperazineethanesulfonic acid (HEPES) pH 7.5, 100mM NaCl, 2mM DTT, 0.01% Brij-35

Snake Venom

Phosphodiesterase: 50mM Tris-Cl pH 8.8, 10mM Magnesium Chloride (MgCl₂)

cGAMP Infusion

cGAMP Infusion Buffer: 50mM HEPES pH 7.0, 100mM KCl, 3mM MgCl₂, 0.1mM DTT, 85mM Sucrose, 0.2%(w/v) Bovine Serum Albumin, 1mM Adenosine triphosphate (ATP), 1mM Guanosine triphosphate (GTP), 5 mg/ml Digitonin

Real Time PCR Solutions

10xDNAse I Buffer: 100mM Tris-HCl pH 7.5, 25mM MgCl₂, 1mM Calcium Chloride (CaCl₂)

cGAMP Extraction Reagents

Reagents used to extract cGAMP for quantitative analysis were prepared as (v/v)% solutions using HiPerSolv H₂O. The following solutions were prepared during the optimization of the protocol detailed further in chapter 3.2:

Protocol Stage	Reagent
Cell Lysis	70% Ethanol, 80% Methanol
Liquid-Liquid Extraction	9% Butanol, 90% Butanol
Solid Phase Extraction	25%-45% Acetyl-Nitrate (C ₂ H ₃ NO ₄) (Increasing gradient with 5% intervals)
	100-700mM Ammonium Acetate (NH ₄ CH ₃ CO ₂) (Increasing gradient with 100mM intervals)
	80% Methanol+4-12% Ammonium Hydroxide (NH ₄ OH) (Increasing gradient with 4% intervals)

Table 2.1: Reagents used in developing a method to extract and quantify cGAMP (v/v)%

2.3 Antibodies:

Primary Antibodies:

Anti-	Supplier	Isotype	Cat. Number	Used at
Beta Actin	Sigma Aldrich	Mouse	A2228	1:10,000
Cas9	Sigma Aldrich	Mouse	SAB4200701	1:1,000
cGAS(MB21D1)	Sigma Aldrich	Rabbit	HPA031700	1:1,000
FLAG Tag	Sigma Aldrich	Mouse	F3165	1:3,000
HA Tag	Cell Signalling Technology	Mouse	2367	1:1,000
IFI16 (C-Terminus)	Santa-Cruz Biotech	Goat	SC-6050	1:1,000
IFI16 (N-Terminus)	Santa-Cruz Biotech	Mouse	SC-8023	1:1,000
IRF3	Cell Signalling Technology	Rabbit	11904	1:1,000
IRF3(Ser396)	Cell Signalling Technology	Rabbit	4847	1:1,000
STING	Cell Signalling Technology	Rabbit	13647	1:1,000
STING(Ser 396)	Cell Signalling Technology	Rabbit	85735	1:1,000
TBK1	Santa-Cruz Biotech	Mouse	SC-398366	1:500
TBK1(Ser 172)	Cell Signalling Technology	Rabbit	5483	1:1,000

Table 2.2: Primary Antibodies and supplier information

Secondary Antibodies:

Anti-	Supplier	Isotype	Cat. Number	Used at
Mouse HRP	Cell Signalling Technology	Mouse	7076	1:3,000
Rabbit HRP	Cell Signalling Technology	Rabbit	7074	1:3,000

Table 2.3 Secondary Antibodies and supplier information

Secondary Antibodies used in Immunofluorescence:

Anti-	Supplier	Isotype	Cat. Number	Used at
Mouse Alexa 647	Life Technologies	Goat	A21236	1:1,500
Rabbit Alexa 488	Life Technologies	Goat	A11034	1:1,500

Table 2.4: Immunofluorescence Secondary Antibodies and supplier information

2.4 Methods:

2.4.1 Cell Culture

Human Immortalised Keratinocyte (HaCaT) and Human Embryonic Kidney (HEK293T) cell lines were maintained in Dulbecco's Modified Eagle's medium (Life Technologies) containing 10% (v/v) Foetal Calf Serum (FCS) and 10 µg/ml Gentamicin. Cells were housed in an incubator at 37°C with 5% CO₂. Adherent cells were split every 2/3 days upon reaching confluence using TrypLE express (Life Technologies) to remove cells from cell culture plastics. Prior to treatment with TrypLE express, cells were twice rinsed in Dulbecco's Phosphate-Buffered Saline (Life Technologies) to remove residual FCS. Cell number per mL was determined using a Bright-Line™ Hemacytometer (Life Technologies). Cell culture plastics were purchased from Greiner Bio-one Inc.

2.4.1.1 Generation of IFI16 Knockout Cell Lines

IFI16 knockout cell lines (*IFI16*^(-/-)) were generated by Leonie Unterholzner using TALEN technology. Left and right TALENs were transfected into HaCaT cell lines by electroporation using the Neon system (Life Technologies). Electroporated cells were allowed to recover overnight before selection for 48 hours in complete DMEM containing 5 µg/ml puromycin. Selected cells were then seeded as single cell clones in 96 well plates. DNA was extracted from individual colonies using Quickextract DNA extraction solution (EpiBio). Modifications of the TALEN target site; *IFI16* exon 5, were screened by PCR using high resolution melting analysis on a LifeCycler 96 system (Roche), using LightCycler480 High Resolution Melting master mix (Roche). Potential *IFI16*^(-/-) candidates were screened for lack of protein expression by western blotting for IFI16 and β-actin. Immunofluorescence analysis was used confirm homogeneity of cell clones.

2.4.2 Nucleic Acid Transfection Conditions

HaCaT cells were seeded at a density of 1.75x10⁵ cells/mL, 16 hours before transfection. HaCaT were transfected with Lipofectamine2000 (1µL/mL;Invitrogen). Polyinosinic–polycytidylic acid (Poly(I:C)), (2',5') cyclic guanosine monophosphate–adenosine monophosphate (cGAMP) and Herring-Testis(HT) DNA were purchased from Sigma. Vaccina Virus (VACV) 70mer, G3 and C3-YDNAs, and their respective reverse

complements were synthesised by Biofins Genomics, Germany. DNA oligomer sequences are detailed in Table 2.6. DNA oligomers were annealed by heating complementary strands at 99°C for 10 mins. Annealed oligomers were allowed to cool to room temperature before storage at -20°C for later use. 5'-triphosphate RNA was generated using the MEGAScript T7 in-vitro transcription kit (Thermo Fisher) with pcDNA3.1: EGFP as template. Cell lines were transfected according to Lipofectamine2000 supplied protocol.

2.4.3 cGAMP Stimulation Conditions

For cGAMP stimulation, cells were incubated in cGAMP infusion buffer containing 15µM cGAMP for 10 minutes at 37°C. cGAMP infusion buffer was then removed and replaced with serum-containing medium without antibiotics for the remainder of the experiment.

Name	5'-3' Strand Sequence	3'-5' Strand Sequence
VACV 70mer	CCATCAGAAAGAGGTTTAATATTTTT GTGAGACCATCGAAGAGAGAAAGAG ATAAACTTTTTTACGACT	AGTCGTAAAAAAGTTTTATCTCTTTC TCTCTTCGATGGTCTCACAAAATAT TAAACCTCTTTCTGATGG
G3-Y DNA	GGGTATATATATATATATATATAGGG	GGGTATATATATATATATATATAGGG
C3-Y DNA	CCCTATATATATATATATATACCC	CCCTATATATATATATATATACCC

Table 2.5: Sequences of DNA Oligomers used to stimulate cell lines

2.4.4 Overexpression Transfection Conditions

HEK293T cells were seeded at a density of 1.75×10^5 cells/mL, 16 hours before transfection and were transfected with GeneJuice(Merck) in a ratio of 1µg Plasmid:3µL Genejuice as advised by the manufacturers protocol. Cells were left post Genejuice transfection for 18-24 hours to facilitate optimal protein expression.

2.4.4.1 Plasmids

Cultivation of Bacterial Strains:

NovaBlue competent bacteria cultures (Novagen) were transformed with 1 μ g of the desired plasmid. Transformed cultures were permitted one hour of growth in antibiotic free SOC media (Novagen) prior to antibiotic-selection on agar plates. Resistant bacterial colonies were grown in a starter culture of 3mL LB broth containing antibiotics for 8 hours to achieve log phase growth. 1 mL of this starter culture was then inoculated into 100mL of LB broth containing appropriate antibiotics, and left to grow overnight (16 hours). Bacteria was collected by centrifugation at 3000xg for 15 minutes. Plasmids were purified from transformed cultures using the Quagen Endofree Maxi-prep kit.

Plasmid Origins:

hSTING-FLAG was obtained from Lei Jin (Albany Medical College). pcDNA 3.1 cGAS was cloned by Jessica F. Almine (Leonie Unterholzner Group postdoc). pCMV-HA was obtained from Clontech and used as an empty vector control. pCMV-HA:IFI16 was cloned by Leonie Unterholzner. The IFI16 DNA binding mutant, pCMV-HA:IFI16-mt4 was received from T. Sam Xiao (National Institutes of Health, Bethesda, USA).

2.4.5 SDS-PAGE and Western Blotting

Cell lysates were diluted in 3x sample buffer, boiled for 5 minutes and resolved on 12% SDS-PAGE gels at 120V. Lysates were resolved alongside SeeBlue Plus2 Pre-stained protein marker (Life technologies) to determine protein size. Gels were transferred to a 0.2 μ m Immobilon™ polyvinylidene difluoride (PVDF) membrane using a semi-dry transfer system at 100mA/Gel for one hour and blocked for 45 minutes in 5%Marvel/PBS-Tween (or for phospho-blot 5%BSA/TBS-Tween) prior to the addition of primary antibody.

Primary antibodies were incubated with membranes overnight at 4°C at the concentrations outlined in Table 2.2. Primary antibody was removed from membranes with 5 washes of TBS-Tween at 10 minute intervals. Secondary antibodies were incubated with membranes for a further 90 minutes and removed with 3 washes of TBS-Tween at 10 minute intervals.

For visualisation, membranes were incubated in Clarity Western enhanced chemiluminescence (ECL) Substrate (Bio-rad) for 5 minutes, and visualised using X-Ray films.

2.4.5.1 Native-PAGE

Native-PAGE gels were pre-run for 30 minutes with 1x Native gel running buffer. This was followed by an additional 30-minute run with Native gel running buffer containing 1% sodium deoxycholate in the inner chamber. Cell lysates were diluted in 2x Native gel sample buffer and resolved for 90 minutes in fresh Native gel running buffer (with 1% deoxycholate in the inner chamber) and transferred as per SDS-gels.

2.4.6 Viral Infections

Cells were infected with viruses at the desired multiplicity of infection(MOI) in 100 μ L/mL of serum free medium for one hour. Virus containing serum free medium was then replaced with complete medium for the remainder of the experiment. MOI was determined using the following formula:

$$MOI = \left(\frac{\text{Plaque forming units of virus used for infection}}{\text{Total number of cells infected}} \right)$$

HSV-1 was used at an MOI of 5. Sendai virus containing defective viral particles was used at a dilution of (1:2,000). Viruses were UV-inactivated by placing the desired concentration of virus in serum free medium for the infection in a Spectrolinker XL-1000 UV Stratlinker at 10 μ J for 1 minute.

2.4.7 Cell Lysis

Cells were scraped from tissue culture plastics into chilled 1xPBS and collected by centrifugation at 4000xg for 10 minutes. PBS supernatants were removed and discarded. Cells were resuspended in lysis buffer and left on ice for one hour. Cell lysates were cleared of cell debris by centrifuging at 8000xg for 10 minutes. Cleared lysates were transferred to Eppendorf tubes and stored at -20°C until required.

2.4.8 Immunoprecipitations

Cells were lysed in the Thermo immunoprecipitation lysis buffer and precleared of debris by centrifuging at 6000xg for 10 minutes. Debris-cleared lysates were incubated with 20 μ L of Protein G beads for 30 minutes. Pre-cleared lysates were then incubated with protein G-antibody coupled overnight at 4°C. Antibody coupled beads were prepared at a ratio of 30 μ L beads to 1 μ L antibody. Immunoprecipitates were washed in lysis buffer three times prior to analysis by SDS-polyacrylamide gel electrophoresis (SDS-PAGE) and Western blot.

2.4.8.1 Benzonase Treatment

For benzonase treatment, immunoprecipitates were washed twice with Thermo IP lysis buffer without EDTA. Immunoprecipitates were resuspended in 50 μ L of Benzonase reaction buffer containing 1.5U/ μ L benzonase. Samples were incubated for 1 hour at 37°C for benzonase treatment. Post-treatment, immunoprecipitates were twice washed in Thermo IP lysis buffer (now containing EDTA) and analysed by SDS-PAGE and Western blot.

2.4.8.2 λ Phosphatase Treatment

λ phosphatase treatment was performed in a similar manner to Benzonase treatment. Following washes in IP lysis buffer without EDTA and resuspension in 50 μ L of λ Phosphatase reaction buffer containing 0.5U/ μ L of λ phosphatase, samples were incubated for 1 hour at 30°C. Post-treatment, samples were washed twice with Thermo IP lysis buffer and analysed analysed by SDS-PAGE and Western blot

2.4.9 Real-Time PCR

RNA Extraction:

RNA was extracted from cells according to the protocol described in the VWR E.Z.N.A Total RNA kit. Genomic DNA contamination was removed which the addition of a DNase I treatment step to the protocol. DNase I was purchased from (Thermo-Fisher). DNase I was used on the columns at a final concentration of 1U/Column. For experiments requiring pre-incubations with fatty acid inhibitors (Such as 2-bromopalmitate; Chapter 3.3), cells were lysed in TriGENE(Sigma) and separated into aqueous and organic phases according to the manufacturer's guidelines. The aqueous phase was removed and used with the VWR E.Z.N.A

kit to facilitate DNase I treatment. RNA was eluted from columns into 50µL of diethyl dicarbonate (DEPC) water and stored at -80°C until required.

cDNA Synthesis and RT-PCR Conditions:

Isolated RNA was quantified using a NanoDrop 2000c(Thermo-Fisher). 200ng of RNA was used for cDNA synthesis reactions. cDNA was synthesised using the iScript cDNA synthesis kit (Bio-Rad).

Real Time(RT)-PCR Primers were designed using the NCBI Primer-Blast tool and ordered from Eurofin genomics. Primer sequences are detailed in Table 2.6. mRNAs were quantified using FastStart Essential DNA Green Master SYBR Green, diluted to concentration of 1x by the addition of cDNA and primers in a 10µL reaction. RT-PCR data was obtained using a Roche Lightcycler® 96. The programmed used to obtain RT-PCR data was as follows: initial denaturation at 95 °C for 600 seconds, 40 cycles of 95°C for 10 seconds then 60°C for 30 seconds, followed by a melt curve step. Results were then analysed using the comparative C_t method, normalising values to β-actin. Data was expressed as fold change over mock treatment/transfection agent alone.

Gene	Forward Primer	Reverse Primer
Beta-Actin	5'-CGCGAGAGAAGATGACCCAGATC -3'	5'-GCCAGAGGGCGTACAGGGATA 3'
IFN Beta	5'-ACGCCGCATTGACCATCTAT 3'	5'-GTCTCA TTCCAGCCAGTGCT-3'
CXCL10	5'-AGCAGAGGAACCTCCAGTCT -3'	5'-AGGTACTCCTTGAATGCCACT -3'
IL6	5'-CAGCCCTGAGAAAGGAGACA T-3'	5'-GGTTCAGGTTGTTTTCTGCCA-3'
ISG56	5'-CAAAGGGCAAACGAGGCAG-3'	5'-CCCAGGCATAGTTTCCCCAG-3'
RANTES	5'-CTGCTTTGCCTACATTGCC-3'	5'-TCGGGTGACAAAGACGACTG-3'

Table 2.6: Primer Sequences for House Keeping Gene and Cytokines

2.4.10 Confocal Microscopy

Slide Preparation

50,000 cells were seeded onto glass coverslips (VWR) 12-18 hours prior to stimulation. Cells were washed in chilled PBS and fixed in -20°C methanol overnight. Cells were then permeabilised in 0.5% Triton-X/PBS for 12 minutes at room temperature, washed and

incubated in a blocking buffer of 5% FCS/0.2% Tween/PBS for 1 hour. Primary antibodies were added to samples in blocking buffer at a concentration of (1:600). Primary antibodies were left to incubate with samples overnight at 4°C. Samples were washed three times using a solution of 0.005% Tween/PBS prior to the addition of fluorescent secondary antibodies in blocking buffer at a concentration of (1:1,500). Samples were permitted to incubate with secondary antibodies for 1 hour at room temperature. Samples were thrice washed again with 0.005% Tween/PBS. Coverslips were mounted in 3µL MOWIOL-488(Calbiochem) containing 1mg/mL DAPI and sealed with nail varnish prior to imaging.

Imaging

Images were taken using a LSM710 laser scanning microscope (Zeiss) with the x60 oil immersion objective lens.

2.4.11 ELISA

Human CXCL10 and CCL5 protein was measured in supernatants using the human CXCL10/IP-10 and CCL5 ELISA Kits (R&D biosystems) and following the protocols provided by the manufacturer. Proteins were quantified using log of standard curve. Absorbance was measured at 450nm and corrected against a background absorbance of 570nm

2.4.12 DNA Sequencing

DNA sequencing was performed by the Division of Signal Transduction Therapy's DNA Sequencing Service at University of Dundee. DNA sequences were compared to the reference sequence using the multiple sequence alignment programme MAFFT (Multiple Alignment using Fast Fourier Transform) to emulate Clustalw via EMBL-EBI's website.

Sequencing Knockout Cell Lines:

TALEN knockout cell lines were verified by amplifying the TALEN target site of the gene of interest using Herculase II Fusion DNA Polymerase (Agilent Technologies #600675).

DNA used in these PCR reactions was extracted from candidate knockout cell lines using QuickExtract™ DNA Extraction Solution (Epicentre). Primers used for sequencing PCRs are detailed in Table 2.8. The PCR product was cloned into a TOP10 vector using the One Shot® TOP10 Chemically Competent kit (Thermo-Fisher) and transformed into One Shot cells. Colonies were grown overnight and plasmid DNA was extracted using a QIAprep Spin Miniprep Kit (Qiagen). Isolated TOP10 vectors were sent for sequencing to determine the changes to the TALEN target site.

STING mRNA Sequencing:

Due to the existence of polymorphisms that impede STING’s capacity to bind to and respond to cyclic di-nucleotides (Diner et al., 2013), the phenotype of STING in HaCaT cell lines was determined by sequencing STING mRNA. A cDNA library was created using SuperScript III Reverse Transcriptase(Thermo-Fisher) with total RNA extracted from the Wild Type/parental cell line. Due to the length of the STING transcript (1200-1900bp depending on the isoform), it was necessary to amplify STING from the cDNA library in two segments to ensure complete coverage. PCR products were cloned into TOP10 vectors and subsequently sequenced. HaCaT cell lines possess the Arg232 variant of STING and contain no other mutations that produced changes in STING protein sequence.

Target	Forward Primer	Reverse Primer
IFI16 ex5	5'-GGGGCCCTGTGTTATACTGAG-3'	5'-TCAGGTGTTGGTGGAAAAATGAA-3'
STING mRNA	5'- GTTCAATTTTCACTCCTCCCTCCTA- 3'	5'- GGTAATCTGAGATGTGCTTTAAAAAG- 3'
STING mRNA- 681	5'-CCTTCACTTGGATGCTTGCC-3'	

Table 2.7: Sequences of Primers used in Sequencing Reactions

2.4.13 cGAMP Quantification

Sample preparation:

A method to quantitatively measure cGAMP production in cells was developed in collaboration with Abdel Abrith of the Fingerprints Proteomic Service at the University of Dundee. Due to the number of optimisation steps required in preparing these samples this portion of the method will be detailed at length in results chapter 3.2.

Liquid Chromatography-Mass Spectrometer Configuration (Performed by Abdel Abrith of Fingerprints Dundee):

cGAMP levels were measured in enriched cell lysates with a TSQ Quantiva interfaced with Ultimate 3000 Liquid Chromatography system (ThermoScientific), equipped with a porous graphitic carbon column (HyperCarb 30 1 mm ID 3 mm; Part No: C-35003- 031030, ThermoScientific). The buffer used for Mobile phase A was comprised of 0.3% (vol/vol) formic acid adjusted to pH 9 with ammonia before a 1/10 dilution. Mobile phase buffer B comprised 80% (vol/vol) acetonitrile. The column was maintained at a controlled temperature of 30 °C and was equilibrated with 13% buffer B for 15 min at a constant flow rate of 0.06 mL/min. Aliquots of 13µL of each sample were injected into the column and compounds were eluted from the column with a linear gradient of 13–80% buffer B over 20 min.

The concentration of Buffer B was then increased to 100% for 5 min and the column was washed for a further 5 min with Buffer B. Eluents were sprayed into the TSQ Quantiva using Ion Max NG ion source with ion transfer tube temperature set to 350 °C and vaporizer temperature 125°C. The TSQ Quantiva was run in negative mode with a spray voltage of 2,600 V, sheath gas 40 and Aux gas 10.

cGAMP and spiked in cyclic di-AMP levels were measured using multiple reaction monitoring mode with optimized collision energies and radio frequencies previously determined by infusing pure compounds. Three transitions (673.054328.03, 673.054343.92

and 673.064522.00) were used to monitor cGAMP and one transition (657.074328.03) was used to detect cyclic di-AMP.

2.4.14 Snake Venom Phosphodiesterase Treatment

cGAMP containing samples were dried under vacuum to remove the presence of residual solvents. Samples were vortexed with 100 μ L of Snake Venom Phosphodiesterase reaction buffer containing 0.05U/ μ L of enzyme and incubated at 37°C for 1 hour. Snake Venom Phosphodiesterase was removed from the sample during subsequent solid phase extraction steps in the protocol (detailed further in results chapter 3.2).

2.5 Statistical Analysis

Results from quantitative analyses (i.e. RT-PCR, ELISA, cGAMP Quantification) are presented as the mean of triplicate samples with error bars representing standard deviation. Two-way ANOVA was used to determine statistical significance. Statistics were analysed using GraphPad Prism 6 for Macintosh.

P-Values; *= $P < 0.05$, **= $P < 0.01$, ***= $P < 0.001$.

2.6 Data Visualisation

Figures were assembled using Adobe Illustrator for Macintosh and GraphPad Prism. Microscopy figures were analysed and assembled using OME Remote Objects(OMERO). Chemical Structures were drawn with Chemdraw Prime 16 (CambridgeSoft).

Chapter Three Part One

IFI16 is required for the induction of innate immune responses to DNA in human immortalised keratinocytes

3.1.1 Human Immortalised Keratinocytes (HaCaT) cells express IFI16 and the cGAS-STING pathway and produce anti-viral cytokines in response to DNA transfection.

We wished to examine the immune response to DNA in keratinocytes, as these cells are a natural host for numerous DNA viruses (e.g. HSV-1, hCMV, HPV). We utilised spontaneously immortalised human keratinocyte (HaCaT) cells as a model system for this investigation (Boukamp et al., 1988). While HaCaT cell lines are known to express PRRs such as TLRs (Mondini et al., 2007) and NLRs (Jang et al., 2015), DNA sensing PRRs had not been studied in this cell type when we began these experiments. Hence, we first needed to determine whether HaCaT cell lines expressed IFI16, cGAS, and the STING pathway, in addition to whether HaCaT cell lines possessed the capability to respond to transfected DNA.

A time course was performed to establish if HaCaT cell lines expressed DNA sensors and could respond to DNA. HaCaT cells were transfected with HT-DNA or transfection agent alone for the times indicated in **Fig 3.1.1**. Cells were lysed and examined for the presence of IFI16, cGAS and STING pathway components by western blot (**Fig 3.1.1A**). HaCaT cells were found to express IFI16 and cGAS at consistent levels throughout the time course. STING is understood to induce IFN- β transcription by providing a platform for TBK1 activation by auto-phosphorylation (Tanaka and Chen, 2012), and enabling TBK1 induced phosphorylation of the transcription factor IRF3 (Ishikawa, 2008; Liu et al., 2015a). Following the activation of IRF3, STING is turned over by the influence of autophagy proteins (Saitoh et al., 2009). Upon DNA transfection, we detect the phosphorylation of IRF3 (**Fig 3.1.1A**). Additionally, the appearance of a second STING band is observed with DNA transfection. We also witness a decrease in the presence of both STING bands following DNA treatment suggesting that STING is turned over at later time points (**Fig 3.1.1A**).

STING is known to be phosphorylated upon activation (Sun et al., 2009; Zhong et al., 2008), specifically on Ser 366 to recruit IRF3 (Liu et al., 2015a). To examine whether this second STING band is representative of phosphorylated STING as reported by (Konno et al., 2013), we immunoprecipitated STING from cell lysates following DNA

stimulation, and treated samples with λ phosphatase (**Fig 3.1.1B**). **Fig 3.1.1B** demonstrates in λ phosphatase treated samples that STING no longer displays the band shift that occurs with DNA transfection, indicating that the upper band corresponds to a phosphorylated form of STING.

Real-Time PCR was used to measure the production of cytokine mRNA to assess whether HaCaT cell lines could induce production of anti-viral cytokines in response to DNA transfection. We elected to measure *IFN- β* mRNA as it is the first IFN produced in response to viral infection through IRF3 transcription (Lin et al., 1998; Schafer et al., 1998). IFN- β acts on cells in an autocrine and paracrine fashion to induce a myriad of ISGs with anti-viral activity (Reviewed by Stetson and Medzhitov, 2006b).

We also chose to measure the induction of several other genes transcribed by IRF3. Namely, *ISG56* and chemokines *CCL5* and *CXCL10*. *ISG56* is an inducible negative regulator of the STING pathway and is required to limit activation of the STING pathway and ensure an eventual return to homeostasis (Li et al., 2009). *CCL5* and *CXCL10* are imperative for the recruitment of dendritic cells, and specialist anti-viral immune cells such as Natural Killer, CD8+ cytotoxic T cells and T Helper-1 cells to the site of infection (Loetscher et al., 1996; Reviewed by Melchjorsen et al., 2003; Schall et al., 1990). Induction of IFN transcription is supported by efficient NF κ B activation, with the RelA subunit of NF κ B forming a transcriptional complex with phosphorylated IRF3 known as the IFN- β enhanceosome on the IFN- β promoter (Schafer et al., 1998). To assess NF κ B activation, we examined the induction of the NF κ B dependent gene *IL-6*. *IL-6* promotes efficient immune responses by promoting fever, inflammation and activation of the acute phase protein response (Reviewed by Netea et al., 2017). As highlighted in the time course depicted in **Fig 3.1.2**, HaCaT cells induce production of *IFN- β* (**Fig 3.1.2A**), *ISG56* (**Fig 3.1.2B**), *CCL5* (**Fig 3.1.2C**), *CXCL10* (**Fig 3.1.2D**) and *IL-6* mRNAs (**Fig 3.1.2E**) most abundantly 4 hours after transfection with HT-DNA, with production decreasing incrementally at 6 and 8 hours post stimulation, and transfection agent alone failing to induce any significant cytokine production at all.

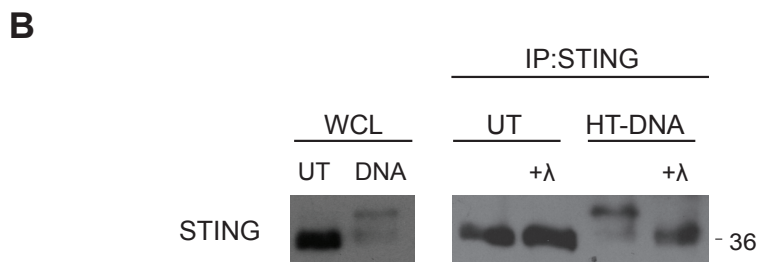
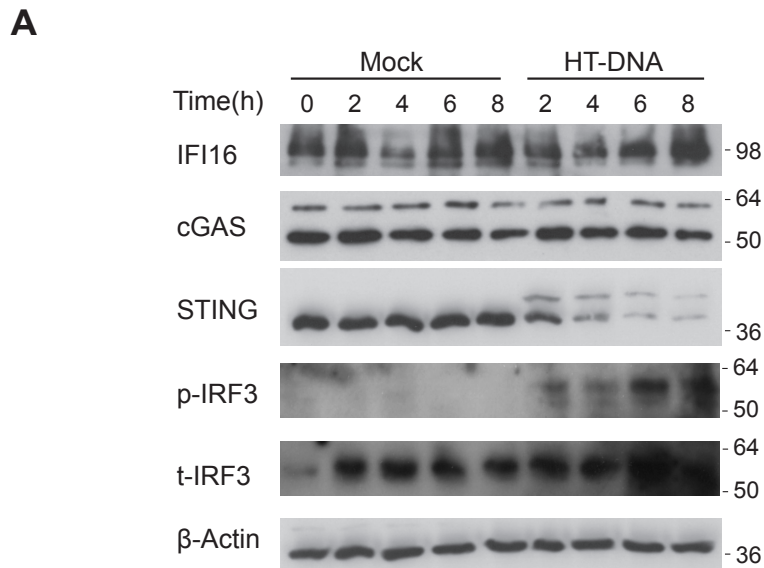


Fig 3.1.1 Human Immortalised Keratinocyte (HaCaT) cell lines express IFI16, cGAS and STING and activate the STING pathway in response to transfected DNA

(A) HaCaT cells were stimulated with 1µg/mL HT-DNA or 1µL/mL Lipofectamine(Mock) for the indicated times. Cells were lysed and examined for the presence of IFI16, cGAS, STING, β-Actin, and total and phosphorylated IRF3(Ser396) by Western blot. **(B)** STING was immunoprecipitated from wild typ HaCaT cells which were left untreated (UT) or stimulated with 1µg/mL HT-DNA for 6 hours. Immunoprecipitates were treated with 100 units of λ phosphatase (or the H₂O control) and incubated for 1 hour at 37°C before analysis by SDS-PAGE and western blot. Data from A and B are representative of three independent experiments.

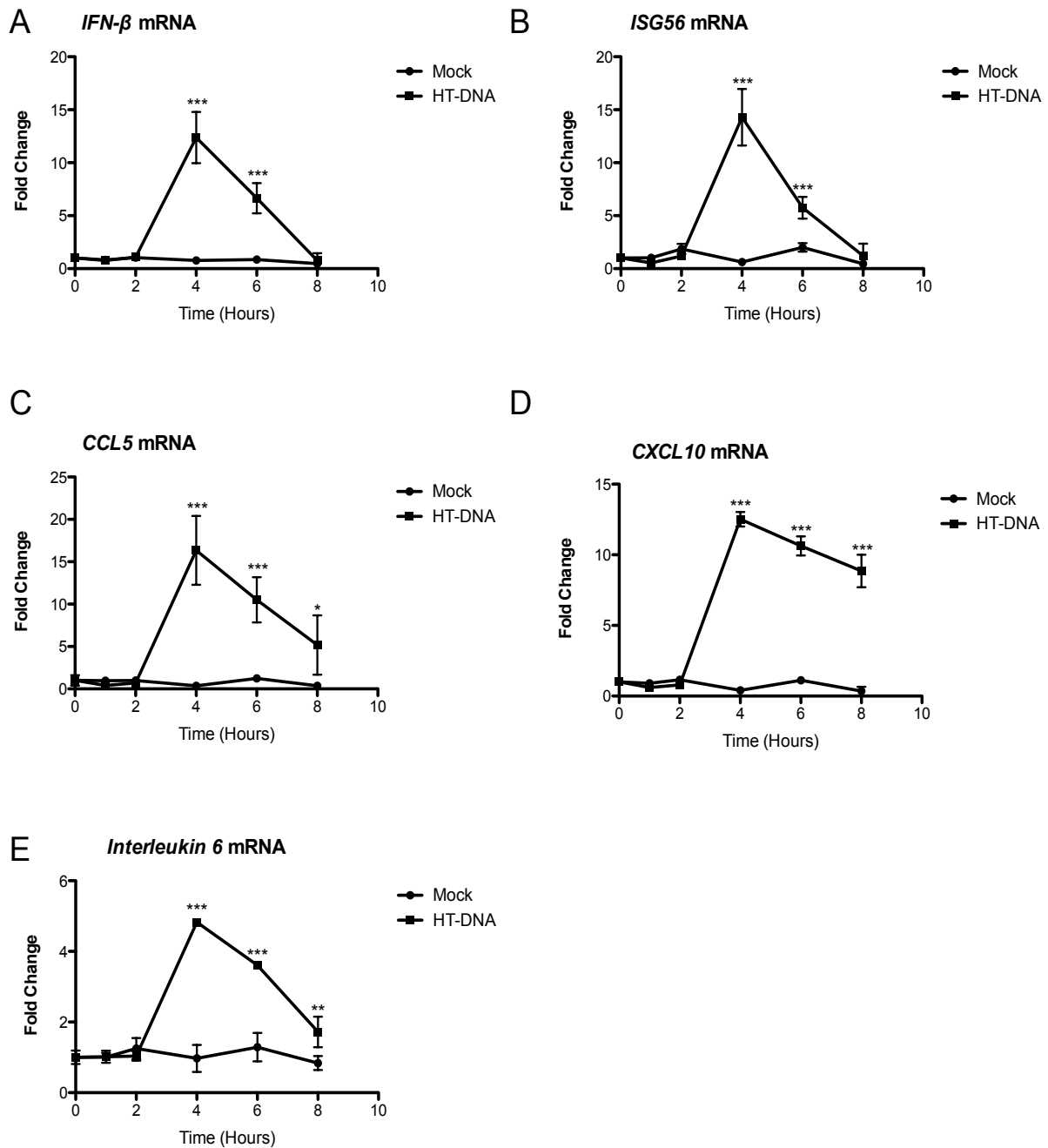


Fig 3.1.2 HaCaT cell lines express IFN-β and anti-viral cytokines in response to DNA transfection

(A-E) HaCaT cells were stimulated with 1μg/mL HT-DNA or 1μL/mL Lipofectamine alone (Mock) at the times indicated. IFN-β (A), ISG56 (B), CCL5 (C), CXCL10 (D) and Interleukin-6 (E) levels were measured by Real-Time PCR. Experiments were carried out with triplicate samples, mean values and standard deviation are shown. Data are representative of three independent experiments. Statistical significance was determined using two-way ANOVA. p-value: * $P < 0.05$, ** $P < 0.01$, *** $P < 0.001$.

To confirm the Real-Time PCR results were reflective of protein production, supernatants were collected from HaCaT cell lines 18 hours post transfection with DNA or transfection agent alone to measure CXCL10 and CCL5 secretion by ELISA. **Fig 3.1.3** demonstrates that CXCL10 and CCL5 are only induced in response to DNA transfection but not in response to transfection agent alone. Collectively these observations demonstrate that HaCaT cell lines possess IFI16, a functional STING pathway, and can produce anti-viral cytokines in response to transfected DNA.

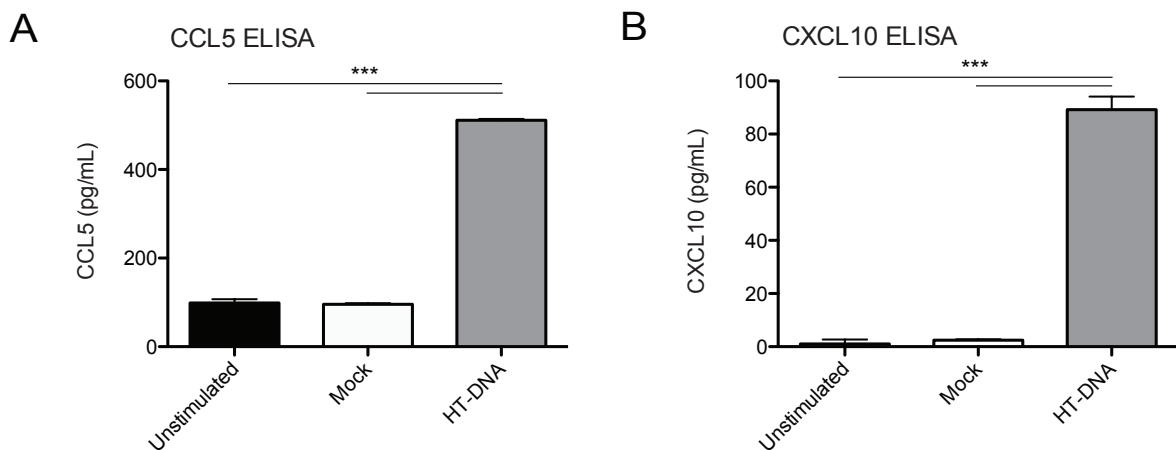


Fig 3.1.3 HaCaT cell lines secrete the chemokines CCL5 and CXCL10 in response to DNA

(A-B) HaCaTs were stimulated with 1µg/mL HT-DNA or mock transfected for 18 hours. Supernatants were collected and examined for the presence of CCL5 **(A)** and CXCL10 **(B)** by ELISA. Experiments were carried out with triplicate samples, mean values and standard deviation are shown. Data are representative of three independent experiments. Statistical significance was determined using one way ANOVA. p-value:*=P<0.05, **=P<0.01, ***=P<0.001

3.1.2 Human Immortalised Keratinocytes (HaCaT) cell lines without IFI16 still possess the other components of the DNA sensing pathway

To conclusively assess the contribution of IFI16 to intracellular IFN induction, we used HaCaT cells lacking IFI16, which had been generated using Transcription activator-like effector nucleases (TALENs). **Fig 3.1.4A** depicts two independently generated *IFI16* knockout HaCaT cell lines which still possess cGAS and the STING-TBK1-IRF3 axis but lack IFI16. By examining the genomic sequence of the TALEN target site (**Fig 3.1.4B**) in the hypotriploid HaCaT cell line, we observe that all three alleles of the *IFI16* gene possess premature stop codons or insertions resulting in frame shift mutations, rendering the cells incapable of producing IFI16 protein.

3.1.3 IFI16 is required for HaCaT cells to produce IFN- β , cytokine and chemokine mRNA in response to DNA

A time course was performed to assess whether the IFI16 knockout (*IFI16*^(-/-)) cell lines could respond to DNA. As illustrated in **Fig 3.1.5**, Wild Type cells behave as previously observed in **Fig 3.1.2** by producing an abundant amount of *IFN- β* , *ISG56*, *CCL5*, *CXCL10* and *IL-6* mRNAs 4 hours post-stimulation with incrementally less mRNA produced at 6 and 8 hour time points (**Fig 3.1.5A-E**). This is in stark contrast to the *IFI16*^(-/-) cells which produce significantly less mRNA for every cytokine examined at 4, 6 and 8 hours post stimulation compared to wild type cells. As *IFI16*^(-/-) cells still display a residual immune response to DNA, it is unlikely that IFI16 is essential for DNA responses and therefore must play a role in enhancing the DNA-induced response.

An investigation by (Thompson et al., 2014) purported IFI16 functioned as a transcriptional regulator of IFN- β and ISGs during infection with DNA and RNA viruses rather than as a DNA sensor as proposed by (Unterholzner et al., 2010). To investigate if *IFI16*^(-/-) cells were responsive to RNA stimulation, Wild Type and *IFI16*^(-/-) cells were stimulated with the dsRNA mimic Poly(I:C). Poly(I:C) was included as a control for TLR3 and RLR pathways, which also induce IFN- β transcription via IRF3 (Alexopoulou et al., 2001; Marshall-Clarke et al., 2007; Yoneyama et al., 2005; Yoneyama et al., 2004) .

To ensure that the results of **Fig 3.1.5** were not somehow unique to HT-DNA stimulation, Wild type and *IFI16*^(-/-) cells were also stimulated with VACV 70mer; a dsDNA oligonucleotide of a reoccurring motif from the Vaccinia virus genome (Unterholzner et al., 2010). 6 hours following stimulation, *IFN-β*, ISG and *IL-6* mRNA was measured using RT-PCR (**Fig 3.1.6A-E**).

Both *IFI16*^(-/-) clones were observed to produce significantly less *IFN-β* mRNA in response to stimulation with either form of DNA, while responses to dsRNA are unaffected (**Fig 3.1.6A**). Similar trends were also observed with *ISG56*, *CCL5*, *CXCL10* and *IL-6* mRNAs in response to HT-DNA and VACV 70mer stimulation (**Fig 3.1.6B-E**). We also witness enhanced production of *ISG56* mRNA in response to RNA stimulation in the absence of IFI16 (**Fig 3.1.6B**).

As a further control, ability of the *IFI16*^(-/-) cell lines to respond to single stranded RNA was also examined. Single stranded viral RNAs are detected by the RIG-I pathway and TLRs7 and 8 (Heil et al., 2004; Pichlmair et al., 2006). We utilised *in-vitro* transcribed GFP mRNA (5'3p-RNA) as a viral RNA mimetic as it lacks the 5' guanine-methyl cap from host mRNA processing, allowing the 5'triphosphates exposed to be detected by RIG-I (Hornung V et al., 2006). Cytokine mRNA levels in Wild Type and *IFI16*^(-/-) HaCaT cell lines were measured 6 hours following stimulation with VACV 70mer and 5'3p-RNA. **Fig 3.1.7A-B** demonstrates that recognition of uncapped single stranded RNAs are largely unaffected by the absence of IFI16, as *IFN-β* (**A**) and *CXCL10* (**B**) mRNA levels in response to GFP 5'3p-RNA are not significantly altered. We observe a modest decrease in *IL-6* mRNA production in response ssRNA stimulation to in one *IFI16*^(-/-) clone (**Fig 3.1.7C**). Responses to VACV 70mer are similar to those depicted in **Fig 3.1.7**.

Taken together, the data presented in **Figures 3.1.5-7** demonstrate that *IFI16*^(-/-) cell lines produce significantly less *IFN-β* and anti-viral cytokine mRNAs in response to DNA transfection. Conversely, RNA responses are broadly unaffected by the absence of IFI16 or even enhanced (**Fig 3.1.6B**).

3.1.4 IFI16 is required for HaCaT cells to produce CCL5 protein in response to transfected DNA and infection with DNA Viruses

We wished to confirm the RT-PCR results by measuring chemokine secretion using ELISA. We examined CCL5 secretion in response to a range of concentrations of HT-DNA and VACV 70mer. CCL5 production is diminished in the *IFI16*^(-/-) HaCaT cells in response to every concentration of DNA examined (**Fig 3.1.8A**). We also examined the CCL5 response to different forms of DNA such as circular bacterial plasmid DNA (**Fig 3.1.8A**), and the Y-DNAs (**Fig 3.1.8B**) described by (Herzner AM et al., 2015). Y-DNAs are DNA oligomers representative of the short ssDNA reverse-transcripts produced early in infection by retroviruses. These are ssDNAs of fewer than 40 base pairs in length that activate dsDNA sensing pathways by self-pairing and forming stem-loop structures (Jakobsen et al., 2013). Herzner et al (2015) observe that the presence of unpaired Guanosines at the ends of the Y-DNAs promote the immunogenicity of the oligomer. CCL5 production in response to circular bacterial plasmid was dependent on IFI16 (**Fig 3.1.8A**). In **Fig 3.1.8B**, we observe that C₃ Y-DNA induced a minimal CCL5 response in both cell lines as expected while G₃ Y-DNA induced CCL5 responses in an IFI16 dependent manner. Collectively, these ELISA results demonstrate that every immunogenic form of DNA examined is detected in an IFI16 dependent manner. As already seen in the RT-PCR experiments (**Fig 3.1.6 and Fig 3.1.7**), chemokine responses to both ssRNA and dsRNAs are unaffected (**Fig 3.1.8C**).

We next investigated CCL5 production in response to infection with the dsDNA virus HSV-1. HSV-1 possesses numerous mechanisms to evade the innate immune response (Reviewed by Christensen and Paludan, 2017) including degradation of IFI16 by the HSV-1 protein ICP0 (Orzalli et al., 2012). UV inactivation of HSV-1 impairs its ability to evade the immune response, but does not impede its entry to the cell (Coohill et al., 1980). **Fig 3.1.9A** demonstrates that UV-inactivated HSV-1 induces a greater CCL5 response in Wild Type HaCaT cells compared to the *IFI16*^(-/-) cells. UV-treatment of the medium alone fails to induce CCL5 production, while HSV-1 does not induce any CCL5 response without UV-inactivation, likely due to the expression of immune evasion factors.

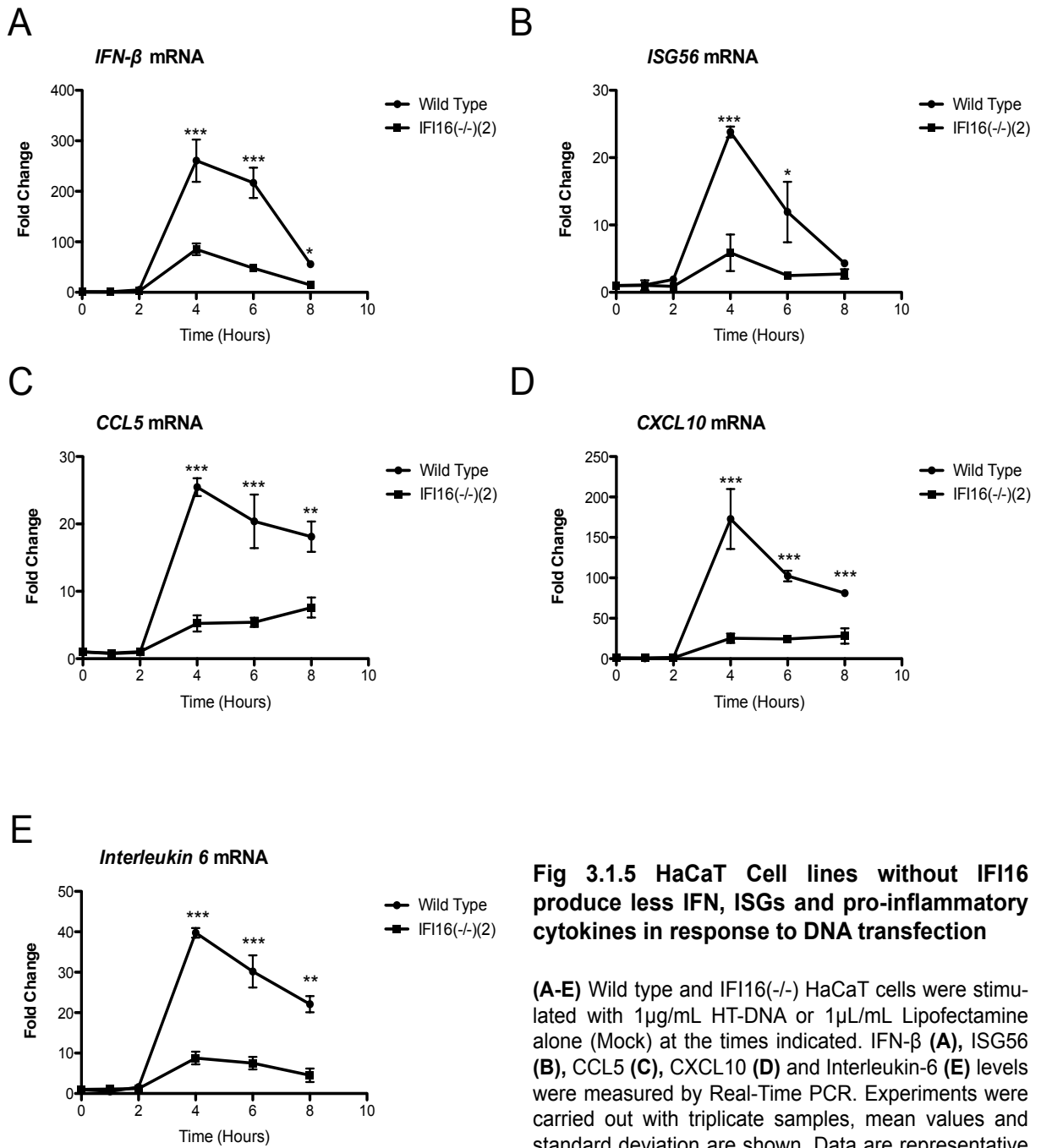


Fig 3.1.5 HaCaT Cell lines without IF16 produce less IFN, ISGs and pro-inflammatory cytokines in response to DNA transfection

(A-E) Wild type and IF16(-/-) HaCaT cells were stimulated with 1µg/mL HT-DNA or 1µL/mL Lipofectamine alone (Mock) at the times indicated. IFN-β (A), ISG56 (B), CCL5 (C), CXCL10 (D) and Interleukin-6 (E) levels were measured by Real-Time PCR. Experiments were carried out with triplicate samples, mean values and standard deviation are shown. Data are representative of three independent experiments. Statistical significance was determined using two-way ANOVA. p-value: * = P < 0.05, ** = P < 0.01, *** = P < 0.001

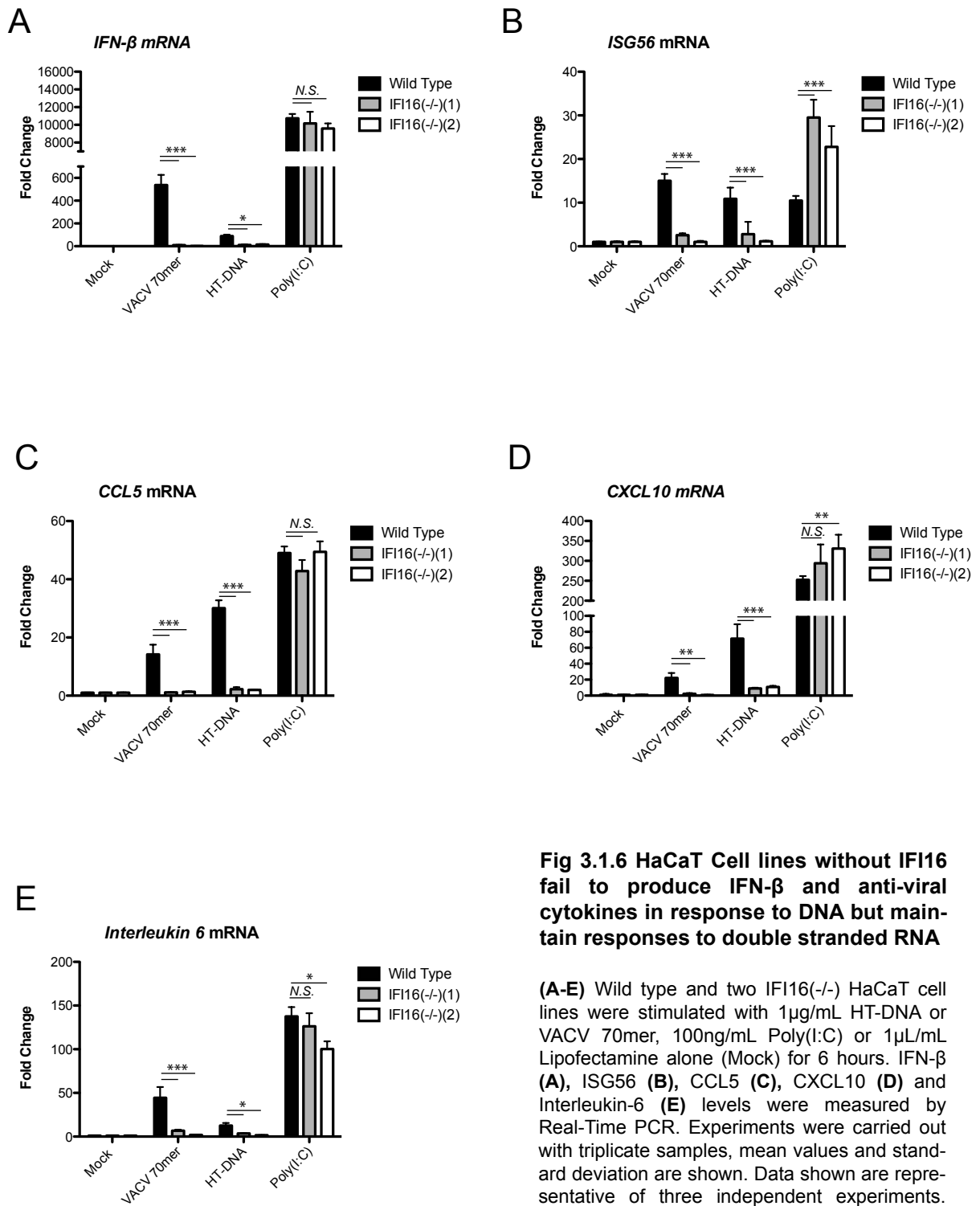


Fig 3.1.6 HaCaT Cell lines without IFI16 fail to produce IFN-β and anti-viral cytokines in response to DNA but maintain responses to double stranded RNA

(A-E) Wild type and two IFI16(-/-) HaCaT cell lines were stimulated with 1μg/mL HT-DNA or VACV 70mer, 100ng/mL Poly(I:C) or 1μL/mL Lipofectamine alone (Mock) for 6 hours. IFN-β (A), ISG56 (B), CCL5 (C), CXCL10 (D) and Interleukin-6 (E) levels were measured by Real-Time PCR. Experiments were carried out with triplicate samples, mean values and standard deviation are shown. Data shown are representative of three independent experiments. Statistical significance was determined using two-way ANOVA. p-value:*=P<0.05, **=P<0.01, ***=P<0.001 N.S=No significance

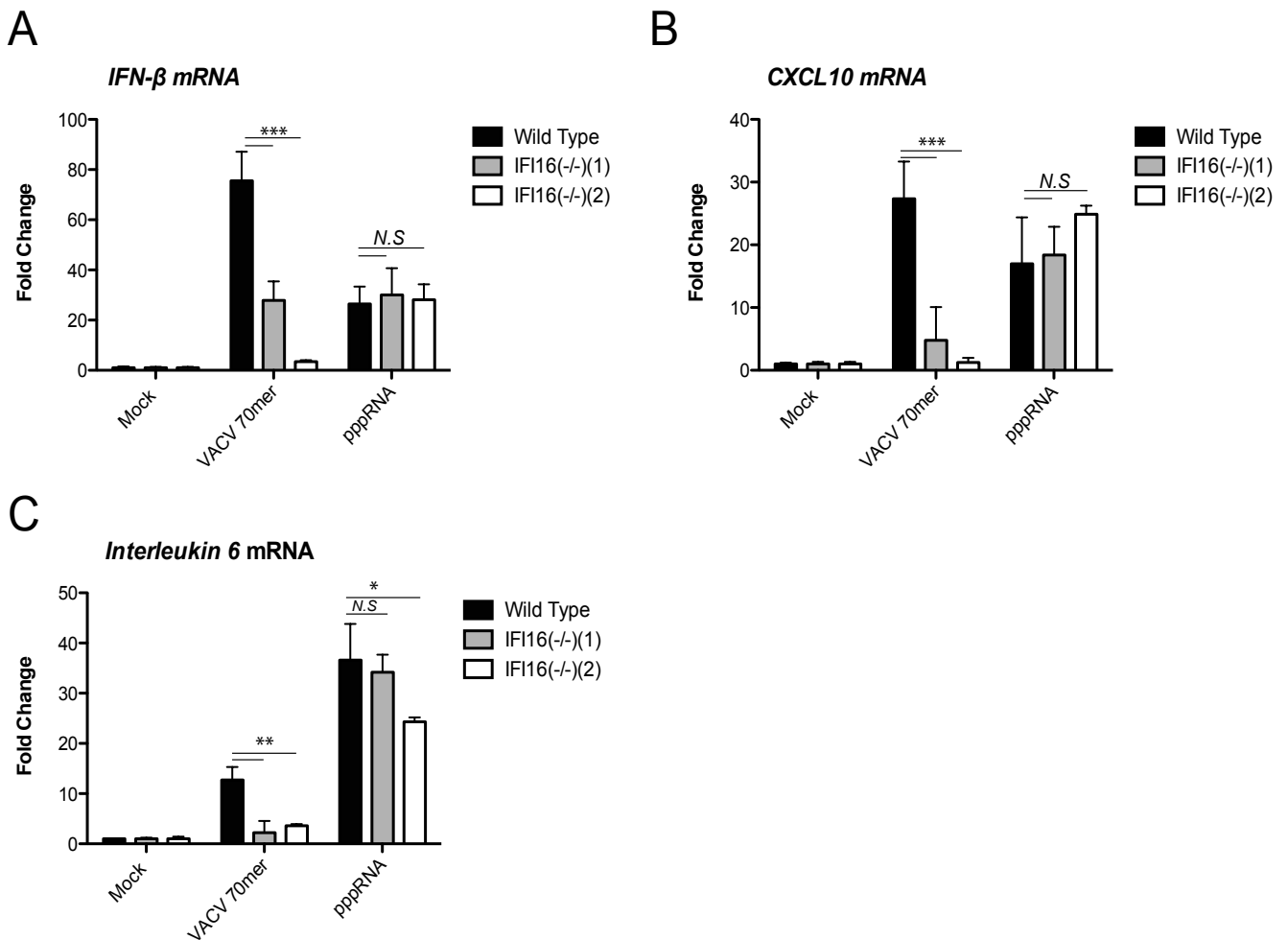
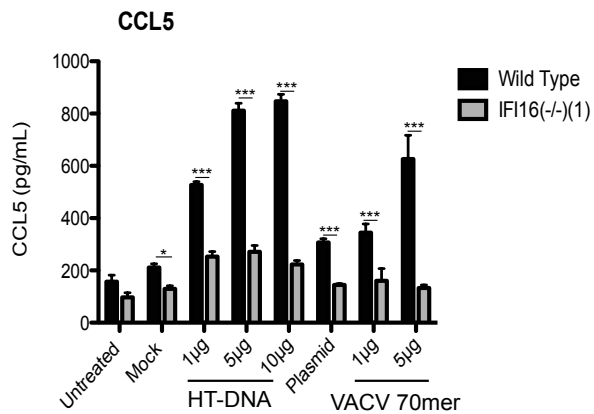


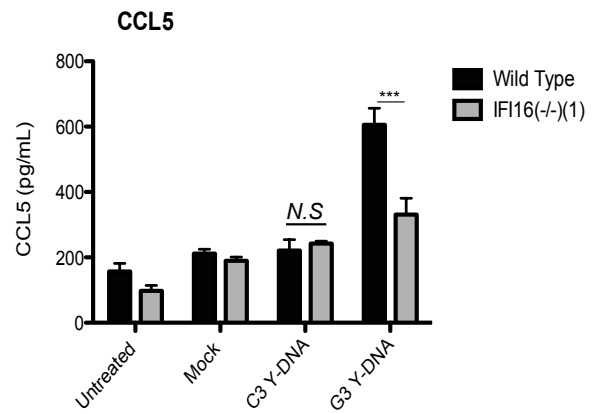
Fig 3.1.7 HaCaT Cell lines do not require IFI16 to produce IFN-β in response to single stranded RNA

(A-C) Wild type and two IFI16(-/-) HaCaT cell lines were stimulated with 1μg/mL VACV 70mer, 50ng/mL pppRNA(GFP) or 1μL/mL Lipofectamine alone (Mock) for 6 hours. IFN-β (A), CXCL10 (B) and Interleukin-6 (C) levels were measured by Real-Time PCR. Experiments were carried out with triplicate samples, mean values and standard deviation are shown. Data are representative of three independent experiments. Statistical significance was determined using two-way ANOVA. p-value: * = P < 0.05, ** = P < 0.01, *** = P < 0.001 N.S. = No Significance

A



B



C

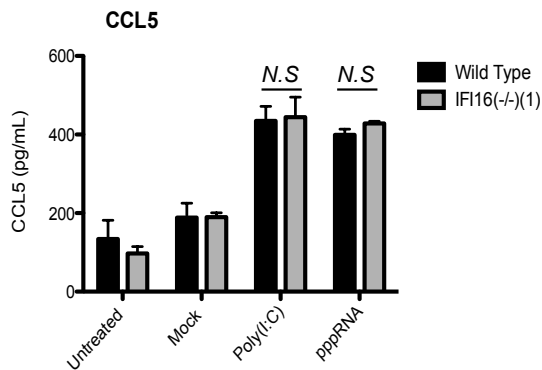
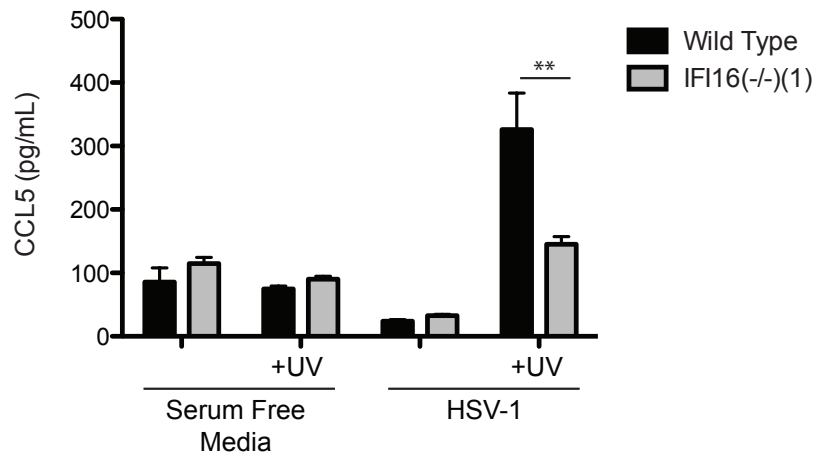


Fig 3.1.8 IF116 is required to produce CCL5 in response to immunogenic DNA but is dispensable for responses to RNA

(A-C) Wild Type and IF116(-/-) HaCaT Cell lines were stimulated with increasing concentrations of HT-DNA and VACV 70mer, 1µg/mL pcDNA(3.1) (A), 1µg/mL of different forms of Y-DNA (B), 50ng/mL of different forms of RNA (C) or transfection agent alone. 18 hours post stimulation cell supernatants were collected and examined for CCL5 production by ELISA. Experiments were carried out with triplicate samples, mean values and standard deviation are shown. Data are representative of three independent experiments. Statistical significance was determined using two-way ANOVA. p-value: * = P < 0.05, ** = P < 0.01, *** = P < 0.001 N.S. = No Significance

A



B

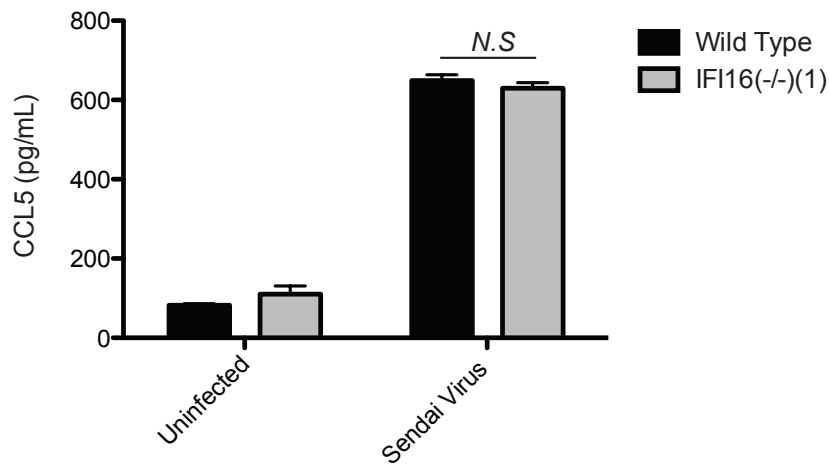


Fig 3.1.9 IFI16 is required for CCL5 production in response to HSV-1 infection in HaCaT cell lines

Wild type and IFI16(-/-) HaCaT cell lines were infected with HSV-1, UV-inactivated HSV-1(MOI=5) (A) or Sendai virus (1:2000) (B) for 18 hours. Supernatants were examined for CCL5 production by ELISA. Experiments were carried out with triplicate samples, mean values and standard deviation are shown. Data are representative at least two independent experiments. Statistical significance was determined using two-way ANOVA. p-value:**=P<0.01. N.S=No significance

Consistent with previous observations examining ssRNA responses by RT-PCR, no difference in CCL5 production was detected between wild type and *IFI16*^(-/-) cells in response to infection with Sendai Virus (**Fig 3.1.9B**) which is detected via the RIG-I pathway (Rehwinkel et al., 2010). Taken together, these ELISA results verify the RT-PCR results of **Fig 3.1.6 and Fig 3.1.7** and demonstrate that IFI16 is required for DNA and DNA virus induced cytokine production, whilst being dispensable for responses to RNA and RNA viruses.

3.1.5 Cells without IFI16 do not efficiently activate the STING pathway

We wished to examine the behaviour of STING in the *IFI16*^(-/-) cell line to determine whether IFI16 acted upstream of STING as proposed by (Unterholzner et al., 2010). Upon activation STING has been observed to translocate from the endoplasmic reticulum into punctuate structures (Ishikawa et al., 2009). These puncta have been described as the trans-golgi ER-Golgi intermediate compartment (ERGIC) by (Dobbs N et al., 2015). Here STING recruits TBK1, which in turn activates IRF3 and initiates IFN- β transcription. Trafficking is understood to be an important component of STING activation, with inhibition of the process by bacterial proteins abrogating IFN- β induction (Dobbs N et al., 2015).

STING trafficking was examined by confocal microscopy to observe if this process was altered in the absence of IFI16. In Wild Type HaCaT cell lines following DNA stimulation, STING traffics from discrete locations around the ER into punctate structures in approximately 40% of cells examined (**Fig 3.1.10A-B**). Conversely, it was observed that DNA induced STING trafficking is severely reduced in *IFI16*^(-/-) cell line with only 10% of cells displaying STING trafficking.

STING is known to be phosphorylated during its activation (Ishikawa, 2008; Zhong et al., 2008). We have previously detected STING phosphorylation with DNA treatment in HaCaT cell lines (**Fig 3.1.1A**). STING phosphorylation was examined between Wild Type and *IFI16*^(-/-) cell lines in response to HT-DNA, VACV 70mer and Poly(I:C) stimulation by observing the appearance of a higher STING band by SDS-PAGE. STING phosphorylation is decreased in the *IFI16*^(-/-) cell line in response to both forms of DNA (**Fig 3.1.11A**). RNA stimulation was found to not induce STING

phosphorylation in either cell line (**Fig 3.1.11A**).

STING is specifically phosphorylated on Ser366 by TBK1 (Liu et al., 2015a; Tanaka and Chen, 2012). Phosphorylation on STING Ser366 has been demonstrated to be important for facilitating recruitment of IRF3 to STING through creating negatively charged residues that IRF3 binds to prior its activation by TBK1 (Liu et al., 2015a). In **Fig 3.1.11B** STING Ser366 phosphorylation and downstream activation of the STING pathway was examined between wild type and *IFI16*^(-/-) cell lines. In Wild Type cell lines, STING Ser366 phosphorylation is present at 2 and 4 hours after DNA stimulation. Phosphorylation of TBK1 and IRF3 can also be detected at these times. In direct contrast, reduced total and Ser366 STING phosphorylation is observed in the *IFI16*^(-/-) cell line along with less TBK1 and IRF3 phosphorylation (**Fig 3.1.11B**). Residual STING and IRF3 phosphorylation is observed at 4 hours in the *IFI16*^(-/-) (**Fig 3.1.11B**). This is consistent with the reduced transcriptional profile observed by RT-PCR in the absence of IFI16 and confirms that the STING pathway is not sufficiently activated in the *IFI16*^(-/-) cells.

Following phosphorylation, IRF3 dimerises and translocates to the nucleus to initiate transcription. We wished to investigate whether IRF3 dimers could still form in *IFI16*^(-/-) cell lines. In **Fig 3.1.11C**, wild type and *IFI16*^(-/-) cell lines were stimulated with HT-DNA or Poly(I:C) to induce IRF3 phosphorylation and dimerisation. These lysates were then run on Native-PAGE gels to assess IRF3 dimerisation. Native-PAGE gels are run without detergents or reducing agents; preserving the quaternary structure of a protein allowing dimers or higher order protein complexes to be observed. IRF3 dimers are observed in the Wild Type cell line in response to both HT-DNA and poly(I:C) stimulation (**Fig 3.1.11D**). As expected from RT-PCR (**Fig 3.1.6**) and ELISA data (**Fig 3.1.8**), the *IFI16*^(-/-) cell line only produced IRF3 dimers with RNA stimulation, and does not produce any phosphorylated IRF3 or IRF3 dimers with HT-DNA stimulation (**Fig 3.1.11D**). Together, these observations confirm that IRF3 is still functioning normally in the absence of IFI16 after RNA recognition and that IFI16 must act upstream of, or on the level of, STING in the DNA sensing pathway.

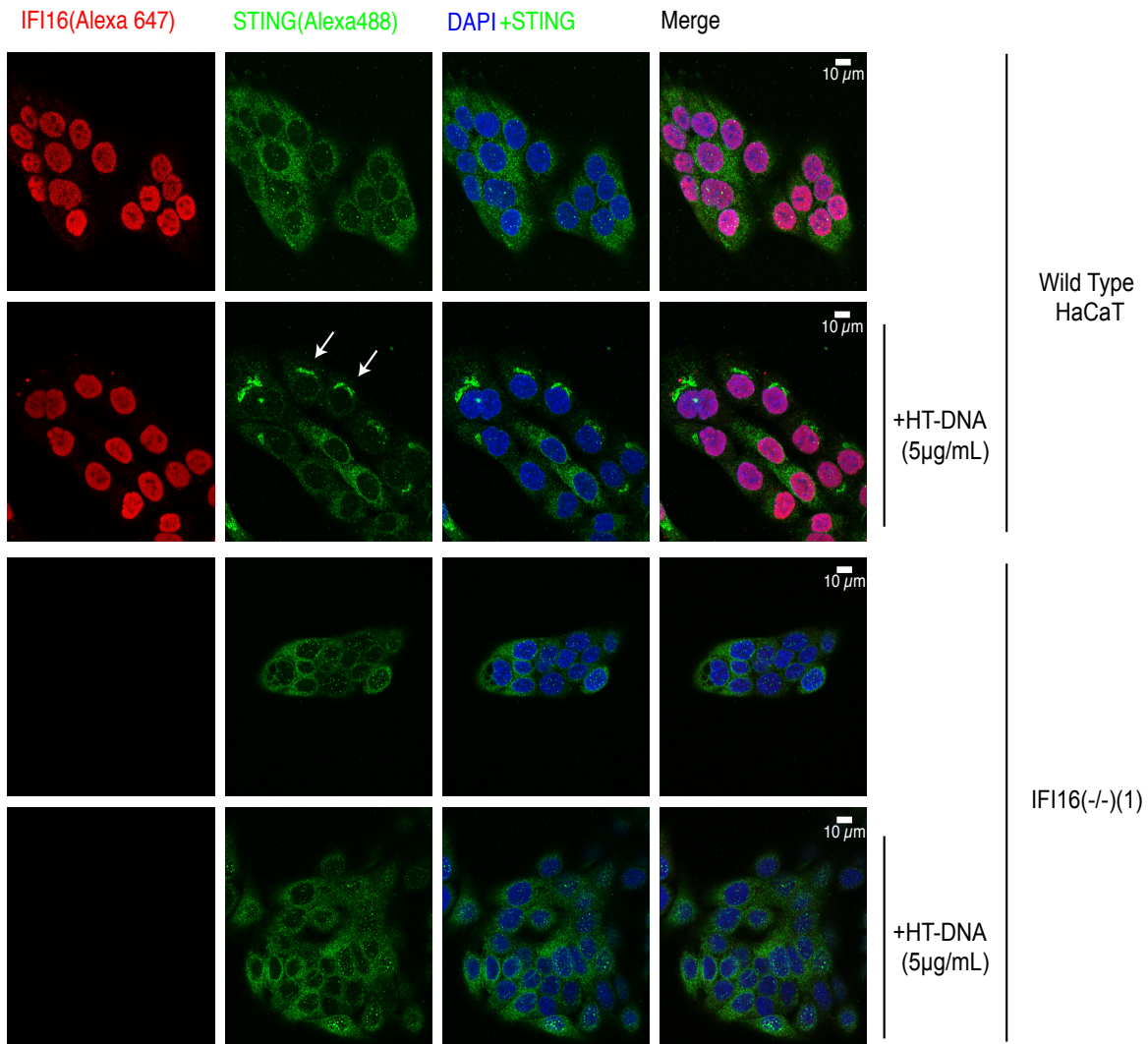
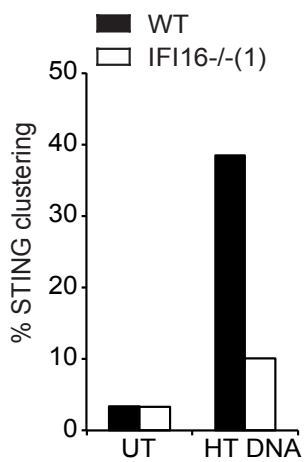
A**B**

Fig 3.1.10 DNA induced STING trafficking is decreased in IFI16(-/-) cell lines

(A) Confocal microscopy analysis of Wild Type and IFI16(-/-) HaCaT cell lines. Cell lines were transfected with 5µg/mL HT-DNA for 1 hour. Cells were stained for IFI16(Red/Alexa 647) and STING(Green/Alexa 488). DNA was visualised with DAPI (Blue). 200 cells were counted and scored for STING clustering. These scores are presented as percentage of STING clustering in **(B)**. Data are representative of two independent experiments.

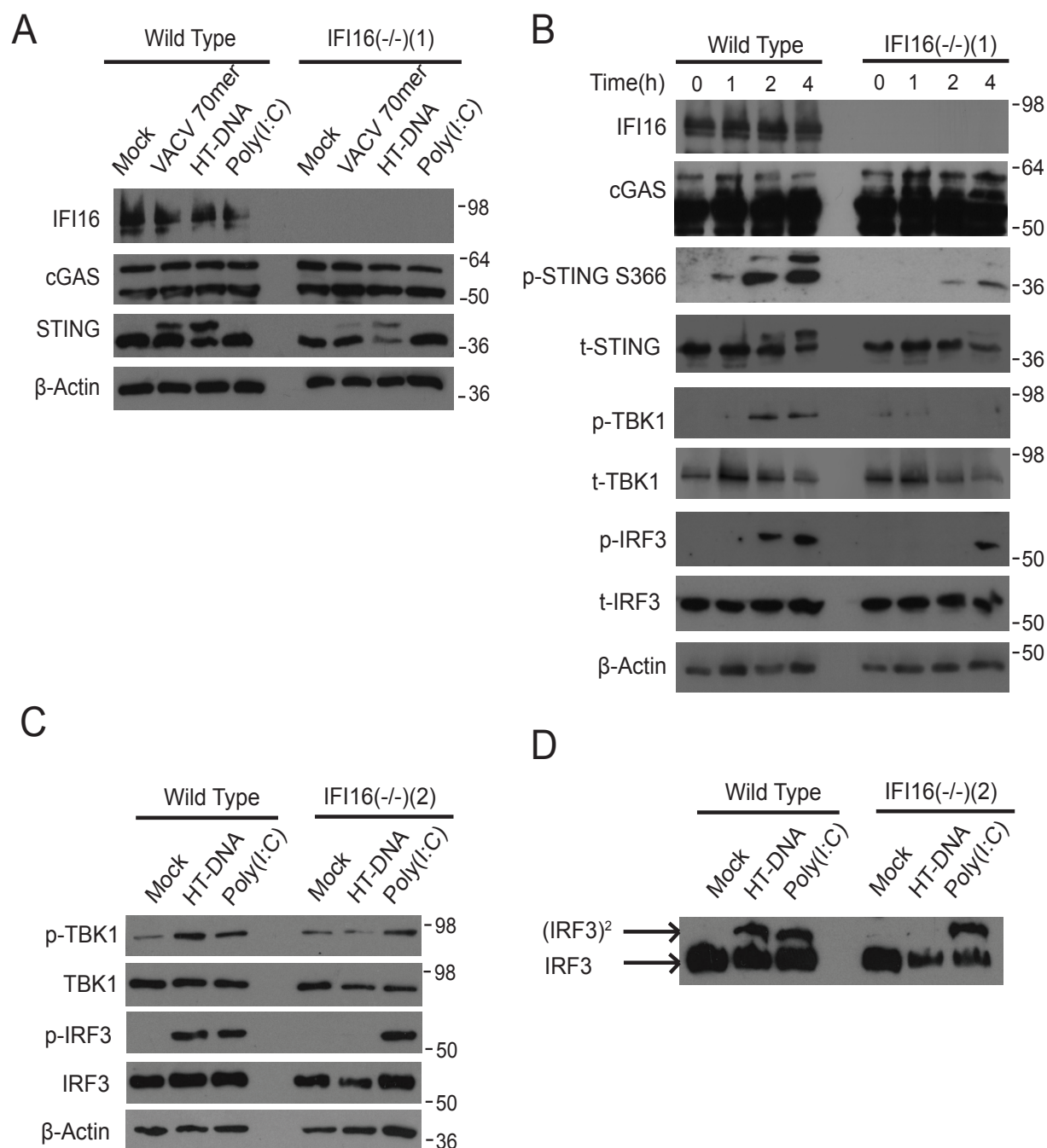


Fig 3.1.11 IFI16(-/-) HaCaT cell lines do not efficiently activate the cGAS-STING pathway

(A) Wild type and IFI16(-/-) HaCaT cell lines were stimulated with 1 μ g/mL HT-DNA and VACV 70mer, 100ng/mL Poly(I:C) or 1 μ L/mL Lipofectamine alone (Mock) for 4 hours. Cells were lysed and activation of STING between cell lines was examined by Western Blot. (B) Wild Type and IFI16(-/-) HaCaT cell lines were stimulated with (5 μ g/ml) of HT-DNA at 0, 1, 2 and 4h. Cell lysates were examined for IFI16, cGAS, Beta-actin and activation of the STING-TBK1-IRF3 axis (p-STING S366, p-TBK1 S172, p-IRF3 S396) by Western blot. (C) Wild type and IFI16(-/-) HaCaT cell lines were stimulated with HT-DNA (5 μ g/mL), poly(I:C) (1 μ g/mL) or transfection agent alone (mock) for 4 hours and examined for TBK1 and IRF3 phosphorylation (p-TBK1 Ser172; p-IRF3 Ser396) by SDS-PAGE and western blotting. (D) Lysates from (C) were also analysed on Native-PAGE gels to examine IRF3 dimerisation. Data shown are representative of three independent experiments.

3.1.6 Discussion

HaCaT cells express all three isoforms of IFI16, cGAS and STING at constant levels throughout an 8 hour time course (**Fig 3.1.1A**). This is distinct from other cells which have been used to study the immune function of IFI16, such as human foreskin fibroblasts, vascular endothelial cells and monocytes. These cells express low basal levels of IFI16 unless stimulated with IFN or DNA (Iqbal et al., 2016; Orzalli et al., 2015; Unterholzner et al., 2010). This suggests that expression of these receptors may be regulated differently in keratinocytes. In contrast to these other cells, keratinocytes constitute the outer most layer of skin and are constantly exposed to pathogens and environmental insults. Keratinocytes could require more consistent PRR expression to provide defence in skin against the near ubiquitous presence of pathogens in the environment.

Skin acts as a mechanical barrier to pathogen invasion and while skin possesses a wealth of nonspecific defence mechanisms (e.g. secretion of anti-microbial peptides), it is not impervious to infection. As a result, skin cells must possess the capacity to communicate infection to localised populations of immune cells and the wider immune system in order to maintain homeostasis (Reviewed by Pasparakis et al., 2014). We show that HaCaT cells produce IFN- β , ISG56, chemokines; CCL5 and CXCL10, and pro-inflammatory cytokine IL-6 when stimulated with DNA, showing that DNA sensors are active within these cells and that keratinocytes can communicate the presence of infection to cells of the immune system. Other cytokines, chemokines and anti-microbial peptides are also likely expressed in response to DNA stimulation and viral infection within these cells but have yet to be tested.

The ability of IFI16 to recognise pathogen DNA has been observed in a wide variety of cell types (**Table 1.3**). However the discovery that cGAS knockout cell lines and mice are unable to respond to DNA stimulation or HSV-1 and HIV-1 infections has obscured the role of IFI16 in innate immunity (Gao et al., 2013; Li et al., 2013). As the studies in (**Table 1.3**) rely on IFI16 or p204 depletion by siRNA it is difficult to ascertain whether IFI16 has essential or redundant functions in initiating IFN- β production. Furthermore (Gray et al., 2016) propose that IFI16 is dispensable for IFN

production in response to hCMV infection in primary fibroblasts. However, it should be noted that the experiment the authors rely on for this conclusion examined IFN- β production using a CRISPR/Cas9 pool of partially depleted cells without selection, thus it is comparable to other depletion approaches such as siRNA. Therefore, the use of complete IFI16 knockout cell lines has afforded us conclusive insights into the role of IFI16 in innate immunity in keratinocytes (**Fig 3.1.4**).

We found that HaCaT cells lacking IFI16 are compromised in their ability to produce IFN- β , anti-viral cytokine or chemokine mRNAs in response to DNA, suggesting that IFI16 is required for complete activation of DNA sensing pathways in keratinocytes (**Fig 3.1.5-7**). We also show that HaCaT cells without IFI16 are compromised in their ability to produce CCL5 in response to a variety of different forms and concentrations of DNA or when faced with HSV1 infection (**Fig 3.1.8-9**). cGAS has been observed to be essential for DNA sensing in every cell type examined thus far (Gao et al., 2013a; Li et al., 2013b). Other experiments performed within our group have confirmed that cGAS is also essential for DNA sensing in keratinocytes (Almine et al., 2017). Therefore, these results indicate that neither IFI16 or cGAS is redundant for the immune response to DNA in keratinocytes and that there is co-operation between both receptors for functional DNA sensing in this cell type.

Since its discovery as a DNA sensor, IFI16 has been proposed to initiate IFN production via STING, albeit through an unknown mechanism (Unterholzner et al., 2010). In contrast, cGAS produces cGAMP which binds to directly to the cyclic dinucleotide cleft of STING, triggering its activation (Gao et al., 2013c; Sun et al., 2013a; Wu et al., 2013b). STING activation is measured by STING trafficking from the ER into activated punctuate structures at ERGIC. This results in the recruitment of TBK1 to STING, which undergoes auto-phosphorylation before phosphorylating STING and the transcription factor IRF3.

The STING pathway is shown to be dysfunctional in IFI16^(-/-) HaCaT cells in (**Fig 3.1.10 and 3.1.11**). In **Fig 3.1.10** we demonstrate that STING trafficking in response to DNA stimulation, widely regarded as an essential hallmark of STING activation, is

severely reduced in the IFI16^(-/-) HaCaT cells. While in **Fig 3.1.11** we confirm the downstream STING signalling pathway is not activated with DNA stimulation in the IFI16 knockout cell line. Cells lacking IFI16 show no activation of TBK1 or IRF3 in response to DNA while these responses persist with RNA stimulation (**Fig 3.1.11**). These results clearly show that IFI16 acts on the level of STING or is involved upstream in the STING signalling pathway. As is unlikely that IFI16 is able to produce cyclic di-nucleotides itself, one mechanism by which IFI16 could potentially function upstream of STING is by promoting cGAS activity thereby enabling cGAMP production.

Chapter Three Part Two

*IFI16 is does not influence
production of cGAMP in human
immortalised keratinocytes*

3.2.1 IFI16 and cGAS associate via DNA when initiating an immune response

The previous phase of this investigation established that the STING pathway was not activated in IFI16^(-/-) HaCaT cells. Yet these experiments were unable to elucidate whether IFI16 influences this phenotype by acting on STING itself or upstream of STING by influencing the activity of cGAS. To investigate the relationship between IFI16 and cGAS, we first wished to examine if IFI16 and cGAS formed a complex when initiating an immune response. Endogenous IFI16 was immunoprecipitated from Wild Type HaCaT cells to determine if IFI16 and cGAS come together during DNA sensing (**Fig 3.2.1**). IFI16^(-/-) cells were included as a measure of the specificity of the IFI16 antibody (**Fig 3.2.1**). IFI16 and cGAS were found to increasingly associate at 2 and 4 hours post DNA stimulation (**Fig 3.2.1**).

Both IFI16 and cGAS have the capacity to bind DNA in a sequence independent manner, albeit through different mechanisms. IFI16 binds to the sugar phosphate backbone of DNA via electrostatic charge from its HIN200 domains (Jin et al., 2012). Similarly, cGAS also binds the DNA sugar phosphate backbone by utilising a zinc thumb motif (Civril et al., 2013). We utilised HEK 293T cells which do not natively express either IFI16 (Unterholzner et al., 2010) or cGAS (Sun et al., 2013b), to express both DNA sensors and determine whether the association observed between IFI16 and cGAS is a direct protein-protein interaction or through IFI16 and cGAS binding to the same piece of DNA. HEK293T cells were transfected with FLAG-cGAS and either HA-IFI16 or HA-IFI16(mt4); a mutant of IFI16 containing several point mutations in the HIN200 domains which impair its ability to bind DNA (described further by Jin et al., 2012). **Fig 3.2.2** highlights that the association between IFI16 and cGAS is via a DNA binding platform, as cGAS does not associate with the IFI16(mt4) DNA binding mutant. The IFI16(mt4) maintains the IFI16 quaternary structure (Jin et al., 2012). This experiment also confirms this by showing that the interaction between wild type IFI16 and cGAS is no longer observed in samples when DNA is removed with Benzonase treatment (**Fig 3.2.2**).

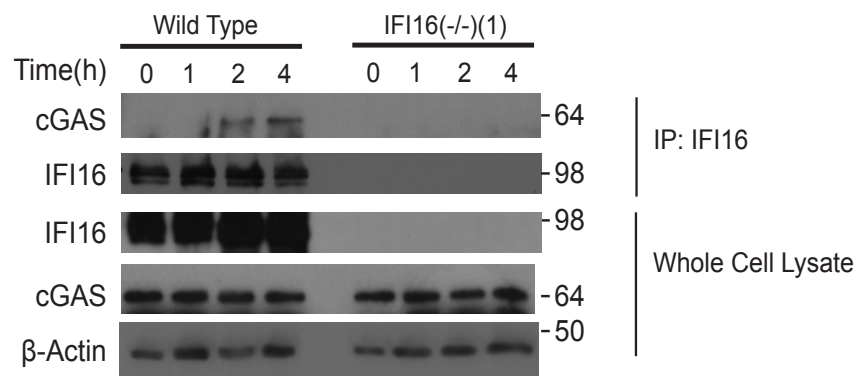


Fig 3.2.1 IFI16 and cGAS associate following DNA stimulation

IFI16 was immunoprecipitated from Wild Type and IFI16(-/-) HaCaT cell lines at 0, 1, 2 and 4h post HT DNA stimulation (5 µg/ml) using anti-IFI16(C-terminus). Immunoprecipitates were analysed for cGAS interactions by immunoblot analysis. Total cGAS, IFI16 and β-actin protein in lysates were determined by Western blot. Data shown are representative of two independent experiments.

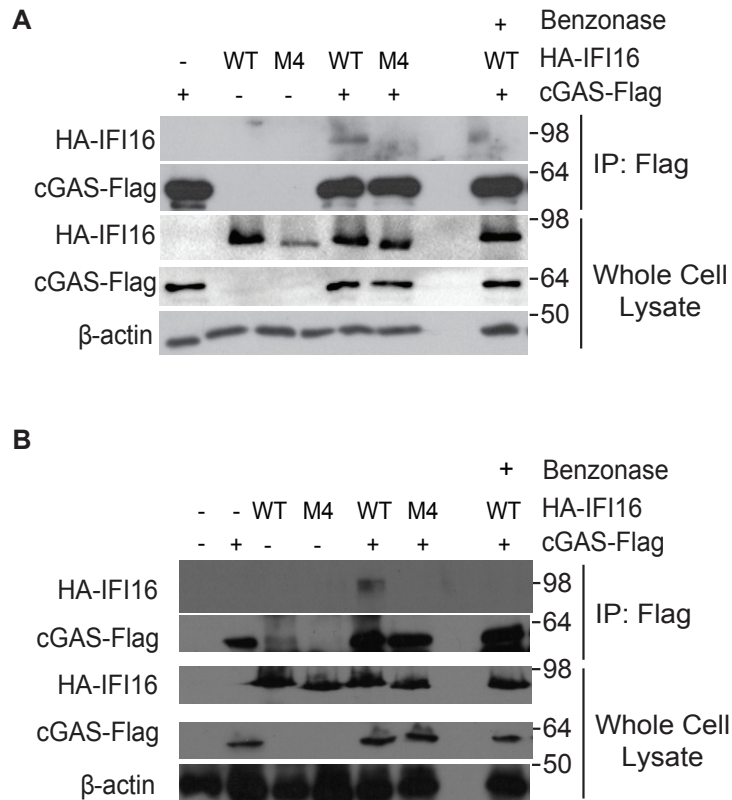


Fig 3.2.2 IFI16 and cGAS associate via DNA

HEK293T cells were transfected with 500ng/mL of cGAS-FLAG and HA-IFI16, either wild-type (WT) or DNA-binding mutant (M4), as indicated. 24 h post transfection, cells were lysed and immunoprecipitated using FLAG antibody. Immunoprecipitates were washed to remove EDTA and treated with 1.5 Units/uL of benzonase where indicated. Lysates and immunoprecipitates (IP) were analysed by SDS-PAGE and western blotting. (A) and (B) are representative of two independent experiments.

3.2.2 Overview of method to extract cGAMP for quantification using LC-MS/MS

The observation that IFI16 and cGAS associate on the same piece of DNA prompts speculation that IFI16 could influence cGAS function. To definitively determine whether IFI16 effects cGAS activity, it was necessary to devise a method to directly measure cGAMP production.

Through collaboration with the Fingerprints Proteomics Service at the University of Dundee, we developed a method for quantifying cGAMP produced in cell lysates using a combined liquid chromatography and mass spectrometry (LC-MS/MS) approach (**outlined in Fig 3.2.3**). Experiments performed to optimise and refine individual components of this method will be described in **3.2.4**. To simplify detection, samples were enriched for cGAMP and similar small molecules. Cells were stimulated with DNA to induce cGAMP production and harvested into cell pellets. Cell pellets were lysed in ice cold solutions of 80% methanol to precipitate proteins and nucleic acids, leaving only small molecules and lipids in solution. 0.45 pmoles of cyclic-di-AMP were added to each sample as internal spike-in to control for losses in sample preparation and injection. Samples were dried using vacuum centrifugation. Lipids were removed through butanol liquid-liquid extraction as described by (Turnock and Ferguson, 2007). Specifically, samples were dissolved in 9% Butanol:H₂O and extracted three times with 90% Butanol:H₂O. Lipids present in the sample move to the upper phase which contains a higher percentage of butanol, in which lipids more readily dissolve. The upper phase is removed during subsequent rounds of extraction leaving only small molecules in the hydrophilic lower phase. The lower phase was dried using vacuum centrifugation to remove butanol from the samples. Samples were resuspended in HiPerSolv H₂O. Samples were further enriched for cyclic di-nucleotides using Hypersep Aminopropyl Solid Phase Extraction columns (Thermo) and later, eluted from columns with a solution of 80% Methanol and 4% Ammonium Hydroxide. Eluates were dried once more using vacuum centrifugation and resuspended in HiPerSolv H₂O for analysis by LC-MS/MS.

3.2.3 Detection of Cyclic Di-Nucleotides by LC-MS/MS

The Fingerprints Proteomics facility utilised a TSQ Quantiva triple quadrupole mass spectrometer interfaced with a Dionex Ultimate 3000 Liquid Chromatography system (Thermo) equipped with a porous graphitic carbon column (HyperCarb 30 × 1 mm ID 3µm; Part No: C-35003-031030, Thermo-Scientific) for sample analysis. Samples were injected onto the liquid chromatography column where their small molecule content was separated based on size and polarity. Each small molecule fraction was then eluted into the mass spectrometer for identification.

Multiple reaction monitoring mass spectrometry was used to identify compounds. Multiple reaction monitoring is highly specific as the first and last mass analysers of the quadrupole mass spectrometer are used as filters to select for a fragment ion of a compound and monitor the abundance of its corresponding daughter ions (Reviewed by Shi et al., 2016). The relative abundance of the daughter ions is measured as function of elution time. The fragmentation step produces specific fragments with mass to charge ratios that are characteristic of each compound of interest as each compound will fragment in a unique way. While highly selective, one disadvantage of multiple reaction monitoring is that significant optimisation is required to determine the optimal elution conditions and mass spectrometry parameters for each compound of interest.

To determine whether cyclic di-nucleotides were compatible with this system and to determine their optimum conditions for elution and detection, 50pg of synthetic cGAMP, cyclic di-AMP and cyclic di-GMP were injected into the LC-MS/MS. As highlighted in **Fig 3.2.4A**, all three cyclic di-nucleotides were eluted from the LC column with distinct retention times. Based on these peaks, cyclic di-AMP was selected for use as an internal standard during sample preparation as cyclic di-GMP was observed to elute over a broader peak. The m/z transitions used for detection of cGAMP and cyclic di-AMP are depicted in **Fig 3.2.4B**.

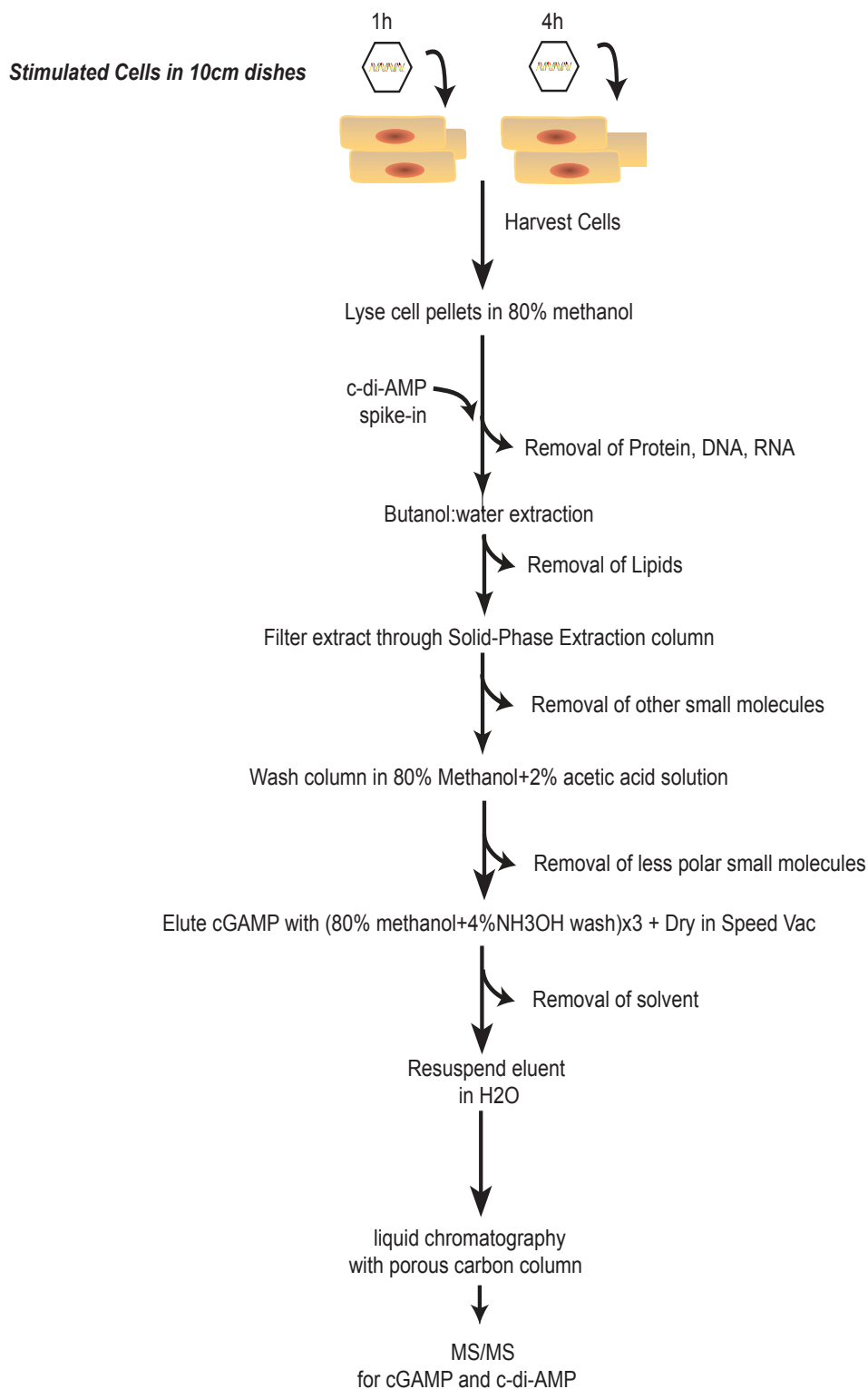
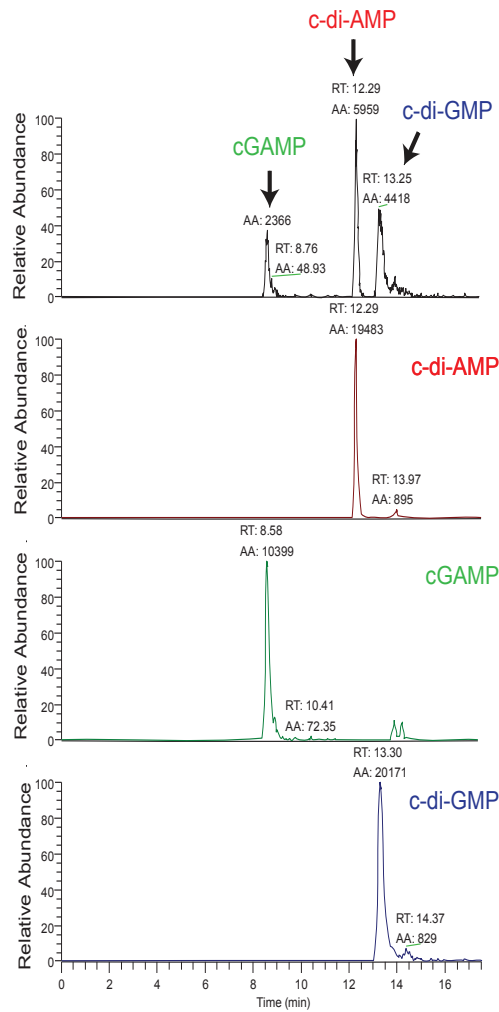


Fig 3.2.3 Schematic of cGAMP extraction protocol

Wild Type and IFI16(-/-) cells are stimulated with (1ug/mL) HT-DNA during a time course to initiate cGAMP production. Samples are scraped into cell pellets and subsequently lysed in a cold solution methanol to precipitate proteins and nucleic acids. The internal standard cyclic di-AMP is added to samples. Samples are then dried under a vacuum and subjected to three rounds of buthanol:water extraction to remove lipids. Dried samples are resuspended in HiPerSolv H₂O and enriched for small nucleotide molecules using aminopropyl solid phase extraction columns. Columns are washed to reduce background from other small molecules and metabolites. cGAMP was eluted from columns in a solution of 80% methanol+4%NH₃OH, which was flushed through the column three times. Column eluents are dried and analysed for cyclic di-AMP and cGAMP by liquid chromatography and mass-spectrometry.

A



B

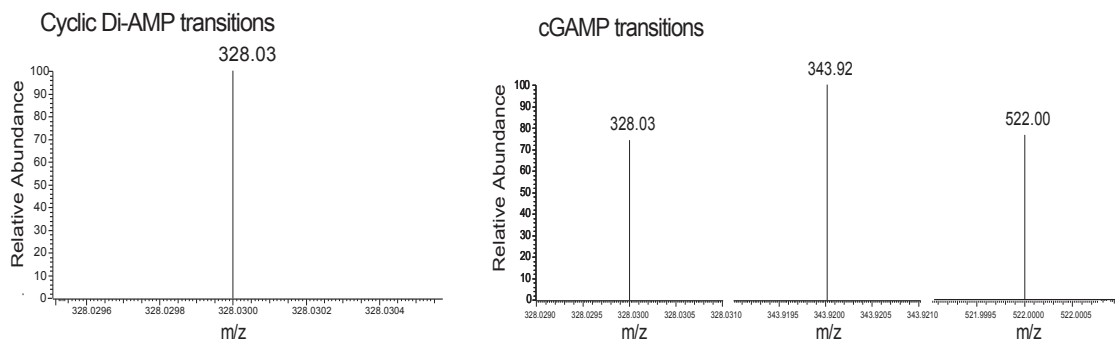


Fig 3.2.4 Detection of cGAMP and ci-di-AMP standards by Liquid Chromatography-Mass Spectrometry

(A) 50pg of synthetic cGAMP, cyclic di-AMP and cyclic di-GMP standards analysed by LC-MS. RT; Retention Time, AA: Area of curve (B) cGAMP and cyclic di-AMP multiple reaction monitoring transitions used for endogenous cGAMP quantification. m/z , mass/charge ratio of fragment ions

3.2.4 Optimisation and refinement steps for cGAMP extraction method:

a) Optimisation of solid phase extraction step:

Solid phase extraction columns were utilised to enrich samples for cGAMP and remove other small molecules such as metabolites and nucleotides. Sample purification using solid phase extraction was deemed necessary as the presence of other small molecules in the sample appeared to be impeding the ability of cGAMP to bind the LC column; resulting in inefficient cGAMP binding and early elution (**Fig 3.2.5**) when compared to synthetic cGAMP standards on a background of HiPerSolv H₂O (**Fig 3.2.4A**).

A range of solid phase extraction columns were tested for their ability to bind and retain cGAMP (**Fig 3.2.6**). The ideal solid phase extraction column would reversibly bind cGAMP and retain no cGAMP on the column after elution. Envi-Carb columns (Sigma Aldrich) utilise graphitized porous carbon matrixes to bind planar molecules in aqueous solutions. WAX columns (Oasis) rely on a neutral primary amine modified divinyl benzene polymer to bind molecules based on anion exchange. Aminopropyl columns (Thermo) use a modified silica polymer bonded to an aminopropyl phase. We suspect WAX and Aminopropyl columns bind the negatively charged phosphates of cGAMP based on their chemistry.

Each solid phase extraction column was tested for its ability to bind cGAMP by loading 20µg cGAMP in a 1mL solution onto each column. cGAMP was loaded onto the Envi-Carb column in a 1M solution of sodium bicarbonate and in H₂O for WAX and Aminopropyl columns. Each column was then washed with a concentration gradient of different elution buffers based on their individual chemistries. As cGAMP possess pyrimidine and imidazole rings in its structure, each column fraction could be examined for the presence of cGAMP by measuring cGAMP's absorbance at 260nm on a nanodrop instrument. While both Envi-Carb and WAX columns were capable of binding cGAMP, both columns retained a significant portion of cGAMP after elution with a concentration gradient of acetyl nitrile (Envi-carb) or ammonium acetate (WAX), rendering them unsuitable for use with biological samples. As illustrated in

Fig3.2.6, the Aminopropyl column retained no cGAMP following elution with 80% methanol and a concentration gradient of ammonium hydroxide, and thus was suitable for use with biological samples. Endogenous cGAMP produced in samples was found to elute with the same retention time as the synthetic cGAMP standard with in LC-MS following sample enrichment with Aminopropyl columns (**Fig3.2.7**).

b) Optimisation of cell lysis conditions:

When this protocol was originally designed samples were initially lysed in 70% Ethanol. However as highlighted in **Fig3.2.7A** this resulted a high background of other small molecules during LC-MS/MS analysis. While developing this method a similar cGAMP quantification protocol was published by (Rongvaux et al., 2014). Lysis of cells with 80% methanol and washing aminopropyl columns with a solution of 80% Methanol and 2% acetic acid prior to elution, as advised by this protocol, reduced the background signal without diminishing the yield of cGAMP (**Fig3.2.7B**).

c) Optimisation of endogenous cGAMP production and detection conditions:

A cGAMP standard curve was constructed to enable the quantification of endogenous cGAMP production and to determine the detection limit of the mass spectrometer. Increasing amounts of synthetic cGAMP were spiked into unstimulated cell lysates. Samples were then processed as outlined in (3.2.2). As illustrated in **Fig 3.2.8A**, we were able to successfully detect increasing levels of cGAMP starting from a detection limit of 3 picograms, which corresponds to 4.5 femtomoles of cGAMP.

To confirm that cGAMP is produced by HaCaT cell lines, wild type HaCaT cells were stimulated with a range of HT-DNA concentrations for 8 hours. cGAMP levels in samples were quantified using the standard curve in **Fig 3.2.8A**. As highlighted in **Fig 3.2.8B**, cGAMP is produced upon DNA stimulation with increasing concentrations of DNA stimulation generally increasing the amount of cGAMP produced. Untreated and mock transfected samples display low basal levels of cGAMP. Treatment of DNA

treated samples with snake venom phosphodiesterase (**Fig 3.2.8C**) removed this cGAMP peak as would be expected based on observations by (Ablasser et al., 2013b). While we were confident we were measuring cGAMP production due the m/z transitions obtained from the cGAMP standard by multiple reaction monitoring, these experiments provide biological evidence that the compound were observe being produced is cGAMP.

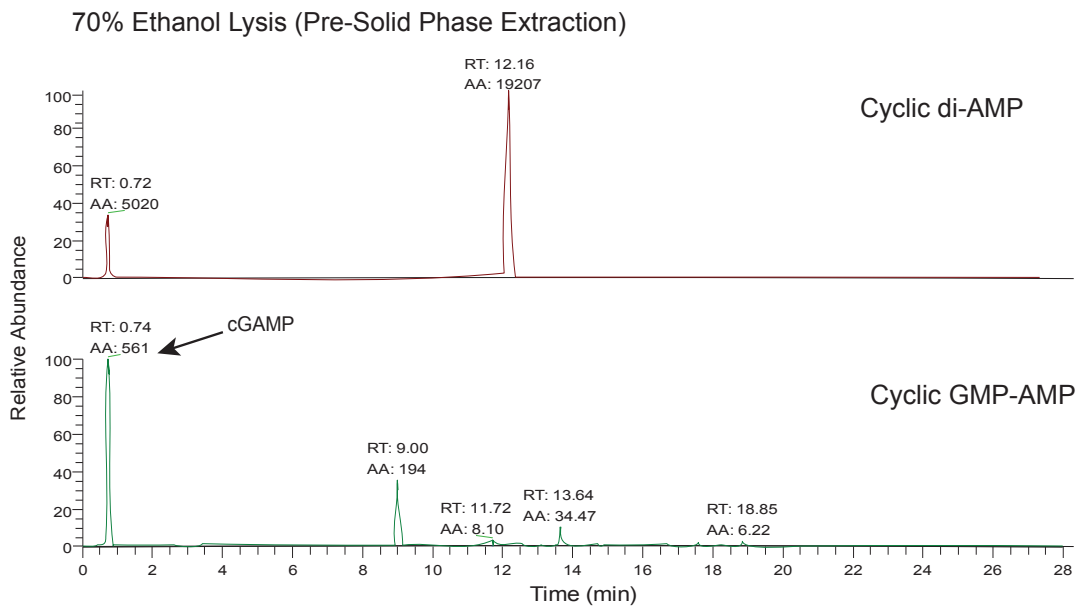


Fig 3.2.5 cGAMP from neat lysates elutes early from the liquid chromatography graphitised carbon column

LC-MS traces of Wild Type HaCaT lysates following stimulation with (1ug/mL) HT-DNA for 4 hours. Samples were lysed in 70% ethanol. Data shown are representative of two independent experiments. RT; retention time. AA; Area under the curve

Envi-carb Column		WAX Column		NH ₂ Column	
Input	Absorbance (260nm)	Input	Absorbance (260nm)	Input	Absorbance (260nm)
20µg/mL cGAMP (1M Amm. Bi-Carbonate Soln)	0.654	20µg/mL cGAMP soln (H ₂ O)	0.583	20µg/mL cGAMP soln (H ₂ O)	0.680
Flow Through	0.002	Flow Through	0.000	Flow Through	0.013
H ₂ O Wash	0.000	H ₂ O Wash	0.017	H ₂ O Wash	0.001
Acetyl-Nitrate Wash	0.000	100 mM NH ₃ Acetate Elute	0.034	80% Methanol Wash	0.025
Tetra-Acetic Acid Wash	0.000	200 mM NH ₃ Acetate Elute	0.091	80% Methanol+4% Amm.OH Elution (Round 1)	0.889
25% Acetyl-Nitrate Elution Round 1	0.089	300 mM NH ₃ Acetate Elute	0.119	80% Methanol+4% Amm.OH Elution (Round 2)	0.900
25% Acetyl-Nitrate Elution Round 2	0.197	400 mM NH ₃ Acetate Elute	0.126	80% Methanol+4% Amm.OH Elution (Round 3)	0.827
25% Acetyl-Nitrate Elution Round 3	0.325	500 mM NH ₃ Acetate Elute	0.083	80% Methanol+8% Amm.OH Elution	0.026
40% Acetyl-Nitrate Elution	0.002	600 mM NH ₃ Acetate Elute	0.046	80% Methanol+10% Amm.OH Elution	0.007
45% Acetyl-Nitrate Elution	0.004	700 mM NH ₃ Acetate Elute	0.002	80% Methanol+12% Amm.OH Elution	0.008
Amount Retained by Column	0.329	Amount Retained by Column	0.084	Amount Retained by Column	0.000
Remaining absorbance approximated to µg cGAMP	10.057	Remaining absorbance approximated to µg cGAMP	2.876	Remaining absorbance approximated to µg cGAMP	0.000

Input	Flow Through	Wash Step(s)	Elution Step(s)
			

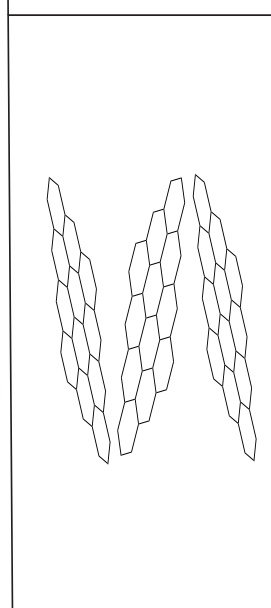
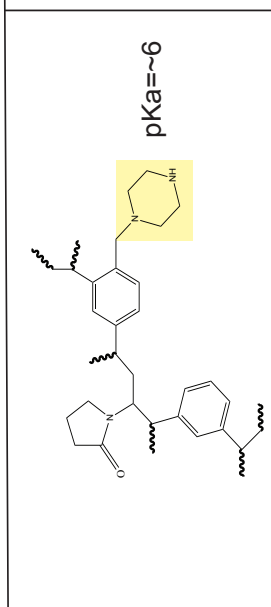
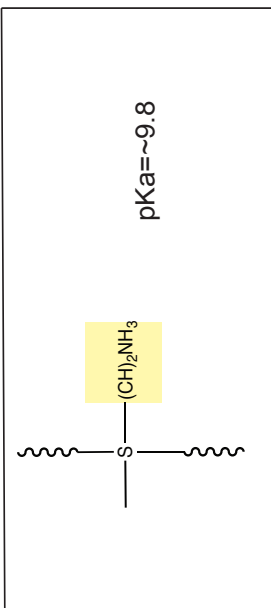


Fig 3.2.6 Comparison of Solid Phase Extraction Columns

Comparison of Envi-Carb, WAX and NH₂ solid phase extraction columns efficiency for isolating cGAMP and their individual chemistries. A 20µg/mL solution of cGAMP is quantified at 260nm and added to each solid phase extraction column. The absorbance of the flow through and each eluent fraction is measured at 260nm and used to assess the ability of the column to bind and retain cGAMP. Data shown are representative of two independent experiments

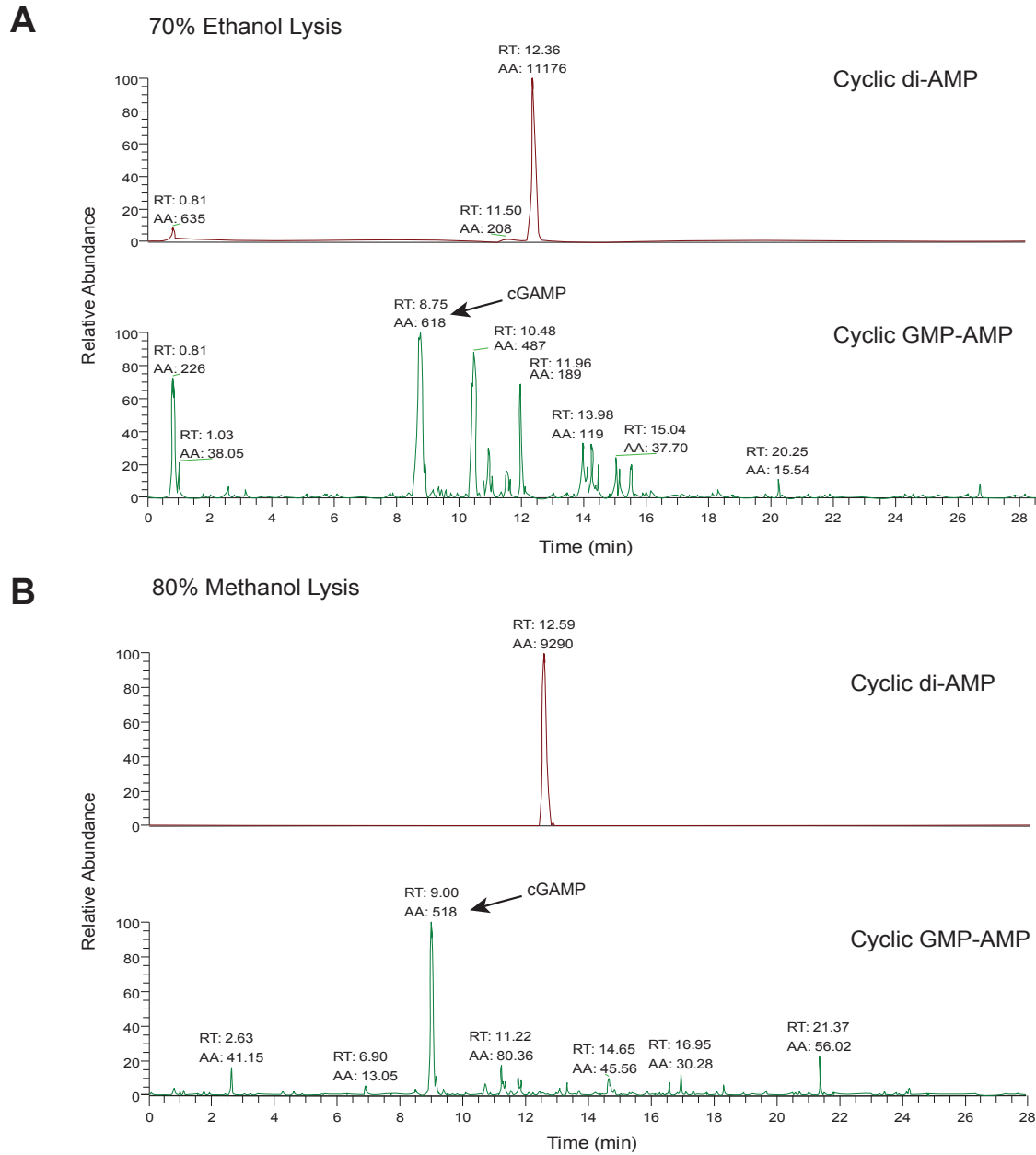


Fig 3.2.7 Optimisation of lysis conditions for cGAMP quantification

(A-B) LC-MS traces of Wild Type HaCaT lysates following stimulation with (1ug/mL) HT-DNA for 4 hours. Samples were lysed in 70% ethanol(**A**) or 80% methanol(**B**) and processed through aminopropyl columns. Data are representative of two independent experiments. RT; retention time. AA; Area under the curve

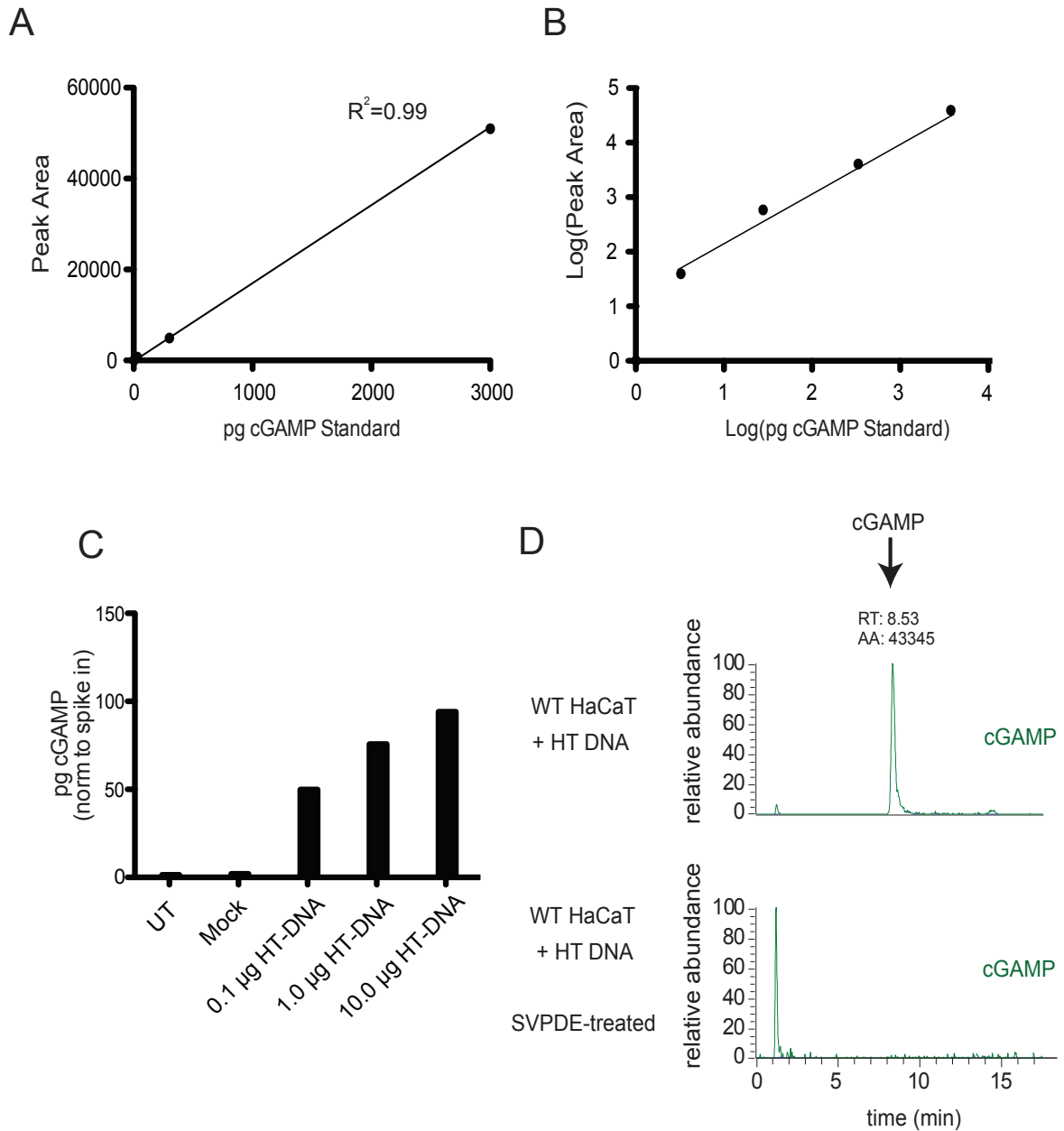


Fig 3.2.8 Verification of endogenous cGAMP production in HaCaT cell lines

(A) Standard curve of synthetic cGAMP spiked into cell lysates and enriched through solid phase extraction columns prior to liquid chromatography and mass spectrometry (LC-MS) analysis. **(B)** Log of Standard Curve. **(C)** Quantification of cGAMP production in WT and IFI16(-/-) cell lines post 8 hours stimulation with increasing concentrations of HT-DNA using reference values from **(B)**. Single injection of one biological sample shown. **(D)** cGAMP extracted LC-MS traces of WT HaCaT cell lines post 4 hours stimulation with 1 µg/ml HT DNA (top) and from parallel lysates treated with 0.05U snake venom phosphodiesterase for 1 h (bottom) prior to solid phase extraction. Data are representative of a single experiment RT: Retention Time AA: Area under the curve

3.2.5 IFI16 does not influence production of cGAMP in HaCaT cells

Production of cGAMP was examined between wild Type and *IFI16*^(-/-) cell lines. HaCaT cell lines were stimulated in triplicate with 1µg/mL of HT-DNA or VACV 70mer for 8 hours, cells were then lysed and cGAMP production was quantified using a standard curve (**Fig 3.2.9**). The standard curve was produced by spiking in increasing amounts of synthetic cGAMP into unstimulated Wild type cell lysates and subjecting the samples to solid phase extraction (**Fig 3.2.9A**). As demonstrated in **Fig 3.2.9B-C** Wild Type and *IFI16*^(-/-) cell lines were found to produce comparable levels of cGAMP in response to both forms of DNA stimulation. These results demonstrate that IFI16 has no role influencing cGAS activity in HaCaT cell lines.

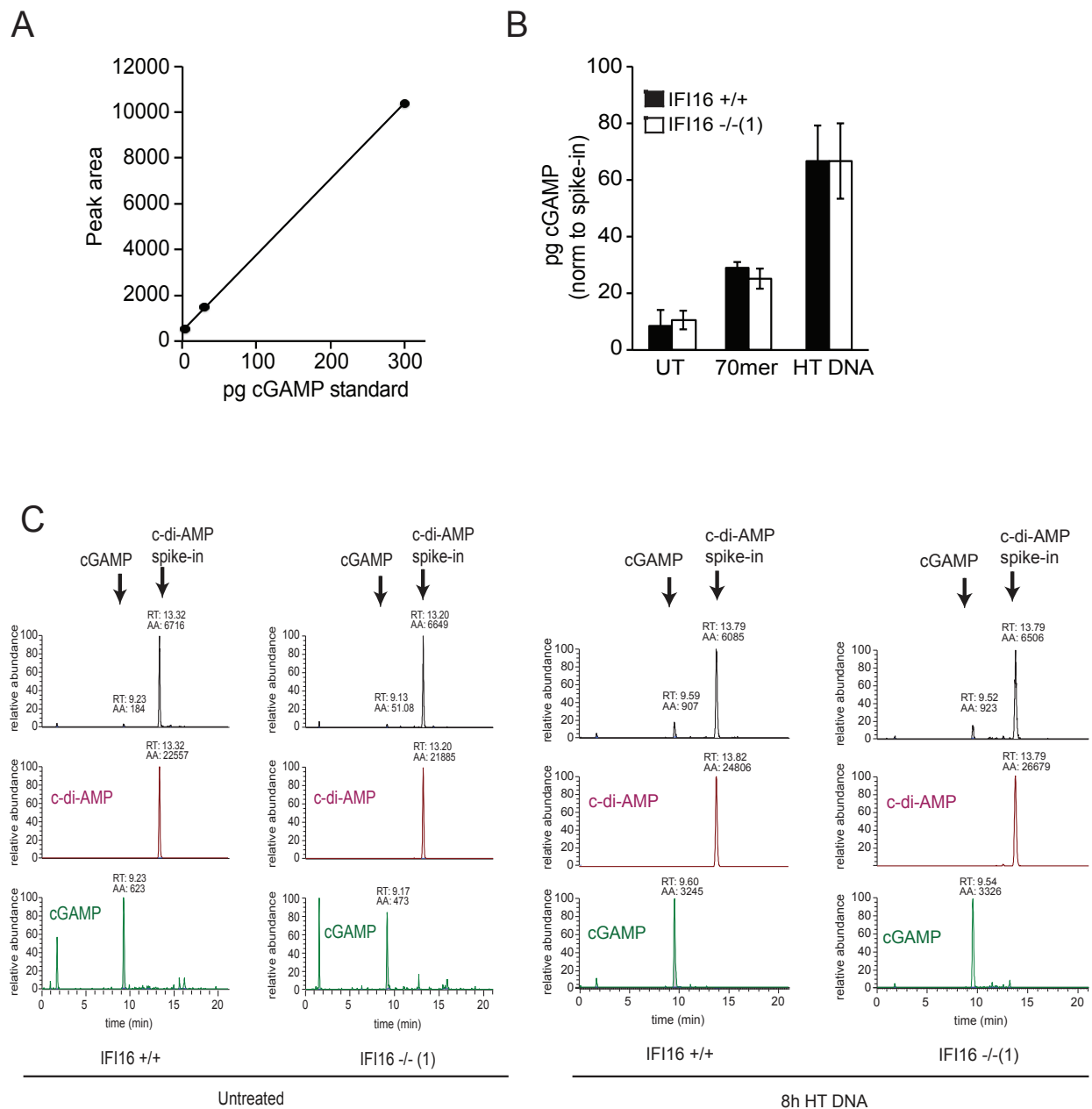


Fig 3.2.9 IFI16 does not influence cGAMP production in HaCaT Cell lines

(A) Standard curve of synthetic cGAMP spiked into cell lysates and enriched through solid phase extraction columns prior to liquid chromatography and mass spectrometry (LC-MS) analysis. (B) Quantification of cGAMP production in WT and IFI16(-/-) cell lines post 8 hours stimulation with (1 μ g/mL) VACV 70mer or HT-DNA, using reference values from (A). (C) LC-MS traces of cGAMP and cyclic-di AMP obtained from samples depicted in (B). One of triplicate of three biological replicates shown. Data are representative of three independent experiments. RT; Retention Time. AA; Area of curve

3.2.6 Discussion:

IFI16 and cGAS both bind to DNA in a sequence-independent manner through the DNA sugar phosphate backbone (Civril et al., 2013; Jin et al., 2012). In-vitro analyses of both DNA sensors have revealed more about their respective DNA-binding affinities and higher order structures upon binding DNA. (Morrone et al., 2014) demonstrate IFI16 co-operatively assembles into filaments along dsDNA oligomers. This observation has provoked speculation that IFI16 may recognise pathogen DNA over host DNA based on DNA length. IFI16 was found to possess a nanomolar affinity for DNA binding. cGAS is believed to bind to the ends of DNA strands as dimers (Li et al., 2013a; Zhang et al., 2014b). Recently, cGAS has also been observed to bind bends and U-turns in DNA created by bacterial and mitochondrion nucleoid proteins HU and mitochondrial transcription factor A, and HMGB1 (Andreeva et al., 2017). However recent studies have shown that the N-terminus of cGAS de-oligomerises cGAS DNA dimers into 1:1 complexes which been recently found to enhance cGAS activity (Lee A et al., 2017; Tao et al., 2017). cGAS possesses comparatively weaker DNA binding affinity than IFI16, binding DNA in the micromolar range (Li et al., 2013a). Human cGAS has been shown to be activated by dsDNA oligonucleotides of at least 40 base pairs in length (Civril et al., 2013; Gao et al., 2013b; Kranzusch et al., 2013). The exception are the short ssDNA stem-loops structures from retroviral transcripts. These are shorter than 40 base pairs in length yet remain potent activators of cGAS (Herzner AM et al., 2015). Y-DNAs (i.e. synthetic oligomers of retrovirus ssDNA transcripts) containing unpaired guanine between 12-20 base pairs in length have also been found to activate cGAS. IFI16 has also been observed to detect HIV DNA stem loop structures (Jakobsen et al., 2013).

When these observations are considered together, IFI16 and cGAS appear to have distinct but not necessarily competing roles in DNA binding. We observe an association between IFI16 and cGAS upon DNA stimulation (**Fig 3.2.1**). Using HEK 293T cells, we determine this association to be dependent on DNA acting as a binding platform due to reduced associations between cGAS and IFI16 when the ability of IFI16 to bind DNA is compromised or if DNA is removed by nuclease treatment (**Fig 3.2.2**).

To conclusively assess if IFI16 influenced the activity of cGAS, we developed and optimised an LC-MS/MS based approach to quantify cGAMP production with femtomolar sensitivity (**Fig 3.2.3**). Synthetic cGAMP was used to determine the elution conditions and optimal phase transitions for cGAMP for multiple reaction monitoring mass spectrometry (**Fig 3.2.4**). Samples were also enriched for cGAMP by optimising solid phase extraction and cell lysis conditions (**Fig 3.2.5-7**). We also confirmed that we were monitoring cGAMP production by confirming that the compound is produced only upon DNA stimulation and by monitoring its corresponding breakdown with snake venom phosphodiesterase as observed by (Ablasser et al., 2013b) (**Fig 3.2.8**).

Although IFI16 and cGAS were found to assemble on the same DNA platform, we observed no change in cGAMP levels between wild type and IFI16^(-/-) cell lines post-stimulation with two forms of DNA (**Fig 3.2.9**). This suggests in keratinocytes that IFI16 does not influence cGAS activity and acts in a complementary manner to cGAS, activating STING during DNA sensing as initially proposed by (Unterholzner et al., 2010).

Chapter Three Results

Part Three

*IFI16 facilitates activation of
STING during DNA sensing in
human immortalised keratinocytes*

3.3.1 *IFI16*^(-/-) HaCaT cells display impaired responses to cGAMP stimulation

Previous experiments in this investigation have established that the STING pathway is not activated in *IFI16*^(-/-) HaCaT cells (**Fig 3.1.11**). By establishing a method to measure cGAMP levels we have also learnt that this cannot be explained by IFI16 influencing cGAS activity, as wild type and *IFI16*^(-/-) HaCaT cells produce equivalent amounts of cGAMP (**Fig 3.2.9**). These results confirm that IFI16 acts in parallel to cGAS and upstream of STING as originally proposed by (Unterholzner et al., 2010), and suggest that IFI16 enables activation of STING after cGAMP is produced.

To investigate whether responses to cGAMP were dependent on IFI16, wild type and *IFI16*^(-/-) cells were directly stimulated with cGAMP; bypassing cGAS function and cGAMP production. Cytokine mRNAs induced by cGAMP stimulation were measured by RT-PCR 6 hours post-stimulation (**Fig 3.3.1**). **Fig 3.3.1** demonstrates that the response to cGAMP is impaired in the absence of IFI16. *IFN-β*, *ISG56*, *Interleukin-6*, *CXCL10* and *CCL5* mRNA production is reduced in response to cGAMP and HT-DNA stimulation in *IFI16*^(-/-) HaCaT cells (**Fig 3.3.1 A-E**). cGAMP stimulation by lipofection induces a comparatively poor response to DNA stimulation in both cell lines. To verify that these results were not an artefact of our choice of delivery mechanism, we also infused cGAMP using digitonin permeabilisation when examining CCL5 production by ELISA (**Fig 3.3.1F**) as described by (Jonsson et al., 2017). **Fig 3.3.1F** demonstrates that cGAMP induced CCL5 protein secretion was also reduced in the absence of IFI16, confirming the RT-PCR results. These results indicate that IFI16 enables STING to respond to cGAMP stimulation.

3.3.2 STING and IFI16 associate during DNA stimulation

STING and IFI16 interactions were investigated to try to understand how IFI16 could influence the ability of STING to respond to cGAMP. STING was immunoprecipitated from wild type HaCaT cells and examined for interactions with IFI16 (**Fig 3.3.2**). In **Fig 3.3.2** we find that there is a weak constitutive association between STING and IFI16, and that IFI16 increasingly associates with STING following DNA stimulation.

We suspect that this interaction is dynamic in keratinocytes as no IFI16 and STING co-localisation was observed by immunofluorescence (**Fig 3.1.10**).

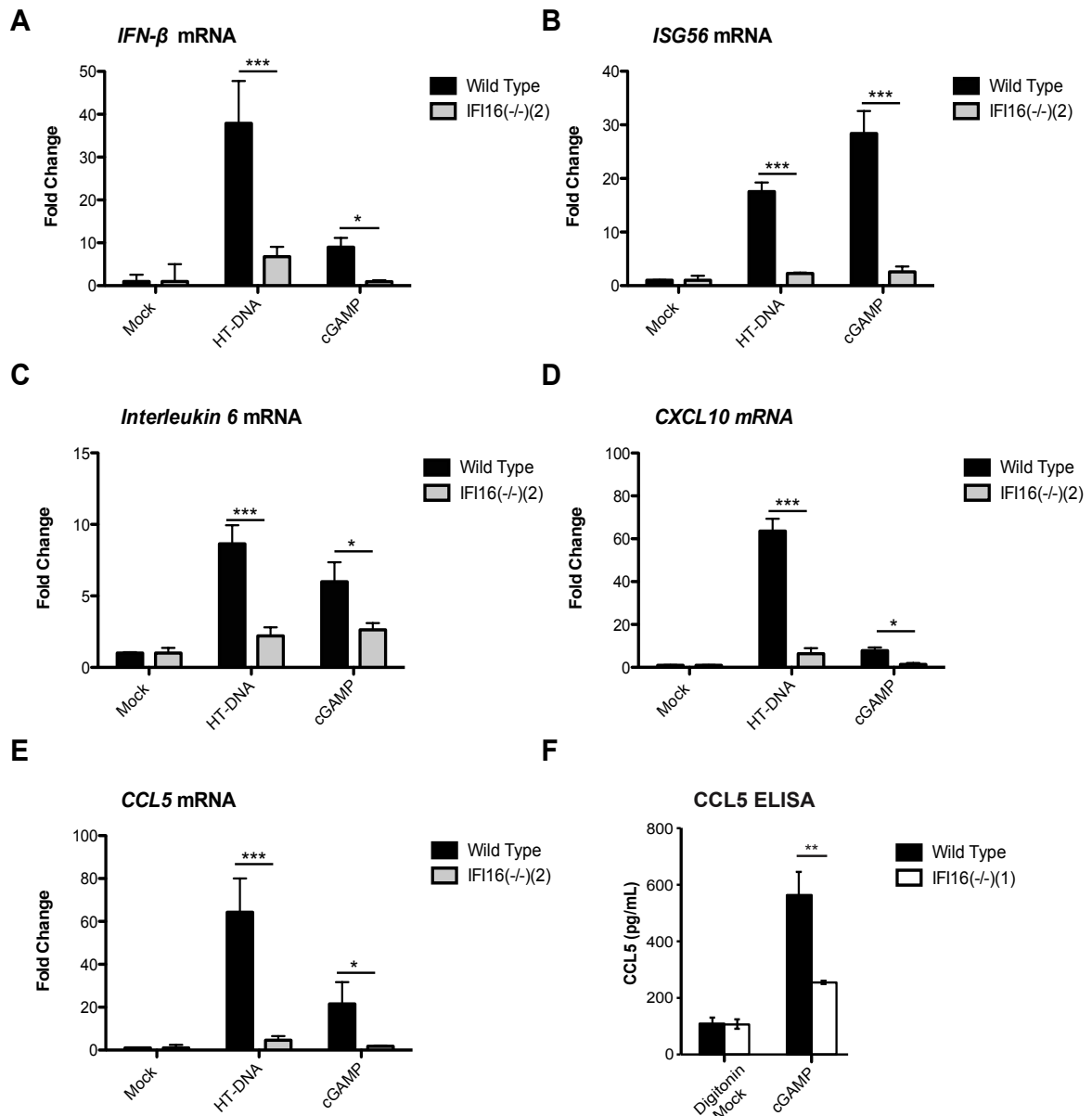


Fig 3.3.1 IFI16(-/-) HaCaT cell lines display impaired responses to cGAMP stimulation

(A-E) HaCaT cells were stimulated with 1µg/mL HT-DNA, 20µg/mL cGAMP or 1µL/mL Lipofectamine alone (Mock) for 6 hours. IFN-β (A), ISG56 (B), Interleukin-6 (C), CXCL10 (D) and CCL5 (G) levels were measured by Real-Time PCR. (F) HaCaTs were infused with 15µM cGAMP or digitonin media containing (5mg/mL) alone for 18 hours. Supernatants were collected and examined for CCL5 production by ELISA. Experiments were carried out with triplicate samples, mean values and standard deviation are shown. Data are representative of three independent experiments. Statistical significance was determined using two-way ANOVA. p-value: * = P < 0.05, ** = P < 0.01, *** = P < 0.001

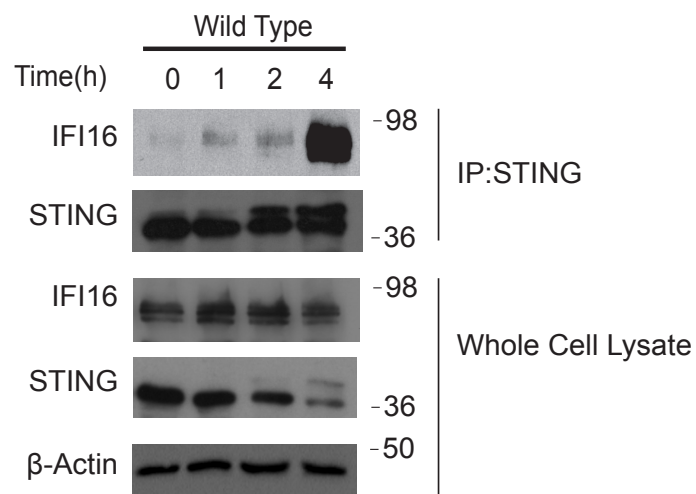


Fig 3.3.2 IFI16 and STING association increases following DNA Stimulation

STING was immunoprecipitated from HaCaT cells at 0, 1, 2 and 4h post stimulation with HT DNA (5 μ g/ml). Immunoprecipitates were analysed for IFI16 interactions by immunoblot analysis. STING, IFI16 and β -actin protein in lysates was determined by Western blot. Data are representative of three independent experiments.

3.3.3 Discussion

It is widely acknowledged that STING is required for IFN induction in response to cytoplasmic DNA, yet how STING was activated during responses to DNA was initially elusive (Ishikawa, 2008; Ishikawa et al., 2009; Sun et al., 2009; Zhong et al., 2008). Although (Abe et al., 2013) report that STING recognises DNA directly, there is a wider consensus that STING functions as an adapter molecule to induce IFN with other proteins upstream of STING detecting DNA such as IFI16 and cGAS (Reviewed by Unterholzner, 2013). STING was then found to directly bind cyclic di-nucleotides; cyclic di-AMP and cyclic di-GMP from bacteria and endogenously produced cGAMP (Burdette et al., 2011; Wu et al., 2013b). Upon binding the cyclic di-nucleotide binding cleft of STING; cyclic di-nucleotides are understood to induce a conformational change in STING enabling its activation. (Diner et al., 2013; Gao et al., 2013c; Zhang et al., 2013).

STING signalling is impaired in *IFI16*^(-/-) HaCaT cell lines (**Fig 3.1.11**). However, this is not due to IFI16 influencing cGAS activity as wild type and *IFI16*^(-/-) cells produce similar levels of cGAMP post stimulation with DNA (**Fig 3.2.9**). We also observed impaired responses to direct cGAMP stimulation in *IFI16*^(-/-) cells (**Fig 3.3.1**). These observations lead us to suspect that IFI16 must act upon STING to enable its activation post cGAMP production.

STING activation is associated with a range of post-translational modifications such as ubiquitination with K11, K27, K48 and K63 ubiquitin chains, SUMOylation and phosphorylation on several residues (Hu et al., 2016; Konno et al., 2013; Liu et al., 2015a; Ni et al., 2017; Qin et al., 2014; Sun et al., 2009; Tsuchida et al., 2010; Wang et al., 2014; Zhang, 2012; Zhong et al., 2008; Zhong et al., 2009). STING is also subject to the influence of a growing number of regulators including NLRC3 (Zhang et al., 2014a), iRhom2 (Luo et al., 2016) and NLRX (Guo et al., 2016). We detect a constitutive association between IFI16 and STING which increases with DNA stimulation (**Fig 3.3.2**), supporting the idea that IFI16 provides an activating signal to STING to facilitate cGAMP responses.

A dynamic IFI16 and STING interaction supports the idea that IFI16 could somehow influence STING signalling in response to cGAMP. IFI16 could affect STING function directly or indirectly by allowing STING post-translational modification. We have already observed that *IFI16*^(-/-) cell lines display reduced STING trafficking and phosphorylation following DNA stimulation within this investigation (**Fig 3.1.10-11**). Additional experiments within our group have identified that *cGAS*^(-/-) HaCaT cell lines display reduced STING phosphorylation upon DNA stimulation (Almine et al., 2017). cGAMP binding is also necessary for STING trafficking (Ablasser et al., 2013b). The association between IFI16 and STING provides further evidence that IFI16 and cGAS provide separate but complementary signals to STING to enable full STING activation.

Chapter Three Results

Part Four

*IFI16 promotes STING
palmitoylation during DNA
sensing in human immortalised
keratinocytes*

3.4.1 Palmitoylation regulates protein trafficking and ligand binding

Recently it has been demonstrated that STING palmitoylation is essential for immune responses to DNA (Mukai et al., 2016). Palmitoylation enables protein trafficking to cholesterol-rich lipid rafts (Reviewed by Linder and Deschenes, 2006). Palmitoylation can also influence the steric orientation of a protein in a membrane with consequences over ligand binding capabilities (Reviewed by Goddard and Watts, 2012). We elected to investigate if IFI16 influenced STING palmitoylation due to the reduced STING trafficking (**Fig 3.1.10**) and impaired response to cGAMP stimulation we observe in IFI16^(-/-) HaCaT cells (**Fig 3.3.1**).

3.4.2 Overview of acyl-RAC method of studying palmitoylation

A modified form of S-acylation resin assisted capture (acyl-RAC) was employed to investigate STING palmitoylation (Forrester et al., 2011) (**Fig 3.4.1**). Briefly, samples were lysed in 2x palmitoylation lysis buffer and mixed with N-ethylmaleimide to irreversibly block free cysteines with an imide functional group. Proteins were then extracted from solution using chloroform-methanol precipitation and re-dissolved in 1x palmitoylation lysis buffer containing 8M urea. Samples were then split in two and mixed with either H₂O or hydroxylamine. Hydroxylamine removes palmitate from proteins, exposing cysteines for binding with thiopropyl sepharose 6b(TPS) beads. H₂O treated samples preserve their palmitoylated cysteines and therefore cannot be pulled down by TPS beads. Thus, protein palmitoylation is assessed by removing palmitate from proteins to enable TPS bead pulldowns, allowing for subsequent analysis by western blot.

3.4.3 Optimisation of conditions for detecting STING palmitoylation

We first investigated STING palmitoylation one hour post DNA stimulation, as STING was previously observed to have trafficked at this time point (**Fig 3.1.10**) and palmitoylation is known to facilitate protein movement into cholesterol rich lipid rafts for signalling (Reviewed by Linder and Deschenes, 2006). As illustrated in **Fig 3.4.2A**, STING is found to be constitutively palmitoylated and STING palmitoylation does not

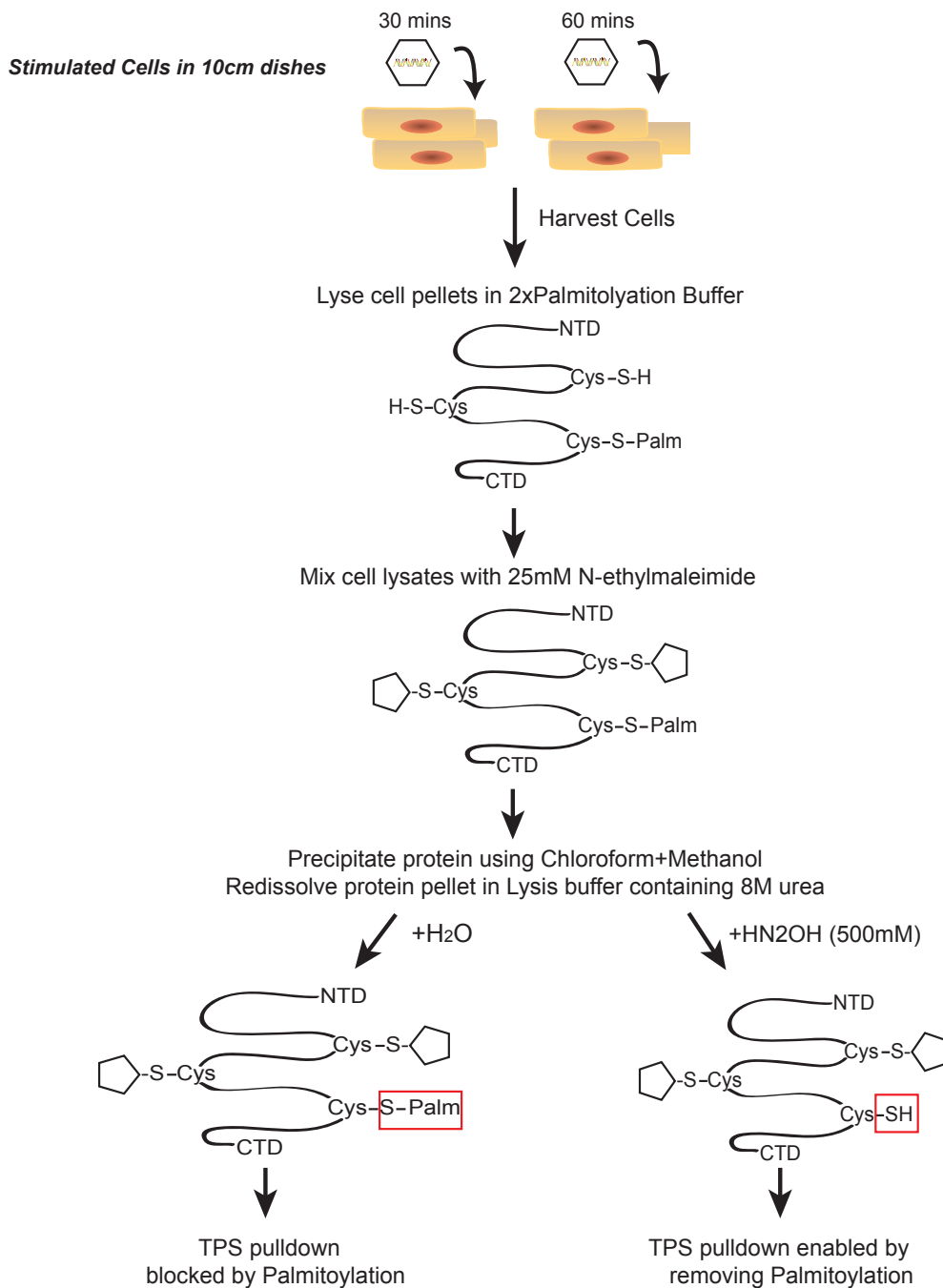
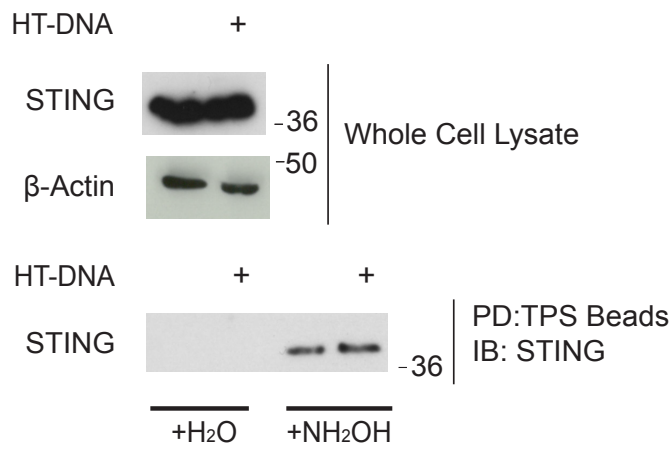


Fig 3.4.1 Schematic of Palmitoylation Pulldown Technique

Cell lines are stimulated with (5ug/mL) HT-DNA during a time course to promote palmitoylation. Samples are scraped into cell pellets and subsequently lysed in 2xPalmitoylation lysis buffer. Lysates are mixed with 25mM N-ethylmaleimide to block free cysteine residues. Samples are subjected to chloroform-methanol precipitation to enrich for protein content. Precipitates are dissolved in a solution of 1xPalmitoylation lysis buffer containing 8M urea. Purified samples are split into three aliquots; loading controls, hydroxylamine treated and H₂O treated (control). Hydroxylamine treatment removes Palmitate from cysteine residues, enabling pulldown by TPS beads to determine palmitoylation. H₂O treated controls retain their palmitate and are utilised to control for non-specific binding by TPS beads.

A



B

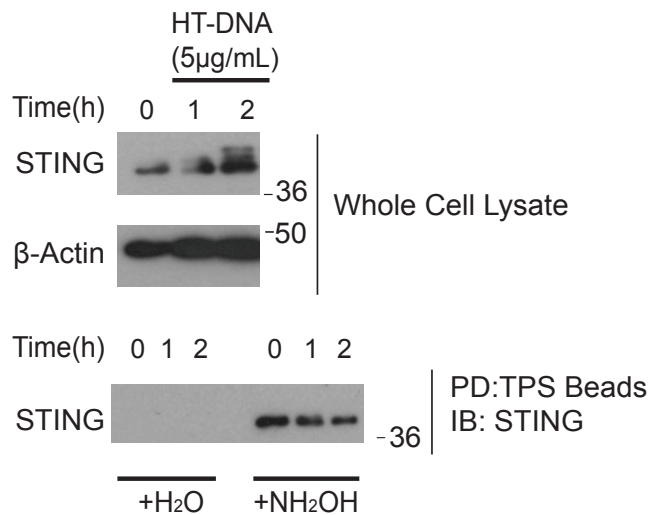


Fig 3.4.2 STING is Palmitoylated

(A) HaCaT cell lines were stimulated with HT DNA (5 μ g/ml) for 1 hour. **(B)** HaCaT cell lines were stimulated with HT DNA (5 μ g/ml) at 0, 1 and 2 hours. Cells were harvested and lysed. Samples were split and treated with Hydroxylamine or H₂O (control). STING, IFI16 and β -actin protein levels in lysates and TPS pulldowns was determined by Western blot. (A) and (B) are representative of two independent experiments.

increase with DNA stimulation. Examining Palmitoylation over a longer time course in **Fig 3.4.2B**, revealed that STING palmitoylation is decreased 2 hours post-stimulation; consistent with a reduction in total-STING levels due to phosphorylation and turnover as previously seen in **Fig 3.1.1A**.

We elected to serum starve HaCaT cells one hour prior to stimulation to see whether inducible STING palmitoylation could be observed by acyl-RAC in HaCaT cells as achieved by (Mukai et al., 2016) using [H^3]-palmitate. As highlighted in **Fig 3.4.3**, serum starvation allowed palmitoylation to be observed as an inducible post-translational modification on STING. **Fig 3.4.3** shows that basal STING palmitoylation is present and greatly increases 30 minutes post DNA stimulation. This time frame is consistent with STING trafficking being enabled, allowing STING to move into punctuate ERGIC structures by 60 minutes for subsequent signalling as observed in **Fig 3.1.10**.

When studying palmitoylation, HaCaT cells were stimulated with 5 μ g/mL of HT-DNA as this concentration allowed STING trafficking to be clearly observed by confocal microscopy (**Fig 3.1.10**). As transfection agents can induce a modest level of STING activation (Holm et al., 2012), we wished to confirm whether STING palmitoylation in HaCaT cells was dependent on DNA stimulation as purposed by (Mukai et al., 2016). We examined STING palmitoylation post-stimulation with transfection agent alone, and 1 μ g/mL and 5 μ g/mL concentrations of HT-DNA (**Fig 3.4.4**). In **Fig 3.4.4** we observe an increase in STING palmitoylation with 1 μ g/mL HT-DNA stimulation which increases further with 5 μ g/mL HT-DNA. We also observe that transfection agent alone induces a slight increase in STING palmitoylation versus untreated samples but not to the same extent as DNA stimulation.

3.4.4 STING palmitoylation is required for immune responses to DNA in HaCaT cells

As STING palmitoylation has only recently been described, we wished to verify if it was essential to for innate immune responses to DNA in HaCaT cells. Palmitoylation

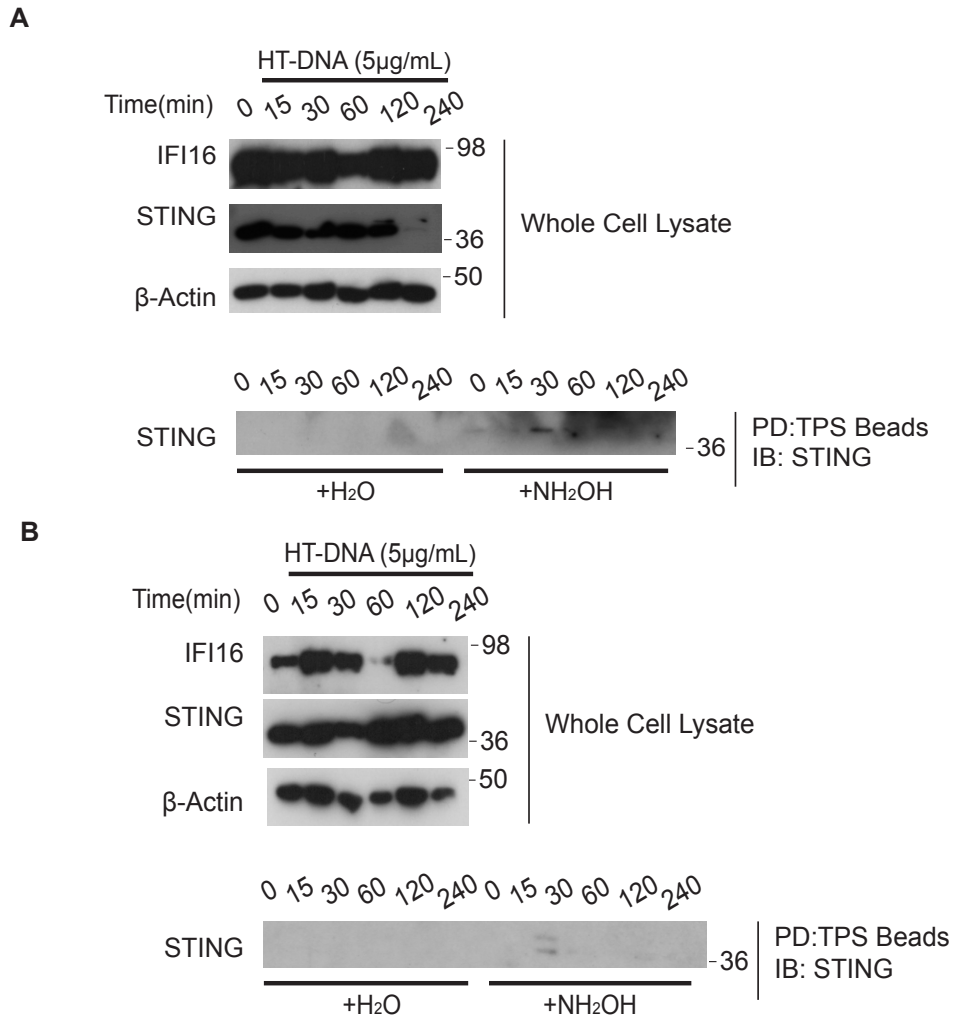


Fig 3.4.3 STING Palmitoylation is inducible with serum starvation

HaCaT cell lines were serum starved for 1 hour and then subjected to stimulation with HT DNA (5µg/ml) at 0,15,30,60,120,240 mins. Samples were split and treated with Hydroxylamine or H₂O(control). STING, IFIDa16 and β-actin protein levels in lysates and TPS pulldowns was determined by Western blot. (A) and (B) are representative of two independent experiments.

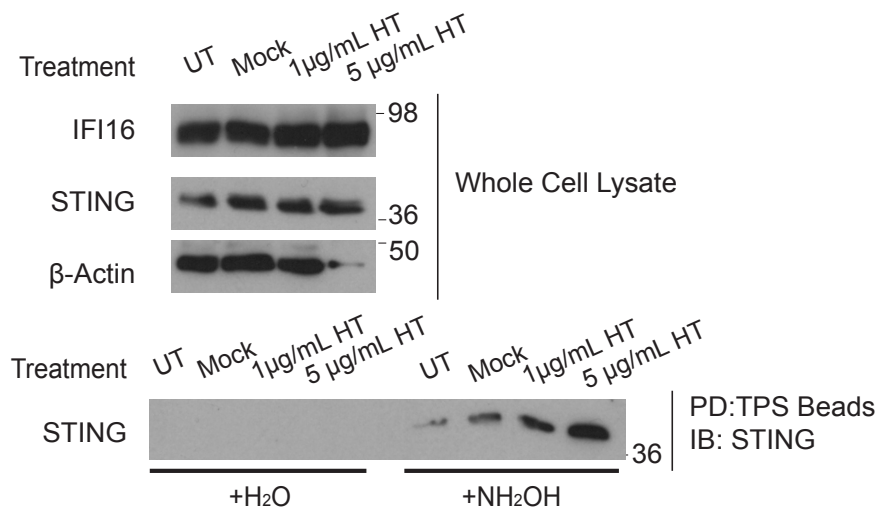


Fig 3.4.4 STING Palmitoylation correlates with increased concentrations of DNA stimulation

HaCaT cell lines were serum starved for 1 hour and then subjected to stimulation with HT DNA (1 or 5 μg/ml) or transfection agent alone for 30 mins. Samples were split and treated with Hydroxylamine or H₂O(control). STING, IFI16 and β-actin protein levels in lysates and TPS pulldowns was determined by Western blot. Data are representative of two independent experiments.

was inhibited using 2-Bromopalmitate (2-BP); an irreversible inhibitor of palmitoyl transferases (Jennings et al., 2009). (Mukai et al., 2016) found in murine fibroblasts that 2-BP inhibited intracellular DNA and RNA sensing pathways, while TLR3 signalling was unaffected by palmitoylation. Therefore, we included ectopic poly(I:C) stimulation as an additional control when examining nucleic acid sensing in this cell type. Wild type HaCaT cells were pre-incubated in serum free media containing 10 μ M 2-BP or (0.01%) DMSO for 1 hour prior to stimulation. Induction of cytokine mRNA was measured 4 hours post-stimulation by RT-PCR. In **Fig 3.4.5** we observe that 2-BP treatment significantly reduces IFN- β , CXCL10 and Interleukin-6 mRNA production in response to intracellular DNA (**3.4.5A-C**). RNA stimulation was also inhibited, suggesting that an aspect of the RLR-MAVS pathway could also be regulated by palmitoylation. In contrast, TLR3 signalling by ectopic poly(I:C) stimulation is unaffected by 2-BP treatment (**3.4.5A-C**).

We next examined whether 2-BP specifically inhibited the STING activation. As in **Fig 3.4.6**, wild type cells were pre-incubated in serum free media containing 10 μ M 2-BP or (0.01%) DMSO for 1 hour and stimulated with HT-DNA for the times indicated in **Fig 3.4.6**. Cells were lysed and STING Ser366 and IRF3 phosphorylation were examined by western blot. **Fig 3.4.6** demonstrates that 2-BP treatment reduces STING Ser366 and IRF3 phosphorylation at 4 hours post DNA stimulation versus samples treated with DMSO vehicle alone. Additionally, we see a delay in total STING phosphorylation with 2-BP treatment as the upper phospho-STING band only appears at 4h hours post DNA stimulation, while it appears at 2 and 4 hours in DMSO treated samples (**Fig 3.4.6**). Thus, we can conclude that inhibiting palmitoylation limits activation of the STING pathway.

Palmitoylation has been reported to facilitate protein trafficking to cholesterol rich lipid rafts (Reviewed by Linder and Deschenes, 2006). We wished to examine if inhibiting STING palmitoylation prevented STING trafficking in HaCaT cells. Wild type cells were treated with either 10 μ M 2-BP or (0.01%) DMSO for 1 hour and stimulated with 5 μ g/mL HT-DNA. In **Fig 3.4.7** we witness STING trafficking in 40% of cells treated with DMSO. Conversely, in 2-BP treated cells we observe no change in STING

trafficking from basal levels of 5%, demonstrating that palmitoylation is required for STING trafficking in HaCaT cells.

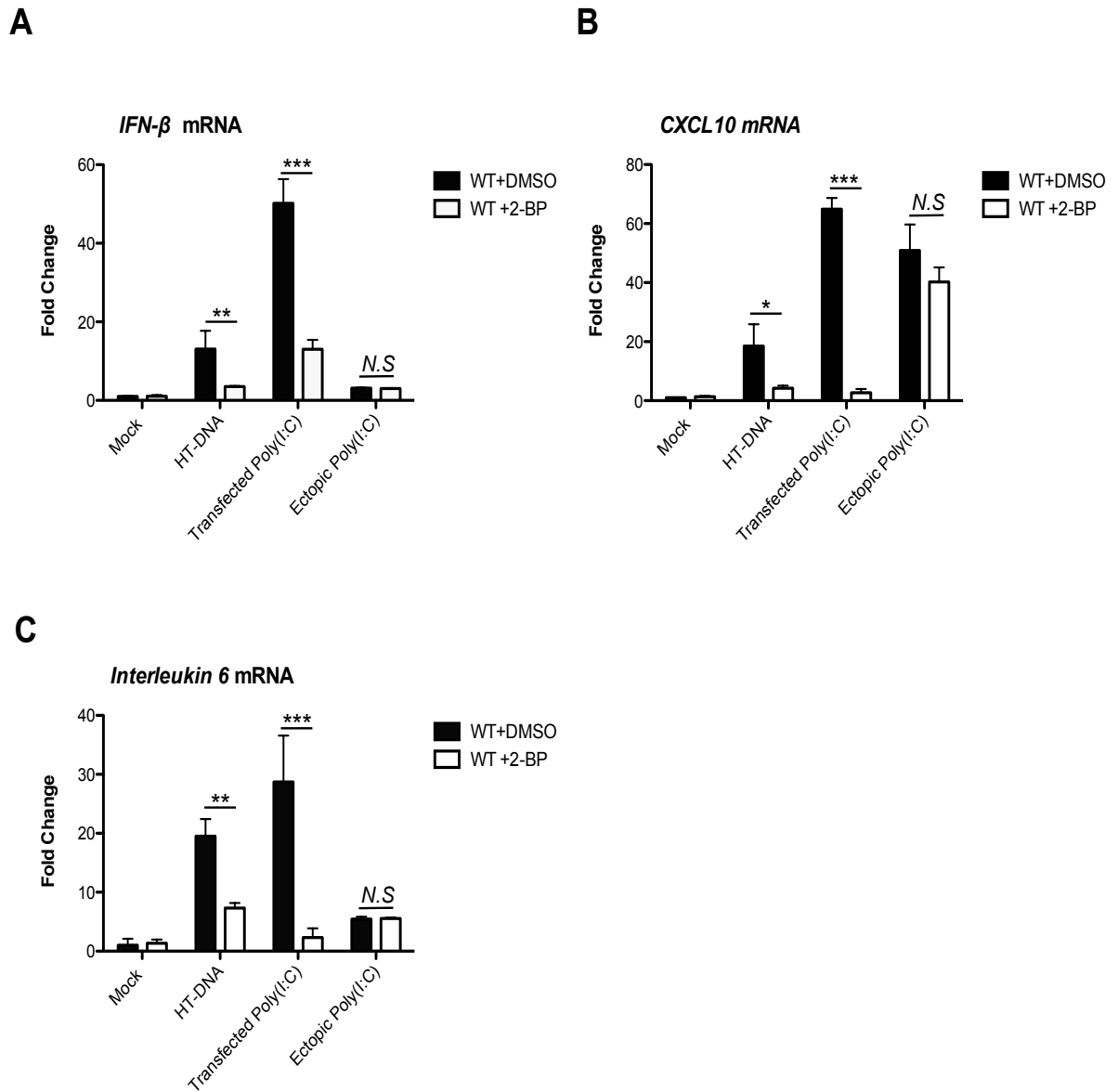


Fig 3.4.5 2-Bromopalmitate suppresses cytosolic nucleic acid sensing

(A-C) Wild Type HaCaT cell lines were starved for one hour in serum free medium containing 10 μ M 2-Bromopalmitate(2-BP) or (0.01%) DMSO and stimulated with 5 μ g/mL HT-DNA, 100ng/mL Poly(I:C) or transfection agent alone. 5 μ g/mL of Poly(I:C) was added directly to the cell culture media to induce ectopic Poly(I:C) stimulation. Cell lines were stimulated for 4 hours before sample lysis. IFN- β **(A)**, CXCL10 **(B)** and Interleukin-6 **(C)** mRNA was measured by RT-PCR. Experiments were carried out with triplicate samples, mean values and standard deviation are shown. Data are representative of three independent experiments. Statistical significance was determined using two-way ANOVA. p-value:*=P<0.05, **=P<0.01, ***=P<0.001 N.S=No significance

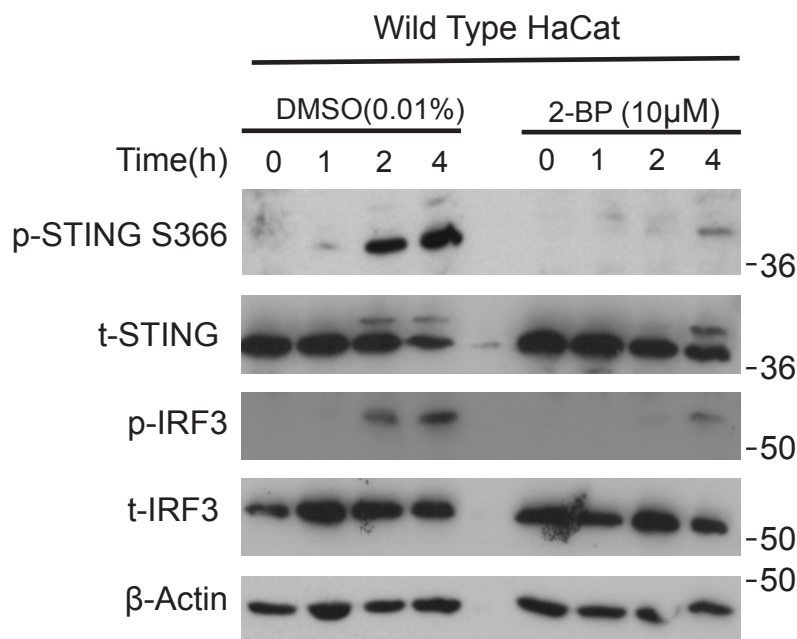


Fig 3.4.6 2-Bromopalmitate inhibits STING Phosphorylation

Wild Type HaCaT cell lines were starved for 1 hour in serum free media containing 10 μ M 2-Bromopalmitate (2-BP) or (0.01%) DMSO stimulated with (1 μ g/ml) of HT-DNA at 0, 1, 2 and 4 h. Cell lysates were examined for activation of STING and IRF3 (p-STING S366,p-IRF 3 S396) by Western blot. Data are representative of two independent experiments.

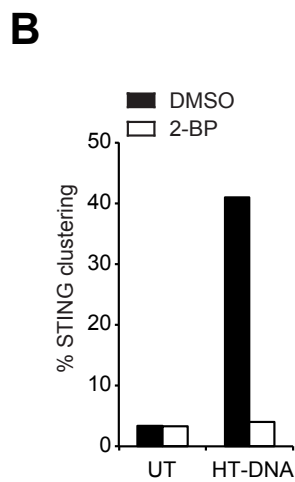
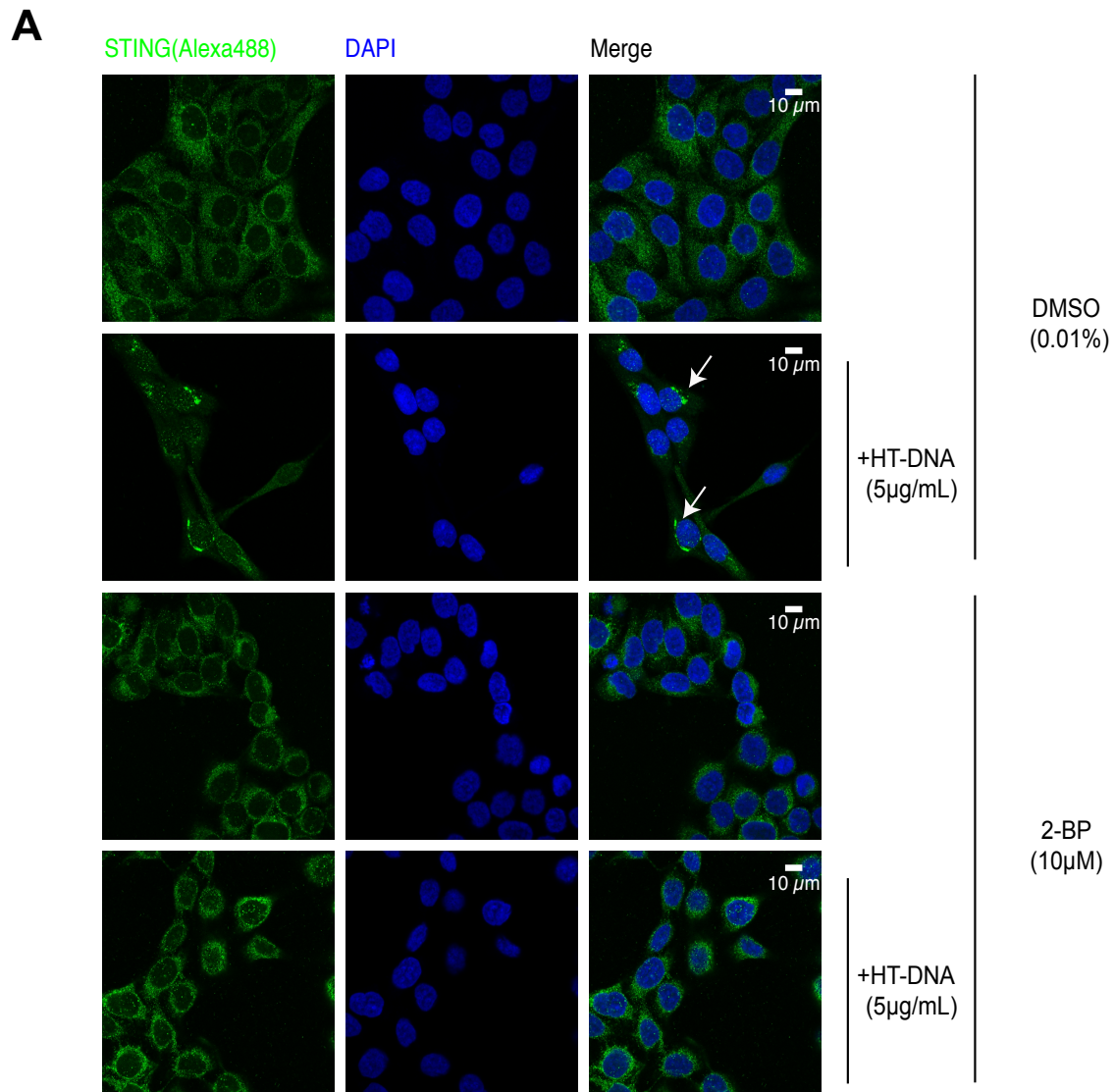


Fig 3.4.7 DNA induced STING activation is decreased following 2-Bromoplamate treatment

(A) Confocal microscopy analysis of Wild Type HaCaT cell lines following treatment with DMSO(0.01%) or 10µM 2-Bromoplamate (2-BP). Cell lines were transfected with 5µg/mL HT-DNA for 1 hour. Cells were stained for STING(Green/Alexa 488), while DNA was visualised with DAPI (Blue). 200 cells were counted and scored for STING clustering. These scores are presented as percentage of STING clustering in (B). Data are representative of two independent experiments.

3.4.5 STING Palmitoylation is dependent on IFI16

To examine STING palmitoylation in *IFI16*^(-/-) cells, wild type and *IFI16*^(-/-) HaCaT cells were serum starved for 1 hour and stimulated with 5µg/mL HT-DNA for 30 minutes before being lysed and subjected to TPS bead pulldown to examine palmitoylation. As highlighted in **Fig 3.4.8**, STING palmitoylation remains at basal levels in the *IFI16*^(-/-) irrespective of DNA stimulation, while STING palmitoylation increases with DNA stimulation in the wild type cell line. This directly implicates IFI16 in enabling the activation of STING during DNA sensing.

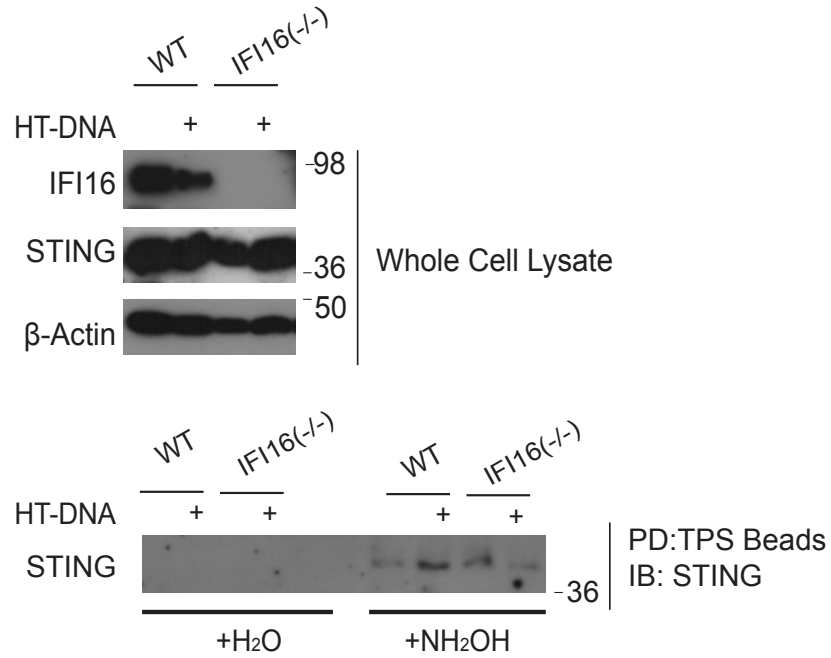


Fig 3.4.8 STING Palmitoylation is decreased in the absence of IFI16

Wild Type, IFI16(-/-) and cGAS(-/-) cell lines were serum starved for 1 hour and then subjected to stimulation with HT DNA (5 μ g/ml) for 30 mins. Samples were split and treated with Hydroxylamine or H₂O(-control). STING, IFI16 and β -actin protein levels in lysates and TPS pulldowns was determined by Western blot. Data are representative of two independent experiments.

3.4.6 Discussion

We chose to examine STING palmitoylation in the context of IFI16, as palmitoylation can regulate protein trafficking and ligand binding, and both processes appeared to be compromised for STING in the IFI16^(-/-) HaCaT (**Fig 3.1.10, Fig 3.3.1**) (Reviewed by Goddard and Watts, 2012; Linder and Deschenes, 2006). Using an acyl-RAC approach (**Fig 3.4.1**), we could detect STING palmitoylation in HaCaT cells (**Fig 3.4.2**). With further optimisation, we could observe STING palmitoylation as an DNA-inducible post-translational modification (**Fig 3.4.3-4**).

As STING palmitoylation had only recently been described by (Mukai et al., 2016), we wished to verify the importance of palmitoylation in HaCaT cells using the palmitoylation inhibitor 2-BP. We found that 2-BP inhibited intracellular nucleic acid sensing pathways (**Fig 3.4.5**) and specifically prevented activation of the STING pathway (**Fig 3.4.6**). Unlike (Mukai et al., 2016), we observed an ablation of STING trafficking with 2-BP treatment (**Fig 3.4.7**) resulting in a phenotype similar to that in IFI16^(-/-) cells. It is worth noting that our investigation examines endogenous STING trafficking, whereas (Mukai et al., 2016) utilise a reconstituted GFP-tagged murine STING in emCOS-1 cells. It is possible that a reconstituted system lessens the influence of 2-BP on STING trafficking by using non-physiological levels of STING.

STING palmitoylation did not increase in IFI16^(-/-) cells with DNA stimulation (**Fig 3.4.8**). This result depicts a possible IFI16 mediated link to STING activation within 30 minutes of DNA stimulation that is necessary for efficient STING activation. This poses the question whether palmitoylation is a unique signal provided by IFI16 to STING. In the future, it would be interesting to examine whether cGAMP stimulation induces STING palmitoylation to confirm if palmitoylation is mediated uniquely by IFI16 or cGAS. This could be investigated by examining STING palmitoylation following stimulation with DNA or cGAMP in Wild Type, IFI16^(-/-) and cGAS^(-/-) cells.

Chapter Four

Discussion

IFI16 and cGAS co-operate to detect exogenous DNA in human keratinocytes

4.1 IFI16 and cGAS are both required for DNA sensing in keratinocytes

The presence of DNA in the cytosol results in the activation of the STING-TBK1-IRF3 axis leading to the induction of IFN- β transcription and the initiation of an anti-viral immune response (Reviewed by Wu and Chen, 2014). In recent years, many DNA sensors have been proposed to recognise pathogen DNA and initiate an immune response through STING (Reviewed by Unterholzner, 2013). IFI16 has been implicated in the immune response to a wide array of pathogens in a variety of different cell types using siRNA depletion strategies (**Table 1.3**). However, the discovery that cells and mice lacking cGAS are unable to respond to DNA has prompted debate about the validity of the other proposed DNA sensors (Gao et al., 2013a; Li et al., 2013b). Additionally, the contribution of the entire ALR locus to IFN signalling has been called into question due to an investigation by (Gray et al., 2016). In this study, the authors demonstrate that mice lacking all 13 ALR genes display normal IFN responses to immune-stimulatory DNA stimulation and infections with lentiviruses and mCMV. This investigation also claims that IFI16 is dispensable for innate immune responses to DNA in human cells using a CRISPR/Cas9 pool of partially depleted primary fibroblasts in human cytomegalovirus (hCMV) infection (Gray et al., 2016). Thus, IFI16's candidacy as a DNA sensor has been met with scepticism (Vance, 2016).

We utilised two independently generated complete IFI16^(-/-) human immortalised keratinocyte clones to conclusively evaluate the role of IFI16 during DNA sensing. Using these cells, I observed that IFI16 is essential for efficient activation of the STING pathway following DNA stimulation and HSV-1 infection. Conversely, I also demonstrate that IFI16 is not required for responses to RNA stimulation or SeV infection. These observations were supported by additional siRNA experiments in our lab using primary human keratinocytes where we witnessed decreased IFN- β mRNA production upon DNA transfection and during HSV-1 infection following IFI16 depletion (Almine et al., 2017). We confirmed that cGAS was also essential for DNA sensing in keratinocytes as cGAS^(-/-) HaCaT cells were also unresponsive to DNA stimulation (Almine et al., 2017). We also observed that expression of increasing amounts of IFI16 with cGAS and STING increased activation of an IFN- β luciferase reporter in HEK293T cells. Similar results were observed by (Jonsson et al., 2017) in

THP1 monocytes in response to HT-DNA stimulation and during HIV-1, HSV-1 and hCMV infections. It is important to note in these studies that although the IFN- β response in IFI16^(-/-) cell lines is severely reduced, it is not entirely absent as in cGAS^(-/-) (Almine et al., 2017; Jonsson et al., 2017). This suggests that IFI16 is not essential for DNA responses but important for amplifying the residual cGAS response. Additionally, (Hansen et al., 2014) report equivalent decreases in IFN- β production following siRNA depletion of IFI16 and cGAS, in THP1 monocytes during *Listeria monocytogenes* infection. Collectively these observations suggest that there is co-operation between IFI16 and cGAS during exogenous DNA sensing.

Keratinocytes and THP1 monocytes lacking IFI16 express normal levels of the rest of the cGAS-STING pathway suggesting that IFI16 and cGAS do not regulate the expression of one another in these cells (**Fig 3.1.4**) (Almine et al., 2017; Jonsson et al., 2017). This is distinct from what has been observed by (Storek et al., 2015) and (Orzalli et al., 2015) who demonstrate that CRISPR/Cas9 removal cGAS in RAW267.4 cells or depletion of cGAS by siRNA in human foreskin fibroblasts, results in equivalent losses of p204 and IFI16. This suggests that IFI16 regulation may vary between cell lines. Normal expression levels of cGAS in the IFI16^(-/-) cells and vice versa, affords us conclusive insights into the contribution of both receptors to DNA sensing in keratinocytes.

4.2 IFI16 does not influence cGAS activity in keratinocytes

IFI16 and cGAS both achieve sequence independent recognition of DNA through binding the DNA sugar-phosphate backbone; IFI16 utilises its HIN200 domain to bind DNA (Jin et al., 2012), while cGAS uses a zinc thumb motif (Civril et al., 2013). IFI16 has been observed to form filaments along strands of DNA in vitro, while cGAS structural studies suggest that cGAS may preferentially bind for the ends of DNA or U-turns and bends in DNA created by nucleoid proteins and HMBG1 (Andreeva et al., 2017; Morrone et al., 2014; Zhang et al., 2014b). Therefore, IFI16 and cGAS have distinct but not necessarily competing mechanisms of DNA binding.

To investigate the relationship between IFI16 and cGAS, I examined if IFI16 and cGAS interacted following DNA stimulation. I observed an association between endogenous IFI16 and cGAS following DNA stimulation in keratinocytes (**Fig 3.2.1**). Using overexpression experiments in 293T cells I inferred that IFI16 and cGAS associations were facilitated using DNA as a binding platform as associations were impaired between cGAS and an IFI16 DNA binding mutant (**Fig 3.2.2**) (Jin et al., 2012). Additionally, treatment of samples with the DNA and RNA endonuclease Benzonase also reduced associations between wild type IFI16 and cGAS (**Fig 3.2.2**). Associations between IFI16 and cGAS have also been observed in other studies. Iqbal et al., (2016) observe an interaction between IFI16 and cGAS in the cytosol using microscopy-based proximity ligation assays in human microvascular endothelial (HMVE) cells. Orzalli et al., (2015) and Diner et al., (2016) detect interactions between IFI16 and cGAS in human foreskin fibroblasts (HFF) by mass spectrometry.

Although cGAS and IFI16 were observed to assemble on exogenous DNA together following stimulation, I observed no change in cGAS activity between wild type and IFI16^(-/-) HaCaT cell lines using LC-MS/MS to directly measure cGAMP production (**Fig 3.2.1-2,3.2.9**). This is distinct from what Jonsson et al., (2017) observe in THP1 monocytes, which display markedly reduced levels of cGAMP production in the absence of IFI16 using a similar LC-MS/MS technique. Jonsson et al., (2017) also observe increased levels of cGAMP production when IFI16 is co-expressed with cGAS in HEK293T cells. Iqbal et al., (2016) do not measure cGAMP production directly. Instead the authors examine induction of IFN- β mRNA in THP1 cells that have been stimulated using lysates from DNA-stimulated cells that contain cGAMP, but have been treated with Benzonase to remove RNAs and DNAs that would also stimulate the immune system. Iqbal et al., (2016) demonstrate that lysates from HMVE cells that have had IFI16 depleted by siRNA induce less of an IFN response in THP1s, correlating with a decrease in cGAMP production.

It is presently unclear why IFI16 appears to have a role in augmenting cGAS activity in THP1s and HMVE cells but not in keratinocytes (Almine et al., 2017; Iqbal et al., 2016; Jonsson et al., 2017). One possible explanation for this observation is the

difference in IFI16 regulation between cell types. THP-1 monocytes upregulate IFI16 upon differentiation, correlating with an increased sensitivity to DNA stimulation (Jonsson et al., 2017; Unterholzner et al., 2010). IFI16 levels in THP1 cells and HMVE cells further increase with DNA stimulation, viral infection and IFN treatment, resulting in a positive feedback loop (Iqbal et al., 2016; Jonsson et al., 2017; Unterholzner et al., 2010). In keratinocytes, I observe that IFI16 is expressed at consistent levels irrespective of DNA stimulation. Unlike monocytes and vascular endothelial cells, keratinocytes constitute a major physical barrier between host and environment and thus may need to regulate DNA sensing differently to cope with an increased pathogen burden. The absence of the IFI16 positive feedback loop therefore could serve to limit excessive activation of the immune response during a localised infection. It is also possible that in cells where IFI16 is expressed at very high levels such as in differentiated or stimulated THP1s that IFI16 may gain additional functions to further amplify the immune response. Thus, it is tempting to speculate that the specific functions of IFI16 are dictated by how it is regulated in a particular cell type.

Due to the discrepancy between different cell types regarding the influence of IFI16 on cGAS activity, it would be interesting to examine the IFI16 and cGAS association using immunoprecipitation and mass spectrometry approaches across different cell types to determine if the nature of the IFI16 and cGAS interaction varies (i.e. from a DNA intermediate to a direct protein:protein interaction) or to examine for the presence of additional cGAS co-factors or regulators in different cellular contexts. For example Polyglutamine binding protein 1 (PQBP1) was recently identified as a proximal sensor to cGAS during HIV-1 infection (Yoh et al., 2015). The authors show PQBP1 binds to reverse transcripts of HIV-1 and augments cGAS activity by direct association in dendritic cells. (Jakobsen et al., 2013) observe that IFI16 binds to these HIV-1 transcripts in THP1 cells. cGAS is subject to regulation by an increasing number of post-translational modifications including K27 ubiquitination, SUMOylation and glutamylation (Cui et al., 2016; Wang et al., 2017; Xia et al., 2016b). Therefore, it could also be interesting to examine whether IFI16 influences cGAS activating post-translational modifications in cells where IFI16 augments cGAMP production.

4.3 IFI16 facilitates STING activation in keratinocytes

IFI16 has been proposed to signal through STING since its discovery as a DNA sensor (Unterholzner et al., 2010). In keratinocytes, I observe a constitutive interaction between IFI16 and STING that increases with DNA stimulation (**Fig 3.3.2**). Similar results are observed in THP1s and HMVE cells in studies by (Ansari et al., 2015; Iqbal et al., 2016; Jonsson et al., 2017). The interaction between IFI16 and STING is likely mediated by the IFI16 PYD, as constructs expressing the IFI16 PYD alone have been observed to drive IFN- β expression when overexpressed with STING (Almine et al., 2017; Jonsson et al., 2017).

I observe that cells lacking IFI16 are unable to respond to stimulation with exogenous cGAMP, which was also reported in the investigation by (Jonsson et al., 2017). We find that IFI16^(-/-) HaCaT cells also do not respond to a non-hydrolysable form of cGAMP, cGAM(PS)₂ (Li, 2014), indicating that the inability of the IFI16^(-/-) cell lines to respond to cGAMP stimulation is due to a failure in STING activation and not due to cGAMP degradation in the absence of IFI16 (Almine et al., 2017). We believe that the function of IFI16 in keratinocytes is to enable STING activation following cGAMP production as STING trafficking and phosphorylation are decreased in the IFI16^(-/-) cell lines despite normal levels of cGAMP production. It would be interesting to examine if the ability of cGAMP to bind to STING was altered by an absence of IFI16. This could be tested by performing biotin-streptavidin pulldowns with biotinylated-cGAMP and comparing if the amount of STING pulldown varies between wild type and IFI16^(-/-) cell lines.

Additionally, it would be interesting to examine whether cGAS or cGAMP regulate IFI16 functions. IFI16 is a predominately nuclear protein which shuttles to the cytoplasm upon detecting viral DNA following acetylation by the p300 acyltransferase (Ansari et al., 2015; Li et al., 2012a; Unterholzner et al., 2010). Cytoplasmic translocation is required for IFI16 to induce *IFN- β* transcription via STING (Ansari et al., 2015), however the signal that activates the p300 acyltransferase during DNA sensing has not been determined. cGAS is capable of inducing immunity in bystander cells by transfer of cGAMP between gap junctions and by the incorporation of cGAMP

into budding viral particles from infected cells (Ablasser et al., 2013b; Bridgeman et al., 2015; Gentili et al., 2015). Through infusion of synthetic cGAMP, we demonstrate that IFI16 is required for STING to respond to cGAMP even in the absence of DNA. This would suggest that cGAS can promote IFI16 translocation and function, perhaps through direct or indirect activation of IFI16 acylation. We could test whether this is directly mediated by cGAS itself, or by cGAMP activating the p300 acyltransferase, through examining if IFI16 translocates to the cytoplasm with DNA and cGAMP stimulation in cellular fractionation experiments using wild type and cGAS^(-/-) cell lines.

4.4 IFI16 promotes STING phosphorylation, translocation palmitoylation in Keratinocytes

There are many mechanisms by which IFI16 could potentially regulate STING activation; IFI16 could promote associations with a STING positive regulator such as iRhom2 or ZDHHC1 (Luo et al., 2016; Zhou et al., 2014) or remove a STING inhibitor such as NLRC3 or NLRX1 (Guo et al., 2016; Zhang et al., 2014a). Alternatively, IFI16 could enable the addition of a STING post-translational modification. STING is subject to regulation by a range of post-translational modifications such as phosphorylation on S358 and S366 by TBK1, ULK1 and unidentified kinases (Konno et al., 2013; Liu et al., 2015a; Tanaka and Chen, 2012; Zhong et al., 2008), K11-, K27-, K48- and K63-linked ubiquitination (Ni et al., 2017; Qin et al., 2014; Wang et al., 2014; Zhang, 2012; Zhong et al., 2009), SUMOylation (Hu et al., 2016) and palmitoylation (Mukai et al., 2016).

I observe a reduction in STING trafficking and STING phosphorylation in IFI16^(-/-) cell lines following DNA stimulation (**Fig 3.1.10-11**). cGAS is already known to be required for STING trafficking to ERGIC, and we demonstrate that STING is still phosphorylated following cGAMP stimulation IFI16^(-/-) HaCaT cells (Almine et al., 2017; Dobbs et al., 2015). Therefore, we were seeking an additional complementary STING activating signal that could be mediated by IFI16. I decided to examine STING palmitoylation as palmitoylation enables trafficking of proteins to cholesterol-rich membranes for subsequent signalling and can regulate the ability of a receptor to bind its ligand by sterically altering its conformation in a membrane (Reviewed by Goddard

and Watts, 2012; Linder and Deschenes, 2006). STING trafficking and STING recognition of cGAMP appeared to be dysfunctional in the *IFI16*^(-/-) cell line (**Fig 3.1.10, 3.3.1**) and STING palmitoylation has recently been identified as an essential signal for STING activation (Mukai et al., 2016). In our experiments with the irreversible palmitoyl transferase inhibitor, 2-BP, we observe that inhibiting palmitoylation produces a similar phenotype to the *IFI16*^(-/-) cell line, resulting in decreased STING phosphorylation, decreased downstream activation of the STING pathway, and decreased STING trafficking (**Fig 3.4.5-7**). We also find that palmitoylation does not increase with DNA stimulation in the *IFI16*^(-/-) cell lines (**Fig 3.4.8**).

In the future, it would be interesting to evaluate whether IFI16 mediates palmitoylation independently of cGAS. This could be examined by testing if cGAMP stimulation can induce palmitoylation in Wild type, *IFI16*^(-/-) and *cGAS*^(-/-) cell lines. If palmitoylation was only induced with DNA stimulation in the wild type and *cGAS*^(-/-) cell lines but not the *IFI16*^(-/-), it would identify palmitoylation as a unique STING activating signal that is mediated by IFI16.

The study by Mukai et al., (2016) was the first to demonstrate that STING is palmitoylated. However, the palmitoyl transferase ZDHHC1 had been already identified as a positive regulator of the STING pathway through direct associations with STING at the ER (Zhou et al., 2014). However it merits attention that the involvement of the palmitoyl transferase activity of ZDHCC1 has not yet been specifically tested (Zhou et al., 2014). Although ZDHHC1 and IFI16 were not found to associate in overexpression experiments in this report, it would be interesting to examine if ZDHHC1 and STING associations are altered in the absence of IFI16 as IFI16 could promote their association indirectly. Additionally, it would be interesting to perform an siRNA or CRIPSR/Cas9 screen of other palmitoyl transferases in keratinocytes and other cell types to observe if regulation of STING pathway requires particular palmitoyl transferases, and whether their involvement varies between different cell types. Administration of 2-BP was found to ameliorate activation of the STING pathway in overexpression experiments of STING induced auto-inflammatory disease (Mukai et

al., 2016). Additionally, dysfunctional palmitoyl transferases have already been implicated in inflammatory diseases such as microbial-driven dermatitis (Chen et al., 2017). Therefore, there are many potential therapeutic benefits to studying how palmitoylation regulates innate immune signalling.

In this investigation we provide evidence that IFI16 and cGAS contribute separate but necessary signals to STING for complete activation. Due to the extensive number and range of STING post-translational modifications it would be useful to employ a proteomics based approach using IFI16^(-/-) and cGAS^(-/-) cell lines to evaluate if certain post-translational modifications are dependent on IFI16 or cGAS alone. As palmitoylation appears to enable STING phosphorylation (**Fig 3.4.5**) and STING trafficking (**Fig 3.4.7**), it would also be interesting to study interplay between STING palmitoylation and other post-translational modifications to assess the influence of this recently described post-translational modification to all aspects of STING behaviour (Mukai et al., 2016). Although cGAS does not directly interact with STING (Sun et al., 2013b), cGAS has been observed to interact with the autophagy regulator beclin-1 and thus could influence STING behaviour and STING post-translational modifications indirectly (Liang et al., 2014).

4.5 Outlook: IFI16 is required for DNA sensing with specific functions that vary with cell type

cGAS has been observed to be essential for DNA sensing in every cell type examined (Gao et al., 2013a; Li et al., 2013b). Within this investigation, we have demonstrated that IFI16 is also essential for efficient activation of the STING pathway during immune responses to DNA in keratinocytes, while Jonsson et al., (2017) observe similar results in monocytes/macrophages. Another study by Diner et al., (2016) demonstrates that while *IFI16*^(-/-) human foreskin fibroblasts display normal activation of the STING pathway, they still present with defects in IFN- β and anti-viral cytokine production, suggesting that IFI16 performs a transcriptional role in these cells or influences STING signalling beyond the readouts examined. Human foreskin fibroblasts without IFI16 also failed to restrict replication of an *ICP0*^(-/-) HSV-1 in this study.

The observations by Diner et al., (2016), when considered with the differences regarding the role of IFI16 in promoting cGAMP production between keratinocytes and monocytes, suggest that the range of functions IFI16 performs may be cell type specific and could reflect the physiological niche or vulnerability of that cell type to infection. The precise role of the ALR murine homologs will require further investigation. Gray et al., (2016) demonstrate that the ALR locus is dispensable for IFN- β production in response to transfected DNA, lentiviral infection and murine models of DNA driven auto-inflammatory disease in mice. While species differences between mice and men are plausible, Nakaya et al., (2017) argue that different mouse strains may regulate expression the ALRs locus differently, resulting in differences in disease severity upon deletion. Alternatively, if the ALRs function as cGAS co-factors they may only be required for immunity in certain cell types or upon challenge with certain viruses, similar to PQBP1 and HIV-1 in dendritic cells in humans (Yoh et al., 2015).

The results of our investigation and others demonstrate that although GAS can induce activation of STING by itself in over expression experiments, however in human cells that naturally respond to DNA, cGAS appears to require additional cofactors for optimal IFN- β induction (Almine et al., 2017; Jonsson et al., 2017; Sun et al., 2013a; Yoh et al., 2015). Considering this hypothesis, it may be beneficial to re-examine the contributions of many of the other putative DNA-sensors with similar knockout studies. Due to discrepancies in specific IFI16 functions between different cell types, it is evident that wider studies are needed to fully appreciate the contributions of IFI16 to innate immunity. However, it is clear from each of these human *IFI16*^(-/-) studies that both IFI16 and cGAS are required for optimal induction of STING mediated anti-viral immunity (**Fig 4.1**) (Almine et al., 2017; Diner et al., 2016; Jonsson et al., 2017).

4.6 Outlook: IFI16 as a DNA Sensor, challenges with experimental models

Perhaps the greatest obstacle to addressing the scepticism surrounding IFI16's candidacy as a DNA sensor is a lack of comparable experimental models. This is due to a lack of conservation in the *alr* locus between humans and mice. Humans possess

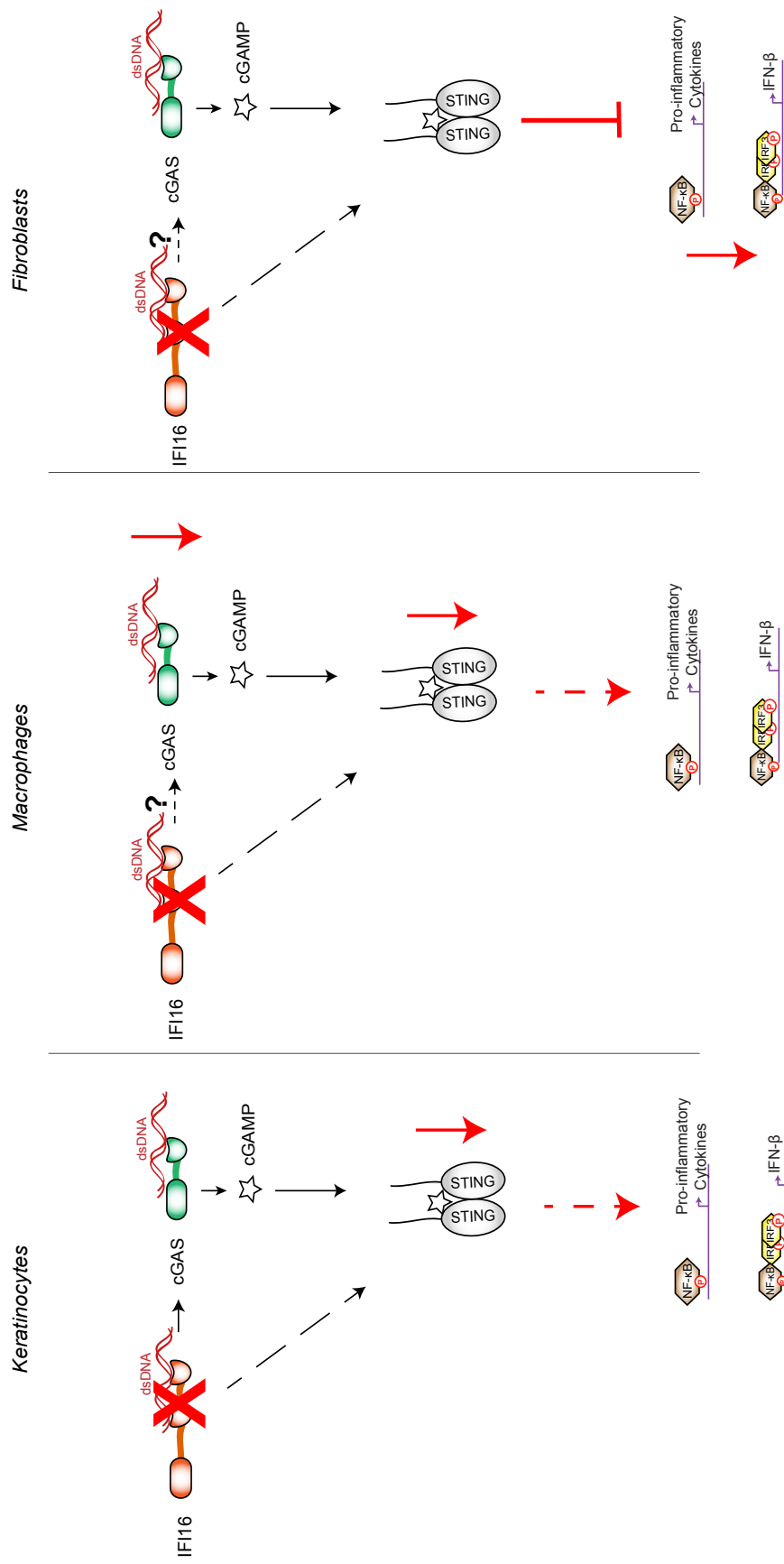


Fig 4.1 Summary of the Roles of IFI16 According to Knockout Studies

IFI16 knockout HaCaT keratinocytes display reduced STING activation, resulting in a reduction in pro-inflammatory cytokines and IFN- β transcription. IFI16 and cGAS associate via DNA in keratinocytes but this has not been examined in other cell types. IFI16 knockout THP1 Macrophages display impaired cGAMP production and STING activation without IFI16. IFI16 knockout fibroblasts display normal activation of the STING pathway, however transcription of pro-inflammatory cytokines and IFN- β transcription was decreased compared to Wild Type fibroblasts.

five ALRs, whereas there are thirteen ALRs present in mice (Cridland et al., 2012). AIM2 is the only ALR conserved between humans and mice.

Our study and the works of Diner et al., (2016) and Jonsson et al., (2017) use *IFI16*^(-/-) immortalised human cell lines generated by TALENs and CRISPR/Cas9 technologies and represent the first models to conclusively study IFI16 function in human cell lines. However, it is important to acknowledge that these models are not without limitations. These limitations include clonal effects within individual cells due to unprecedented off target effects of genetic manipulation, or that may have been generated through the clonal-selection process. Additionally, there are obvious practical limitations to extrapolating observations about a single homogenous cell population outwith a whole organism. As many cancer cell lines have been in use in pre-clinical research laboratories for decades, the clinical relevance of these models has been continuously questioned, hence the need to verify these observations with several independently generated knockout cell clones or with depletion experiments in primary human tissues (Gillet et al., 2013).

Within this investigation, we generated two *IFI16*^(-/-) HaCaT cell lines and extrapolated our experimental observations to primary human keratinocytes using siRNA experiments (Almine et al., 2017). Similarly, Jonsson et al., (2017) utilise siRNA experiments in PBMCs taken from HIV-1 patients to demonstrate IFI16's role in restricting retroviral infection and IFN production. However, although the insights gained from these samples are immensely valuable, it is equally important to acknowledge that primary human tissues are of similarly a limited scope for extrapolating to the biology of a whole organism, and may be of limited practical use depending on the condition of the tissue donor. For example, many of the primary cells used in our investigation were donated from patients undergoing gastric bypass surgeries. Recent work by York et al., (2015), has demonstrated that excessive dietary cholesterol can limit the activation of the STING pathway, potentially resulting in impaired IFN induction in these patients.

Animal models have routinely been used to verify the contributions of different components of innate immune signalling pathways including cGAS (Li et al., 2013b), AIM2 (Rathinam et al., 2010) and STING (Ishikawa, 2008). Due to the lack of conservation of the *alr* locus between humans and mice, it has been difficult to model the contributions of the ALRs to human biology (Cridland et al., 2012). The *alr* locus has also been observed to possess significant diversity between different strains of laboratory mice, further complicating the development of a model to study their relevance to immunity. For example, the gene region of *mnda1* is not present in the DBA/2J, AKR/N, and NZB/BIN lab strains (Cridland et al., 2012). Additionally, there are two duplications of *ifi202* and a pseudogene in the 129 mouse genome but only one copy of *ifi202* is present in C57BL/6 (Wang et al., 1999). The DBA lab strain is also contains a partial deletion in *ifi203* (Zhang et al., 2009). A recent paper by (Nakaya et al., 2017) mapped and compared the entire *alr* locus between C57BL/6 and 129 mice and observed considerable differences in the complement of *alr* genes between strains, and has raised concerns for how this will impact on the interpretation of autoimmune disease models used to discredit the contribution of the ALRs to immunity. Thus, it is clear that the murine *alr* locus has been subjected to frequent rearrangement and is not strongly conserved between murine species. Similarly, bioinformatic analysis of the *alr* locus in humans and primates has revealed that the locus has been a subject of long-standing balancing selection likely due to an evolutionary arms race between virus and host (Cagliani et al., 2014).

4.7 Outlook: Clinical Importance of IFI16 to Immunity; Lessons from Infection and Auto-immunity

Clinical evidence of the involvement of IFI16 in immunity has been observed across an array of different varieties of viral infections and auto-immune diseases. Analysis of a cohort of Swedish patients infected with HSV-2 revealed that IFN induction was largely dependent on IFI16 (Eriksson et al., 2017). Specific subgroup analysis of these patients revealed that the minor G allele of the IFI16 SNP rs2276404 was associated with resistance to infection. This allele was observed to frequently occur with the C allele of rs1417806 and together these SNPs are significantly overrepresented in uninfected individuals. PBMCs from patients with both of these SNPs possessed higher

levels of IFI16 and induced more IFN upon challenge with HSV-2. Pyroptosis induced by IFI16 inflammasomes in HIV infected CD4⁺ T cells leads to progression of HIV to AIDS (Monroe et al., 2014). Further analysis of this phenomenon by (Booiman and Kootstra, 2014) found that IFI16 influences HIV pathogenesis early in the HIV infection cycle and that patients with the IFI16 SNP rs1417806 possessed lower CD4⁺ T cell counts and progressed to AIDS faster than other patients following seroconversion.

Increased levels of IFI16 have been observed in psoriatic lesions (Cao et al., 2016a). Anti-IFI16 antibodies are commonly found in rheumatic diseases such as Systemic Lupus Erythematosus, Sjögren's syndrome and limited Cutaneous Systemic Sclerosis (Baer et al., 2016; Caneparo et al., 2013; Mondini et al., 2006; Seelig et al., 1994). As the aetiology of these autoimmune diseases is complex, the role of these IFI16 autoantibodies in disease pathogenesis is difficult to infer and even differs between diseases. For example, IFI16 antibodies negatively correlate with disease severity in Systemic Lupus Erythematosus but is strongly associated with disease severity in Sjögren's syndrome (Baer et al., 2016; Caneparo et al., 2013).

4.8 What are the benefits to the host of having more than one receptor for viral DNA?

Viruses are obligate parasites that require their host's cells to replicate and spread to new hosts. Due to the restrictive size of their genomes, viruses have had to evolve efficient ways of evading their host's immune system to enable their continued survival (Reviewed by Bowie and Unterholzner, 2008; Reviewed by Chan and Gack, 2016b). A mass spectrometry based analysis of 70 viral immune modulators compiled from 30 viral species revealed that these viruses targeted 579 host proteins, many of which have been implicated in host immune processes (Pichlmair et al., 2012).

Vaccinia virus, the prototypic poxvirus, is the best studied model for viral immune evasion and has been observed to block the innate immune response at several levels of induction such as TLR activation, downstream signalling and IRF3 activation (Reviewed by Smith et al., 2013). DNA viruses have been observed to target IFI16,

cGAS and STING for degradation during infection to continue their replication (Reviewed by Orzalli and Knipe, 2014). The primary function of cGAS is to produce cGAMP, while IFI16 is required to enable activation of STING (Almine et al., 2017; Jonsson et al., 2017; Sun et al., 2013a). cGAS is capable of triggering immunity in bystander cells through spread of cGAMP through gap junctions and by longitudinal transfer through virions emerging from infected cells (Albasser et al., 2013a, Bridgeman et al., 2015; Gentili et al., 2015). IFI16 is also capable of inhibiting the replication of viruses by acting as a restriction factor by through binding to, and inhibiting translation of, viral DNA as observed in HSV-1, HPV-18, HIV-1 and hCMV infections (Gariano et al., 2012; Jakobsen et al., 2013; Johnson et al., 2014; Lo Cigno et al., 2015).

Thus, it is tempting to speculate that due to the numerous strategies that viruses possess to evade the signalling mechanisms of the innate immune system that these additional functions have evolved to help prevent the host becoming overwhelmed by infection if one component of the DNA sensing pathway is compromised. For this reason, it would be interesting to examine the functions of the other putative DNA sensors to see if they compensate for IFI16's STING activating functions or possess additional anti-viral functions if IFI16, cGAS or STING have been degraded during infection.

4.9 Conclusion

The results presented within this thesis demonstrate that IFI16 is required for the complete induction of anti-viral immunity in human immortalised keratinocytes. Other recently published studies of IFI16 knockouts in different cell types also suggest that IFI16 is required for functional anti-viral immunity, but when considered together, prompt speculation that IFI16 may possess additional functions in other cell types such as augmenting cGAMP production or regulating expression of anti-viral cytokines. Further research and knockout studies are therefore required to fully appreciate the contribution of IFI16 to innate immunity.

Bibliography

- Abe, T., and Barber, G. (2014). Cytosolic-DNA-mediated, STING-dependent proinflammatory gene induction necessitates canonical NF- κ B activation through TBK1. *Journal of Virology* *88*, 5328-5341.
- Abe, T., Harashima, A., Xia, T., Konno, H., Konno, K., Morales, A., Ahn, J., Gutman, D., and Barber, G.N. (2013). STING recognition of cytoplasmic DNA instigates cellular defence. *Molecular Cell* *50*, 5-15.
- Ablasser, A., Bauernfeind, F., Hartmann, G., Latz, E., Fitzgerald, K.A., and Hornung, V. (2009). RIG-I-dependent sensing of poly(dA:dT) through the induction of an RNA polymerase III-transcribed RNA intermediate. *Nat Immunol* *10*, 1065-1072.
- Ablasser, A., Goldeck, M., Cavlar, T., Deimling, T., Witte, G., Röhl, I., Hopfner, K.-P., Ludwig, J., and Hornung, V. (2013a). cGAS produces a 2'-5'-linked cyclic dinucleotide second messenger that activates STING. *Nature* *498*, 380-384.
- Ablasser, A., Hemmerling, I., Schmid-Burgk, J.L., Behrendt, R., Roers, A., and Hornung, V. (2014). TREX1 deficiency triggers cell-autonomous immunity in a cGAS-dependent manner. *J Immunol* *192*, 5993-5997.
- Ablasser, A., Schmid-Burgk, J.L., Hemmerling, I., Horvath, G.L., Schmidt, T., Latz, E., and Hornung, V. (2013b). Cell intrinsic immunity spreads to bystander cells via the intercellular transfer of cGAMP. *Nature* *503*, 530-534.
- Aguirre, S., Luthra, P., Sanchez-Aparicio, M., Maestre, A., Patel, J., Lamothe, F., Fredericks, A., Tripathi, S., and Zhu T1, Pintado-Silva J1,3, Webb LG1,3, Bernal-Rubio D1, Solovyov A4, Greenbaum B4, Simon V1,2,5, Basler CF1, Mulder LC1,2, García-Sastre A1,2,5, Fernandez-Sesma A1,3,5 (2017). Dengue virus NS2B protein targets cGAS for degradation and prevents mitochondrial DNA sensing during infection. *Nature Microbiology* *27*, 17037.
- Aguirre, S., Maestre, A., Pagni, S., Patel, J., Savage, T., Gutman, D., Maringer, K., Bernal-Rubio, D., Shabman, R., Simon, V., *et al.* (2012). DENV inhibits type I IFN production in infected cells by cleaving human STING. *Plos Pathog* *8*, e1002934.
- Ahn, J., Ruiz, P., and Barber, G.N. (2014). Intrinsic self-DNA triggers inflammatory disease dependent on STING. *J Immunol* *193*, 4634-4642.
- Akutsu, M., Dikic, I., and Bremm, A. (2016). Ubiquitin chain diversity at a glance. *Journal of Cell Science* *129*, 875-878.
- Alexopoulou, L., Holt, A., Medzhitov, R., and Flavell, R. (2001). Recognition of double-stranded RNA and activation of NF-kappaB by Toll-like receptor 3. *Nature* *413*, 732-738.
- Almine, J.F., O'Hare, C.A., Dunphy, G., Haga, I.R., Naik, R.J., Atrih, A., Connolly, D.J., Taylor, J., Kelsall, I.R., Bowie, A.G., *et al.* (2017). IFI16 and cGAS cooperate in the activation of STING during DNA sensing in human keratinocytes. *Nat Commun* *8*, 14392.

- Andrade, W., Agarwal, S., Mo, S., Shaffer, S., Dillard, J., Schmidt, T., Hornung, V., Fitzgerald, K., Kurt-Jones, E., and Golenbock, D. (2016). Type I Interferon Induction by *Neisseria gonorrhoeae*: Dual Requirement of Cyclic GMP-AMP Synthase and Toll-like Receptor 4. *Cell Reports* *15*, 2438-2448.
- Andreeva, L., Hiller, B., Kostrewa, D., Lässig, C., de Oliveira Mann, C., Jan Drexler, D., Maiser, A., Gaidt, M., Leonhardt, H., Hornung, V., and Hopfner, K. (2017). cGAS senses long and HMGB/TFAM-bound U-turn DNA by forming protein-DNA ladders. *Nature* *549*, 394-398.
- Ank, N., Iversen, M., Bartholdy, C., Staeheli, P., Hartmann, R., Jensen, U., Dagnaes-Hansen, F., Thomsen, A., Chen, Z., Haugen, H., *et al.* (2008). An Important Role for Type III Interferon (IFN- λ /IL-28) in TLR-Induced Antiviral Activity. *Journal of Immunology* *180*, 2474-2485.
- Ansari, M.A., Dutta, S., Veetil, M.V., Dutta, D., Iqbal, J., Kumar, B., Roy, A., Chikoti, L., Singh, V.V., and Chandran, B. (2015). Herpesvirus Genome Recognition Induced Acetylation of Nuclear IFI16 Is Essential for Its Cytoplasmic Translocation, Inflammasome and IFN-beta Responses. *Plos Pathog* *11*, e1005019.
- Ansari, M.A., Singh, V.V., Dutta, S., Veetil, M.V., Dutta, D., Chikoti, L., Lu, J., Everly, D., and Chandran, B. (2013). Constitutive interferon-inducible protein 16-inflammasome activation during Epstein-Barr virus latency I, II, and III in B and epithelial cells. *J Virol* *87*, 8606-8623.
- Baer, A., Petri M., Sohn J., Rosen A., and L., C.-R. (2016). Association of Antibodies to Interferon-Inducible Protein-16 With Markers of More Severe Disease in Primary Sjögren's Syndrome. *Arthritis Care Res (Hoboken)* *68*, 254-260.
- Barber, G. (2015). STING: infection, inflammation and cancer. *Nature Reviews Immunology* *15*, 760-770.
- Barton, G., and Kagan, J. (2009). A cell biological view of Toll-like receptor function: regulation through compartmentalization. *Nature Reviews Immunology* *9*, 535-542.
- Bauer, S., Kirschning, C., Häcker, H., Redecke, V., Hausmann, S., Akira, S., Wagner, H., and Lipford, G. (2001). Human TLR9 confers responsiveness to bacterial DNA via species-specific CpG motif recognition. *Proc Natl Acad Sci U S A* *98*, 9237-9242.
- Baum, A., Sachidanandam, R., and García-Sastre, A. (2010). Preference of RIG-I for short viral RNA molecules in infected cells revealed by next-generation sequencing. *Proc Natl Acad Sci U S A* *07*, 16303-16308.
- Bell, J., Askins, J., Hall, P., Davies, D., and Segal, D. (2006). The dsRNA binding site of human Toll-like receptor 3. *Proc Natl Acad Sci U S A* *103*, 8792-8797.
- Berg, R.K., Rahbek, S.H., Kofod-Olsen, E., Holm, C.K., Melchjorsen, J., Jensen, D.G., Hansen, A.L., Jorgensen, L.B., Ostergaard, L., Tolstrup, M., *et al.* (2014). T

cells detect intracellular DNA but fail to induce type I IFN responses: implications for restriction of HIV replication. *PLoS One* *9*, e84513.

Biolatti, M., Dell'Oste, V., Pautasso, S., von Einem, J., Marschall, M., Plachter, B., Gariglio, M., De Andrea, M., and Landolfo, S. (2016). Regulatory Interaction between the Cellular Restriction Factor IFI16 and Viral pp65 (pUL83) Modulates Viral Gene Expression and IFI16 Protein Stability. *Journal of Virology* *90*, 8238-8250.

Bishop, K., Holmes RK., Sheehy AM., Davidson NO., Cho SJ., and MH., M. (2004). Cytidine deamination of retroviral DNA by diverse APOBEC proteins. *Curr Biol.* *14*, 1392-1396.

Booiman, T., and Kootstra, N. (2014). Polymorphism in IFI16 affects CD4(+) T-cell counts in HIV-1 infection. *Int J Immunogenet.* *41*, 518-520.

Boukamp, P., Petrussevska, R.T., Breitkreutz, D., Hornung, J., Markham, A., and Fusenig, N.E. (1988). Normal keratinization in a spontaneously immortalized aneuploid human keratinocyte cell line. *J Cell Biol* *106*, 761-771.

Bowie, A.G., and Unterholzner, L. (2008). Viral evasion and subversion of pattern-recognition receptor signalling. *Nat Rev Immunol* *8*, 911-922.

Brass, A., Huang, I., Benita, Y., and John, S., Krishnan MN, Feeley EM, Ryan BJ, Weyer JL, van der Weyden L, Fikrig E, Adams DJ, Xavier RJ, Farzan M, Elledge SJ. (2009). The IFITM proteins mediate cellular resistance to influenza A H1N1 virus, West Nile virus, and dengue virus. *Cell* *139*, 1243-1254.

Bridgeman, A., Maelfait, J., Davenne, T., Partridge, T., Peng, Y., Mayer, A., Dong, T., Kaeffer, V., Borrow, P., and Rehwinkel, J. (2015). Viruses transfer the antiviral second messenger cGAMP between cells. *Science* *349*, 1228-1232.

Broz, P., and Dixit, V. (2016). Inflammasomes: mechanism of assembly, regulation and signalling. *Nature Reviews Immunology* *16*, 407-420.

Bürckstümmer, T., Baumann, C., Blüml, S., Dixit, E., Dürnberger, G., Jahn, H., Panyavsky, M., Bilban, M., Colinge, J., Bennett, K., and Superti-Furga, G. (2009). An orthogonal proteomic-genomic screen identifies AIM2 as a cytoplasmic DNA sensor for the inflammasome. *Nature Immunology* *10*, 266-272.

Burdette, D.L., Monroe, K.M., Sotelo-Troha, K., Iwig, J.S., Eckert, B., Hyodo, M., Hayakawa, Y., and Vance, R.E. (2011). STING is a direct innate immune sensor of cyclic di-GMP. *Nature* *478*, 515-518.

Cagliani, R., Forni, D., Biasin, M., Comabella, M., Guerini, F., Riva, S., Pozzoli, U., Agliardi, C., Caputo, D., Malhotra, S., *et al.* (2014). Ancient and recent selective pressures shaped genetic diversity at AIM2-like nucleic acid sensors. *Genome Biol Evol.* *6*, 830-845.

- Caneparo, V., Cena T, De Andrea M, Dell'oste V, Stratta P, Quaglia M, Tincani A, Andreoli L, Ceffa S, Taraborelli M, *et al.* (2013). Anti-IFI16 antibodies and their relation to disease characteristics in systemic lupus erythematosus. *Lupus* 22, 607-613.
- Cao, T., Shao S., Li B., Jin L., Lei J., Qiao H., and G., W. (2016a). Up-regulation of Interferon-inducible protein 16 contributes to psoriasis by modulating chemokine production in keratinocytes. *Nature Scientific Reports* 3, 25381.
- Cao, Y., Guan, K., He, X., Wei, C., Zheng, Z., Zhang, Y., Ma, S., Zhong, H., and Shi, W. (2016b). *Yersinia* YopJ negatively regulates IRF3-mediated antibacterial response through disruption of STING-mediated cytosolic DNA signaling. *Biochem Biophys Acta* 1863, 3148-3159.
- Casrouge, A., Zhang, S., Eidenschenk, C., Jouanguy, E., Puel, A., Yang, K., Alcais, A., Picard, C., Mahfoufi, N., Nicolas, N., *et al.* (2006). Herpes simplex virus encephalitis in human UNC-93B deficiency.
- Chan, Y., and Gack, M. (2016a). A phosphomimetic-based mechanism of dengue virus to antagonize innate immunity. *Nature Immunology* 17, 523-530.
- Chan, Y., and Gack, M. (2016b). Viral evasion of intracellular DNA and RNA sensing. *Nature Reviews Microbiology* 14, 360-373.
- Chen, H., Sun, H., You, F., Sun, W., Zhou, X., and Chen L, Y.J., Wang Y, Tang H, Guan Y, Xia W, Gu J, Ishikawa H, Gutman D, Barber G, Qin Z, Jiang Z. (2011). Activation of STAT6 by STING is critical for antiviral innate immunity. *Cell* 147, 436-446.
- Chen, L., Yang-Yen, H., Tsai, C., Thio, C., Chuang, H., Yang, L., Shen, L., Song, I., Liu, K., Huang, Y., *et al.* (2017). Protein Palmitoylation by ZDHHC13 Protects Skin against Microbial-Driven Dermatitis. *Journal of Investigative Dermatology* 137, 894-904.
- Chen, M., Meng, Q., Qin, Y., Liang, P., Tan, P., and He, L., Zhou Y4, Chen Y1, Huang J5, Wang RF6, Cui J7. (2016). TRIM14 Inhibits cGAS Degradation Mediated by Selective Autophagy Receptor p62 to Promote Innate Immune Responses. *Molecular Cell* 64, 105-119.
- Chin, K., and Cresswell, P. (2001). Viperin (cig5), an IFN-inducible antiviral protein directly induced by human cytomegalovirus. *Proc Natl Acad Sci U S A* 98, 15125-15130.
- Chiu, Y.H., Macmillan, J.B., and Chen, Z.J. (2009). RNA polymerase III detects cytosolic DNA and induces type I interferons through the RIG-I pathway. *Cell* 138, 576-591.
- Christensen, M.H., and Paludan, S.R. (2017). Viral evasion of DNA-stimulated innate immune responses. *Cell Mol Immunol* 14, 4-13.

- Civril, F., Deimling, T., de Oliveira Mann, C.C., Ablasser, A., Moldt, M., Witte, G., Hornung, V., and Hopfner, K.P. (2013). Structural mechanism of cytosolic DNA sensing by cGAS. *Nature* *498*, 332-337.
- Collart, M., Baeuerle, P., and Vassalli, P. (1990). Regulation of tumor necrosis factor alpha transcription in macrophages: involvement of four kappa B-like motifs and of constitutive and inducible forms of NF-kappa B. *Molecular and Cellular Biology* *10*, 1498-1506.
- Collins, A.C., Cai, H., Li, T., Franco, L.H., Li, X.D., Nair, V.R., Scharn, C.R., Stamm, C.E., Levine, B., Chen, Z.J., and Shiloh, M.U. (2015). Cyclic GMP-AMP Synthase Is an Innate Immune DNA Sensor for Mycobacterium tuberculosis. *Cell Host Microbe* *17*, 820-828.
- Coolhill, T.P., Babich, M., Taylor, W.D., and Snipes, W. (1980). A comparison of herpes simplex virus plaque development after viral treatment with anti-DNA or antilipid agents. *Biophys J* *30*, 517-521.
- Cridland, J.A., Curley, E.Z., Wykes, M.N., Schroder, K., Sweet, M.J., Roberts, T.L., Ragan, M.A., Kassahn, K.S., and Stacey, K.J. (2012). The mammalian PYHIN gene family: phylogeny, evolution and expression. *BMC Evol Biol* *12*, 140.
- Cui, Y., Yu, H., Zheng, X., Peng, R., Wang, Q., Zhou, Y., Wang, R., Wang, J., Qu, B., and Shen N2, G.Q., Liu X3, Wang C1,4. (2016). SENP7 Potentiates cGAS Activation by Relieving SUMO-Mediated Inhibition of Cytosolic DNA Sensing. *Plos Pathog* *13*, e1006156.
- Cui, Y., Yu, H., Zheng, X., Peng, R., Wang, Q., Zhou, Y., Wang, R., Wang, J., Qu, B., Shen, N., *et al.* (2017). SENP7 Potentiates cGAS Activation by Relieving SUMO-Mediated Inhibition of Cytosolic DNA Sensing. *Plos Pathog* *13*, e1006156.
- Daffis, S., Szretter, K., Schriewer J, Li J, Youn S, Errett J, Lin TY, Schneller S, Zust R, and Dong H, T.V., Sen GC, Fensterl V, Klimstra WB, Pierson TC, Buller RM, Gale M Jr, Shi PY, Diamond MS. (2010). 2'-O methylation of the viral mRNA cap evades host restriction by IFIT family members. *Nature* *468*, 452-462.
- Dai, P., Wang, W., Cao, H., Avogadri, F., Dai, L., Drexler, I., Joyce, J.A., Li, X.D., Chen, Z., Merghoub, T., *et al.* (2014). Modified vaccinia virus Ankara triggers type I IFN production in murine conventional dendritic cells via a cGAS/STING-mediated cytosolic DNA-sensing pathway. *Plos Pathog* *10*, e1003989.
- Dai, P., Wang, W., Yang, N., Serna-Tamayo, C., Ricca, J., Zamarin, D., Shuman, S., Merghoub, T., Wolchok, J., and Deng, L. (2017). Intratumoral delivery of inactivated modified vaccinia virus Ankara (iMVA) induces systemic antitumor immunity via STING and Batf3-dependent dendritic cells. *Science Immunology* *2*, eaal1713.
- Davies, M., Chang HW., Jacobs BL., and RJ., K. (1993). The E3L and K3L vaccinia virus gene products stimulate translation through inhibition of the double-stranded RNA-dependent protein kinase by different mechanisms. *Journal of Virology* *67*, 1688-1692.

- Deddouche, S., Goubau D., Rehwinkel J., Chakravarty P., Begum S., Maillard PV., Borg A., Matthews N., Feng Q., van Kuppeveld FJ., and C., R.e.S. (2014). Identification of an LGP2-associated MDA5 agonist in picornavirus-infected cells. *Elife*. *18*; e01535.
- Dell'Oste, V., Gatti, D., Gugliesi, F., De Andrea, M., Bawadekar, M., Lo Cigno, I., Biolatti, M., Vallino, M., Marschall, M., Gariglio, M., and Landolfo, S. (2014). Innate nuclear sensor IFI16 translocates into the cytoplasm during the early stage of in vitro human cytomegalovirus infection and is entrapped in the egressing virions during the late stage. *J Virol* *88*, 6970-6982.
- Deschamps, T., , and Kalamvoki, M. (2017). Evasion of the STING DNA-Sensing Pathway by VP11/12 of Herpes Simplex Virus 1. *Journal of Virology* *91*, pii: e00535-00517.
- Dey, B., Dey, R., Cheung, L., Pokkali, S., Guo, H., Lee, J., and Bishai, W. (2015). A bacterial cyclic dinucleotide activates the cytosolic surveillance pathway and mediates innate resistance to tuberculosis. *Nature Medicine* *21*, 401-406.
- Dey, R., Dey, B., Zheng, Y., Cheung, L., Zhou, J., Sayre, D., Kumar, P., Guo, H., Lamichhane, G., Sintim, H., and Bishai, W. (2017). Inhibition of innate immune cytosolic surveillance by an *M. tuberculosis* phosphodiesterase. *Nature Chemical Biology* *13*, 210-217.
- Diebold, S., Kaisho, T., Hemmi, H., Akira, S., and Reis e Sousa, C. (2004). Innate antiviral responses by means of TLR7-mediated recognition of single-stranded RNA. *Science* *303*, 1529-1531.
- Diner, B., Li , T., Greco, T., Crow, M., Fuesler, J., Wang, J., and Cristea, I. (2015). The functional interactome of PYHIN immune regulators reveals IFIX is a sensor of viral DNA. *Molecular Systems Biology* *11*.
- Diner, B.A., Lum, K.K., Toettcher, J.E., and Cristea, I.M. (2016). Viral DNA Sensors IFI16 and Cyclic GMP-AMP Synthase Possess Distinct Functions in Regulating Viral Gene Expression, Immune Defenses, and Apoptotic Responses during Herpesvirus Infection. *MBio* *7*.
- Diner, E.J., Burdette, D.L., Wilson, S.C., Monroe, K.M., Kellenberger, C.A., Hyodo, M., Hayakawa, Y., Hammond, M.C., and Vance, R.E. (2013). The innate immune DNA sensor cGAS produces a noncanonical cyclic dinucleotide that activates human STING. *Cell Rep* *3*, 1355-1361.
- Ding, Q., Cao, X., Lu, J., Huang, B., Liu, Y.J., Kato, N., Shu, H.B., and Zhong, J. (2013). Hepatitis C virus NS4B blocks the interaction of STING and TBK1 to evade host innate immunity. *J Hepatol* *59*, 52-58.
- Dobbs N, Burnaevskiy N, Chen D, Gonugunta VK, Alto NM, and N., Y. (2015). STING Activation by Translocation from the ER Is Associated with Infection and Autoinflammatory Disease. *Cell Host and Microbe* *18*, 157-168.

- Dobbs, N., Burnaevskiy, N., Chen, D., Gonugunta, V., Alto NM, and N., Y. (2015). STING Activation by Translocation from the ER Is Associated with Infection and Autoinflammatory Disease. *Cell Host and Microbe* *18*, 157-168.
- Dupuis, S., Jouanguy, E., Al-Hajjar, S., Fieschi, C., Al-Mohsen, I., Al-Jumaah, S., Yang, K., Chapgier, A., Eidenschenk, C., Eid, P., *et al.* (2003). Impaired response to interferon-alpha/beta and lethal viral disease in human STAT1 deficiency. *Nature Genetics* *33*, 388-391.
- Dutta, D., Dutta, S., Veettil, M., Roy, A., Ansari, M., Iqbal, J., Chikoti, L., and Kumar B1, J.K., Chandran B1. (2015). BRCA1 Regulates IFI16 Mediated Nuclear Innate Sensing of Herpes Viral DNA and Subsequent Induction of the Innate Inflammasome and Interferon- β Responses. *Plos Pathogens* *11*, e1005030.
- Edelmann, K., Richardson-Burns, S., Alexopoulou, L., Tyler, K., Flavell, R., and Oldstone, M. (2004). Does Toll-like receptor 3 play a biological role in virus infections? *Virology* *322*, 231-238.
- Eriksson, K., Svensson, A., Hait, A., Schlüter, K., Tunbäck, P., Nordström, I., Padyukov, L., Liljeqvist, J., Mogensen, T., and SR., P. (2017). Cutting Edge: Genetic Association between IFI16 Single Nucleotide Polymorphisms and Resistance to Genital Herpes Correlates with IFI16 Expression Levels and HSV-2-Induced IFN- β Expression. *Journal of Immunology* *199*, 2613-2617.
- Ferguson, B.J., Mansur, D.S., Peters, N.E., Ren, H., and Smith, G.L. (2012). DNA-PK is a DNA sensor for IRF-3-dependent innate immunity. *Elife* *1*, e00047.
- Fernandes-Alnemri, T., Wu, J., Yu, J.W., Datta, P., Miller, B., Jankowski, W., Rosenberg, S., Zhang, J., and Alnemri, E.S. (2007). The pyroptosome: a supramolecular assembly of ASC dimers mediating inflammatory cell death via caspase-1 activation. *Cell Death Differ* *14*, 1590-1604.
- Fernandes-Alnemri, T., Yu, J.W., Datta, P., Wu, J., and Alnemri, E.S. (2009). AIM2 activates the inflammasome and cell death in response to cytoplasmic DNA. *Nature* *458*, 509-513.
- Fieber, C., Janos, M., Koestler, T., Gratz, N., Li, X., Castiglia, V., Aberle, M., Sauert, M., Wegner, M., Alexopoulou, L., *et al.* (2013). Innate immune response to *Streptococcus pyogenes* depends on the combined activation of TLR13 and TLR2. *Plos ONE* *10*, :e0119727.
- Forrester, M.T., Hess, D.T., Thompson, J.W., Hultman, R., Moseley, M.A., Stamler, J.S., and Casey, P.J. (2011). Site-specific analysis of protein S-acylation by resin-assisted capture. *J Lipid Res* *52*, 393-398.
- Fu, X., Kessler, D., Veals, S., Levy, D., and Darnell, J.J. (1990). ISGF3, the transcriptional activator induced by interferon alpha, consists of multiple interacting polypeptide chains. *Proc Natl Acad Sci U S A* *87*, 8555-8559.

Fung, K., Mangan, N., Cumming, H., Horvat, J., Mayall, J., and Stifter, S., De Weerd N, Roisman LC, Rossjohn J, Robertson SA, Schjenken JE, Parker B, Gargett CE, Nguyen HP, Carr DJ, Hansbro PM, Hertzog PJ. (2013). Interferon- ϵ protects the female reproductive tract from viral and bacterial infection. *Science* 339, 1088-1092.

Gabay, C., and Kushner, I. (1999). Acute-Phase Proteins and Other Systemic Responses to Inflammation. *New England Journal of Medicine* 340, 448-454.

Gack, M., Shin, Y., Joo, C., Urano, T., Liang, C., Sun, L., Takeuchi, O., Akira, S., Chen, Z., Inoue, S., and Jung, J. (2007). TRIM25 RING-finger E3 ubiquitin ligase is essential for RIG-I-mediated antiviral activity. *Nature* 446, 916-920.

Gaidt, M., Ebert TS., Chauhan D., Ramshorn K., Pinci F., Zuber S., O'Duill F., Schmid-Burgk JL., Hoss F., Buhmann R., *et al.* (2017). The DNA Inflammasome in Human Myeloid Cells Is Initiated by a STING-Cell Death Program Upstream of NLRP3. *Cell*.

Gao, D., Wu, J., Wu, Y.T., Du, F., Aroh, C., Yan, N., Sun, L., and Chen, Z.J. (2013a). Cyclic GMP-AMP synthase is an innate immune sensor of HIV and other retroviruses. *Science* 341, 903-906.

Gao, P., Ascano, M., Wu, Y., Barchet, W., Gaffney, B.L., Zillinger, T., Serganov, A.A., Liu, Y., Jones, R.A., Hartmann, G., *et al.* (2013b). Cyclic [G(2',5')pA(3',5')p] is the metazoan second messenger produced by DNA-activated cyclic GMP-AMP synthase. *Cell* 153, 1094-1107.

Gao, P., Ascano, M., Zillinger, T., Wang, W., Dai, P., Serganov, A.A., Gaffney, B.L., Shuman, S., Jones, R.A., Deng, L., *et al.* (2013c). Structure-function analysis of STING activation by c[G(2',5')pA(3',5')p] and targeting by antiviral DMXAA. *Cell* 154, 748-762.

Gariano, G.R., Dell'Oste, V., Bronzini, M., Gatti, D., Luganini, A., De Andrea, M., Gribaudo, G., Gariglio, M., and Landolfo, S. (2012). The intracellular DNA sensor IFI16 gene acts as restriction factor for human cytomegalovirus replication. *Plos Pathog* 8, e1002498.

Génin, P., Algarté, M., Roof, P., Lin, R., and Hiscott, J. (2000). Regulation of RANTES Chemokine Gene Expression Requires Cooperativity Between NF- κ B and IFN-Regulatory Factor Transcription Factors. *Journal of Immunology* 164, 5352-5361.

Gentili, M., Kowal, J., Tkach, M., Satoh, T., Lahaye, X., Conrad, C., Boyron, M., Lombard, B., Durand, S., Kroemer, G., *et al.* (2015). Transmission of innate immune signaling by packaging of cGAMP in viral particles. *Science* 349, 1232-1236.

Gibbert, K., Schlaak, J., Yang, D., and Dittmer, U. (2013). IFN- α subtypes: distinct biological activities in anti-viral therapy. *British Journal of Pharmacology* 168, 1048-1058.

Gillet, J., Varma, S., and Gottesman, M. (2013). The Clinical Relevance of Cancer Cell Lines. *Journal of the National Cancer Institute*, *105*, 452–458.

Goddard, A.D., and Watts, A. (2012). Regulation of G protein-coupled receptors by palmitoylation and cholesterol. *BMC Biol* *10*, 27.

Goldstone, D., Ennis-Adeniran V., Hedden JJ., Groom HC., Rice GI., Christodoulou E., Walker PA, K.G., Haire LF., Yap MW., de Carvalho LP., *et al.* (2011). HIV-1 restriction factor SAMHD1 is a deoxynucleoside triphosphate triphosphohydrolase. *Nature* *480*, 379-382.

Goubau, D., Schlee, M., Deddouche, S., Pruijssers, A., Zillinger, T., Goldeck, M., Schuberth, C., Van der Veen, A., Fujimura, T., Rehwinkel, J., *et al.* (2014). Antiviral immunity via RIG-I-mediated recognition of RNA bearing 5'-diphosphates. *Nature* *514*, 372-375.

Gough, D., Messina, N., Clarke, C., Johnstone, R., and Levy, D. (2002). Constitutive type I interferon modulates homeostatic balance through tonic signaling. *Immunity* *36*, 166-174.

Grandvaux, N., Servant, M., tenoever, B., Sen, G., Balachandran, S., Barber, G., Lin, R., and Hiscott, J. (2002). Transcriptional profiling of interferon regulatory factor 3 target genes: direct involvement in the regulation of interferon-stimulated genes. *Journal of Virology* *76*, 5532-5539.

Gray, E.E., Winship, D., Snyder, J.M., Child, S.J., Geballe, A.P., and Stetson, D.B. (2016). The AIM2-like Receptors Are Dispensable for the Interferon Response to Intracellular DNA. *Immunity* *45*, 255-266.

Guo, H., Konig, R., Deng, M., Riess, M., Mo, J., Zhang, L., Petrucelli, A., Yoh, S.M., Barefoot, B., Samo, M., *et al.* (2016). NLRX1 Sequesters STING to Negatively Regulate the Interferon Response, Thereby Facilitating the Replication of HIV-1 and DNA Viruses. *Cell Host Microbe* *19*, 515-528.

Hansen, K., Prabakaran, T., Laustsen, A., Jorgensen, S.E., Rahbaek, S.H., Jensen, S.B., Nielsen, R., Leber, J.H., Decker, T., Horan, K.A., *et al.* (2014). *Listeria monocytogenes* induces IFN β expression through an IFI16-, cGAS- and STING-dependent pathway. *Embo J* *33*, 1654-1666.

Hauptmann, R., and Swetly, P. (1985). A novel class of human type I interferons. *Nucleic Acids Res* *13*, 4739-4749.

Heil, F., Hemmi, H., Hochrein, H., Ampenberger, F., Kirschning, C., Akira, S., Lipford, G., Wagner, H., and Bauer, S. (2004). Species-specific recognition of single-stranded RNA via toll-like receptor 7 and 8. *Science* *303*, 1526-1529.

Hemmi, H., Takeuchi, O., Kawai, T., Kaisho, T., Sato, S., Sanjo, H., Matsumoto, M., Hoshino, K., Wagner, H., Takeda, K., and S., A. (2000). A Toll-like receptor recognizes bacterial DNA. *Nature* *408*, 740-745.

Herbert, A., Alfken J., Kim YG., Mian IS., Nishikura K., and A., R. (1997). A Z-DNA binding domain present in the human editing enzyme, double-stranded RNA adenosine deaminase. *Proc Natl Acad Sci U S A* *94*, 8421-8426.

Herzner AM, Hagmann CA, Goldeck M, Wolter S, Kübler K, Wittmann S, Gramberg T, Andreeva L, Hopfner KP, Mertens C, *et al.* (2015). Sequence-specific activation of the DNA sensor cGAS by Y-form DNA structures as found in primary HIV-1 cDNA. *Nature Immunology* *6*, 1025-1033.

Hillyer, P., Mane, V., Schramm, L., Puig, M., Verthelyi, D., Chen, A., Zhao, Z., Navarro, M., Kirschman, K., Bykadi, S., *et al.* (2012). Expression profiles of human interferon-alpha and interferon-lambda subtypes are ligand- and cell-dependent. *Immunology and Cell Biology* *90*, 774-783.

Hiscott, J., Marois, J., Garoufalidis, J., D'Addario, M., Roulston, A., Kwan, I., Pepin, N., Lacoste, J., Nguyen, H., and Bensi, G., *et al.* (1993). Characterization of a functional NF-kappa B site in the human interleukin 1 beta promoter: evidence for a positive autoregulatory loop. *Mol Cell Bio* *13*, 6231-6240.

Holm, C.K., Jensen, S.B., Jakobsen, M.R., Cheshenko, N., Horan, K.A., Moeller, H.B., Gonzalez-Dosal, R., Rasmussen, S.B., Christensen, M.H., Yarovinsky, T.O., *et al.* (2012). Virus-cell fusion as a trigger of innate immunity dependent on the adaptor STING. *Nat Immunol* *13*, 737-743.

Holm, C.K., Rahbek, S.H., Gad, H.H., Bak, R.O., Jakobsen, M.R., Jiang, Z., Hansen, A.L., Jensen, S.K., Sun, C., Thomsen, M.K., *et al.* (2016). Influenza A virus targets a cGAS-independent STING pathway that controls enveloped RNA viruses. *Nat Commun* *7*, 10680.

Horan, K.A., Hansen, K., Jakobsen, M.R., Holm, C.K., Soby, S., Unterholzner, L., Thompson, M., West, J.A., Iversen, M.B., Rasmussen, S.B., *et al.* (2013). Proteasomal degradation of herpes simplex virus capsids in macrophages releases DNA to the cytosol for recognition by DNA sensors. *J Immunol* *190*, 2311-2319.

Hornung V, Ellegast J, Kim S, Brzózka K, Jung A, Kato H, Poeck H, Akira S, Conzelmann KK, Schlee M, *et al.* (2006). 5'-Triphosphate RNA Is the Ligand for RIG-I. *Science* *314*, 994-997.

Hornung, V., Ablasser, A., Charrel-Dennis, M., Bauernfeind, F., Horvath, G., Caffrey, D.R., Latz, E., and Fitzgerald, K.A. (2009). AIM2 recognizes cytosolic dsDNA and forms a caspase-1-activating inflammasome with ASC. *Nature* *458*, 514-518.

Hou, F., Sun, L., Zheng, H., Skaug, B., Jiang, Q., and Chen, Z. (2011). MAVS forms functional prion-like aggregates to activate and propagate antiviral innate immune response. *Cell* *146*, 448-461.

Hu, M., Liao, C., Yang, Q., Xie, X., and Shu, H. (2017). Innate immunity to RNA virus is regulated by temporal and reversible sumoylation of RIG-I and MDA5. *Journal of Experimental Medicine* *214*, 973.

Hu, M.M., Yang, Q., Xie, X.Q., Liao, C.Y., Lin, H., Liu, T.T., Yin, L., and Shu, H.B. (2016). Sumoylation Promotes the Stability of the DNA Sensor cGAS and the Adaptor STING to Regulate the Kinetics of Response to DNA Virus. *Immunity* 45, 555-569.

Huang, Y.H., Liu, X.Y., Du, X.X., Jiang, Z.F., and Su, X.D. (2012). The structural basis for the sensing and binding of cyclic di-GMP by STING. *Nat Struct Mol Biol* 19, 728-730.

Hwang, S., Hertzog, P., Holland, K., Sumarsono, S., Tymms, M., Hamilton, J., Whitty, G., Bertonecello, I., and Kola, I. (1995). A null mutation in the gene encoding a type I interferon receptor component eliminates antiproliferative and antiviral responses to interferons α and β and alters macrophage responses. *Proc Natl Acad Sci U S A* 92, 11284-11288.

Iqbal, J., Ansari, M.A., Kumar, B., Dutta, D., Roy, A., Chikoti, L., Pisano, G., Dutta, S., Vahedi, S., Veetil, M.V., and Chandran, B. (2016). Histone H2B-IFI16 Recognition of Nuclear Herpesviral Genome Induces Cytoplasmic Interferon-beta Responses. *Plos Pathog* 12, e1005967.

Ishii, K.J., Kawagoe, T., Koyama, S., Matsui, K., Kumar, H., Kawai, T., Uematsu, S., Takeuchi, O., Takeshita, F., Coban, C., and Akira, S. (2008). TANK-binding kinase-1 delineates innate and adaptive immune responses to DNA vaccines. *Nature* 451, 725-729.

Ishikawa, H., and Barber, G.N. (2008). STING is an endoplasmic reticulum adaptor that facilitates innate immune signalling. *Nature* 455, 674-678.

Ishikawa, H., Ma, Z., and Barber, G.N. (2009). STING regulates intracellular DNA-mediated, type I interferon-dependent innate immunity. *Nature* 461, 788-792.

Ivashkiv, L., and Donlin, L. (2014). Regulation of type I interferon responses. *Nature Reviews Immunology* 14, 36-49.

Jakobsen, M.R., Bak, R.O., Andersen, A., Berg, R.K., Jensen, S.B., Tengchuan, J., Laustsen, A., Hansen, K., Ostergaard, L., Fitzgerald, K.A., *et al.* (2013). IFI16 senses DNA forms of the lentiviral replication cycle and controls HIV-1 replication. *Proc Natl Acad Sci U S A* 110, E4571-4580.

Janeway, C. (2001). How the immune system works to protect the host from infection: a personal view. *Proc Natl Acad Sci U S A* 98, 7461-7468.

Jang, Y., Lee, A.Y., Jeong, S.H., Park, K.H., Paik, M.K., Cho, N.J., Kim, J.E., and Cho, M.H. (2015). Chlorpyrifos induces NLRP3 inflammasome and pyroptosis/apoptosis via mitochondrial oxidative stress in human keratinocyte HaCaT cells. *Toxicology* 338, 37-46.

Jennings, B.C., Nadolski, M.J., Ling, Y., Baker, M.B., Harrison, M.L., Deschenes, R.J., and Linder, M.E. (2009). 2-Bromopalmitate and 2-(2-hydroxy-5-nitro-

benzylidene)-benzo[b]thiophen-3-one inhibit DHHC-mediated palmitoylation in vitro. *J Lipid Res* 50, 233-242.

Jiang, X., Kinch, L., Brautigam, C., Chen, X., Du, F., Grishin, N., and Chen, Z. (2012). Ubiquitin-induced oligomerization of the RNA sensors RIG-I and MDA5 activates antiviral innate immune response. *Immunity* 36, 959-973.

Jin, L., Hill, K.K., Filak, H., Mogan, J., Knowles, H., Zhang, B., Perraud, A.L., Cambier, J.C., and Lenz, L.L. (2011). MPYS is required for IFN response factor 3 activation and type I IFN production in the response of cultured phagocytes to bacterial second messengers cyclic-di-AMP and cyclic-di-GMP. *J Immunol* 187, 2595-2601.

Jin, L., Waterman, P., Jonscher, K., Short, C., Reisdorph, N., and Cambier, J. (2008). MPYS, a novel membrane tetraspanner, is associated with major histocompatibility complex class II and mediates transduction of apoptotic signals. *Mol Cell Bio* 28, 5014-5026.

Jin, T., Perry, A., Jiang, J., Smith, P., Curry, J.A., Unterholzner, L., Jiang, Z., Horvath, G., Rathinam, V.A., Johnstone, R.W., *et al.* (2012). Structures of the HIN domain:DNA complexes reveal ligand binding and activation mechanisms of the AIM2 inflammasome and IFI16 receptor. *Immunity* 36, 561-571.

Johnson, K., Bottero, V., Flaherty, S., Dutta, S., Singh, V., and Chandran, B. (2014). IFI16 restricts HSV-1 replication by accumulating on the hsv-1 genome, repressing HSV-1 gene expression, and directly or indirectly modulating histone modifications. *Plos Pathogens* 10, e1004503.

Johnson, K.E., Chikoti, L., and Chandran, B. (2013). Herpes simplex virus 1 infection induces activation and subsequent inhibition of the IFI16 and NLRP3 inflammasomes. *J Virol* 87, 5005-5018.

Jonsson, K.L., Laustsen, A., Krapp, C., Skipper, K.A., Thavachelvam, K., Hotter, D., Egedal, J.H., Kjolby, M., Mohammadi, P., Prabakaran, T., *et al.* (2017). IFI16 is required for DNA sensing in human macrophages by promoting production and function of cGAMP. *Nat Commun* 8, 14391.

Kaiser, W.J., Upton, J.W., and Mocarski, E.S. (2008). Receptor-interacting protein homotypic interaction motif-dependent control of NF-kappa B activation via the DNA-dependent activator of IFN regulatory factors. *J Immunol* 181, 6427-6434.

Kato, H., Takeuchi, O., Mikamo-Satoh, E., Hirai, R., Kawai, T., Matsushita, K., Hiiragi, A., Dermody, T., Fujita, T., and Akira, S. (2008). Length-dependent recognition of double-stranded ribonucleic acids by retinoic acid-inducible gene-I and melanoma differentiation-associated gene 5. *Journal of Experimental Medicine* 205, 1601-1610.

Kato, H., Takeuchi, O., Sato, S., Yoneyama, M., Yamamoto, M., Matsui, K., Uematsu, S., Jung, A., Kawai, T., Ishii, K., *et al.* (2006). Differential roles of MDA5 and RIG-I helicases in the recognition of RNA viruses. *Nature* 441, 101-105.

- Kawai, T., and Akira, S. (2011). Toll-like receptors and their crosstalk with other innate receptors in infection and immunity. *Immunity* 34, 637-650.
- Kawai, T., Takahashi, K., Sato, S., Coban, C., Kumar, H., Kato, H., Ishii, K., Takeuchi, O., and Akira, S. (2005). IPS-1, an adaptor triggering RIG-I- and Mda5-mediated type I interferon induction. *Nature Immunology* 6, 981-988.
- Kayagaki, N., Stowe, I., Lee, B., O'Rourke, K., Anderson, K., Warming, S., Cuellar, T., Haley, B., Roose-Girma, M., Phung, Q., *et al.* (2015). Caspase-11 cleaves gasdermin D for non-canonical inflammasome signalling. *Nature* 526, 666-671.
- Keating, S., Maloney, G., Moran, E., and Bowie, A. (2007). IRAK-2 participates in multiple toll-like receptor signaling pathways to NFkappaB via activation of TRAF6 ubiquitination. *Journal of Biological Chemistry* 282, 33435-33443.
- Kerur, N., Veetil, M.V., Sharma-Walia, N., Bottero, V., Sadagopan, S., Otageri, P., and Chandran, B. (2011). IFI16 acts as a nuclear pathogen sensor to induce the inflammasome in response to Kaposi Sarcoma-associated herpesvirus infection. *Cell Host Microbe* 9, 363-375.
- Khare, S., Ratsimandresy, R.A., de Almeida, L., Cuda, C.M., Rellick, S.L., Misharin, A.V., Wallin, M.C., Gangopadhyay, A., Forte, E., Gottwein, E., *et al.* (2014). The PYRIN domain-only protein POP3 inhibits ALR inflammasomes and regulates responses to infection with DNA viruses. *Nat Immunol* 15, 343-353.
- Kim, S., Bauernfeind, F., Ablasser, A., Hartmann, G., Fitzgerald, K.A., Latz, E., and Hornung, V. (2010). *Listeria monocytogenes* is sensed by the NLRP3 and AIM2 inflammasome. *Eur J Immunol* 40, 1545-1551.
- Kim, T., Kim, T.Y., Song, Y.H., Min, I.M., Yim, J., and Kim, T.K. (1999). Activation of interferon regulatory factor 3 in response to DNA-damaging agents. *J Biol Chem* 274, 30686-30689.
- Kim, T.K., Kim, T., Kim, T.Y., Lee, W.G., and Yim, J. (2000). Chemotherapeutic DNA-damaging drugs activate interferon regulatory factor-7 by the mitogen-activated protein kinase kinase-4-cJun NH2-terminal kinase pathway. *Cancer Res* 60, 1153-1156.
- Kim, Y., Brinkmann, M., Paquet, M., and Ploegh, H. (2008). UNC93B1 delivers nucleotide-sensing toll-like receptors to endolysosomes. *Nature* 452, 234-238.
- Kis-Toth, K., Szanto, A., Thai, T.H., and Tsokos, G.C. (2011). Cytosolic DNA-activated human dendritic cells are potent activators of the adaptive immune response. *J Immunol* 187, 1222-1234.
- Kolakofsky, D., Kowalinski, E., and Cusack, S. (2012). A structure-based model of RIG-I activation. *RNA* 18, 2118-2127.
- Kondo, T., Kobayashi, J., Saitoh, T., Maruyama, K., Ishii, K.J., Barber, G.N., Komatsu, K., Akira, S., and Kawai, T. (2013). DNA damage sensor MRE11

recognizes cytosolic double-stranded DNA and induces type I interferon by regulating STING trafficking. *Proc Natl Acad Sci U S A* 110, 2969-2974.

Konno, H., Konno, K., and Barber, G.N. (2013). Cyclic dinucleotides trigger ULK1 (ATG1) phosphorylation of STING to prevent sustained innate immune signaling. *Cell* 155, 688-698.

Koppe, U., Hogner, K., Doehn, J.M., Muller, H.C., Witzenth, M., Gutbier, B., Bauer, S., Pribyl, T., Hammerschmidt, S., Lohmeyer, J., *et al.* (2012). Streptococcus pneumoniae stimulates a STING- and IFN regulatory factor 3-dependent type I IFN production in macrophages, which regulates RANTES production in macrophages, cocultured alveolar epithelial cells, and mouse lungs. *J Immunol* 188, 811-817.

Kotenko, S., and Durbin, S. (2017). Contribution of type III interferons to antiviral immunity: location, location, location. *Journal of Biological Chemistry* 292, 7295–7303.

Kranzusch, P.J., Lee, A.S., Berger, J.M., and Doudna, J.A. (2013). Structure of human cGAS reveals a conserved family of second-messenger enzymes in innate immunity. *Cell Rep* 3, 1362-1368.

Kristiansen, H., Scherer CA., McVean M., Iadonato SP., Vends S., Thavachelvam K., Steffensen TB, Horan KA., Kuri T., Weber F., *et al.* (2010). Extracellular 2'-5' oligoadenylate synthetase stimulates RNase L-independent antiviral activity: a novel mechanism of virus-induced innate immunity. *Journal of Virology* 84, 11898-11904.

Kumar, H., Kawai, T., Kato, H., Sato, S., Takahashi, K., Coban, C., Yamamoto, M., Uematsu, S., Ishii, K., Takeuchi, O., and S., A. (2006). Essential role of IPS-1 in innate immune responses against RNA viruses. *Journal of Experimental Medicine* 203, 1795-1803.

LaFleur, D., Nardelli, B., Tsareva, T., Mather, D., Feng, P., Semenuk, M., Taylor, K., Buergin, M., Chinchilla, D., Roshke V, *et al.* (2001). Interferon-kappa, a novel type I interferon expressed in human keratinocytes. *Journal of Biological Chemistry* 276, 39765-39771.

Lahaye, X., Satoh, T., Gentili, M., Cerboni, S., Conrad, C., and Hurbain I2, E.M.A., Lacabaratz C3, Lelièvre JD4, Manel N5. (2013a). The capsids of HIV-1 and HIV-2 determine immune detection of the viral cDNA by the innate sensor cGAS in dendritic cells. *Immunity* 39, 1132-1142.

Lahaye, X., Satoh, T., Gentili, M., Cerboni, S., Conrad, C., Hurbain, I., El Marjou, A., Lacabaratz, C., Lelièvre, J.D., and Manel, N. (2013b). The capsids of HIV-1 and HIV-2 determine immune detection of the viral cDNA by the innate sensor cGAS in dendritic cells. *Immunity* 39, 1132-1142.

Lam, E., Stein, S., and Falck-Pedersen, E. (2014). Adenovirus detection by the cGAS/STING/TBK1 DNA sensing cascade. *J Virol* 88, 974-981.

- Lamphier, M., Sirois, C., Verma, A., Golenbock, D., and Latz, E. (2006). TLR9 and the recognition of self and non-self nucleic acids. *Ann N Y Acad Sci.*, 31-43.
- Lang, X., Tang, T., Jin, T., Ding, C., Zhou, R., and Jiang, W. (2016). TRIM65-catalyzed ubiquitination is essential for MDA5-mediated antiviral innate immunity. *Journal of Experimental Medicine* 214, 459-473.
- Lavin, M., Kozlov, S., Gatei, M., and Kijas, A. (2015). ATM-Dependent Phosphorylation of All Three Members of the MRN Complex: From Sensor to Adaptor. *Biomolecules* 5, 2877-2902.
- Lee A, Park EB, Lee J, Choi BS, and SJ., K. (2017). The N terminus of cGAS de-oligomerizes the cGAS:DNA complex and lifts the DNA size restriction of core-cGAS activity. *FEBS Letters* 591, 954-961.
- Lee, A., Park, E.B., Lee, J., Choi, B.S., and Kang, S.J. (2017). The N terminus of cGAS de-oligomerizes the cGAS:DNA complex and lifts the DNA size restriction of core-cGAS activity. *FEBS Lett* 591, 954-961.
- Lee, B., Moon, J., Shu, J., Yuan, L., Newman, Z., Schekman, R., and Barton, G. (2013). UNC93B1 mediates differential trafficking of endosomal TLRs. *Elife* 2.
- Leonard, J., Ghirlando, R., Askins, J., Bell, J., Margulies, D., Davies, D., and Segal, D. (2008). The TLR3 signaling complex forms by cooperative receptor dimerization. *Proc Natl Acad Sci U S A* 105, 258-263.
- Li, L., Yin, Q., Kuss, P., Maliga, Z., Millán, J.L., Wu, H., and Mitchison, T.J. (2014). Hydrolysis of 2'3'-cGAMP by ENPP1 and design of nonhydrolyzable analogs. *Nature Chemical Biology*.
- Li, T., Diner, B.A., Chen, J., and Cristea, I.M. (2012a). Acetylation modulates cellular distribution and DNA sensing ability of interferon-inducible protein IFI16. *Proc Natl Acad Sci U S A* 109, 10558-10563.
- Li, W., Avey, D., Fu, B., Wu, J., Ma, S., Liu, X., and Zhu, F. (2016). Kaposi's Sarcoma-Associated Herpesvirus Inhibitor of cGAS (KicGAS), Encoded by ORF52, Is an Abundant Tegument Protein and Is Required for Production of Infectious Progeny Viruses. *Journal of Virology* 90, 5329-5342.
- Li, X., and Chen, Z. (2012). Sequence specific detection of bacterial 23S ribosomal RNA by TLR13. *Elife* 1, :e00102.
- Li, X., Shu, C., Yi, G., Chaton, C.T., Shelton, C.L., Diao, J., Zuo, X., Kao, C.C., Herr, A.B., and Li, P. (2013a). Cyclic GMP-AMP synthase is activated by double-stranded DNA-induced oligomerization. *Immunity* 39, 1019-1031.
- Li, X.D., Wu, J., Gao, D., Wang, H., Sun, L., and Chen, Z.J. (2013b). Pivotal roles of cGAS-cGAMP signaling in antiviral defense and immune adjuvant effects. *Science* 341, 1390-1394.

Li, Y., Chen, R., Zhou, Q., Xu, Z., Li, C., Wang, S., Mao, A., Zhang, X., He, W., and Shu, H.-B. (2012b). LSm14A is a processing body-associated sensor of viral nucleic acids that initiates cellular antiviral response in the early phase of viral infection. *PNAS*.

Li, Y., Li C, Xue P, Zhong B, Mao AP, Ran Y, Chen H, Wang YY, Yang F, and HB., S. (2009). ISG56 is a negative-feedback regulator of virus-triggered signaling and cellular antiviral response. *PNAS* *12*; 7945-7950.

Liang, Q., Seo, G., Choi, Y., Kwak, M., Ge, J., Rodgers, M., Shi, M., Leslie, B., Hopfner, K., Ha, T., *et al.* (2014). Crosstalk between the cGAS DNA sensor and Beclin-1 autophagy protein shapes innate antimicrobial immune responses. *Cell Host and Microbe* *15*, 228-238.

Lin, R., Heylbroeck, C., Pitha, P.M., and Hiscott, J. (1998). Virus-dependent phosphorylation of the IRF-3 transcription factor regulates nuclear translocation, transactivation potential, and proteasome-mediated degradation. *Mol Cell Biol* *18*, 2986-2996.

Linder, M., and Deschenes, R. (2006). Palmitoylation: policing protein stability and traffic. *Nature Reviews Cell Biology* *8*, 74-84.

Lio, C.W., McDonald, B., Takahashi, M., Dhanwani, R., Sharma, N., Huang, J., Pham, E., Benedict, C.A., and Sharma, S. (2016). cGAS-STING Signaling Regulates Initial Innate Control of Cytomegalovirus Infection. *J Virol* *90*, 7789-7797.

Lippmann, J., Rothenburg, S., and Deigendesch, N. (2008). IFN β responses induced by intracellular bacteria or cytosolic DNA in different human cells do not require ZBP1 (DLM-1/DAI). *Microbiology*.

Liu, H., Loo, Y., Horner, S., Zornetzer, G., Katze, M., and Gale, M.J. (2012). The mitochondrial targeting chaperone 14-3-3 ϵ regulates a RIG-I translocon that mediates membrane association and innate antiviral immunity. *Cell Host and Microbe* *11*, 528-537.

Liu, S., Cai, X., Wu, J., Cong, Q., Chen, X., Li, T., Du, F., Ren, J., Wu, Y.T., Grishin, N.V., and Chen, Z.J. (2015a). Phosphorylation of innate immune adaptor proteins MAVS, STING, and TRIF induces IRF3 activation. *Science* *347*, aaa2630.

Liu, S., Chen, J., Cai, X., Wu, J., Chen, X., Wu, Y., Sun, L., and Chen, Z. (2013). MAVS recruits multiple ubiquitin E3 ligases to activate antiviral signaling cascades. *eLife* *2*; e00785.

Liu, X., Zhang, Z., Ruan, J., Pan, Y., Magupalli, V., Wu, H., and Lieberman, J. (2016). Inflammasome-activated gasdermin D causes pyroptosis by forming membrane pores. *Nature* *535*, 153-158.

Liu, Y., Li, J., Chen, J., Li, Y., Wang, W., Du, X., Song, W., Zhang, W., Lin, L., and Yuan, Z. (2015b). Hepatitis B virus polymerase disrupts K63-linked ubiquitination of STING to block innate cytosolic DNA-sensing pathways. *J Virol* *89*, 2287-2300.

- Lo Cigno, I., De Andrea, M., Borgogna, C., Albertini, S., Landini, M.M., Peretti, A., Johnson, K.E., Chandran, B., Landolfo, S., and Gariglio, M. (2015). The Nuclear DNA Sensor IFI16 Acts as a Restriction Factor for Human Papillomavirus Replication through Epigenetic Modifications of the Viral Promoters. *J Virol* *89*, 7506-7520.
- Loetscher, M., Gerber, B., Loetscher, P., Jones, S.A., Piali, L., Clark-Lewis, I., Baggiolini, M., and Moser, B. (1996). Chemokine receptor specific for IP10 and mig: structure, function, and expression in activated T-lymphocytes. *J Exp Med* *184*, 963-969.
- Loo, Y., Fornek, J., Crochet, N., Bajwa, G., Perwitasari, O., Martinez-Sobrido, L., Akira, S., Gill, M., García-Sastre, A., Katze, M., and Gale, M.J. (2008). Distinct RIG-I and MDA5 signaling by RNA viruses in innate immunity. *Journal of Virology* *82*, 335-345.
- Loo, Y., and Gale, M., Jr. (2011). Immune signaling by RIG-I-like receptors. *Immunity* *34*, 680-692.
- Lotze, M.T., Zeh, H.J., Rubartelli, A., Sparvero, L.J., Amoscato, A.A., Washburn, N.R., Devera, M.E., Liang, X., Tor, M., and Billiar, T. (2007). The grateful dead: damage-associated molecular pattern molecules and reduction/oxidation regulate immunity. *Immunol Rev* *220*, 60-81.
- Lu, A., Magupalli, V.G., Ruan, J., Yin, Q., Atianand, M.K., Vos, M.R., Schroder, G.F., Fitzgerald, K.A., Wu, H., and Egelman, E.H. (2014). Unified polymerization mechanism for the assembly of ASC-dependent inflammasomes. *Cell* *156*, 1193-1206.
- Luecke, S., Holleufer, A., Christensen, M., Jønsson, K., Boni, G., Sørensen, L., Johannsen, M., Jakobsen, M., Hartmann, R., and SR., P. (2017). cGAS is activated by DNA in a length-dependent manner. *EMBO Reports* *18*, 1707-1715.
- Lund, J., Alexopoulou, L., Sato, A., Karow, M., Adams, N., Gale, N., Iwasaki, A., and RA., F. (2004). Recognition of single-stranded RNA viruses by Toll-like receptor 7. *Proc Natl Acad Sci U S A* *101*, 5598-5603.
- Lund, J., Sato, A., Akira, S., Medzhitov, R., and A., I. (2003). Toll-like receptor 9-mediated recognition of Herpes simplex virus-2 by plasmacytoid dendritic cells. *Journal of Experimental Medicine* *198*, 513-520.
- Luo, D., Ding, S., Vela, A., Kohlway, A., Lindenbach, B., and Pyle, A. (2011). Structural insights into RNA recognition by RIG-I. *Cell* *147*, 409-422.
- Luo, W.W., Li, S., Li, C., Lian, H., Yang, Q., Zhong, B., and Shu, H.B. (2016). iRhom2 is essential for innate immunity to DNA viruses by mediating trafficking and stability of the adaptor STING. *Nat Immunol* *17*, 1057-1066.

- Maelfait, J., Liverpool, L., Bridgeman, A., Ragan, K., Upton, J., and Rehwinkel, J. (2017). Sensing of viral and endogenous RNA by ZBP1/DAI induces necroptosis. *Embo J* *e201796476*.
- Majlessi, L., and Brosch, R. (2015). Mycobacterium tuberculosis Meets the Cytosol: The Role of cGAS in Anti-mycobacterial Immunity. *Cell Host Microbe* *17*, 733-735.
- Malathi, K., Dong, B., Gale, M.J., and Silverman, R. (2007). Small self-RNA generated by RNase L amplifies antiviral innate immunity. *Nature* *448*, 816-819.
- Mankan, A.K., Schmidt, T., Chauhan, D., Goldeck, M., Honing, K., Gaidt, M., Kubarenko, A.V., Andreeva, L., Hopfner, K.P., and Hornung, V. (2014). Cytosolic RNA:DNA hybrids activate the cGAS-STING axis. *Embo J* *33*, 2937-2946.
- Marié, I., Durbin, J., and Levy, D. (1998). Differential viral induction of distinct interferon-alpha genes by positive feedback through interferon regulatory factor-7. *Embo J* *17*, 6660-6669.
- Marshall-Clarke, S., Downes JE, Haga IR, Bowie AG, Borrow P, Pennock JL, Grecnis RK, and P., R. (2007). Polyinosinic acid is a ligand for toll-like receptor 3. *Journal of Biological Chemistry* *282*, 24759-24766.
- Martinon, F., Burns, K., and Tschopp, J. (2002). The inflammasome: a molecular platform triggering activation of inflammatory caspases and processing of proIL1-beta. *Molecular Cell*.
- Matsumoto, M., Funami, K., Tanabe, M., Oshiumi, H., Shingai, M., Seto, Y., Yamamoto, A., and Seya, T. (2003). Subcellular localization of Toll-like receptor 3 in human dendritic cells. *Journal of Immunology* *171*, 3154-3162.
- Matsusaka, T., Fujikawa, K., Nishio, Y., Mukaida, N., and Matsushima K, K.T., Akira S. (1993). Transcription factors NF-IL6 and NF-kappa B synergistically activate transcription of the inflammatory cytokines, interleukin 6 and interleukin 8. *Proc Natl Acad Sci U S A* *90*, 10193-10197.
- McNab, F., Mayer-Barber, K., Sher, A., Wack, A., and O'Garra, A. (2015). Type I interferons in infectious disease. *Nat Rev Immunol* *15*, 87-103.
- McWhirter, S.M., Barbalat, R., Monroe, K.M., Fontana, M.F., Hyodo, M., Joncker, N.T., Ishii, K.J., Akira, S., Colonna, M., Chen, Z.J., *et al.* (2009). A host type I interferon response is induced by cytosolic sensing of the bacterial second messenger cyclic-di-GMP. *J Exp Med* *206*, 1899-1911.
- Melchjorsen, J., Sorensen, L.N., and Paludan, S.R. (2003). Expression and function of chemokines during viral infections: from molecular mechanisms to in vivo function. *J Leukoc Biol* *74*, 331-343.
- Meylan, E., Curran, J., Hofmann, K., Moradpour, D., Binder, M., Bartenschlager, R., and Tschopp, J. (2005). Cardif is an adaptor protein in the RIG-I antiviral pathway and is targeted by hepatitis C virus. *Nature* *437*, 1167-1172.

- Mondini, M., Vidali M, De Andrea M, Azzimonti B, Airò P, D'Ambrosio R, Riboldi P, Meroni PL, Albano E, Shoenfeld Y, *et al.* (2006). A novel autoantigen to differentiate limited cutaneous systemic sclerosis from diffuse cutaneous systemic sclerosis: the interferon-inducible gene IFI16. *Arthritis Rheum.* 54, 3939-3944.
- Mondini, M., Vidali, M., Airo, P., De Andrea, M., Riboldi, P., Meroni, P.L., Gariglio, M., and Landolfo, S. (2007). Role of the interferon-inducible gene IFI16 in the etiopathogenesis of systemic autoimmune disorders. *Ann N Y Acad Sci* 1110, 47-56.
- Monroe, K.M., Yang, Z., Johnson, J.R., Geng, X., Doitsh, G., Krogan, N.J., and Greene, W.C. (2014). IFI16 DNA sensor is required for death of lymphoid CD4 T cells abortively infected with HIV. *Science* 343, 428-432.
- Morrone, S.R., Wang, T., Constantoulakis, L.M., Hooy, R.M., Delannoy, M.J., and Sohn, J. (2014). Cooperative assembly of IFI16 filaments on dsDNA provides insights into host defense strategy. *Proc Natl Acad Sci U S A* 111, E62-71.
- Mukai, K., Konno, H., Akiba, T., Uemura, T., Waguri, S., Kobayashi, T., Barber, G., Arai, H., and Taguchi, T. (2016). Activation of STING requires palmitoylation at the Golgi. *Nature Communications*, 11932.
- Müller, U., Steinhoff, U., Reis, L., Hemmi, S., Pavlovic, J., Zinkernagel, R., and Aguet, M. (1994). Functional role of type I and type II interferons in antiviral defense. *Science* 264, 1918-1921.
- Muruve, D.A., Petrilli, V., Zaiss, A.K., White, L.R., Clark, S.A., Ross, P.J., Parks, R.J., and Tschopp, J. (2008). The inflammasome recognizes cytosolic microbial and host DNA and triggers an innate immune response. *Nature* 452, 103-107.
- Nakaya, Y., Lilue, J., Stavrou, S., Moran, E., and Ross, S. (2017). AIM2-Like Receptors Positively and Negatively Regulate the Interferon Response Induced by Cytosolic DNA. *MBio* 8, pii: e00944-00917.
- Negishi, H., Osawa, T., Ogami, K., Ouyang, X., Sakaguchi, S., Koshiba, R., Yanai, H., Seko, Y., Shitara, H., Bishop, K., *et al.* (2008). A critical link between Toll-like receptor 3 and type II interferon signaling pathways in antiviral innate immunity. *Proc Natl Acad Sci U S A* 105, 20446-20451.
- Neil, S., Zang T., and PD., B. (2008). Tetherin inhibits retrovirus release and is antagonized by HIV-1 Vpu. *Nature* 451, 425-430.
- Netea, M., Balkwill, F., and Chonchol, M. (2017). A guiding map for inflammation. *Nature Immunology* 18, 826-831.
- Ni, G., Konno, H., and Barber, G. (2017). Ubiquitination of STING at lysine 224 controls IRF3 activation. *Science Immunology* 2, eaah7119.
- Nissen, S.K., Hojen, J.F., Andersen, K.L., Kofod-Olsen, E., Berg, R.K., Paludan, S.R., Ostergaard, L., Jakobsen, M.R., Tolstrup, M., and Mogensen, T.H. (2014).

Innate DNA sensing is impaired in HIV patients and IFI16 expression correlates with chronic immune activation. *Clin Exp Immunol* 177, 295-309.

Nitta, S., Sakamoto, N., Nakagawa, M., Kakinuma, S., Mishima, K., Kusano-Kitazume, A., Kiyohashi, K., Murakawa, M., Nishimura-Sakurai, Y., Azuma, S., *et al.* (2013). Hepatitis C virus NS4B protein targets STING and abrogates RIG-I-mediated type I interferon-dependent innate immunity. *Hepatology* 57, 46-58.

Ohto, U., Shibata, T., Tanji, H., Ishida, H., Krayukhina, E., Uchiyama, S., Miyake, K., and Shimizu, T. (2015). Structural basis of CpG and inhibitory DNA recognition by Toll-like receptor 9. *Nature* 520, 702-705.

Oldenburg, M., Krüger, A., Ferstl, R., Kaufmann, A., Nees, G., Sigmund, A., Bathke, B., Lauterbach, H., Suter, M., Dreher, S., *et al.* (2012). TLR13 Recognizes Bacterial 23S rRNA Devoid of Erythromycin Resistance-Forming Modification. *Science* 337, 1111-1115.

Orzalli, M., Conwell, S., Berrios, C., DeCaprio, J., and Knipe, D. (2013). Nuclear interferon-inducible protein 16 promotes silencing of herpesviral and transfected DNA. *Proc Natl Acad Sci U S A* 110, E4492-4501.

Orzalli, M., and Knipe, D. (2014). Cellular sensing of viral DNA and viral evasion mechanisms. *Annu Rev Microbiol.*, 477-492.

Orzalli, M.H., Broekema, N.M., Diner, B.A., Hancks, D.C., Elde, N.C., Cristea, I.M., and Knipe, D.M. (2015). cGAS-mediated stabilization of IFI16 promotes innate signaling during herpes simplex virus infection. *Proc Natl Acad Sci U S A* 112, E1773-1781.

Orzalli, M.H., DeLuca, N.A., and Knipe, D.M. (2012). Nuclear IFI16 induction of IRF-3 signaling during herpesviral infection and degradation of IFI16 by the viral ICP0 protein. *Proc Natl Acad Sci U S A* 109, E3008-3017.

Oshiumi, H., Matsumoto, M., Hatakeyama, S., and Seya, T. (2009). Riplet/RNF135, a RING Finger Protein, Ubiquitinates RIG-I to Promote Interferon- β Induction during the Early Phase of Viral Infection. *Journal of Biological Chemistry* 284, 807-817.

Oshiumi, H., Miyashita, M., Inoue, N., Okabe, M., Matsumoto, M., and Seya, T. (2010). The ubiquitin ligase Riplet is essential for RIG-I-dependent innate immune responses to RNA virus infection. *Cell Host and Microbe* 8, 496-509.

Ouyang, S., Song, X., Wang, Y., Ru, H., Shaw, N., Jiang, Y., Niu, F., Zhu, Y., Qiu, W., Parvatiyar, K., *et al.* (2012). Structural analysis of the STING adaptor protein reveals a hydrophobic dimer interface and mode of cyclic di-GMP binding. *Immunity* 36, 1073-1086.

Paijo, J., Döring, M., Spanier, J., Grabski, E., Nooruzzaman, M., Schmidt, T., Witte, G., Messerle, M., Hornung, V., Kaefer, V., and Kalinke, U. (2016). cGAS Senses Human Cytomegalovirus and Induces Type I Interferon Responses in Human Monocyte-Derived Cells. *Plos Pathogens* 12, e1005546.

- Parker, D., Martin, F., Soong, G., Harfenist, B., Aguilar, J., Ratner, A., Fitzgerald, K., Schindler, C., and Prince, A. (2011). *Streptococcus pneumoniae* DNA initiates type I interferon signaling in the respiratory tract. *MBio* 2, e00016-00011.
- Parvatiyar, K., Zhang, Z., Teles, R.M., Ouyang, S., Jiang, Y., Iyer, S.S., Zaver, S.A., Schenk, M., Zeng, S., Zhong, W., *et al.* (2012). The helicase DDX41 recognizes the bacterial secondary messengers cyclic di-GMP and cyclic di-AMP to activate a type I interferon immune response. *Nat Immunol* 13, 1155-1161.
- Pasparakis, M., Haase, I., and Nestle, F.O. (2014). Mechanisms regulating skin immunity and inflammation. *Nat Rev Immunol* 14, 289-301.
- Pavlovic, J., Haller, O., and P., S. (1992). Human and mouse Mx proteins inhibit different steps of the influenza virus multiplication cycle. *Journal of Virology* 66, 2564-2569.
- Pestka, S., Krause, C., and Walter, M. (2004). Interferons, interferon-like cytokines, and their receptors. *Immunological Reviews*, 8-32.
- Peters, N., Ferguson, B., Mazzon, M., Fahy, A., Krysztofinska, E., Arribas-Bosacoma, R., Pearl, L., Ren, H., and Smith, G. (2013). A mechanism for the inhibition of DNA-PK-mediated DNA sensing by a virus. *Plos Pathog* 9, e1003649.
- Pichlmair, A., Kandasamy, K., Alvisi, G., Mulhern, O., Sacco, R., Habjan, M., Binder, M., Stefanovic, A., and Eberle, C., Goncalves A, Bürckstümmer T, Müller AC, Fauster A, Holze C, Lindsten K, Goodbourn S, Kochs G, Weber F, Bartenschlager R, Bowie AG, Bennett KL, Colinge J, Superti-Furga G. (2012). Viral immune modulators perturb the human molecular network by common and unique strategies. *Nature* 487, 486-490.
- Pichlmair, A., Lassnig C., Eberle CA., Górna MW., Baumann CL., Burkard TR., Bürckstümmer T., Stefanovic A., Krieger S., Bennett KL., *et al.* (2011). IFIT1 is an antiviral protein that recognizes 5'-triphosphate RNA. *Nature Immunology* 12, 624-630.
- Pichlmair, A., Schulz, O., Tan, C., Rehwinkel, J., Kato, H., Takeuchi, O., Akira, S., Way, M., Schiavo, G., and Reis e Sousa, C. (2009). Activation of MDA5 requires higher-order RNA structures generated during virus infection. *Journal of Virology* 83, 10761-10769.
- Pichlmair, A., Schulz, O., Tan, C.P., Naslund, T.I., Liljestrom, P., Weber, F., and Reis e Sousa, C. (2006). RIG-I-mediated antiviral responses to single-stranded RNA bearing 5'-phosphates. *Science* 314, 997-1001.
- Platanias, L. (2005). Mechanisms of type-I- and type-II-interferon-mediated signalling. *Nature Reviews Immunology*, 375-386.
- Qin, Y., Zhou, M.T., Hu, M.M., Hu, Y.H., Zhang, J., Guo, L., Zhong, B., and Shu, H.B. (2014). RNF26 temporally regulates virus-triggered type I interferon induction by two distinct mechanisms. *Plos Pathog* 10, e1004358.

- Rathinam, V., Jiang, Z., Waggoner, S., Sharma, S., Cole, L., Waggoner, L., Vanaja, S., Monks, B., Ganesan, S., Latz, E., *et al.* (2010). The AIM2 inflammasome is essential for host defense against cytosolic bacteria and DNA viruses. *Nature Immunology* *11*, 395-402.
- Rebsamen, M., Heinz, L.X., Meylan, E., Michallet, M.-C.E.C., Schroder, K., Hofmann, K., Vazquez, J., Benedict, C.A., and Tschopp, J.U.R. (2009). DAI/ZBP1 recruits RIP1 and RIP3 through RIP homotypic interaction motifs to activate NF-kappaB. *EMBO Reports*.
- Rehwinkel, J., Tan, C.P., Goubau, D., Schulz, O., Pichlmair, A., Bier, K., Robb, N., Vreede, F., Barclay, W., Fodor, E., and Reis e Sousa, C. (2010). RIG-I detects viral genomic RNA during negative-strand RNA virus infection. *Cell* *140*, 397-408.
- Reinert, L., Lopusná, K., Winther, H., Sun, C., Thomsen, M., Nandakumar, R., Mogensen, T., Meyer, M., Vægter, C., Nyengaard, J., *et al.* (2017). Sensing of HSV-1 by the cGAS-STING pathway in microglia orchestrates antiviral defence in the CNS. *Nature Communications* *10*, 13348.
- Reinholz, M., Kawakami, Y., Salzer, S., Kreuter, A., Dombrowski, Y., Koglin, S., Kresse, S., Ruzicka, T., and Schaubert, J. (2013). HPV16 activates the AIM2 inflammasome in keratinocytes. *Arch Dermatol Res* *305*, 723-732.
- Rigby, R., Webb, L., Mackenzie, K., Li, Y., Leitch, A., Reijns, M., Lundie, R., Revuelta, A., Davidson, D., Diebold, S., *et al.* (2014). RNA:DNA hybrids are a novel molecular pattern sensed by TLR9. *Embo J* *33*, 542-558.
- Roy, A., Dutta, D., Iqbal, J., Pisano, G., Gjyshi, O., Ansari, M.A., Kumar, B., and Chandran, B. (2016). Nuclear Innate Immune DNA Sensor IFI16 Is Degraded during Lytic Reactivation of Kaposi's Sarcoma-Associated Herpesvirus (KSHV): Role of IFI16 in Maintenance of KSHV Latency. *J Virol* *90*, 8822-8841.
- Saito, T., Owen, D., Jiang, F., Marcotrigiano, J., and Gale, M.J. (2008). Innate immunity induced by composition-dependent RIG-I recognition of hepatitis C virus RNA. *Nature* *454*, 523-527.
- Saitoh, T., Fujita, N., Hayashi, T., Takahara, K., Satoh, T., Lee, H., Matsunaga, K., Kageyama, S., Omori, H., Noda, T., *et al.* (2009). Atg9a controls dsDNA-driven dynamic translocation of STING and the innate immune response. *Proc Natl Acad Sci U S A* *106*, 20842-20846.
- Samanta, M., Iwakiri, D., Kanda, T., Imaizumi, T., and Takada, K. (2006). EB virus-encoded RNAs are recognized by RIG-I and activate signaling to induce type I IFN. *Embo J* *25*, 4207-4214.
- Sanchez David, R., Combredet C., Sismeiro O., Dillies MA., Jagla B., Coppée JY., Mura M., Guerbois Galla M., Despres P., Tangy F., and AV., K. (2016). Comparative analysis of viral RNA signatures on different RIG-I-like receptors. *Elife* *24*, e11275. .

- Sarkar, A., and Hochedlinger, K. (2013). The sox family of transcription factors: versatile regulators of stem and progenitor cell fate. *Cell Stem Cell* *12*, 15–30.
- Sato, M., Hata, N., Asagiri, M., Nakaya, T., Taniguchi, T., and Tanaka, N. (1998). Positive feedback regulation of type I IFN genes by the IFN-inducible transcription factor IRF-7. *FEBS Letters* *441*, 106-110.
- Satoh, T., Kato, H., Kumagai, Y., Yoneyama, M., Sato, S., Matsushita, K., Tsujimura, T., Fujita, T., Akira, S., and Takeuchi, O. (2010). LGP2 is a positive regulator of RIG-I- and MDA5-mediated antiviral responses. *Proc Natl Acad Sci U S A* *107*, 1512-1517.
- Schafer, S.L., Lin, R., Moore, P.A., Hiscott, J., and Pitha, P.M. (1998). Regulation of type I interferon gene expression by interferon regulatory factor-3. *J Biol Chem* *273*, 2714-2720.
- Schall, T.J., Bacon, K., Toy, K.J., and Goeddel, D.V. (1990). Selective attraction of monocytes and T lymphocytes of the memory phenotype by cytokine RANTES. *Nature* *347*, 669-671.
- Schlee, M., Roth, A., Hornung, V., Hagmann, C., Wimmenauer, V., Barchet, W., Coch, C., Janke, M., Mihailovic, A., Wardle, G., *et al.* (2009). Recognition of 5' triphosphate by RIG-I helicase requires short blunt double-stranded RNA as contained in panhandle of negative-strand virus. *Immunity* *31*, 25–34.
- Schoggins, J., Wilson, S., Panis, M., Murphy, M., Jones, C., Bieniasz, P., and Rice, C. (2011). A diverse range of gene products are effectors of the type I interferon antiviral response. *Nature* *472*, 481-485.
- Schoggins, J.W., MacDuff, D.A., Imanaka, N., Gainey, M.D., Shrestha, B., Eitson, J.L., Mar, K.B., Richardson, R.B., Ratushny, A.V., Litvak, V., *et al.* (2014). Pan-viral specificity of IFN-induced genes reveals new roles for cGAS in innate immunity. *Nature* *505*, 691-695.
- Seelig, H., Ehrfeld H., and M., R. (1994). Interferon-gamma-inducible protein p16. A new target of antinuclear antibodies in patients with systemic lupus erythematosus. *Arthritis Rheum.* *37*, 1672-1683.
- Seth, R., Sun, L., Ea, C., and Chen, Z. (2005). Identification and Characterization of MAVS, a Mitochondrial Antiviral Signaling Protein that Activates NF- κ B and IRF3. *Cell* *122*, 669-682.
- Sharma, S., DeOliveira, R.B., Kalantari, P., Parroche, P., Goutagny, N., Jiang, Z., Chan, J., Bartholomeu, D.C., Lauw, F., Hall, J.P., *et al.* (2011). Innate immune recognition of an AT-rich stem-loop DNA motif in the *Plasmodium falciparum* genome. *Immunity* *35*, 194-207.
- Shi, J., Zhao, Y., Wang, K., Shi, X., Wang, Y., Huang, H., Zhuang, Y., Cai, T., Wang, F., and Shao, F. (2015). Cleavage of GSDMD by inflammatory caspases determines pyroptotic cell death. *Nature* *526*, 660-665.

- Shi, T., Song, E., Nie, S., Rodland, K., Liu, T., Qian, W., and Smith, R. (2016). Advances in targeted proteomics and applications to biomedical research. *Proteomics* 16, 2160-2182.
- Shibata, T., Ohto, U., Nomura, S., Kibata, K., Motoi, Y., Zhang, Y., Murakami, Y., Fukui, R., Ishimoto, T., Sano, S., *et al.* (2015). Guanosine and its modified derivatives are endogenous ligands for TLR7. *International Immunology* 28, 211-222.
- Shimizu, T. (2017). Structural insights into ligand recognition and regulation of nucleic acid-sensing Toll-like receptors. *Current Opinion in Structural Biology* 34, 52-59.
- Shu, C., Sankaran, B., Chaton, C.T., Herr, A.B., Mishra, A., Peng, J., and Li, P. (2013). Structural insights into the functions of TBK1 in innate antimicrobial immunity. *Structure* 21, 1137-1148.
- Shu, C., Yi, G., Watts, T., Kao, C.C., and Li, P. (2012). Structure of STING bound to cyclic di-GMP reveals the mechanism of cyclic dinucleotide recognition by the immune system. *Nat Struct Mol Biol* 19, 722-724.
- Singh, V.V., Kerur, N., Bottero, V., Dutta, S., Chakraborty, S., Ansari, M.A., Paudel, N., Chikoti, L., and Chandran, B. (2013). Kaposi's sarcoma-associated herpesvirus latency in endothelial and B cells activates gamma interferon-inducible protein 16-mediated inflammasomes. *J Virol* 87, 4417-4431.
- Smith, G., Benfield, C., Maluquer de Motes, C., Mazzon, M., Ember, S., and Ferguson, B., Sumner RP. (2013). Vaccinia virus immune evasion: mechanisms, virulence and immunogenicity. *J Gen Virol.* 94, 2367-2392.
- Soby, S., Laursen, R.R., Ostergaard, L., and Melchjorsen, J. (2012). HSV-1-induced chemokine expression via IFI16-dependent and IFI16-independent pathways in human monocyte-derived macrophages. *Herpesviridae* 3, 6.
- Sparrer, K., and Gack, M. (2015). Intracellular detection of viral nucleic acids. *Current Opinion in Microbiology* 26, 1-9.
- Sridharan, H., Ragan, K., Guo, H., Gilley, R., Landsteiner, V., Kaiser, W., and Upton, J. (2017). Murine cytomegalovirus IE3-dependent transcription is required for DAI/ZBP1-mediated necroptosis. *Embo J* 18, 1429-1441.
- Stetson, D.B., and Medzhitov, R. (2006a). Recognition of cytosolic DNA activates an IRF3-dependent innate immune response. *Immunity* 24, 93-103.
- Stetson, D.B., and Medzhitov, R. (2006b). Type I interferons in host defense. *Immunity* 25, 373-381.
- Storek, K.M., Gertsvolf, N.A., Ohlson, M.B., and Monack, D.M. (2015). cGAS and Ifi204 cooperate to produce type I IFNs in response to Francisella infection. *J Immunol* 194, 3236-3245.

- Stratmann, S., Morrone, S., van Oijen, A., and Sohn, J. (2015). The innate immune sensor IFI16 recognizes foreign DNA in the nucleus by scanning along the duplex. *Elife* 16, e11721.
- Stremlau, M., Owens CM., Perron MJ., Kiessling M., Autissier P., and J., S. (2004). The cytoplasmic body component TRIM5alpha restricts HIV-1 infection in Old World monkeys. *Nature* 427, 848-853.
- Sun, B., Sundström, K., Chew, J., Bist, P., Gan, E., Tan, H., Goh, K., Chawla, T., Tang, C., and Ooi, E. (2017). Dengue virus activates cGAS through the release of mitochondrial DNA. *Nature Scientific Reports* 7, 3594.
- Sun, L., Wu, J., Du, F., Chen, X., and Chen, Z.J. (2013a). Cyclic GMP-AMP synthase is a cytosolic DNA sensor that activates the type I interferon pathway. *Science* 339, 786-791.
- Sun, L., Xing, Y., Chen, X., Zheng, Y., Yang, Y., Nichols, D., Clementz, M., Banach, B., Li, K., Baker, S., and Chen, Z. (2012). Coronavirus papain-like proteases negatively regulate antiviral innate immune response through disruption of STING-mediated signaling. *Plos One* 7, e30802.
- Sun, L.J., Wu, J.X., Du, F.H., Chen, X., and Chen, Z.J.J. (2013b). Cyclic GMP-AMP Synthase Is a Cytosolic DNA Sensor That Activates the Type I Interferon Pathway. *Science* 339, 786-791.
- Sun, Q., Sun, L., Liu, H., Chen, X., Seth, R., Forman, J., and Chen, Z. (2006). The specific and essential role of MAVS in antiviral innate immune responses. *Immunity* 24, 633-642.
- Sun, W., Li, Y., Chen, L., Chen, H., You, F., Zhou, X., Zhou, Y., Zhai, Z., Chen, D., and Jiang, Z. (2009). ERIS, an endoplasmic reticulum IFN stimulator, activates innate immune signaling through dimerization. *Proc Natl Acad Sci U S A* 106, 8653-8658.
- Suthar, M., Ramos HJ., Brassil MM., Netland J., Chappell CP., Blahnik G., McMillan A., Diamond MS., Clark EA., Bevan MJ., and Jr., G.M. (2012). The RIG-I-like receptor LGP2 controls CD8(+) T cell survival and fitness. *Immunity* 37, 235-248.
- Tabeta, K., Hoebe, K., Janssen, E., Du, X., Georgel, P., Crozat, K., Mudd, S., Mann, N., Sovath, S., Goode, J., *et al.* (2006). The Unc93b1 mutation 3d disrupts exogenous antigen presentation and signaling via Toll-like receptors 3, 7 and 9.
- Takaoka, A., Wang, Z., Choi, M.K., Yanai, H., Negishi, H., Ban, T., Lu, Y., Miyagishi, M., Kodama, T., Honda, K., *et al.* (2007). DAI (DLM-1/ZBP1) is a cytosolic DNA sensor and an activator of innate immune response. *Nature* 448, 501-505.
- Tamassia, N., Bazzoni, F., Le Moigne, V., Calzetti, F., Masala, C., Grisendi, G., Bussmeyer, U., Scutera, S., De Gironcoli, M., Costantini, C., *et al.* (2012). IFN- β expression is directly activated in human neutrophils transfected with plasmid DNA and is further increased via TLR-4-mediated signaling. *Journal of Immunology*.

- Tanaka, Y., and Chen, Z.J. (2012). STING specifies IRF3 phosphorylation by TBK1 in the cytosolic DNA signaling pathway. *Science Signalling* 5.
- Tanaka, Y., and Chen, Z.J. (2012). STING specifies IRF3 phosphorylation by TBK1 in the cytosolic DNA signaling pathway. *Sci Signal* 5, ra20.
- Tanji, H., Ohto, U., Shibata, T., Taoka, M., Yamauchi, Y., Isobe, T., Miyake, K., and Shimizu, T. (2015). Toll-like receptor 8 senses degradation products of single-stranded RNA. *Nature Structural and Molecular Biology* 22, 109-115.
- Tao, J., Zhang, X.W., Jin, J., Du, X.X., Lian, T., Yang, J., Zhou, X., Jiang, Z., and Su, X.D. (2017). Nonspecific DNA Binding of cGAS N Terminus Promotes cGAS Activation. *J Immunol* 198, 3627-3636.
- Thompson, M.R., Sharma, S., Atianand, M., Jensen, S.B., Carpenter, S., Knipe, D.M., Fitzgerald, K.A., and Kurt-Jones, E.A. (2014). Interferon gamma-inducible protein (IFI) 16 transcriptionally regulates type I interferons and other interferon-stimulated genes and controls the interferon response to both DNA and RNA viruses. *J Biol Chem* 289, 23568-23581.
- Thornberry, N., Bull, H., Calaycay, J., Chapman, K., Howard, A., Kostura, M., and Miller, D., Molineaux SM, Weidner JR, Aunins J, et al. (1992). A novel heterodimeric cysteine protease is required for interleukin-1 beta processing in monocytes. *Nature* 356, 768-774.
- Tian, J., Avalos, A.M., Mao, S.-Y., Chen, B., Senthil, K., Wu, H., Parroche, P., Drabic, S., Golenbock, D., Sirois, C., et al. (2007). Toll-like receptor 9-dependent activation by DNA-containing immune complexes is mediated by HMGB1 and RAGE. *Nature Immunology*.
- Tsuchida, T., Zou, J., Saitoh, T., Kumar, H., Abe, T., Matsuura, Y., Kawai, T., and Akira, S. (2010). The ubiquitin ligase TRIM56 regulates innate immune responses to intracellular double-stranded DNA. *Immunity* 33, 765-776.
- Turnell, A.S., and Grand, R.J. (2012). DNA viruses and the cellular DNA-damage response. *J Gen Virol* 93, 2076-2097.
- Turnock, D., and Ferguson, M.A.J. (2007). Sugar Nucleotide Pools of *Trypanosoma brucei*, *Trypanosoma cruzi*, and *Leishmania major*. *Eukaryotic Cell* 6 1450-1463.
- Unterholzner, L. (2013). The interferon response to intracellular DNA: why so many receptors? *Immunobiology* 218, 1312-1321.
- Unterholzner, L., Keating, S.E., Baran, M., Horan, K.A., Jensen, S.B., Sharma, S., Sirois, C.M., Jin, T., Latz, E., Xiao, T.S., et al. (2010). IFI16 is an innate immune sensor for intracellular DNA. *Nat Immunol* 11, 997-1004.
- Upton, J.W., Kaiser, W.J., and Mocarski, E.S. (2012). DAI/ZBP1/DLM-1 complexes with RIP3 to mediate virus-induced programmed necrosis that is targeted by murine cytomegalovirus vIRA. *Cell Host Microbe* 11, 290-297.

- Vance, R.E. (2016). Cytosolic DNA Sensing: The Field Narrows. *Immunity* 45, 227-228.
- Venkataraman, T., Valdes, M., Elsby, R., Kakuta, S., Caceres, G., Saijo, S., Iwakura, Y., and Barber, G. (2007). Loss of DExD/H box RNA helicase LGP2 manifests disparate antiviral responses. *Journal of Immunology* 178, 6444-6455.
- Wang, H., Chatterjee, G., Meyer, J., Liu, C., Manjunath, N., Bray-Ward, P., and P., L. (1999). Characteristics of three homologous 202 genes (Ifi202a, Ifi202b, and Ifi202c) from the murine interferon-activatable gene 200 cluster. *Genomics* 60, 281-294.
- Wang, Q., Huang, L., Hong, Z., Lv, Z., Mao, Z., Tang, Y., and Kong, X., Li S2, Cui Y2, Liu H2, Zhang L2, Zhang X4, Jiang L4, Wang C2,3, Zhou Q1. (2017). The E3 ubiquitin ligase RNF185 facilitates the cGAS-mediated innate immune response. *Plos Pathog* 13, e1006264.
- Wang, Q., Liu, X., Cui, Y., Tang, Y., Chen, W., Li, S., Yu, H., Pan, Y., and Wang, C. (2014). The E3 ubiquitin ligase AMFR and INSIG1 bridge the activation of TBK1 kinase by modifying the adaptor STING. *Immunity* 41, 919-933.
- Wang, X., Hinson, E., and P., C. (2007). The interferon-inducible protein viperin inhibits influenza virus release by perturbing lipid rafts. *Cell Host and Microbe* 2, 96-105.
- Wang, Z., Choi, M.K., Ban, T., Yanai, H., Negishi, H., Lu, Y., Tamura, T., Takaoka, A., Nishikura, K., and Taniguchi, T. (2008). Regulation of innate immune responses by DAI (DLM-1/ZBP1) and other DNA-sensing molecules. *Proc Natl Acad Sci U S A* 105, 5477-5482.
- Weber, F., Wagner, V., Rasmussen, S., Hartmann, R., and Paludan, S. (2006). Double-stranded RNA is produced by positive-strand RNA viruses and DNA viruses but not in detectable amounts by negative-strand RNA viruses. *Journal of Virology* 80, 5059-5064.
- West, A.P., Khoury-Hanold, W., Staron, M., Tal, M.C., Pineda, C.M., Lang, S.M., Bestwick, M., Duguay, B.A., Raimundo, N., MacDuff, D.A., *et al.* (2015). Mitochondrial DNA stress primes the antiviral innate immune response. *Nature* 520, 553-557.
- White, R.J. (2011). Transcription by RNA polymerase III: more complex than we thought. *Nature Reviews Genetics*.
- Wu, B., Peisley, A., Richards, C., Yao, H., Zeng, X., Lin, C., Chu, F., Walz, T., and Hur, S. (2013a). Structural basis for dsRNA recognition, filament formation, and antiviral signal activation by MDA5. *Cell* 52(276-289).
- Wu, J., and Chen, Z.J. (2014). Innate immune sensing and signaling of cytosolic nucleic acids. *Annu Rev Immunol* 32, 461-488.

- Wu, J., Sun, L., Chen, X., Du, F., Shi, H., Chen, C., and Chen, Z.J. (2013b). Cyclic GMP-AMP is an endogenous second messenger in innate immune signaling by cytosolic DNA. *Science* *339*, 826-830.
- Xia, P., Wang, S., Ye, B., Du, Y., Huang, G., Zhu, P., and Fan, Z. (2015). Sox2 functions as a sequence-specific DNA sensor in neutrophils to initiate innate immunity against microbial infection. *Nature Immunology* *16*, 366-375.
- Xia, P., Ye, B., Wang, S., Zhu, X., Du, Y., Xiong, Z., Tian, Y., and Fan, Z. (2016a). Glutamylation of the DNA sensor cGAS regulates its binding and synthase activity in antiviral immunity. *Nat Immunol* *17*, 369-378.
- Xia, P., Ye, B., Wang, S., Zhu, X., Du, Y., Xiong, Z., Tian, Y., and Fan, Z. (2016b). Glutamylation of the DNA sensor cGAS regulates its binding and synthase activity in antiviral immunity. *Nature Immunology* *17*, 369-378.
- Xie, Q., Whisnant, R., and Nathan, C. (1993). Promoter of the mouse gene encoding calcium-independent nitric oxide synthase confers inducibility by interferon gamma and bacterial lipopolysaccharide. *Journal of Experimental Medicine* *177*, 1779-1784.
- Xu, L., Wang, Y., Han, K., Li, L., Zhai, Z., and Shu, H. (2005). VISA is an adapter protein required for virus-triggered IFN-beta signaling. *Molecular Cell* *19*, 727-740.
- Yamamoto, M., Sato, S., Hemmi, H., Hoshino, K., Kaisho, T., Sanjo, H., Takeuchi, O., Sugiyama, M., Okabe, M., Takeda, K., and S., A. (2003). Role of adaptor TRIF in the MyD88-independent toll-like receptor signaling pathway. *Science* *301*, 640-643.
- Yanai, H., Ban, T., Wang, Z., Choi, M.K., Kawamura, T., Negishi, H., Nakasato, M., Lu, Y., Hangai, S., Koshiba, R., *et al.* (2009). HMGB proteins function as universal sentinels for nucleic-acid-mediated innate immune responses. *Nature* *462*, 99-103.
- Yang, P., An, H., Liu, X., Wen, M., Zheng, Y., Rui, Y., and Cao, X. (2010). The cytosolic nucleic acid sensor LRRFIP1 mediates the production of type I interferon via a beta-catenin-dependent pathway. *Nat Immunol* *11*, 487-494.
- Yi, G., Brendel, V., Shu, C., Li, P., Palanathan, S., and Cheng Kao, C. (2013). Single nucleotide polymorphisms of human STING can affect innate immune response to cyclic dinucleotides. *PLoS One* *8*, e77846.
- Yin, Q., Sester, D.P., Tian, Y., Hsiao, Y.-S., Lu, A., Cridland, J.A., Sagulenko, V., Thygesen, S.J., Choubey, D., and Hornung, V., *et al.* (2011a). Molecular mechanism for p202-mediated specific inhibition of AIM2 inflammasome activation. *Cell Reports*.
- Yin, Q., Sester, D.P., Tian, Y., Hsiao, Y.-S., Lu, A., Cridland, J.A., Sagulenko, V., Thygesen, S.J., Choubey, D., and Hornung, V., *et al.* (2011b). Molecular mechanism for p202-mediated specific inhibition of AIM2 inflammasome activation. *Cell Reports*.

Yoh, S., Schneider, M., Seifried, J., Soonthornvacharin, S., Akleh, R., Olivieri, K., De Jesus, P., Ruan, C., de Castro, E., Ruiz, P., *et al.* (2015). PQBP1 Is a Proximal Sensor of the cGAS-Dependent Innate Response to HIV-1. *Cell* *161*, 1293-1305.

Yoneyama, M., Kikuchi, M., Matsumoto, K., Imaizumi, T., Miyagishi, M., Taira, K., Foy, E., Loo, Y.M., Gale, M. Jr., Akira, S., *et al.* (2005). Shared and unique functions of the DExD/H-box helicases RIG-I, MDA5, and LGP2 in antiviral innate immunity. *Journal of Immunology* *175*, 2851-2858.

Yoneyama, M., Kikuchi, M., Natsukawa, T., Shinobu, N., Imaizumi, T., Miyagishi, M., Taira, K., Akira, S., and Fujita, T. (2004). The RNA helicase RIG-I has an essential function in double-stranded RNA-induced innate antiviral responses. *Nature Immunology* *5*, 730-737.

York, A., Williams, K., Argus, J., Zhou, Q., Brar, G., Vergnes, L., Gray, E., Zhen, A., Wu, N., Yamada, D., *et al.* (2015). Limiting Cholesterol Biosynthetic Flux Spontaneously Engages Type I IFN Signaling. *Cell* *163*, 1716-1729.

Yu, X., Cai, B., Wang, M., Tan, P., Ding, X., Wu, J., Li, J., Li, Q., and Liu, P., Xing C5, Wang HY5, Su XZ8, Wang RF9. (2016). Cross-Regulation of Two Type I Interferon Signaling Pathways in Plasmacytoid Dendritic Cells Controls Anti-malaria Immunity and Host Mortality. *Immunity* *45*, 1093-1107.

Zeng, W., Sun, L., Jiang, X., Chen, X., Hou, F., Adhikari, A., Xu, M., and Chen, Z. (2010). Reconstitution of the RIG-I pathway reveals a signaling role of unanchored polyubiquitin chains in innate immunity. *Cell* *141*, 315-330.

Zhang, J., Hu, M.M., Wang, Y.Y., and Shu, H.B. (2012). RIM32 Protein Modulates Type I Interferon Induction and Cellular Antiviral Response by Targeting MITA/STING Protein for K63-linked Ubiquitination. *Journal of Biological Chemistry*.

Zhang, K., Kagan, D., DuBois, W., Robinson, R., Bliskovsky, V., Vass, W., Zhang, S., and BA., M. (2009). Mndal, a new interferon-inducible family member, is highly polymorphic, suppresses cell growth, and may modify plasmacytoma susceptibility. *Blood* *114* 2952-2960.

Zhang, L., Mo, J., Swanson, K., Wen, H., Petrucelli, A., Gregory, S., and Zhang, Z., Schneider M, Jiang Y, Fitzgerald KA, Ouyang S, Liu ZJ, Damania B, Shu HB, Duncan JA, Ting JP. (2014a). NLRC3, a member of the NLR family of proteins, is a negative regulator of innate immune signaling induced by the DNA sensor STING. *Immunity* *40*, 329-341.

Zhang, X., Brann, T.W., Zhou, M., Yang, J., Oguariri, R.M., Lidie, K.B., Imamichi, H., Huang, D.W., Lempicki, R.A., Baseler, M.W., *et al.* (2011a). Cutting edge: Ku70 is a novel cytosolic DNA sensor that induces type III rather than type I IFN. *J Immunol* *186*, 4541-4545.

- Zhang, X., Shi, H., Wu, J., Zhang, X., Sun, L., Chen, C., and Chen, Z.J. (2013). Cyclic GMP-AMP containing mixed phosphodiester linkages is an endogenous high-affinity ligand for STING. *Mol Cell* *51*, 226-235.
- Zhang, X., Wu, J., Du, F., Xu, H., Sun, L., Chen, Z., Brautigam, C.A., Zhang, X., and Chen, Z.J. (2014b). The cytosolic DNA sensor cGAS forms an oligomeric complex with DNA and undergoes switch-like conformational changes in the activation loop. *Cell Rep* *6*, 421-430.
- Zhang, Y., Yeruva, L., Marinov, A., Prantner, D., Wyrick, P.B., Lupashin, V., and Nagarajan, U.M. (2014). The DNA sensor, cyclic GMP-AMP synthase, is essential for induction of IFN- β during *Chlamydia trachomatis* infection. *Journal of Immunology*.
- Zhang, Z., Ohto, U., Shibata, T., Krayukhina, E., Taoka, M., Yamauchi, Y., Tanji, H., Isobe, T., Uchiyama, S., Miyake, K., and Shimizu, T. (2016). Structural Analysis Reveals that Toll-like Receptor 7 Is a Dual Receptor for Guanosine and Single-Stranded RNA. *Immunity* *45*, 737-748.
- Zhang, Z., Yuan, B., Bao, M., Lu, N., Kim, T., and Liu, Y.J. (2011b). The helicase DDX41 senses intracellular DNA mediated by the adaptor STING in dendritic cells. *Nat Immunol* *12*, 959-965.
- Zhong, B., Yang, Y., Li, S., Wang, Y.Y., Li, Y., Diao, F., Lei, C., He, X., Zhang, L., Tien, P., and Shu, H.B. (2008). The adaptor protein MITA links virus-sensing receptors to IRF3 transcription factor activation. *Immunity* *29*, 538-550.
- Zhong, B., Zhang, L., Lei, C., Li, Y., Mao, A.P., Yang, Y., Wang, Y.Y., Zhang, X.L., and Shu, H.B. (2009). The ubiquitin ligase RNF5 regulates antiviral responses by mediating degradation of the adaptor protein MITA. *Immunity* *30*, 397-407.
- Zhou, Q., Lin, H., Wang, S., Wang, S., Ran, Y., and Liu, Y., Ye W1, Xiong X1, Zhong B1, Shu HB3, Wang YY4. (2014). The ER-associated protein ZDHHC1 is a positive regulator of DNA virus-triggered, MITA/STING-dependent innate immune signaling. *Cell Host and Microbe* *6*, 450-461.
- Zhu, J., and Paul, W. (2008). CD4 T cells: fates, functions, and faults. *Blood* *112*, 1557-1569.

Appendix

ARTICLE

Received 15 Dec 2015 | Accepted 22 Dec 2016 | Published 13 Feb 2017

DOI: 10.1038/ncomms14392

OPEN

IFI16 and cGAS cooperate in the activation of STING during DNA sensing in human keratinocytes

Jessica F. Almine^{1,2,*}, Craig A.J. O'Hare^{1,2,*}, Gillian Dunphy^{1,2}, Ismar R. Haga³, Rangeetha J. Naik¹, Abdelmadjid Atrih⁴, Dympna J. Connolly⁵, Jordan Taylor¹, Ian R. Kelsall¹, Andrew G. Bowie⁵, Philippa M. Beard^{3,6} & Leonie Unterholzner^{1,2}

Many human cells can sense the presence of exogenous DNA during infection through the cytosolic DNA receptor cyclic GMP-AMP synthase (cGAS), which produces the second messenger cyclic GMP-AMP (cGAMP). Other putative DNA receptors have been described, but whether their functions are redundant, tissue-specific or integrated in the cGAS-cGAMP pathway is unclear. Here we show that interferon- γ inducible protein 16 (IFI16) cooperates with cGAS during DNA sensing in human keratinocytes, as both cGAS and IFI16 are required for the full activation of an innate immune response to exogenous DNA and DNA viruses. IFI16 is also required for the cGAMP-induced activation of STING, and interacts with STING to promote STING phosphorylation and translocation. We propose that the two DNA sensors IFI16 and cGAS cooperate to prevent the spurious activation of the type I interferon response.

¹Division of Cell Signalling and Immunology, School of Life Sciences, University of Dundee, Dundee DD1 5EH, UK. ²Division of Biomedical and Life Sciences, Faculty of Health and Medicine, Lancaster University, Lancaster LA1 4YQ, UK. ³The Pirbright Institute, Pirbright, Surrey GU24 0NF, UK. ⁴Fingerprints Proteomics Facility, School of Life Sciences, University of Dundee, Dundee DD1 5EH, UK. ⁵School of Biochemistry and Immunology, Trinity Biomedical Sciences Institute, Trinity College Dublin, Dublin 2, Ireland. ⁶The Roslin Institute and The Royal (Dick) School of Veterinary Studies, University of Edinburgh, Edinburgh EH25 9RG, UK. * These authors contributed equally to this work. Correspondence and requests for materials should be addressed to L.U. (email: l.unterholzner@lancaster.ac.uk).

Keratinocytes constitute the outermost layer of the skin, and as such are the first point of contact for many pathogens, including DNA viruses. Keratinocytes not only provide a physical barrier to infection and environmental insults but are also thought to function as sentinels of infection and injury that initiate and shape local immune responses¹. However, their antiviral defence mechanisms are relatively under-studied. Like many other cell types, keratinocytes are able to sense the presence of pathogens through pattern recognition receptors that detect pathogen-associated molecular patterns (PAMPs) as part of the immediate innate immune response to infection. Pattern recognition receptors include the Toll-like receptors at the cell surface and in endosomes, as well as intracellular receptors that sense the presence of viruses and intracellular bacteria inside infected host cells. The PAMPs that constitute the major tell-tale signs of viral infection are viral nucleic acids. Double-stranded RNA and single-stranded RNA with a 5'-triphosphate group for instance are detected as 'foreign' by the cytosolic RNA receptors MDA5 and RIG-I, whereas pathogen-derived dsDNA can be detected by intracellular DNA receptors².

Several cytosolic and nuclear DNA receptors promote the transcription of type I interferons, cytokines and chemokines upon recognition of DNA viruses, retroviruses and intracellular bacteria. An important DNA receptor in the cytosol is cyclic GMP-AMP synthase (cGAS), which catalyses the formation of the second messenger cyclic GMP-AMP (2'3'cGAMP, referred to as cGAMP throughout this manuscript)^{3,4}. cGAMP then binds to the adaptor protein STING in the endoplasmic reticulum (ER), causing a conformational change in the STING dimer⁵. Activation of STING results in its relocalization from the ER to ER-Golgi intermediate compartments (ERGIC)⁶, where STING associates with TANK binding kinase 1 (TBK1). This interaction leads to the subsequent phosphorylation of STING by TBK1, which causes the recruitment of interferon regulatory factor 3 (IRF3)⁷, IRF3 phosphorylation and nuclear translocation. Together with nuclear factor κ B (NF- κ B), IRF3 is an important transcription factor for the activation of the *IFN- β* promoter, as well as for the expression of other cytokines, chemokines and IFN-stimulated genes during the innate immune response to viral infection.

Studies using cGAS-deficient mice, as well as mouse and human cell lines lacking cGAS expression, have provided evidence for a central role of cGAS during DNA sensing in a variety of infection contexts and cell types⁸. The discovery of cGAS has called into question the function of other, previously identified DNA receptors, which have also been described to detect viral dsDNA and activate STING⁹. One of the best described DNA sensors is interferon- γ -inducible protein 16 (IFI16), which shuttles between the nucleus and the cytosol, but is predominantly nuclear at steady state^{10,11}. IFI16 is related to the inflammasome-inducing cytosolic DNA sensor AIM2 (ref. 12), and possesses an N-terminal pyrin domain and two HIN domains, which bind DNA in a sequence-independent manner¹³. IFI16 involvement in the type I interferon response to foreign DNA has been demonstrated using RNA interference (RNAi) approaches in a variety of mouse and human cells, and IFI16 and its mouse orthologue p204 have been shown to function in the innate immune response to DNA viruses such as HSV-1 in human and mouse myeloid cells, epithelial cells and fibroblasts^{10,14–17}. IFI16 is also required for the response to infection with retroviruses such as HIV-1 in macrophages¹⁸ as well as to infection with intracellular bacteria such as *Listeria monocytogenes* in human myeloid cells¹⁹, and *Francisella novicida* in mouse macrophages²⁰. In many of these cases, an essential role for cGAS has also been observed in the same cell type, during infection with the same pathogen or following

stimulation with identical DNA ligands^{15,18–21}. However, due to the reliance on RNAi approaches to diminish, rather than abolish IFI16 expression, the extent of redundancy or cooperation between IFI16 and cGAS has been difficult to ascertain. Furthermore, it has been reported that the entire family of murine AIM2-like receptors is dispensable for the interferon response to exogenous DNA in mice²², thus casting doubts over the role of IFI16 in the anti-viral response.

Here, we examine the role of IFI16 and cGAS in human keratinocytes, which are the target cells and first point of contact for a variety of DNA viruses. We use gene targeting to generate human immortalized HaCaT keratinocytes lacking IFI16 or cGAS, in order to investigate the function of these DNA receptors during the detection of exogenous DNA. We find that IFI16 and cGAS are not redundant during DNA sensing, but that both are required for the full activation of the innate immune response to exogenous DNA. Although the presence of cGAS is central for DNA sensing in keratinocytes, as it is in other cell types, IFI16 is closely integrated into the cGAS-cGAMP-STING signalling pathway by promoting the activation of STING in synergy with cGAMP. Thus, we propose that cGAS does not act in isolation, but rather cooperates with other factors such as IFI16 to activate STING in human cells.

Results

IFI16 is required for DNA sensing in HaCaT keratinocytes. We used immortalized HaCaT keratinocytes as a model system to study the detection of viral DNA in a human cell type that is the initial point of contact for DNA viruses such as herpesviruses and poxviruses. Using transcription activator-like effector nuclease (TALEN) technology, two independent clonal cell lines were generated, where all IFI16 alleles contained insertions or deletions resulting in frameshift mutations. This resulted in the absence of detectable IFI16 protein expression as confirmed by Western blotting (Fig. 1a). HaCaT keratinocytes expressed cGAS, STING, TBK1 and IRF3 to similar extents in the presence and absence of IFI16 (Fig. 1a).

In order to assess the ability of HaCaT cells to respond to exogenous DNA, we transfected wild-type (*IFI16* +/+) HaCaT cells and the two *IFI16* -/- clones with herring testis (HT) DNA, and quantified the expression of *IFN- β* mRNA over time by real-time PCR. *IFI16* +/+ HaCaT keratinocytes generated a robust *IFN- β* response peaking at 4–6 h post DNA transfection. This response was severely blunted in both *IFI16* -/- clones (Fig. 1b). It has previously been suggested that IFI16 is dispensable for the early response to foreign DNA, but plays a role at later time points after DNA transfection in some cell types^{15,23}. This does not seem to be the case in human keratinocytes, as the absence of IFI16 affected *IFN- β* mRNA expression as soon as induction was observed, at 2 h post stimulation (Fig. 1b). While we do observe a residual response in IFI16-deficient cells, this response occurs with similar kinetics as that in wild-type HaCaT cells. A similar deficiency in *IFN- β* mRNA production was observed following transfection with a 70 nt long dsDNA oligonucleotide (70mer, see ref. 10) or a circular dsDNA plasmid (Fig. 1c), or when HT DNA was introduced into cells by digitonin-mediated permeabilization (Supplementary Fig. 1a).

IFN- β expression induced by transfection of the dsRNA mimic poly(I:C) was not impaired in the absence of IFI16, even at the lowest poly(I:C) concentrations tested, and indeed often caused an enhanced response in IFI16-deficient cells (Fig. 1d). Both IFI16-deficient cell clones exhibited a similar impairment in the response to DNA, but not to poly(I:C) (Supplementary Fig. 1b,c), or to *in vitro* transcribed RNA containing 5'-triphosphates

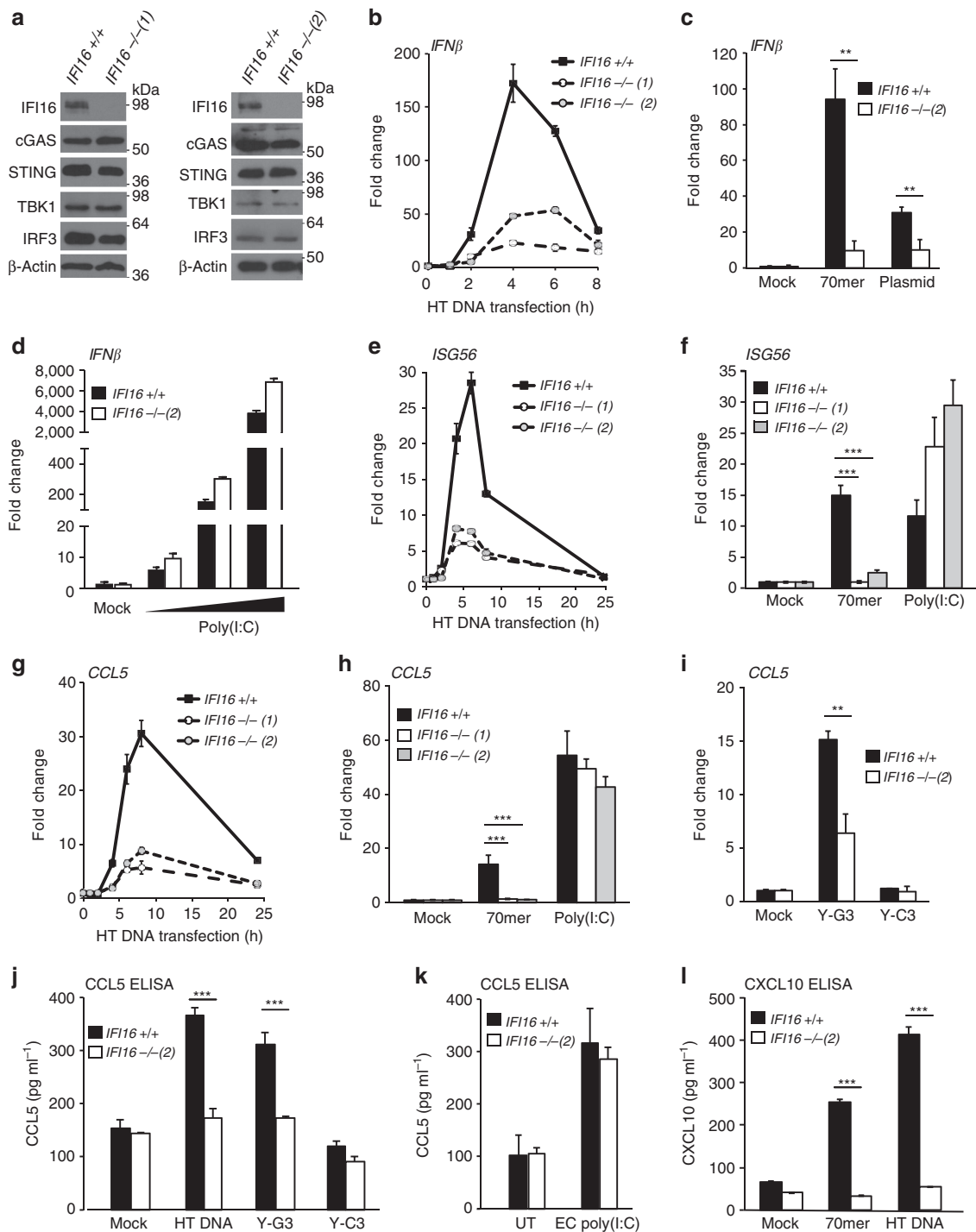


Figure 1 | IFI16 is required for DNA but not RNA sensing in HaCaT keratinocytes. (a) Immunoblot analysis of wild-type (*IFI16* +/+) HaCaT and two *IFI16* -/- HaCaT clones. (b–i) Quantitative real-time PCR (qRT-PCR) analysis of mRNA expression levels normalized to β -actin mRNA and mock transfection in *IFI16* +/+ and *IFI16* -/- HaCaT cells, as indicated. (b) qRT-PCR analysis of *IFN- β* mRNA expression in *IFI16* +/+ and two *IFI16* -/- HaCaT cells clones transfected with $1 \mu\text{g ml}^{-1}$ HT DNA for the times indicated. (c) qRT-PCR analysis of *IFN- β* mRNA 6 h post transfection with $1 \mu\text{g ml}^{-1}$ of a 70nt dsDNA oligonucleotide (70mer) or circular pcDNA3.1 plasmid. (d) *IFN- β* mRNA induction 6 h after transfection with 1, 10 or 100 ng ml^{-1} poly(I:C). (e) Time course of *ISG56* mRNA expression following transfection with $1 \mu\text{g ml}^{-1}$ HT DNA. (f) *ISG56* mRNA expression 6 h post transfection with $1 \mu\text{g ml}^{-1}$ 70mer oligonucleotide or 100 ng ml^{-1} poly(I:C). (g) qRT-PCR analysis of *CCL5* mRNA expression following transfection with $1 \mu\text{g ml}^{-1}$ HT DNA for the times indicated. (h) Relative *CCL5* mRNA expression levels 6 h post transfection with $1 \mu\text{g ml}^{-1}$ 70mer oligonucleotide or 100 ng ml^{-1} poly(I:C). (i) *CCL5* mRNA expression levels 6 h post transfection with $1 \mu\text{g ml}^{-1}$ of Y-G3 or Y-C3 oligonucleotides. (j) Secreted CCL5 (Rantes) protein detected by ELISA in the supernatants of *IFI16* +/+ or *IFI16* -/- HaCaT cells transfected with $1 \mu\text{g ml}^{-1}$ HT DNA, Y-G3 or Y-C3 DNA for 24 h. (k) ELISA quantitation of CCL5 protein in supernatants from *IFI16* +/+ and *IFI16* -/- HaCaT cells stimulated with $5 \mu\text{g ml}^{-1}$ extracellular (EC) poly(I:C) added to the medium for 24 h. (l) ELISA quantitation of CXCL10 (IP-10) protein in supernatants of *IFI16* +/+ or *IFI16* -/- HaCaT cells transfected with $1 \mu\text{g ml}^{-1}$ 70mer oligonucleotide or HT DNA. All qRT-PCR and ELISA data are presented as mean values of biological triplicates. Error bars indicate s.d. * $P < 0.05$, ** $P < 0.01$, *** $P < 0.001$ Student's *t*-test. Data are representative of at least two experiments in two independent *IFI16*-deficient cell clones.

(Supplementary Fig. 1d). This demonstrates that HaCaT cells lacking IFI16 are still capable of mounting a type I interferon response, but are specifically impaired in their response to foreign DNA.

The activation of the *IFN- β* promoter relies on the transcription factors IRF3 and NF- κ B, which are both activated by the adaptor protein STING. We found that the IRF3-dependent expression of the *interferon stimulated gene 56 (ISG56)* was strongly impaired by the absence of IFI16 in response to DNA, but not poly(I:C) transfection (Fig. 1e,f). The same was true for the NF- κ B-dependent transcription of *IL-6* mRNA (Supplementary Fig. 1e–g). IFI16 was also required for the DNA-, but not RNA-induced expression of the chemokines *CCL5* (Rantes, Fig. 1g,h) and *CXCL10* (IP-10, Supplementary Fig. 1h,i). IFI16-dependent *CCL5* mRNA induction was also observed following transfection of a short dsDNA oligonucleotide with single-stranded guanosine-containing overhangs (Y-G3 DNA), which has previously been implicated in the sequence-specific activation of cGAS in THP-1 monocytes²⁴. In agreement with the mRNA expression data, we find that cells lacking IFI16 are unable to secrete *CCL5* (Rantes) protein in response to transfected HT DNA or Y-G3 DNA (Fig. 1j), but *CCL5* secretion is unaffected following stimulation with extracellular poly(I:C; Fig. 1k). Cells lacking IFI16 are also unable to induce *CXCL10* (IP-10) secretion in response to exogenous DNA (Fig. 1l). Overall, we show that the innate immune response to exogenous DNA is strongly impaired in HaCaT cells lacking IFI16, while the response to poly(I:C) or to 5'-triphosphate-containing RNA is generally unaffected, or even enhanced. This confirms a specific involvement of IFI16 in the sensing of intracellular DNA.

IFI16 is required for the response to DNA viruses. Keratinocytes are natural host cells for many viruses including poxviruses such as vaccinia virus (VACV) and Modified Vaccinia virus Ankara (MVA) which replicate in the cytosol, and herpesviruses, such as herpes simplex virus 1 (HSV-1) which replicates in the nucleus of permissive cells. While IFI16 can shuttle between the nucleus and the cytosol¹¹, it is predominantly nuclear at steady state in HaCaT keratinocytes (Fig. 2a), with low but detectable levels in the cytosol, as has been observed in other cell types^{10,11}. We observed that during infection with VACV, endogenous IFI16 relocalized to viral factories in the cytosol, which also contain DNA and the VACV virus protein A3, as visualized during infection with VACV expressing an A3-mCherry fusion protein (Fig. 2a). During infection with HSV-1, which replicates in the nucleus, we observed a relocalization of IFI16 to nuclear puncta (Fig. 2b), which have previously been shown to be sites of HSV-1 replication^{25,26}. Thus, during infection with DNA viruses IFI16 localizes to viral factories in both the nucleus and the cytosol, consistent with a role in the detection of foreign DNA in both compartments.

We next tested whether IFI16 is required for the sensing of DNA viruses. HSV-1 infection induced the expression of *IFN- β* , *ISG56* and *IL-6* mRNA in HaCaT keratinocytes, even though gene induction levels were modest, presumably due to the many countermeasures employed by wild-type HSV-1 to dampen the anti-viral response, which include the degradation of IFI16 and STING^{25,27,28}. Nevertheless, the HSV-1-induced expression of *IFN- β* , *ISG56* and *IL-6* mRNA was impaired in IFI16-deficient cells (Fig. 2c–e and Supplementary Fig. 2a,b). HaCaT cells lacking IFI16 were also impaired in the secretion of *CCL5* protein following infection with ultraviolet light-inactivated HSV-1 (Fig. 2f).

We were unable to detect an innate immune response to infection with VACV in HaCaT keratinocytes, as VACV

also possess a large repertoire of inhibitors of innate immune signalling²⁹. Thus, we examined the transcriptional response to the poxvirus Modified Vaccinia virus Ankara (MVA), an attenuated vaccine strain that lacks many of the immunomodulators of its relatives. MVA-induced *CCL5* and *ISG56* mRNA induction was significantly reduced in IFI16-deficient cells (Fig. 2g,h). Cells lacking IFI16 also secreted less *CCL5* protein 24 h post infection with MVA (Fig. 2i).

We also infected HaCaT cells with a preparation of the Sendai virus (SeV) that contains a high proportion of defective viral particles allowing its RNA genome to be recognized by RIG-I^{30,31}. SeV-induced *CCL5* secretion was unaffected by the absence of IFI16 (Fig. 2j). Analogously, the induction of *IFN- β* , *ISG56* and *IL-6* mRNA expression in response to SeV was equally potent in wild-type and IFI16-deficient cells (Fig. 2k,l, Supplementary Fig. 2c,d).

We further confirmed the involvement of IFI16 in the sensing of DNA viruses in primary human cells by RNAi. Treatment of primary human keratinocytes from adult donors with a pool of four IFI16 siRNAs resulted in the potent knock-down of IFI16 protein expression (Fig. 2m). IFI16-depleted primary keratinocytes were unable to induce *IFN- β* or *IL-6* mRNA following infection with HSV-1 (Fig. 2n,o). Knock-down of IFI16 in embryonic lung fibroblast MRC-5 cells also reduced the interferon response to transfected DNA, but not to transfected poly(I:C) (Fig. 2p,q). This effect was also observed when individual IFI16-targeting siRNAs were used, confirming that the effects were not due to off-target effects of a particular siRNA sequence (Supplementary Fig. 2e).

IFI16 is required for the DNA-induced activation of STING.

We have previously shown that IFI16 can interact with the DNA sensing adaptor protein STING, and that p204, a mouse orthologue of IFI16, promotes the activation of IRF3 and NF- κ B in mouse myeloid cells^{10,14}. However, one study proposed that IFI16 can induce the transcription of *IFN- α* and *IFN- β* at the promoter level, and promotes IFN expression irrespective of stimulus³².

To confirm a role for IFI16 at the level of STING and transcription factor activation, we examined the individual steps in the signalling cascade activated by exogenous DNA. Upon stimulation with intracellular DNA, STING translocates away from the ER to the ERGIC and clusters in membrane-bound peri-nuclear foci^{6,33–35}. STING signalling at the ERGIC results in the recruitment and activation of the kinase TBK1 (ref. 6). TBK1-mediated phosphorylation of STING is then thought to lead to the recruitment and activation of IRF3 (ref. 7), resulting in IRF3 phosphorylation, dimerization and nuclear translocation.

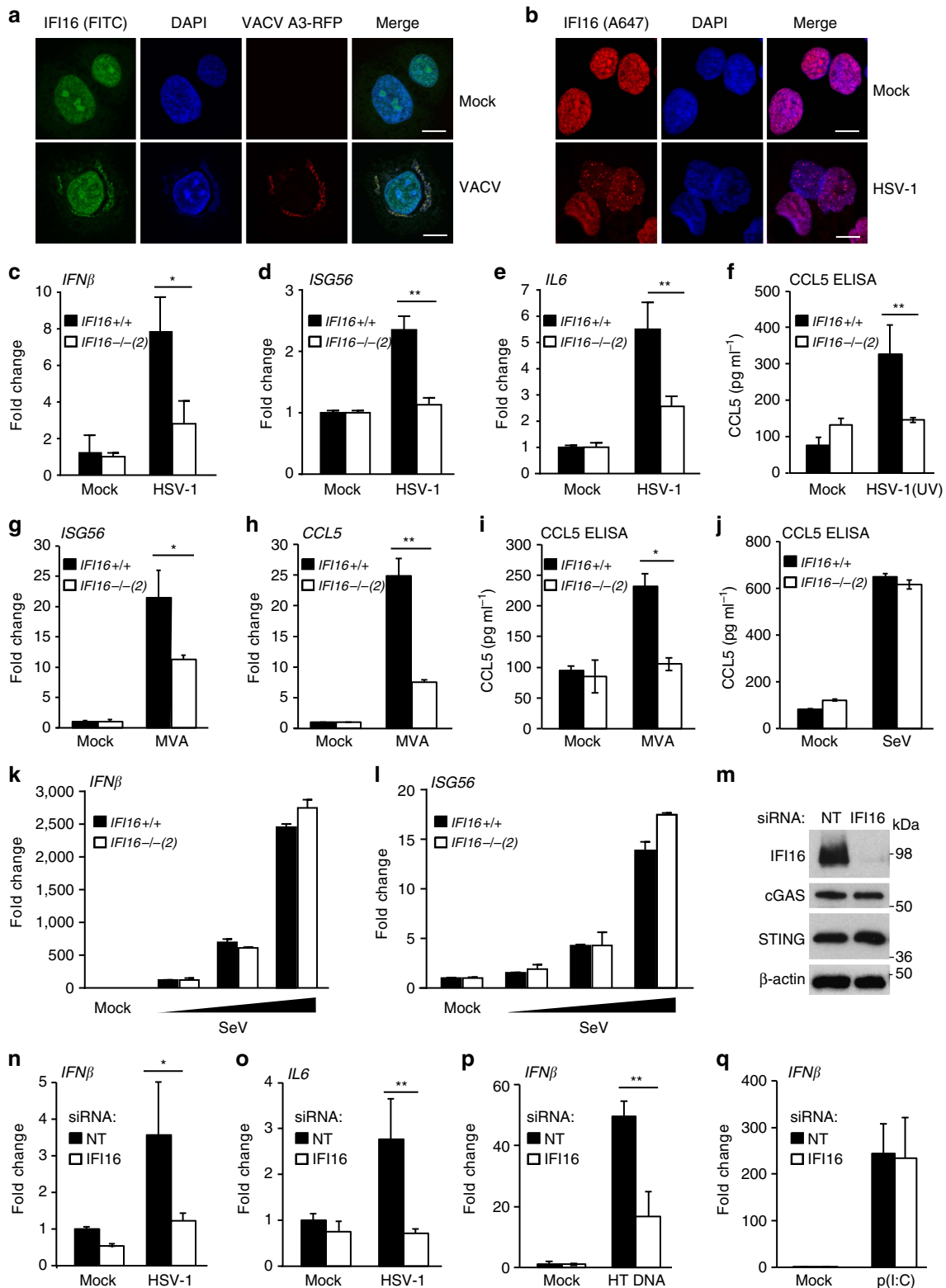
To place IFI16 in this signalling cascade, we first investigated the localization of endogenous STING protein in HaCaT keratinocytes by confocal microscopy. We found that STING relocalizes after 1 h stimulation with dsDNA, and moves from the ER to peri-nuclear foci in 46% of wild-type HaCaT cells (Fig. 3a,b). In HaCaT cells lacking IFI16, much fewer cells (12%) displayed DNA-induced STING clustering (Fig. 3a,b), suggesting that IFI16 affects the function of STING upon DNA transfection. This effect was also observed in a second *IFI16*-deficient cell clone (Supplementary Fig. 3a,b). Importantly, we were able to reconstitute *IFI16*-deficient cells with *in vitro* transcribed, capped and polyadenylated mRNA encoding *IFI16*. Reconstitution of cells with mRNA rather than expression plasmid allowed us to stimulate the cells by DNA transfection, and quantify STING translocation upon stimulation. *IFI16*-deficient cells transfected with mRNA expressing GFP displayed low levels of STING clustering after stimulation with exogenous DNA (12% of cells), like the *IFI16* –/– cells before mRNA transfection (Fig. 3c,d).

In *IFI16*-deficient cells reconstituted with mRNA encoding *IFI16*, more cells (24%) showed DNA-induced STING translocation (Fig. 3c,d). This shows unequivocally that *IFI16* is involved in the DNA-induced translocation of STING.

The presence of exogenous DNA induces the phosphorylation of STING by TBK1 and other kinases^{7,36}. We observe the appearance of a more slowly migrating STING band by SDS-polyacrylamide gel electrophoresis (SDS-PAGE) following

transfection with HT DNA and Y-G3 DNA in wild-type HaCaT cells, which is reduced in the absence of *IFI16* (Fig. 3e and Supplementary Fig. 3c). This band is indeed a phosphorylated form of STING, as shown by STING immunoprecipitation followed by treatment with λ phosphatase (Fig. 3f). Thus, *IFI16* plays a role in the DNA-induced phosphorylation of STING.

We also tracked the phosphorylation of TBK1 (at Serine 172) and IRF3 (at Serine 396) over time after DNA transfection.



Phosphorylation of TBK1 and IRF3 peaked at 4 h post DNA transfection in wild-type HaCaT cells. TBK1 and IRF3 phosphorylation levels were much reduced, but not completely absent in cells lacking IFI16 (Fig. 3g), consistent with a reduced transcriptional response to exogenous DNA. In agreement with the unimpaired transcriptional response to poly(I:C), the phosphorylation of TBK1 and IRF3 induced by poly(I:C) was able to proceed in the absence of IFI16 (Supplementary Fig. 3d). Both IFI16-deficient cell clones also showed impaired translocation of IRF3 to the nucleus at 4 h post transfection, as observed by confocal microscopy (Fig. 3h,i and Supplementary Fig. 3e,f). Taken together, our data indicate that IFI16 acts ‘upstream’ of STING and transcription factor activation during DNA sensing, consistent with a role as *bona fide* co-receptor in this signalling pathway.

DNA sensing in HaCaT keratinocytes also requires cGAS. HaCaT keratinocytes also express cGAS (Fig. 1a). In order to assess whether the function of cGAS is as critical during DNA sensing in human keratinocytes, as it is in many other cell types⁸, we generated HaCaT cells lacking cGAS, using a CRISPR-Cas9 nickase approach. cGAS-deficient HaCaT cells still contained similar IFI16 protein levels as wild-type cells (Fig. 4a). Thus, deletion of cGAS in HaCaT cells does not automatically result in the reduction of IFI16 protein levels which has been observed in other cell contexts^{15,20}, and the relative function of the two DNA sensors can be examined in isolation.

We find that cGAS-deficient HaCaT cells are unable to induce *IFN-β*, *CCL5*, *ISG56* and *IL-6* mRNA at 6 h post stimulation with transfected DNA (Fig. 4b–e). cGAS-deficient cells are also impaired in their response to infection with the cytosolic DNA virus MVA (Fig. 4f), as measured by *CCL5* mRNA induction. Thus, as in many other cells, cGAS is essential for the response to foreign DNA and DNA viruses in HaCaT keratinocytes. Given that we have shown here that IFI16 also has an important role in the same cells and in response to the same DNA ligands and viruses, our data suggest that IFI16 and cGAS each have important, but functionally different, roles in the innate immune response to DNA, and need to cooperate to achieve full activation of an anti-viral response.

To test whether the cooperation between IFI16 and cGAS can also be observed in HEK293T cells, which do not express endogenous STING and are unable to mount an innate immune response upon DNA transfection^{10,37}, we transfected HEK293T cells with expression constructs encoding *STING*, *cGAS* and *IFI16* and measured *IFNβ* promoter activation using luciferase assays. We found that IFI16 synergizes with cGAS and STING in the activation of the *IFNβ* promoter in a dose-dependent manner (Fig. 4g). Furthermore, the activities of IFI16 and cGAS were

critically dependent on the presence of STING in this system (Fig. 4g). IFI16 did not synergize to the same extent with other signalling factors such as the TLR3 adaptor protein TRIF, even when STING was co-expressed (Fig. 4h). This indicates that the strong synergy between IFI16 and cGAS is specific to their roles in the DNA sensing pathway, rather than simply being due to an additive effect of two independent IFN-inducing factors.

IFI16 interacts with cGAS in a DNA-dependent manner. The molecular function of cGAS in the DNA sensing pathway is well-defined. Upon recognition of DNA, cGAS catalyses the production of the second messenger cGAMP from ATP and GTP. cGAMP then binds to STING dimers, resulting in a conformational change in STING that is thought to contribute to STING activation⁵. We find that IFI16 also influences STING phosphorylation and translocation in response to DNA (Fig. 3a–f). To place the function of IFI16 in the context of the cGAS-cGAMP-STING pathway, we examine whether IFI16 plays a role in the DNA-induced production of cGAMP, and/or in the cGAMP-induced activation of STING.

We first tested whether IFI16 and cGAS would form a complex during DNA sensing. We were able to detect an interaction between endogenous IFI16 and cGAS that was enhanced by stimulation with DNA (Fig. 5a). We could also detect the interaction in FlipIn HEK293 cells expressing GFP-IFI16, but not GFP alone (Supplementary Fig. 4a) and in HEK293T cells expressing HA-tagged IFI16 and Flag-tagged cGAS (Fig. 5b). The interaction between the two proteins is facilitated by DNA as a binding platform, as cGAS does not interact with a IFI16 protein containing several point mutations that impair its ability to bind DNA (IFI16-m4, described in ref. 13) (Fig. 5b). Furthermore, treatment of the IFI16-cGAS complex with benzonase, a nuclease which degrades DNA and RNA, also reduced the interaction (Fig. 5b). Thus, IFI16 and cGAS are brought together by assembling on exogenous DNA.

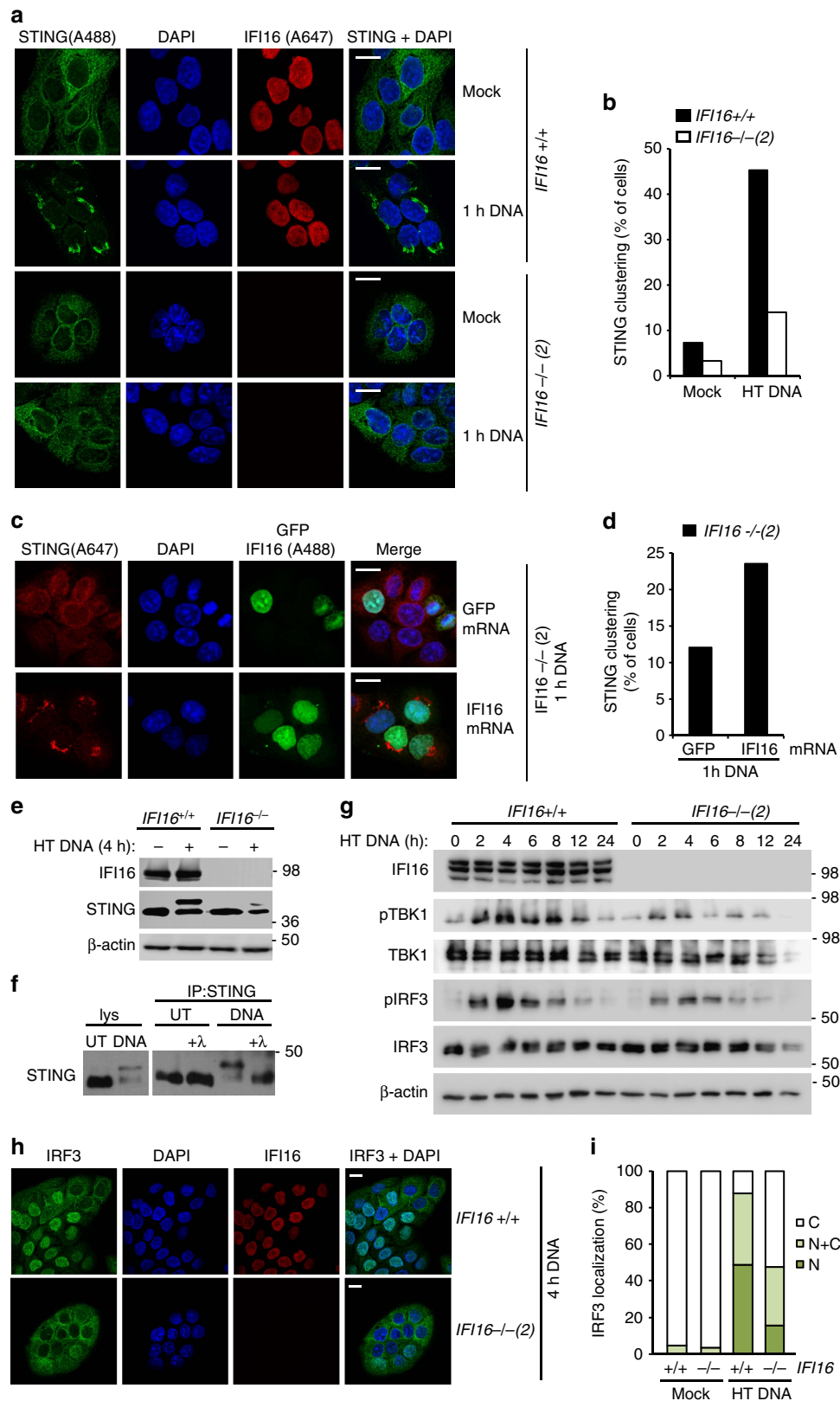
IFI16 is not required for cGAMP production in HaCaT cells.

We next tested whether IFI16 would be able to influence cGAS function in production of the second messenger cGAMP. To measure the production of cGAMP during DNA sensing, we quantified endogenous cGAMP levels in cell extracts after DNA stimulation using a liquid chromatography and mass spectrometry (LC-MS/MS) approach outlined in Supplementary Fig. 4b. Multiple reaction monitoring allowed us to unambiguously identify cGAMP, as well as cyclic-di-AMP which we used as internal spike-in control to account for losses during the sample preparation and injection. Three *m/z* transitions were used for the identification of cGAMP, and one for c-di-AMP (Fig. 5c),

Figure 2 | IFI16 is required for the innate immune response to DNA viruses. (a) Confocal imaging of HaCaT cells infected with VACV-A3-RFP (MOI = 0.1) for 24 h and stained with FITC-labelled IFI16 antibody (green). A3-RFP is shown in red, DNA is stained with DAPI (blue). (b) Confocal imaging of HaCaT cells infected with HSV-1 (MOI = 1) for 6 h and stained with anti-IFI16 antibody (red). DNA is visualized with DAPI (blue). Scale bars, 20 μm. (c–e) qRT-PCR analysis of IFI16 +/+ and IFI16 –/– HaCaT cells infected with HSV-1 (MOI = 1) for 6 h. mRNA expression levels normalized to *β-actin* mRNA were determined for *IFNβ* (c), *ISG56* (d) and *IL6* (e). (f) Secreted CCL5 protein from HaCaT cells infected with UV inactivated HSV-1 (MOI = 5) for 24 h, quantified by ELISA. (g,h) qRT-PCR analysis of *ISG56* (g) and *CCL5* (h) mRNA expression in HaCaT cells infected with MVA (MOI = 5) for 6 h. (i) ELISA quantitation of CCL5 protein in supernatants from HaCaT cells infected with MVA (MOI = 5) for 24 h. (j) ELISA analysis of CCL5 protein from HaCaT cells infected with a Sendai virus (SeV) preparation containing defective viral particles (1:2,000 dilution) for 24 h. (k,l) qRT-PCR analysis of *IFNβ* (k) and *ISG56* (l) mRNA expression in HaCaT cells infected with Sendai virus (SeV) at dilutions of 1: 20 000, 1: 2,000 and 1:200 for 6 h. (m) Primary human keratinocytes (NHEK) were transfected with a non-targeting (NT) or IFI16-targeting siRNA pool for 48 h. Protein expression was examined by Western blotting. (n,o) NHEK were treated with siRNA pools for 48 h, and infected with HSV-1 (MOI = 1) for 6 h. *IFN-β* (n) and *IL-6* (o) mRNA expression levels were quantified by qRT-PCR. (p,q) qRT-PCR analysis of *IFN-β* mRNA expression in MRC-5 human embryonic lung fibroblasts treated with siRNA pools for 48 h, and transfected for 6 h with 1 μg ml⁻¹ HT DNA (p) or 100 ng ml⁻¹ poly(I:C) (q). Data are representative of at least two independent experiments, and presented as mean values of biological triplicates, with error bars indicating s.d. **P* < 0.05, ***P* < 0.01, ****P* < 0.001 Student's *t*-test.

allowing us to accurately detect synthetic cGAMP and c-di-AMP standards (Supplementary Fig. 4c), and quantify cGAMP in a background of processed cell lysates with pg sensitivity (standard curve in Fig. 5d). Unstimulated HaCaT cells contain low, but detectable amounts of cGAMP (Fig. 5e and Supplementary

Fig. 4d). Following stimulation with HT DNA or VACV 70mer oligonucleotide, cGAMP levels increase in both wild-type and IFI16-deficient HaCaT cells (Fig. 5e,f and Supplementary Fig. 4e). Treatment of cell extracts with snake venom phosphodiesterase removes the cGAMP peak following DNA stimulation



(Supplementary Fig. 4f), as would be predicted³⁸. Thus, we conclude that IFI16 is not required for cGAMP production in HaCaT keratinocytes.

IFI16 is required for the response to exogenous cGAMP. We next tested whether IFI16 affects the activation of STING by cGAMP. Cells can be stimulated by the intracellular delivery of cGAMP, thus by-passing cGAS function and the production of endogenous cGAMP.

In order to assess the function of IFI16 in this context, we transfected HaCaT cells with synthetic 2'3' cGAMP, and quantified the gene expression response over time. The delivery of synthetic cGAMP induced the expression of *CCL5* and *ISG56* mRNA in wild-type HaCaT cells, peaking at 12 and 6 h post transfection. *IFI16*-deficient cells exhibited a severely blunted response that occurred with similar kinetics to the response in wild-type cells (Fig. 6a and Supplementary Fig. 5a). As lipofection has also been described to induce a STING-dependent innate immune response in some cells³⁹, we tested other means of delivering cGAMP. A similar reduction in cGAMP-induced gene expression was observed when cGAMP was infused into the cells by digitonin-mediated permeabilization (Supplementary Fig. 5b,c). *IFI16*-deficient cells also secreted less *CCL5* protein quantified by ELISA (Fig. 6b). In analogy to our observations in cells stimulated by DNA transfection, *IFI16* deficiency also impaired the phosphorylation of STING, TBK1 and IRF3 following stimulation with cGAMP (Fig. 6c), and the translocation of IRF3 to the nucleus (Fig. 6d,e).

Finally, we tested the response of HaCaT cells to endogenously produced cGAMP delivered through gap junctions. For this, we over-expressed cGAS in HEK293T cells, which acted as producer cells for endogenous cGAMP, and co-cultured these with wild-type or *IFI16*-deficient HaCaT cells (schematic representation in Fig. 6f). The expression levels of FLAG-tagged cGAS in the co-culture were confirmed by western blotting (Fig. 6g). As HEK293T cells do not express STING, they cannot respond to the cGAMP they produce and are not stimulated by the over-expression of cGAS alone (Fig. 4g). However, neighbouring HaCaT cells that are in direct contact with the cGAS-expressing HEK293T cells take up cGAMP through gap junctions, resulting in the activation of STING and the induction of an innate immune response in the HaCaT cells. Co-culture with cGAS-expressing HEK293T cells, but not HEK293T cells transfected with empty vector, induced the phosphorylation of endogenous STING in the HaCaT cells, which was reduced in HaCaT cells lacking IFI16 (Fig. 6g). As a consequence of STING activation, HaCaT cells co-cultured with cGAS-expressing HEK293T cells induce the expression of *CCL5* mRNA, compared with HaCaT monocultures or co-cultures with HEK293T cells containing

empty vector (Fig. 6h). In agreement with our data using synthetic cGAMP, *CCL5* mRNA levels induced by endogenous cGAMP were significantly lower in *IFI16*-deficient HaCaT cells (Fig. 6h), despite similar levels of cGAS expression in the co-culture (Fig. 6g). *IFI16* was also required for the expression of *ISG56* and *IFN-β* in these co-culture experiments (Supplementary Fig. 5d–f). Taken together, we find that *IFI16* is required for the response to cGAMP, whether delivered into the cells by permeabilization, transfection or through gap junctions from neighbouring cells.

IFI16 provides an additional signal for STING activation. The observed effects of *IFI16* on cGAMP-induced STING activation could potentially be explained by a role of *IFI16* in the stabilization of cGAMP. For this reason, we tested whether the use of a non-hydrolysable analogue of cGAMP, cGAM(PS)₂ (ref. 40), would overcome the effect of *IFI16* on cGAMP-induced activation of an innate immune response. We found that *CCL5* mRNA expression following the exposure of cells to cGAMP or its non-hydrolysable analogue was equally affected by the absence of *IFI16* (Fig. 7a). Analogously, STING phosphorylation and the activation of TBK1 and IRF3 were reduced in *IFI16*-deficient cells, regardless of whether the cells were stimulated with cGAMP or cGAM(PS)₂ (Fig. 7b). While we cannot formally exclude a role of *IFI16* in affecting cGAMP turnover, our results indicate that *IFI16* has an important function in cGAMP-induced STING activation that is independent of cGAMP hydrolysis.

We also examined whether *IFI16* is required for the response to other cyclic di-nucleotides that are sensed by STING. STING can detect molecules such as cyclic di-AMP and cyclic di-GMP which are produced by bacteria, and constitute a PAMP during infection with intracellular pathogens³⁷. Some common STING sequence variants display impaired sensing of bacterial cyclic di-nucleotides⁴¹. Sequencing of STING cDNA in HaCaT cells did not reveal the presence of alleles containing such sequence polymorphisms, and, in agreement with this, HaCaT cells can respond to the transfection of synthetic cyclic di-AMP. The response to cyclic di-AMP was also dependent on *IFI16* (Fig. 7c). Thus, the involvement of *IFI16* in STING activation is not limited to the DNA sensing pathway, but also encompasses the innate immune response to bacterial cyclic di-nucleotide PAMPs in human keratinocytes.

We next tested the interaction between *IFI16* and STING during DNA sensing. Using co-immunoprecipitation, we can detect a constitutive weak interaction between endogenous STING and *IFI16* in HaCaT cells, and complex formation increases in the hours following DNA transfection (Fig. 7d). However, we do not observe a clear co-localization of *IFI16* and STING in DNA-stimulated HaCaT cells (see Fig. 3a),

Figure 3 | IFI16 is required for the DNA-induced activation of STING and IRF3. (a) Confocal analysis of *IFI16* +/+ and *IFI16* -/- HaCaT cells that were mock transfected or transfected for 1 h with 5 μg ml⁻¹ HT DNA. Cells were stained for endogenous *IFI16* (red) and STING (green). DNA is visualized with DAPI (blue). (b) Cells as in (a) were observed by confocal microscopy and scored for STING clustering. At least 200 cells were counted per sample. (c) Confocal analysis of *IFI16* -/- HaCaT cells reconstituted for 6 h with 1 μg ml⁻¹ *in vitro* transcribed, capped and polyadenylated mRNA encoding GFP or *IFI16*, followed by transfection with 5 μg ml⁻¹ HT DNA for 1 h. Cells were stained for STING (red), and DNA (DAPI, blue). GFP or AlexaFluor488-stained *IFI16* are shown in green. (d) Cells as in (c) were scored for STING clustering, with at least 300 cells counted per sample. (e) Immunoblot analysis of HaCaT cells treated with 1 μg ml⁻¹ HT DNA for 4 h, and probed for *IFI16*, STING and β-actin protein levels by Western blotting. (f) HaCaT cells were stimulated with 1 μg ml⁻¹ HT DNA for 6 h or left untreated (UT). STING immunoprecipitates (IP) were treated with λ phosphatase where indicated, and analysed by western blotting. (g) Western blot analysis of IRF3 phosphorylation at Ser396 (pIRF3) and TBK1 phosphorylation at Ser172 (pTBK1) in HaCaT cells transfected with 1 μg ml⁻¹ HT DNA for the times indicated. (h) HaCaT cells were transfected with 5 μg ml⁻¹ HT DNA for 4 h, and the translocation of endogenous IRF3 was analysed by confocal microscopy. Cells were stained for IRF3 (green) and *IFI16* (red), DNA is visualized with DAPI (blue). (i) Cells as in (h) were scored for predominately cytosolic (C), predominantly nuclear (N) and evenly distributed nuclear and cytosolic (N + C) localization of IRF3. At least 200 cells were counted per sample. Results are representative of at least two experiments each in two independent *IFI16* -/- cell clones. Scale bars, 20 μm.

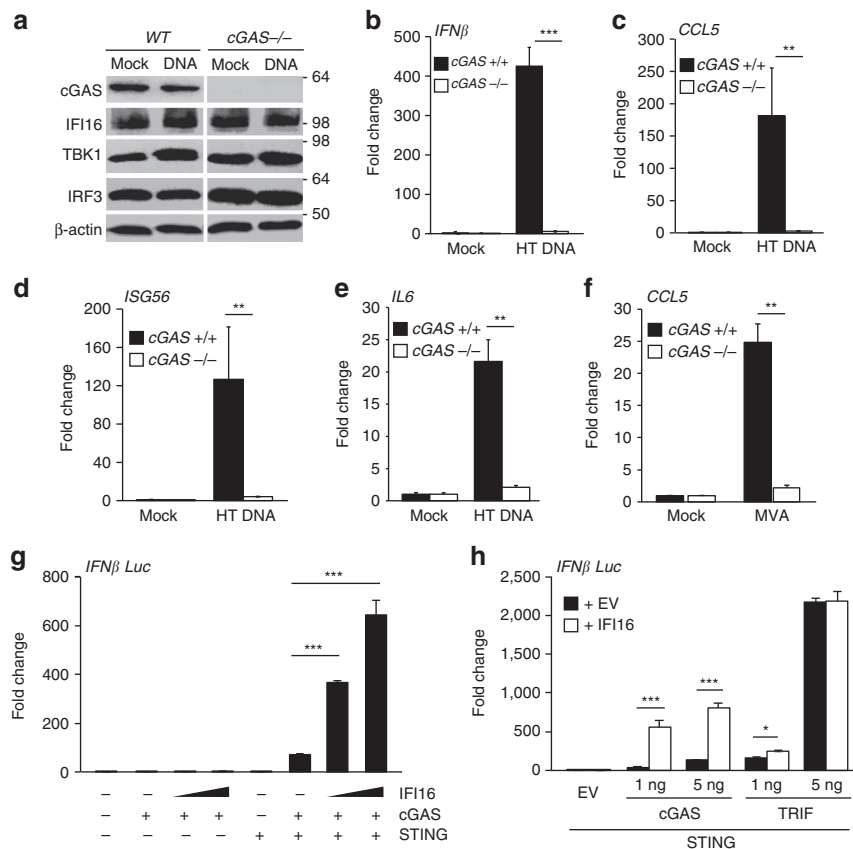


Figure 4 | cGAS is required for the innate immune response to DNA in HaCaT keratinocytes. (a) Immunoblot analysis of wild-type (WT) and cGAS^{-/-} HaCaT cells, mock transfected or transfected with $1 \mu\text{g ml}^{-1}$ HT DNA for 6 h. (b–e) qRT-PCR analysis of cGAS^{+/+} and cGAS^{-/-} HaCaT cells that were mock transfected or transfected with $1 \mu\text{g ml}^{-1}$ HT DNA for 6 h. mRNA levels were normalized to β -actin mRNA levels and mock transfections. *IFN β* (b), *CCL5* (c), *ISG56* (d) and *IL6* (e) mRNA levels are shown. (f) qRT-PCR analysis *CCL5* mRNA from cGAS^{+/+} and cGAS^{-/-} HaCaT cells infected with MVA (MOI = 5) for 6 h. (g) HEK293T cells were transfected with a firefly luciferase reporter construct under the control of the *IFN β* promoter, a Renilla luciferase transfection control, 10 ng STING-Flag plasmid, 1 ng cGAS-Flag and 35 or 70 ng HA-IFI16 expression plasmids, as indicated. Firefly luciferase activity was measured 24 h post transfection, and normalized to Renilla luciferase activity. (h) HEK293T cells were transfected with a firefly luciferase reporter construct under the control of the *IFN β* promoter, Renilla luciferase transfection control and 10 ng STING-Flag expression plasmid. In addition, 1 or 5 ng cGAS or TRIF expression constructs were co-expressed with 35 ng HA-IFI16 plasmid or empty vector, as indicated. Relative Firefly luciferase activity was quantified 24 h post transfection. Data are representative of at least three independent experiments, and presented as mean values of triplicate samples. Error bars indicate s.d. * $P < 0.05$, ** $P < 0.01$, *** $P < 0.001$ Student's *t*-test.

suggesting that the association between the two proteins is likely dynamic.

Given that IFI16 binds to STING and synergizes with cGAMP in STING activation, we tested whether IFI16 would be able to influence STING function in the absence of cGAS and cGAMP. When IFI16 is transiently expressed in HEK293T cells in the presence of a luciferase reporter system driven by the *IFN β* promoter, IFI16 is only able to activate the *IFN β* promoter if STING is also co-expressed (Fig. 7e). IFI16 contains two C-terminal HIN domains which bind DNA¹³ and an N-terminal pyrin domain (PYD) which is thought to mediate its signalling functions. We found that over-expression of the PYD alone is able to drive STING activation in this assay, while expression of the DNA-binding HINb domain is not (Fig. 7e). We have previously shown that the DNA-binding function of IFI16 is required for full STING activation in the context of the full-length IFI16 protein in this assay, where plasmid DNA likely provides the stimulus¹³. This correlates with the DNA-induced interaction between endogenous IFI16 and STING that we observe under more physiological conditions in HaCaT keratinocytes (Fig. 7d). Over-expression of the pyrin domain likely drives the activation of STING constitutively, by-passing the requirement for DNA

detection by the HIN domain. Taken together, we find that IFI16 acts on STING via its pyrin domain, and cooperates with cGAMP and other cyclic di-nucleotides to promote the phosphorylation and translocation of STING.

Discussion

The function of IFI16 as a receptor for foreign DNA during infection with DNA viruses and intracellular bacteria is supported by a large body of evidence, mostly relying on the use of RNAi approaches⁴². It has been reported that p204, a mouse orthologue of IFI16, cooperates with cGAS during *Francisella novicida* infection in murine RAW264.7 monocytic cells²⁰, and synergy between IFI16 and cGAS has also been observed during *Listeria monocytogenes* infection in human myeloid cells, and during HSV-1 infection in primary human foreskin fibroblasts^{15,19}, using RNAi approaches to study the effect of IFI16 and cGAS depletion. However, one study suggested that IFI16 may have a more generic function in the transcriptional activation of type I IFN regardless of stimulus³², and it has recently been shown that the locus containing all murine homologues of IFI16 is dispensable for DNA sensing in mice²². This study also reported that pools of

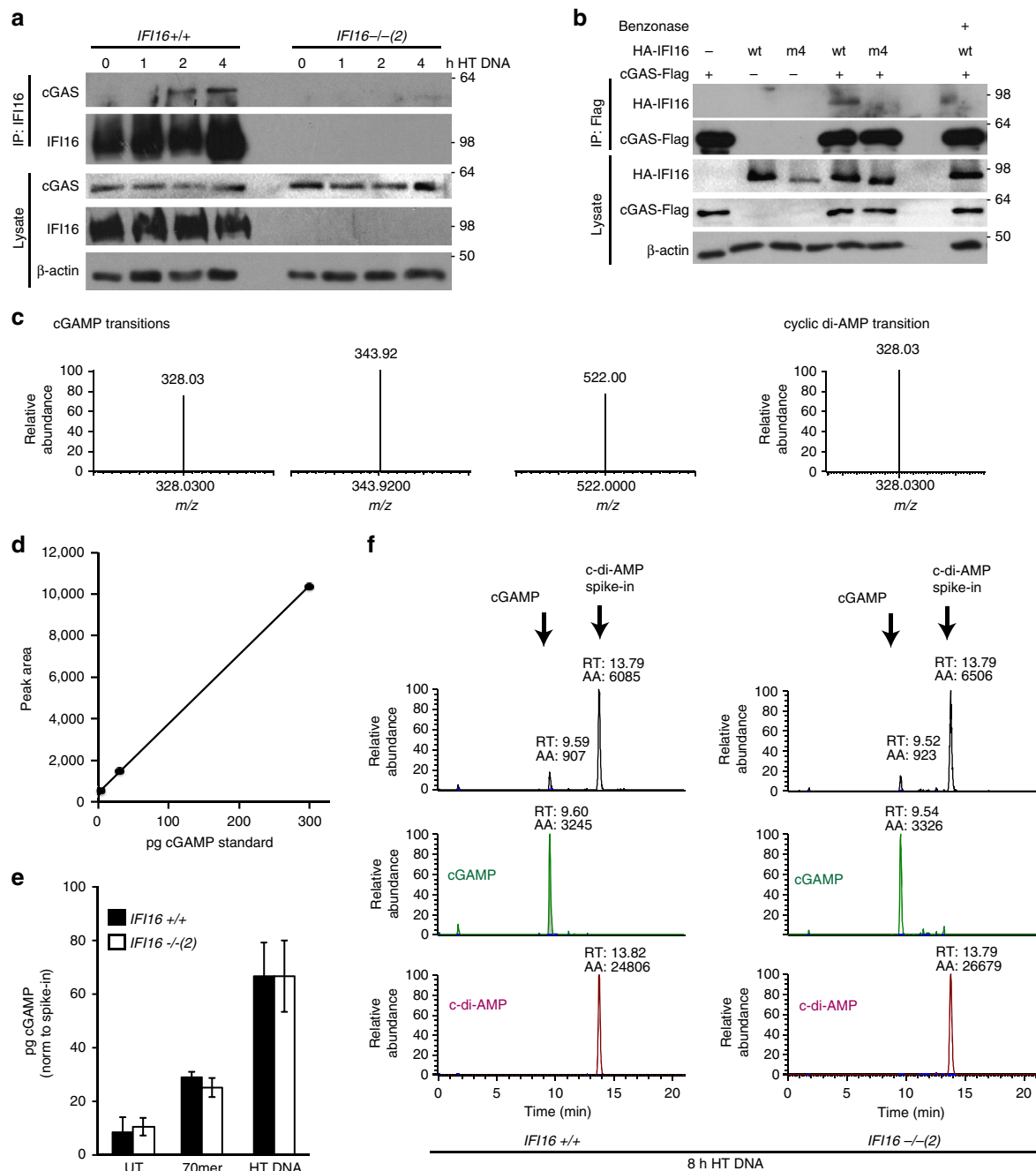


Figure 5 | IFI16 interacts with cGAS but does not affect cGAMP production. (a) *IFI16*^{+/+} or *IFI16*^{-/-} HaCaT cells were stimulated with 5 $\mu\text{g ml}^{-1}$ HT DNA for the times indicated, and IFI16 was immunoprecipitated from cell lysates. Lysates and immunoprecipitates (IP) were analysed by SDS-PAGE and western blotting. (b) HEK293T cells were transfected with constructs for the expression of cGAS-FLAG and HA-IFI16, either wild-type (wt) or DNA-binding mutant (m4), as indicated. 24 h post transfection, cells were subjected to lysis and immunoprecipitation using FLAG antibody. Immunoprecipitates were washed, and treated with benzonase where indicated. Lysates and immunoprecipitates (IP) were analysed by SDS-PAGE and western blotting. (c) Multiple reaction monitoring transitions for cGAMP and cyclic di-AMP, used for the quantification of endogenous cGAMP and internal standard cyclic di-AMP. *m/z*, mass/charge ratio of fragment ions. (d) Standard curve for synthetic cGAMP spiked into cell lysates before sample preparation and liquid chromatography and mass spectrometry (LC-MS) analysis. (e) *IFI16*^{+/+} and *IFI16*^{-/-} HaCaT cells were treated with 1 $\mu\text{g ml}^{-1}$ 70mer oligonucleotide or HT DNA for 8 h, followed by lysis in methanol, spike-in of c-di-AMP and sample preparation. cGAMP levels were determined by LC-MS, and normalized to c-di-AMP levels to account for losses in sample preparation and injection. Data are representative of at least four experiments; values are shown as mean of triplicate samples, with error bars representing s.d. (f) Total and extracted ion chromatogram of cGAMP and cyclic di-AMP in representative samples from (e), showing *IFI16*^{+/+} and *IFI16*^{-/-} cells treated with HT DNA for 8 h. AA, integral peak area; RT, retention time.

gene targeted human fibroblasts with low or undetectable levels of IFI16 protein displayed unimpaired *IFN β* mRNA expression in response to infection with human cytomegalovirus²². Thus, the role of IFI16 during DNA sensing has remained controversial.

Here, we generated human immortalized keratinocytes lacking IFI16, in order to unambiguously determine to what extent IFI16 is required for the innate immune response to DNA in these cells. We show that IFI16 is specifically required for the innate immune

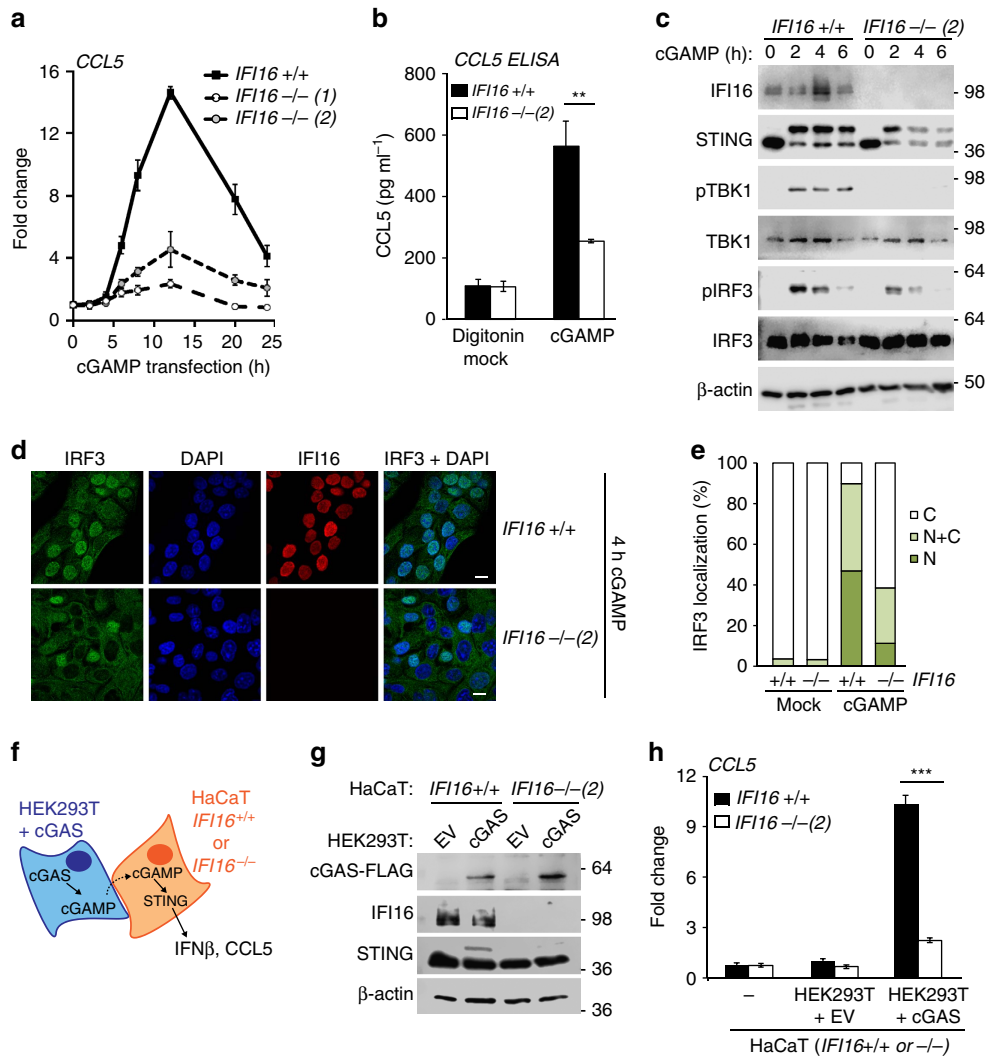


Figure 6 | IFI16 is required for cGAMP-induced STING activation. (a) *IFI16* +/+ and *IFI16* -/- HaCaT cells were transfected with 20 μg ml⁻¹ synthetic cGAMP, and *CCL5* mRNA induction was analysed by qRT-PCR at the time points indicated, and normalized to β-actin mRNA. (b) *IFI16* +/+ and *IFI16* -/- HaCaT cells were infused with 15 μM cGAMP by digitonin-mediated permeabilization, and *CCL5* protein in supernatants was quantified by ELISA 24 h post stimulation. (c) HaCaT cells were permeabilized with digitonin and infused with 15 μM cGAMP for 2, 4 or 6 h. Phosphorylation of STING, of IRF3 at Ser396 (pIRF3) and TBK1 at Ser172 (pTBK1) was analysed by SDS-PAGE and western blotting. (d) HaCaT cells were transfected with 20 μg ml⁻¹ cGAMP for 4 h, and the translocation of endogenous IRF3 was observed by confocal microscopy. Cells were stained for IRF3 (green), IFI16 (red) and DNA (DAPI, blue). Scale bar, 20 μm. (e) Cells as in d were scored for predominantly cytosolic (C), predominantly nuclear (N) and evenly distributed nuclear and cytosolic (N + C) localization of IRF3. At least 200 cells were counted per sample. (f) Schematic representation of the co-culture of HaCaT cells with cGAS-expressing HEK293T cells. Endogenously produced cGAMP can diffuse through gap junctions from the cGAS-expressing producer HEK293T cells to HaCaT cells, where it can bind STING to induce an innate immune response. (g,h) HEK293T cells were transiently transfected with a cGAS-FLAG expression construct or empty vector (EV) for 6 h, then co-cultured with *IFI16* +/+ or *IFI16* -/- HaCaT cells for 18 h. (g) Immunoblot analysis of cGAS-FLAG, IFI16 and STING protein expression in the co-culture. (h) qRT-PCR analysis of *CCL5* mRNA expression in *IFI16* +/+ or *IFI16* -/- HaCaT cells grown in monoculture (-) or co-cultured with HEK293T cells expressing cGAS-FLAG or empty vector (EV). Data show means of triplicate samples with s.d. Shown are representatives of at least two independent experiments each in two *IFI16* -/- cell clones.

response to transfected DNA and to infection with nuclear and cytosolic DNA viruses, but is dispensable for the response to poly(I:C), *in vitro* transcribed RNA, and during infection with Sendai virus. Indeed, the RNA-induced responses are frequently enhanced in the absence of IFI16, possibly due to the competition between DNA and RNA sensing pathways for downstream signalling factors such as TBK1 and IRF3. By analysing the events that follow the detection of foreign DNA in more detail, we find that IFI16 synergizes with cGAMP in the activation of STING. Our data suggest that the activation of STING relies on two independent signals from cGAMP and IFI16, and both are required for optimal STING phosphorylation and trans-

location, and the full activation of the resulting signalling cascades.

It is clear that in HEK293T cells, which lack many of the key components of the DNA sensing pathway, the activation of STING can be driven by cGAS and cGAMP alone (Fig. 4g), or alternatively by IFI16 in the absence of cGAS (Fig. 7e and refs 11,13). In keratinocytes, which naturally respond to DNA, this is not the case, as both IFI16 and cGAS are required for the full activation of STING after DNA stimulation. Thus, the activation of STING is likely more complex and more tightly controlled under physiological conditions, where STING protein levels may be limiting, and additional regulatory mechanisms are

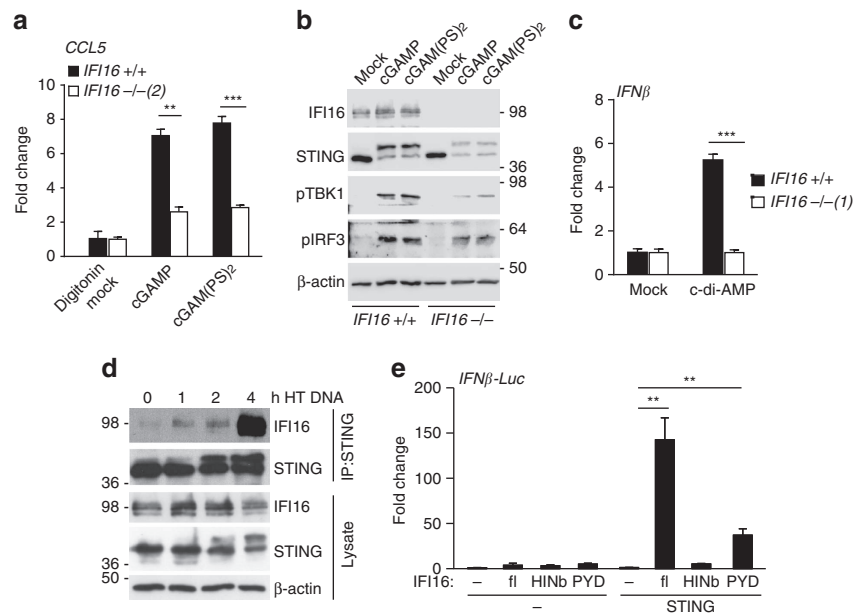


Figure 7 | IFI16 acts on STING to promote its activation by cyclic di-nucleotides. (a) *IFI16*^{+/+} or *IFI16*^{-/-} HaCaT cells were permeabilized with digitonin and infused with 15 μ M cGAMP or its non-hydrolysable analogue cGAM(PS)₂ for 6 h. *CCL5* mRNA expression was analysed by qRT-PCR. (b) Cells were permeabilized and infused with 15 μ M cGAMP or cGAM(PS)₂ for 4 h, and lysates were analysed by western blotting for phosphorylation of STING, TBK1 at Ser172 (pTBK1) and IRF3 at Ser396 (pIRF3). (c) Cells were transfected with 100 μ g ml⁻¹ cyclic di-AMP for 6 h, and *IFN* β mRNA levels were quantified by qRT-PCR. (d) STING was immunoprecipitated from HaCaT cells transfected with 5 μ g ml⁻¹ HT DNA for the times indicated. Lysates and immunoprecipitates (IP) were analysed by SDS-PAGE and western blotting. (e) HEK293T cells were transfected with a firefly luciferase reporter construct under the control of the *IFN* β promoter, a Renilla luciferase transfection control, 2 ng STING-FLAG plasmid and 150 ng empty vector (EV) or *IFI16* expression constructs as indicated: full-length *IFI16* (fl), the *IFI16* HINb domain (HINb), or the *IFI16* pyrin domain (PYD). Firefly luciferase activity was measured 24 h post transfection, and normalized to Renilla luciferase activity. Data are representative of at least two independent experiments. qRT-PCR and luciferase data are expressed as means of triplicate samples; error bars represent s.d. **P* < 0.05, ***P* < 0.01, ****P* < 0.001 Student's *t*-test.

likely to exist. Thus, while HEK293T cells provide a convenient model to test some of the signalling mechanisms at play, the more complex regulation of this signalling pathway will require detailed analysis in more appropriate cell systems that have evolved to respond to exogenous DNA with a high level of selectivity to prevent potentially damaging responses.

In recent years, a multitude of regulatory mechanisms that can influence STING function have been described. In addition to the conformation change caused by cGAMP binding, STING is regulated by a variety of post-translational modifications, including phosphorylation by TBK1 and other kinases^{7,36}, ubiquitylation with K48-, K63- and K27-linked ubiquitin chains⁴³⁻⁴⁷, and palmitoylation⁴⁸. These and other signals may be involved in the translocation of STING from the ER to the signalling compartments where TBK1 recruitment takes place, and further trafficking for the subsequent degradation of STING^{6,34}. In addition, a number of positive and negative regulators that interact with STING have been described⁴⁹⁻⁵¹, but their precise molecular function during DNA-mediated activation of STING has not yet been fully elucidated. Our data indicate that *IFI16* is required for STING phosphorylation, and for STING translocation away from the ER following DNA stimulation. It would be of great interest to determine whether this effect is a direct consequence of *IFI16* association, or whether the function of *IFI16* is mediated by the addition or removal of a post-translational modification or the dissociation of a negative regulator. The detailed analysis of STING modifications and interaction partners following stimulation with DNA in cells lacking *IFI16* or cGAS is required to provide additional insights into the precise molecular mechanisms of STING activation that is elicited by the cooperation of DNA sensors and co-factors. In this context, it would also be important to characterize the

degradation of STING that usually follows its activation. Our data suggest that the absence of *IFI16* causes an un-coupling of STING activation and degradation, as degradation appears to proceed normally, despite reduced levels of STING phosphorylation and trafficking in *IFI16*-deficient cells (see Supplementary Fig. 3c and Figs 6c and 7b).

It is interesting to note that a parallel study on *IFI16* function in human THP-1 monocytes and primary monocyte-derived macrophages found an analogous function of *IFI16* in promoting the phosphorylation of STING in response to exogenous DNA and cGAMP⁵², with a similar impairment in IFN induction in the absence of *IFI16*. However, the authors also show, that in this cellular context, *IFI16* can perform an additional function during DNA sensing in also promoting the production of cGAMP by cGAS. Thus, there may be cell-type-specific differences in the regulation of the DNA sensing pathway.

We find that in human keratinocytes, cGAS and *IFI16* function more independently of each other, only co-operating at the level of STING activation. Furthermore, while in other cell types cGAS promotes *IFI16* protein expression after DNA stimulation^{15,20}, this is not the case in human keratinocytes, where *IFI16* protein levels remain unchanged over a 12 h time course after DNA transfection (see Fig. 3g).

Thus, it is conceivable that the range of *IFI16* functions may depend on its relative abundance in the cell, which is particularly dynamic in monocytes and macrophages. In monocytes and THP1 cells, *IFI16* protein expression is induced very strongly by differentiation, and this correlates with an increased sensitivity to exogenous DNA in those cells¹⁰. In these cells, *IFI16* levels increase even further upon DNA stimulation, providing a positive feedback loop. This positive feedback loop is absent in human keratinocytes, which may serve to prevent excessive immune

activation after localized infection. Differences in the relative expression levels of cGAS, IFI16 or other AIM2-like receptors may also account for some of the observed differences between mouse and human cells, and between different mouse strains²². While we and others provide strong evidence for an involvement of IFI16 in DNA sensing in human cells, the function of IFI16 homologues in mice may need to be investigated further.

In summary, we show here that cGAS and IFI16 cooperate in the sensing of intracellular DNA in human keratinocytes. While we still observe a weak transcriptional response to exogenous DNA in the absence of IFI16 in these cells, IFI16 is critical for the full activation of STING, and cooperates with cGAMP in the activation of this key signalling adaptor. The integration of IFI16 into the cGAS-cGAMP-STING signalling cascade provides a further level of regulation of STING activation that may be important to prevent the spurious activation of the innate immune system.

Methods

Cells and viruses. Immortalized human keratinocytes (HaCaT), MRC-5 human embryonic lung fibroblasts and immortalized human embryonic kidney HEK293T cells were cultured in Dulbecco's Modified Eagle's Medium (DMEM, Gibco) supplemented with 10% (v/v) FCS and 50 $\mu\text{g ml}^{-1}$ gentamicin. Primary human keratinocytes from adult donors were obtained from Lonza, and grown in KGM-Gold Keratinocyte Basal Medium supplemented with KGM-Gold Single-Quots (Lonza). Cell lines were regularly tested for mycoplasma contamination.

Sendai virus (SeV, strain Cantell) was kindly provided by R. Randall (University of St. Andrews, UK). Vaccinia virus with RFP-tagged A3L protein (VACV-RFP)⁵³ was propagated in RK13 cells and sucrose-purified. MVA was kindly provided by B. Ferguson (University of Cambridge, UK). MVA was propagated in BHK cells and sucrose-purified. GFP-tagged Herpes Simplex Virus 1 (HSV-1-GFP) was kindly provided by F. Grey (The Roslin Institute, University of Edinburgh, UK) and propagated in Vero cells. All viruses were titrated on BSC cells.

Generation of IFI16^{-/-} and cGAS^{-/-} HaCaT cells. HaCaT cells lacking cGAS or IFI16 were generated using CRISPR-Cas9 nickase or TALE nuclease technology, respectively. Plasmids encoding left and right TALEN arms, or Cas9 nickase and two guide RNAs, were transfected into HaCaT cells using electroporation with the Neon system (Life Technologies). Cells were selected for 48 h with puromycin, then allowed to recover and seeded as single cells in 96-well plates. DNA was extracted from individual colonies using Quickextract DNA extraction solution (EpiBio), and screened for modifications of the target site, using high resolution melting analysis on a LifeCycler 96 system (Roche), using Light-Cycler480 High Resolution Melting master mix (Roche). Candidate clones displaying mutated target sites were screened for lack of protein expression by western blotting of IFI16 or cGAS and β -actin, and by immunofluorescence analysis to confirm homogeneity of cell clones.

Virus infection. HaCaT cells were seeded 24 h before infection and were infected with VACV or MVA in DMEM supplemented with 2.5% (v/v) FCS for 1 h, before replacing the inoculum with DMEM containing 2.5% (v/v) FCS. HSV-1-GFP infections (MOI = 1) were performed in serum-free DMEM for 1 h, followed by the maintenance of cells in complete DMEM containing 10% (v/v) FCS. Infections with a SeV preparation containing defective viral particles was carried out in serum-free DMEM for 1 h, followed by replacement of the medium with complete DMEM containing 10% (v/v) FCS. Infections were allowed to proceed for 6 h, unless indicated otherwise.

Transfection of nucleic acids and cGAMP. Cells were seeded at $1-1.5 \times 10^5$ cells per ml 24 h before transfection, and stimulated with $1 \mu\text{g ml}^{-1}$ HT DNA (HT DNA, Sigma), a double-stranded 70mer oligonucleotide derived from VACV (5'-CCATCAGAAAAGAGGTTTAAATATTTTTGTGAGACCATCGAAGAGAGAAAGAGATAAAACTTTTTACGACT-3')¹⁰, Y-G3 DNA (5'-GGGAACTCCAGCAGGACCATTGGGG-3') or Y-C3 DNA (5'-CCCGAACTCCAGCAGGAC CATTGCC-3')²⁴. DNA oligonucleotides were synthesized by Biofins Genomics, Germany. *In vitro* transcribed RNA containing a 5'-triphosphate was generated using the MEGAScript T7 transcription kit (Thermo Fisher) with pcDNA3.1:EGFP as template. 50 ng ml^{-1} of *in vitro* transcribed RNA and 100 ng ml^{-1} poly(I:C) (Sigma) were used, unless indicated otherwise. 2'3' cGAMP (Invivogen) or cyclic di-AMP (Invivogen) were transfected at 20 and 100 $\mu\text{g ml}^{-1}$, respectively. All transfections were carried out with 1 μl Lipofectamine 2000 (Life Technologies) per ml medium.

Transfection by digitonin permeabilization was carried out in a buffer containing 50 mM HEPES (pH 7), 100 mM KCl, 3 mM MgCl_2 , 0.1 mM DTT, 85 mM saccharose, 1 mM ATP, 0.1 mM GTP and 0.2% (v/v) BSA. 25 $\mu\text{g ml}^{-1}$ HT DNA

(Sigma). 15 μM 2'3' cGAMP or 2'3' cGAMP(PS)₂ (both Invivogen) was transfected using 5 $\mu\text{g ml}^{-1}$ digitonin in permeabilization buffer for 10 min at 37 °C before replacing the permeabilization buffer with DMEM containing 10% (v/v) FCS.

Quantitative real-time PCR (qRT-PCR). RNA was extracted using HighPure RNA Isolation Kits (Roche), and cDNA was synthesized using the iScript cDNA Synthesis Kit (Bio-Rad Laboratories). Real-time PCR amplification was performed in a 10 μl reaction containing FastStart Universal SYBR Green Master Mix (Roche) on a LifeCycler 96 system (Roche). The real-time PCR program was as follows: initial denaturation at 95 °C for 600 s; 40 cycles of 95 °C for 10 s then 60 °C for 30 s; followed by a melt curve step. Quantification cycle (C_q) of mRNAs of interest were normalized to C_q of β -actin reference mRNA and data was expressed as fold change over mock treatment. Primers were synthesized by Eurofins Genomics. Primer sequences were: β -actin forward (FWD): 5'-CGCGAGAGAAGATGACC CAG;ATC-3'; β -actin reverse (REV): 5'-GCCAGAGCGGTACAGGGATA-3'; *IFN β* FWD: 5'-ACGCCGATTGACCATCTAT-3'; *IFN β* REV: 5'-GTCTCA TTCCAGCCAGTGCT-3'; *CXCL10* FWD: 5'-AGCAGAGGAACCTCCAGTCT-3'; *CXCL10* REV: 5'-AGGTACTCCTTGAATGCCACT-3'; *CCL5* FWD: 5'-CTGC TTTGCCTACATTGCC-3'; *CCL5* REV: 5'-TCGGGTGACAAAGACGACTG-3'; *ISG56* FWD: 5'-CAAAGGGCAAACGAGGCAG-3'; *ISG56* REV: 5'-CCCAG GCATAGTTTCCCCAG-3'; *IL6* FWD: 5'-CAGCCCTGAGAAAGGAGACAT-3'; *IL6* REV: 5'-GGTTCAGTTGTTTTCTGCCA-3'.

ELISA. For the quantification of secreted chemokines by ELISA, cells were stimulated for 24 h as indicated. Supernatants were harvested and secreted CCL5 or CXCL10 protein levels were quantified using Human CCL5/Rantes (DY278) and Human CXCL10/IP-10 (DY266) DuoSet ELISA kits (R&D Systems) according to manufacturer's instructions. Absorbance was measured at 450 nm and corrected against absorbance at 570 nm.

Western blotting and antibodies. For western blotting, cells were harvested in lysis buffer containing 50 mM Tris (pH 7.4), 150 mM NaCl, 30 mM NaF, 5 mM EDTA, 10% (v/v) glycerol, 40 mM β -glycerophosphate, 1% (v/v) Triton X-100, 1 mM sodium orthovanadate, 0.1 mM phenylmethanesulfonylfluoride and 0.07 μM aprotinin. Proteins were separated by SDS-PAGE and transferred to polyvinylidene (PVDF) membranes using semi-dry transfer. Membranes were blocked with 5% (w/v) non-fat milk in PBS containing 0.1% (v/v) Tween-20 (PBS-T) for 1 h before incubation with antibodies. Western blots using antibodies against phosphorylated proteins were performed with TBS containing 0.1% (v/v) Tween-20 and 5% bovine serum albumin (BSA).

The antibodies used were anti-IFI16 (1G7, Santa Cruz Biotechnology), anti-cGAS (HPA031700, Sigma Aldrich), anti-STING (D2P2F, Cell Signaling Technology), anti-TBK1 (D1B4, Cell Signaling Technology), anti-IRF3 (D614C, Cell Signaling Technology), anti- β -actin (A2228, Sigma Aldrich), anti-phospho(Ser172)-TBK1 (D52C2, Cell Signaling Technology) and anti-phospho(Ser396)-IRF3 (4D4G, Cell Signaling Technology). Primary antibodies were used at a dilution of 1:1,000. Secondary horse radish peroxidase-coupled anti-mouse (7076 S) and anti-rabbit (7074 S) antibodies were from Cell Signaling Technology and used at a dilution of 1:3,000. Full immunoblots including size markers are shown in Supplementary Fig. 6.

Luciferase assays. HEK293T cells were seeded in 96-well plates at 1×10^5 cells per ml, and transfected with 60 ng of a firefly luciferase construct under the control of an *IFN β* promoter (IFN β -luciferase, obtained from T Taniguchi, University of Tokyo) and 60 ng pGL3-Renilla luciferase transfection control¹⁰ per well. In addition, pcDNA3.1:STING-FLAG (kindly provided by Lei Jin, Albany Medical Centre) and cGAS or IFI16 expression constructs were co-transfected as indicated. Empty vector (pCMV-HA, Clontec) was added to keep amounts of DNA constant. Transfections were carried out using 0.8 μl GeneJuice Transfection Reagent (Merck Millipore) per well, and cells were lysed in Passive Lysis Buffer (Merck Millipore) 24 h post transfection. Firefly luciferase activity was measured and normalized to Renilla luciferase activity in each sample. IFI16 truncations (Pyrin domain, aa 1-91; HINb domain, aa 507-730) were cloned into pIRESpuro2 containing an N-terminal HA tag.

Co-culture of HEK293T and HaCaT cells. For the co-culture with cGAS-expressing cells, HEK293T cells were transfected with pCMV6-Entry:cGAS-myc-FLAG (OriGene) or empty vector for 6 h using GeneJuice Transfection Reagent (Merck Millipore). cGAS-expressing HEK293T and wild-type or *IFI16^{-/-}* HaCaT cells were seeded together in 12-well plates at a ratio of 1:4 (HEK293T:HaCaT) at a total of 1.5×10^5 cells per ml. RNA and protein samples were harvested after 18 h of co-culture.

siRNA transfection. Pools of four dual strand modified siRNAs were obtained from GE Dharmacon (ON-TARGETplus SMARTpool siRNA), and used as pool or individually, as indicated. Primary human keratinocytes or MRC-5 fibroblasts were seeded in 24-well plates at 1.5×10^5 cells ml^{-1} and transfected with 5 nM of non-targeting siRNA pools or IFI16-targeting siRNA using 3 $\mu\text{l ml}^{-1}$ of Lipofectamine

RNAimax (Life Technologies). Cells were stimulated 48 h after treatment with siRNA.

Immunofluorescence and confocal microscopy. Cells were seeded on coverslips 24 h before stimulation with DNA or infection as indicated. Cells were washed with PBS, and fixed in methanol at -20°C . Cells were permeabilized for 12 min in 0.5% Triton-X in PBS, washed in PBS, and incubated for 1 h in blocking solution (5% FBS, 0.2% Tween-20 in PBS). Cells were stained with primary antibodies (1:600 in blocking solution) at room temperature over night. Primary antibodies used were anti-IFI16 (1G7, Santa Cruz Biotechnology), anti-STING (D2P2F, Cell Signaling Technology) and anti-IRF3 (D614C, Cell Signaling Technology). Coverslips were washed in PBS, and incubated for 3 h with fluorescently labelled secondary antibodies, used at a dilution of 1:1,500 in blocking solution. Anti-mouse IgG labelled with AlexaFluor647 (A21236) or AlexaFluor488 (A11029), and anti-rabbit IgG labelled with AlexaFluor488 (A11034) were from Life Technologies. Coverslips were washed in PBS and mounted in MOWIOL 4-88 containing $1\ \mu\text{g ml}^{-1}$ DAPI. Images were obtained using a $\times 100$ oil immersion objective on a LSM710 laser scanning microscope (Zeiss).

mRNA reconstitution. DNA plasmids pcDNA3.1(+):GFP or pcDNA3.1(+):IFI16 were used as templates for the *in vitro* synthesis of capped and polyadenylated mRNA using the mMESAGE mMACHINE T7 Transcription Kit (ThermoScientific). *IFI16* $-/-$ HaCaT cells were seeded at 1×10^5 cells/ml on coverslips 24 h before transfection with $1\ \mu\text{g ml}^{-1}$ GFP mRNA or *IFI16* mRNA for 6 h using using $1\ \mu\text{l ml}^{-1}$ of Lipofectamine 2000 (Life Technologies). Cells were then stimulated with $5\ \mu\text{g ml}^{-1}$ HT DNA (Sigma) for 1 h.

cGAMP detection by LC-MS. 5×10^6 HaCaT cells per sample were lysed in cold 80% methanol, followed by the addition of 0.45 pmol cyclic-di-AMP, as internal spike-in to control for losses in sample preparation and injection. Cell debris was removed by centrifugation, samples were dried by vacuum centrifugation, and then subjected to three rounds of butanol:water extraction. Dried samples were resuspended in 1 ml H_2O and subjected to solid phase extraction using HyperSep Aminopropyl columns (ThermoFisher). Columns were activated using 80% methanol before the addition of samples. The columns were then washed twice with a solution of 2% (v/v) acetic acid/80% (v/v) methanol. Elution was performed using a solution of 4% (v/v) ammonium hydroxide/80% (v/v) methanol. Samples were dried again by vacuum centrifugation and resuspended in 40 μl H_2O for analysis by liquid chromatography and mass spectrometry (LC-MS).

cGAMP levels were measured using a TSQ Quantiva interfaced with Ultimate 3000 Liquid Chromatography system (ThermoScientific), equipped with a porous graphitic carbon column (HyperCarb $30 \times 1\ \text{mm ID } 3\ \mu\text{m}$; Part No: C-35003-031030, Thermo-Scientific). Mobile phase buffer A consisted of 0.3% (v/v) formic acid adjusted to pH 9 with ammonia before a 1/10 dilution. Mobile phase buffer B was 80% (v/v) acetonitrile. The column was maintained at a controlled temperature of 30°C and was equilibrated with 13% buffer B for 15 min at a constant flow rate of $0.06\ \text{ml min}^{-1}$. Aliquots of 13 μl of each sample were loaded onto the column and compounds were eluted from the column with a linear gradient of 13–80% buffer B over 20 min. Buffer B was then increased to 100% for 5 min and the column was washed for a further 5 min with Buffer B. Eluents were sprayed into the TSQ Quantiva using Ion Max NG ion source with ion transfer tube temperature set to 350°C and vaporizer temperature 125°C . The TSQ Quantiva was run in negative mode with a spray voltage of 2,600 V, sheath gas 40 and Aux gas 10. cGAMP and spiked in cyclic di-AMP levels were measured using multiple reaction monitoring mode with optimized collision energies and radio frequencies previously determined by infusing pure compounds. Three transitions ($673.05 > 328.03$, $673.05 > 343.92$ and $673.06 > 522.00$) were used to monitor cGAMP and one transition ($657.07 > 328.03$) was used to detect cyclic di-AMP.

Co-immunoprecipitation. Cells were lysed in IP lysis buffer (25 mM Tris-HCl pH 7.4, 150 mM NaCl, 1% NP-40, 1 mM EDTA, 50 mM NaF and 5% glycerol), supplemented with Complete protease inhibitor cocktail (Roche). Samples were pre-cleared by centrifugation at 2,000 g for 10 min before incubation with antibodies overnight at 4°C , followed by the addition of protein G beads (ThermoFisher) for 3 h. Immunoprecipitates were washed three times with the IP lysis buffer. Bound proteins were eluted by boiling in SDS-sample buffer and analysed by western blot.

Treatment with phosphatase and benzonase. For phosphatase treatment, immunoprecipitates containing STING were incubated with 25 U λ phosphatase for 1 h at 30°C . For treatment with benzonase, immunoprecipitates were washed in lysis buffer without EDTA, and incubated in 100 μl benzonase reaction buffer (50 mM Tris-Cl, pH 8, 2 mM MgCl_2 , 150 mM NaCl) with $1.5\ \text{U } \mu\text{l}^{-1}$ benzonase for 1 h at 37°C . Immunoprecipitates were washed twice in lysis buffer and analysed by SDS-PAGE and western blotting.

Statistical analysis. Results from real-time PCR analysis, luciferase assays, ELISA and cGAMP quantification are presented as averages of triplicate samples with error bars representing s.d. Data were subjected to a multiple *t*-test statistical analysis with the Holm-Sidak method. * $P < 0.05$, ** $P < 0.01$, *** $P < 0.001$.

Data availability. The data that support the findings of this study are available from the corresponding author upon request.

References

- Nestle, F. O., Di Meglio, P., Qin, J.-Z. & Nickoloff, B. J. Skin immune sentinels in health and disease. *Nat. Rev. Immunol.* **9**, 679–691 (2009).
- Sparrer, K. M. J. & Gack, M. U. Intracellular detection of viral nucleic acids. *Curr. Opin. Microbiol.* **26**, 1–9 (2015).
- Sun, L., Wu, J., Du, F., Chen, X. & Chen, Z. J. Cyclic GMP-AMP synthase is a cytosolic DNA sensor that activates the type I interferon pathway. *Science* **339**, 786–791 (2013).
- Li, X.-D. *et al.* Pivotal roles of cGAS-cGAMP signaling in antiviral defense and immune adjuvant effects. *Science* **341**, 1390–1394 (2013).
- Zhang, X. *et al.* Cyclic GMP-AMP containing mixed phosphodiester linkages is an endogenous high-affinity ligand for STING. *Mol Cell* **51**, 226–235 (2013).
- Dobbs, N. *et al.* STING activation by translocation from the ER is associated with infection and autoinflammatory disease. *Cell Host Microbe* **18**, 157–168 (2015).
- Liu, S. *et al.* Phosphorylation of innate immune adaptor proteins MAVS, STING, and TRIF induces IRF3 activation. *Science* **347**, aaa2630 (2015).
- Cai, X., Chiu, Y.-H. & Chen, Z. J. The cGAS-cGAMP-STING pathway of cytosolic DNA sensing and signaling. *Mol Cell* **54**, 289–296 (2014).
- Unterholzner, L. The interferon response to intracellular DNA: why so many receptors? *Immunobiology* **218**, 1312–1321 (2013).
- Unterholzner, L. *et al.* IFI16 is an innate immune sensor for intracellular DNA. *Nat. Immunol.* **11**, 997–1004 (2010).
- Li, T., Diner, B. A., Chen, J. & Cristea, I. M. Acetylation modulates cellular distribution and DNA sensing ability of interferon-inducible protein IFI16. *Proc. Natl Acad. Sci. USA* **109**, 10558–10563 (2012).
- Hornung, V. *et al.* AIM2 recognizes cytosolic dsDNA and forms a caspase-1-activating inflammasome with ASC. *Nature* **458**, 514–518 (2009).
- Jin, T. *et al.* Structures of the HIN domain:DNA complexes reveal ligand binding and activation mechanisms of the AIM2 inflammasome and IFI16 receptor. *Immunity* **36**, 561–571 (2012).
- Horan, K. A. *et al.* Proteasomal degradation of herpes simplex virus capsids in macrophages releases DNA to the cytosol for recognition by DNA sensors. *J. Immunol.* **190**, 2311–2319 (2013).
- Orzalli, M. H. *et al.* cGAS-mediated stabilization of IFI16 promotes innate signaling during herpes simplex virus infection. *Proc. Natl Acad. Sci. USA* **112**, E1773–E1781 (2015).
- Chiliveru, S. *et al.* Inflammatory cytokines break down intrinsic immunological tolerance of human primary keratinocytes to cytosolic DNA. *J. Immunol.* **192**, 2395–2404 (2014).
- Conrady, C. D., Zheng, M., Fitzgerald, K. A., Liu, C. & Carr, D. J. J. Resistance to HSV-1 infection in the epithelium resides with the novel innate sensor, IFI-16. *Mucosal Immunol.* **5**, 173–183 (2012).
- Jakobsen, M. R. *et al.* IFI16 senses DNA forms of the lentiviral replication cycle and controls HIV-1 replication. *Proc. Natl Acad. Sci. USA* **110**, E4571–E4580 (2013).
- Hansen, K. *et al.* *Listeria monocytogenes* induces IFN expression through an IFI16-, cGAS- and STING-dependent pathway. *EMBO J.* **33**, 1654–1666 (2014).
- Storek, K. M., Gertsvolf, N. A., Ohlson, M. B. & Monack, D. M. cGAS and Ifi204 cooperate to produce type I IFNs in response to *Francisella* infection. *J. Immunol.* **194**, 3236–3245 (2015).
- Gao, D. *et al.* Cyclic GMP-AMP synthase is an innate immune sensor of HIV and other retroviruses. *Science* **341**, 903–906 (2013).
- Gray, E. E. *et al.* The AIM2-like receptors are dispensable for the interferon response to intracellular DNA. *Immunity* **45**, 255–266 (2016).
- Zhang, Z. *et al.* The helicase DDX41 senses intracellular DNA mediated by the adaptor STING in dendritic cells. *Nat. Immunol.* **12**, 959–965 (2011).
- Herzner, A. M. *et al.* Sequence-specific activation of the DNA sensor cGAS by Y-form DNA structures as found in primary HIV-1 cDNAs. *Nat. Immunol.* **16**, 1025–1033 (2015).
- Orzalli, M. H., DeLuca, N. A. & Knipe, D. M. Nuclear IFI16 induction of IRF-3 signaling during herpesviral infection and degradation of IFI16 by the viral ICP0 protein. *Proc. Natl Acad. Sci. USA* **109**, E3008–E3017 (2012).
- Everett, R. D. The dynamic response of IFI16 and PML nuclear body components to HSV-1 infection. *J. Virol.* **90**, 167–179 (2015).
- Kalamvoki, M. & Roizman, B. HSV-1 degrades, stabilizes, requires, or is stung by STING depending on ICP0, the US3 protein kinase, and cell derivation. *Proc. Natl Acad. Sci. USA* **111**, E611–E617 (2014).

28. Cuchet-Lourenço, D., Anderson, G., Sloan, E., Orr, A. & Everett, R. D. The viral ubiquitin ligase ICP0 is neither sufficient nor necessary for degradation of the cellular DNA sensor IFI16 during herpes simplex virus 1 infection. *J. Virol.* **87**, 13422–13432 (2013).
29. Smith, G. L. *et al.* Vaccinia virus immune evasion: mechanisms, virulence and immunogenicity. *J. Gen. Virol.* **94**, 2367–2392 (2013).
30. Strähle, L., Garcin, D. & Kolakofsky, D. Sendai virus defective-interfering genomes and the activation of interferon- β . *Virology* **351**, 101–111 (2006).
31. Rehwinkel, J. *et al.* RIG-I detects viral genomic RNA during negative-strand RNA virus infection. *Cell* **140**, 397–408 (2010).
32. Thompson, M. R. *et al.* Interferon γ -inducible protein (IFI) 16 transcriptionally regulates type I interferons and other interferon-stimulated genes and controls the interferon response to both DNA and RNA viruses. *J. Biol. Chem.* **289**, 23568–23581 (2014).
33. Ishikawa, H. & Barber, G. N. STING is an endoplasmic reticulum adaptor that facilitates innate immune signalling. *Nature* **455**, 674–678 (2008).
34. Ishikawa, H., Ma, Z. & Barber, G. N. STING regulates intracellular DNA-mediated, type I interferon-dependent innate immunity. *Nature* **461**, 788–792 (2009).
35. Saitoh, T. *et al.* Atg9a controls dsDNA-driven dynamic translocation of STING and the innate immune response. *Proc. Natl Acad. Sci. USA* **106**, 20842–20846 (2009).
36. Konno, H., Konno, K. & Barber, G. N. Cyclic dinucleotides trigger ULK1 (ATG1) phosphorylation of STING to prevent sustained innate immune signaling. *Cell* **155**, 688–698 (2013).
37. Burdette, D. L. *et al.* STING is a direct innate immune sensor of cyclic di-GMP. *Nature* **478**, 515–518 (2011).
38. Ablasser, A. *et al.* cGAS produces a 2'-5'-linked cyclic dinucleotide second messenger that activates STING. *Nature* **498**, 380–384 (2013).
39. Holm, C. K. *et al.* Virus-cell fusion as a trigger of innate immunity dependent on the adaptor STING. *Nat. Immunol.* **13**, 737–743 (2012).
40. Li, L. *et al.* Hydrolysis of 2'3'-cGAMP by ENPP1 and design of nonhydrolyzable analogs. *Nat. Chem. Biol.* **10**, 1043–1048 (2014).
41. Yi, G. *et al.* Single nucleotide polymorphisms of human STING can affect innate immune response to cyclic dinucleotides. *PLoS ONE* **8**, e77846 (2013).
42. Dempsey, A. & Bowie, A. G. Innate immune recognition of DNA: a recent history. *Virology* **479–480**, 146–152 (2015).
43. Zhong, B. *et al.* The ubiquitin ligase RNF5 regulates antiviral responses by mediating degradation of the adaptor protein MITA. *Immunity* **30**, 397–407 (2009).
44. Tsuchida, T. *et al.* The ubiquitin ligase TRIM56 regulates innate immune responses to intracellular double-stranded DNA. *Immunity* **33**, 765–776 (2010).
45. Zhang, J., Hu, M. M., Wang, Y. Y. & Shu, H. B. TRIM32 protein modulates type I interferon induction and cellular antiviral response by targeting MITA/STING protein for K63-linked ubiquitination. *J. Biol. Chem.* **287**, 28646–28655 (2012).
46. Wang, Q. *et al.* The E3 ubiquitin Ligase AMFR and INSIG1 bridge the activation of TBK1 kinase by modifying the adaptor STING. *Immunity* **41**, 919–933 (2014).
47. Wang, Y. *et al.* TRIM30 α is a negative-feedback regulator of the intracellular DNA and DNA virus-triggered response by targeting STING. *PLoS Pathog.* **11**, e1005012 (2015).
48. Mukai, K. *et al.* Activation of STING requires palmitoylation at the Golgi. *Nat. Commun.* **7**, 11932 (2016).
49. Zhang, L. *et al.* NLRC3, a member of the NLR family of proteins, is a negative regulator of innate immune signaling induced by the DNA sensor STING. *Immunity* **40**, 329–341 (2014).
50. Li, Z. *et al.* PPM1A regulates antiviral signaling by antagonizing TBK1-mediated STING phosphorylation and aggregation. *PLoS Pathog.* **11**, e1004783 (2015).
51. Okabe, Y., Sano, T. & Nagata, S. Regulation of the innate immune response by threonine-phosphatase of Eyes absent. *Nature* **460**, 520–524 (2009).
52. Jönsson, K. L. *et al.* IFI16 is required for DNA sensing in human macrophages by promoting production and function of cGAMP. *Nat. Commun.* **8**, 14391 (2017).
53. Carter, G. C. *et al.* Vaccinia virus cores are transported on microtubules. *J. Gen. Virol.* **84**, 2443–2458 (2003).

Acknowledgements

We thank Mike Ferguson and the Fingerprints Proteomics Facility, University of Dundee, for help with the quantification of cGAMP samples. We are grateful to Finn Grey (The Roslin Institute, University of Edinburgh), Brian Ferguson (University of Cambridge) and Richard Randall (University of St. Andrews) for generously providing viruses. The work was supported by the Medical Research Council (Career Development Award to L.U., MR/K00655X/1), the British Skin Foundation (Innovative Project Grant, 6057i), Tenovus Scotland (Ref. T14/14), the Biotechnology and Biological Sciences Research Council (BB/J004324/1), the National Institutes of Health (AI093752) and Science Foundation Ireland (11/PI/1056). C.A.J.O.H. and G.D. were supported through a Wellcome Trust ISSF grant and the MRC doctoral training program at the University of Dundee.

Author contributions

J.F.A. and C.A.J.O.H. designed and performed most experiments, and analysed data. G.D. generated and characterized cGAS-deficient cells; I.R.H., R.J.N., J.T., D.J.C. and I.R.K. performed additional experiments; A.A. optimized the cGAMP detection by LC-MS; A.G.B. and P.M.B. designed and supervised experiments; L.U. conceived the study, designed and performed experiments, and wrote the manuscript with input from all authors.

Additional information

Supplementary Information accompanies this paper at <http://www.nature.com/naturecommunications>

Competing financial interests: The authors declare no competing financial interests.

Reprints and permission information is available online at <http://npg.nature.com/reprintsandpermissions/>

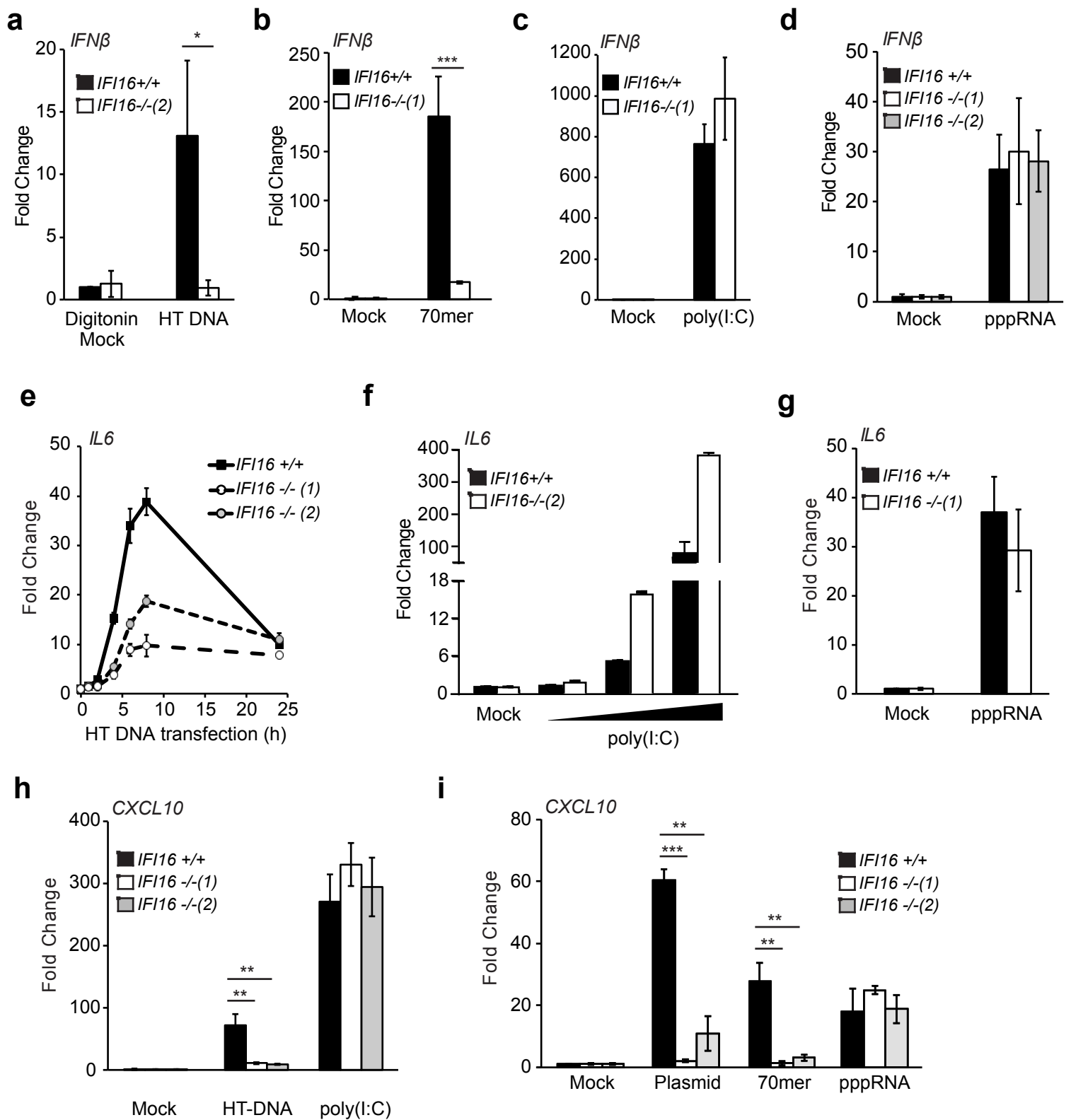
How to cite this article: Almine, J. F. *et al.* IFI16 and cGAS cooperate in the activation of STING during DNA sensing in human keratinocytes. *Nat. Commun.* **8**, 14392 doi: 10.1038/ncomms14392 (2017).

Publisher's note: Springer Nature remains neutral with regard to jurisdictional claims in published maps and institutional affiliations.



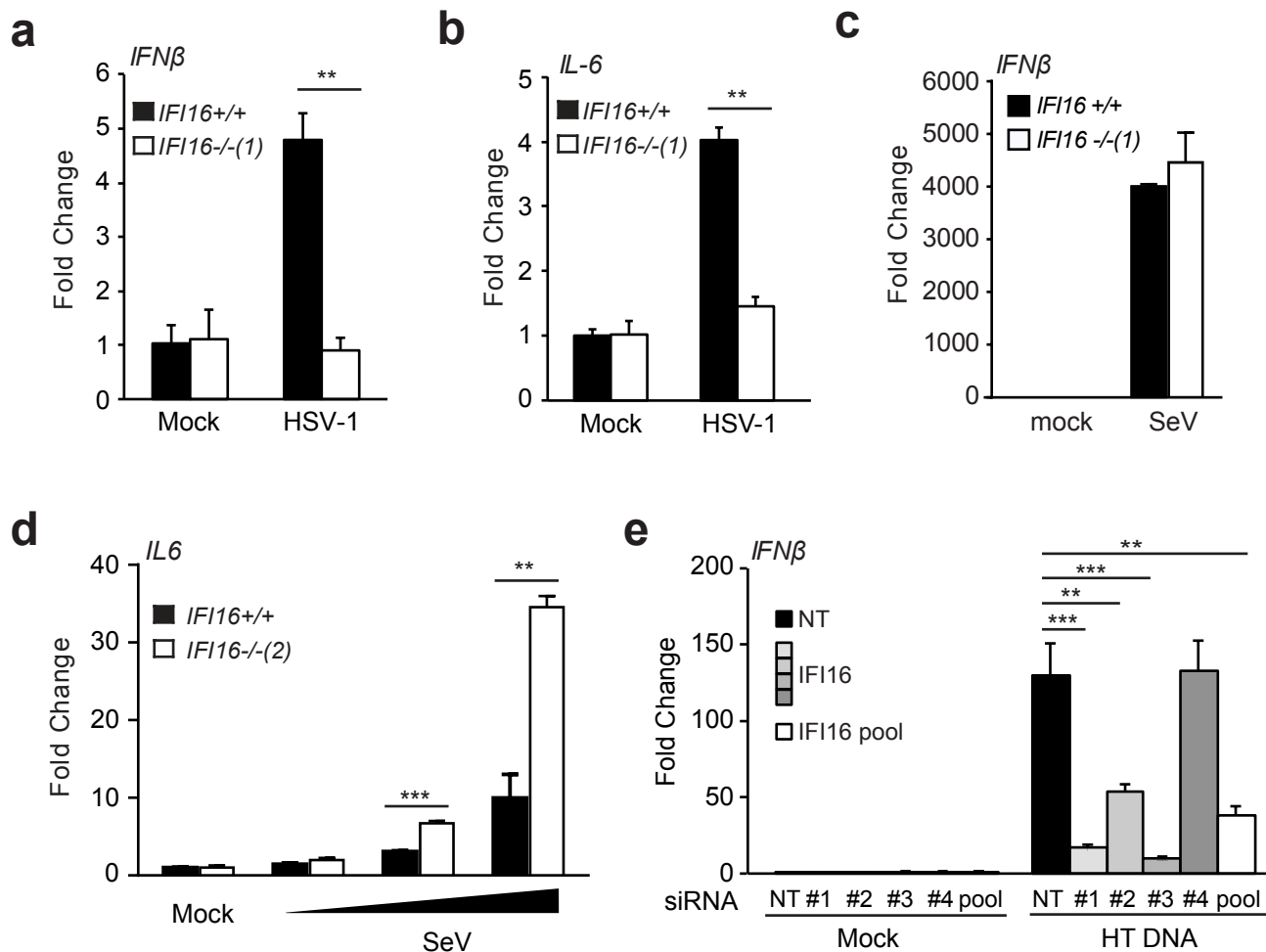
This work is licensed under a Creative Commons Attribution 4.0 International License. The images or other third party material in this article are included in the article's Creative Commons license, unless indicated otherwise in the credit line; if the material is not included under the Creative Commons license, users will need to obtain permission from the license holder to reproduce the material. To view a copy of this license, visit <http://creativecommons.org/licenses/by/4.0/>

© The Author(s) 2017



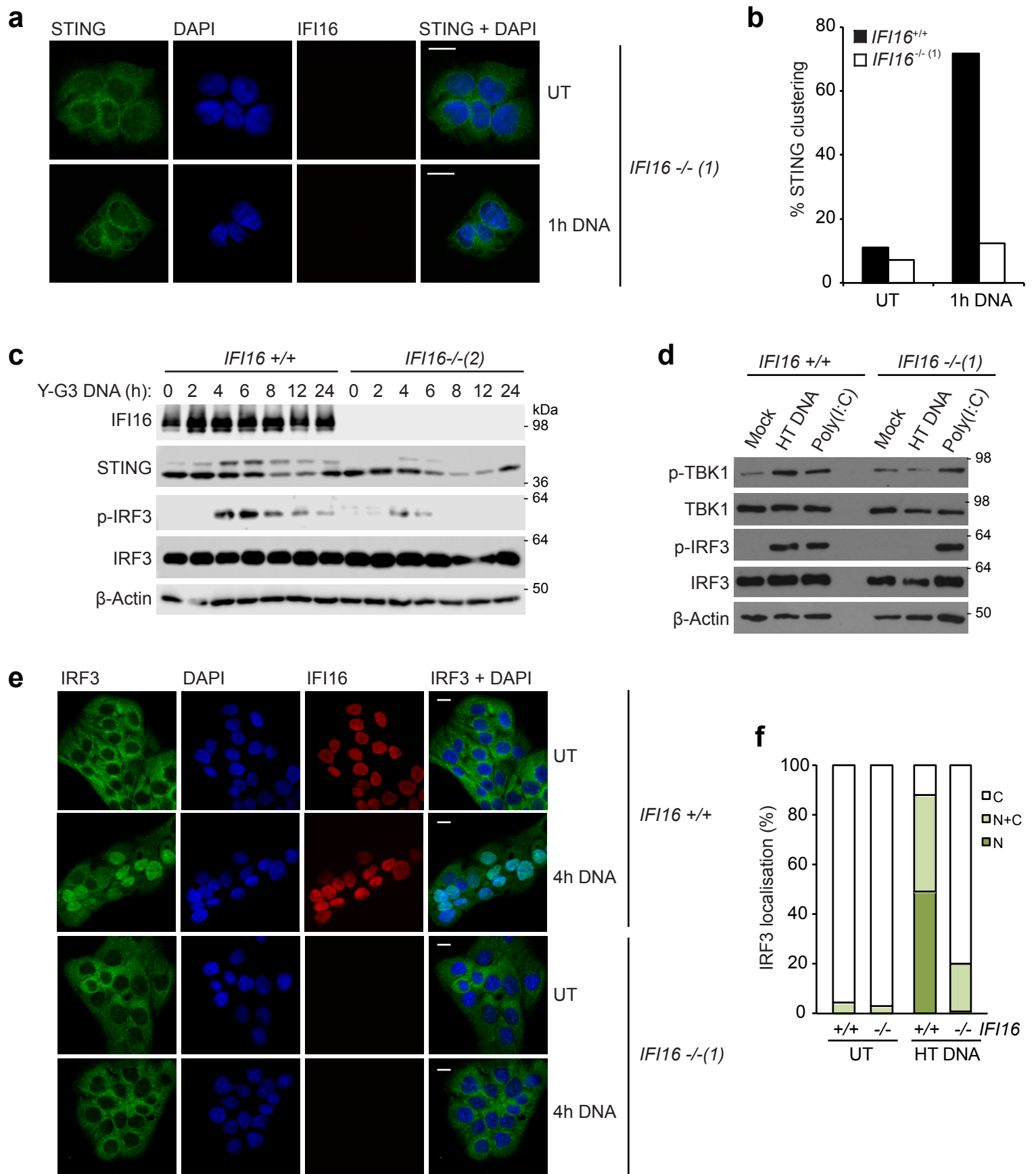
Supplementary Figure 1. IFI16 is required for DNA, but not RNA sensing in HaCaT keratinocytes.

(a-i) qRT-PCR analysis of mRNA expression levels normalised to β -actin mRNA and mock treatment in wild type (*IFI16*^{+/+}) HaCaT keratinocytes or two *IFI16*-deficient HaCaT clones, *IFI16*^{-/-}(1) or (2), as indicated. Data are presented as mean values of biological triplicates. Error bars indicate standard deviation (sd). * p < 0.05, ** p < 0.01, *** p < 0.001 Student's t-test. (a) Cells were permeabilised with digitonin, and infused with 25 μg/ml herring testis (HT) DNA for 6 h. *IFN* β mRNA expression levels were quantified by qRT-PCR. (b) *IFN* β mRNA expression 6 h post mock transfection, or transfection with 1 μg/ml 70mer oligonucleotide. (c) *IFN* β mRNA expression after transfection of 100 ng/ml poly(I:C). (d) *IFN* β mRNA levels after transfection with 50 ng/ml *in vitro* transcribed GFP mRNA containing 5' triphosphate groups (pppRNA). (e) Time course analysis of *IL-6* mRNA expression following transfection with 1 μg/ml HT DNA for the times indicated. (f) *IL-6* mRNA expression 6 h post transfection with 1, 10 or 100 ng/ml poly(I:C). (g) *IL-6* mRNA expression 6 h post transfection with 50 ng/ml *in vitro* transcribed mRNA (pppRNA). (h) *CXCL10* mRNA 6 h post transfection with 1 μg/ml HT DNA or 100 ng/ml poly(I:C). (i) *CXCL10* mRNA expression 6 h post transfection with 1 μg/ml plasmid DNA or 70mer oligonucleotide, or 50 ng/ml *in vitro* transcribed RNA (pppRNA).



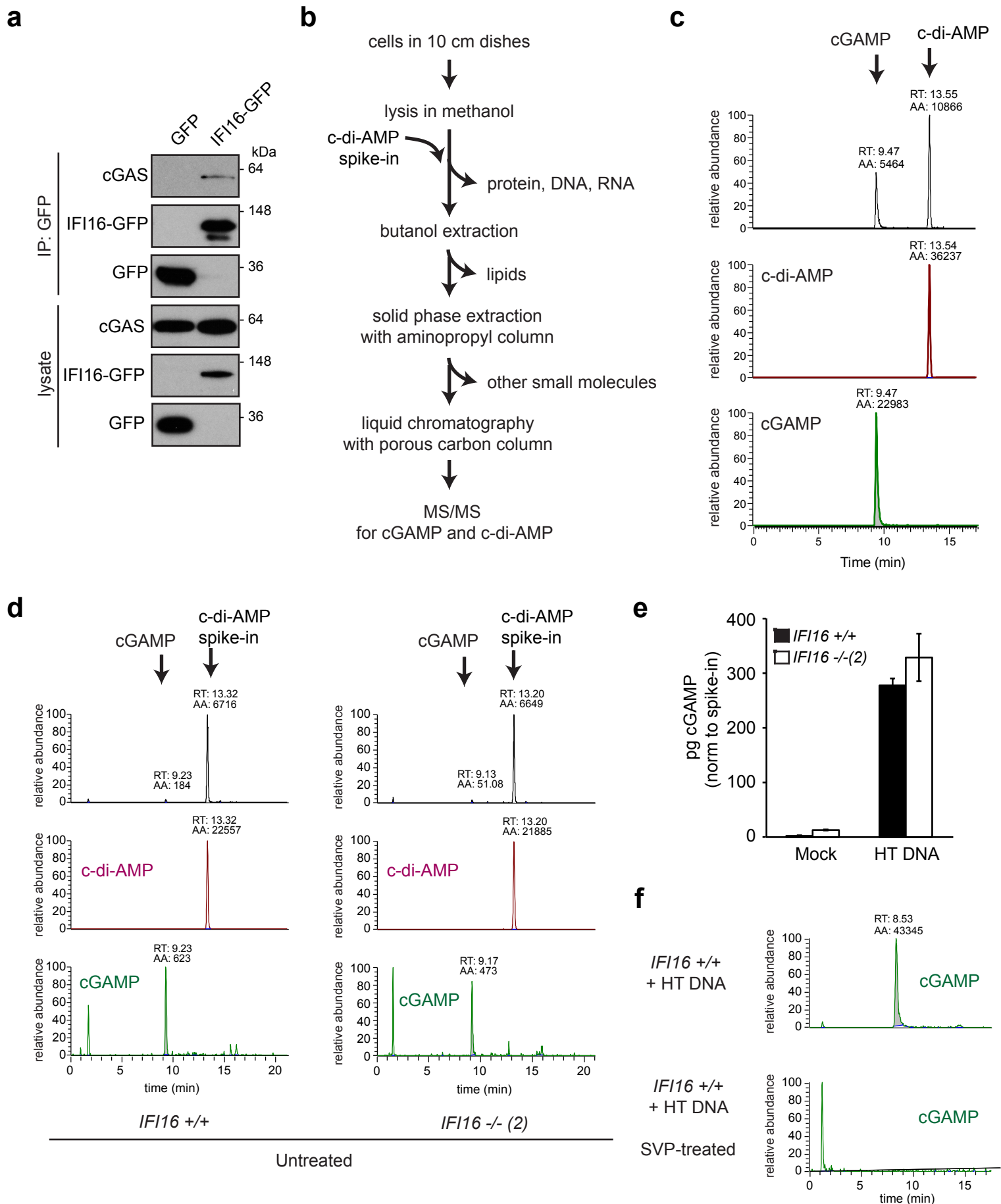
Supplementary Figure 2. IFI16 is required for the response to DNA viruses

(a,b) Wild type (IFI16^{+/+}) or IFI16-deficient HaCaT cells were infected with HSV-1 (MOI=1) for 6 h. IFN- β (a) or IL-6 (b) mRNA expression was analysed by qRT-PCR. (c) HaCaT cells were infected with a preparation of Sendai virus containing defective viral particles for 6h, and IFN- β mRNA expression was measured by qRT-PCR. (d) HaCaT cells were infected with a preparation of Sendai virus, at dilutions of 1:20,000, 1:2,000 and 1:200. After 6h, levels of IL-6 mRNA were quantified by qRT-PCR. (e) MRC-5 human embryonic lung fibroblasts were treated with a non-targeting (NT) or IFI16-targeting pool of siRNAs, or the four IFI16-targeting siRNAs individually as indicated. Expression of IFN- β mRNA was quantified following transfection of 1 μ g/ml HT DNA for 6h. All data are presented as mean values of biological triplicates. Error bars indicate standard deviation (sd). * $p < 0.05$, ** $p < 0.01$, *** $p < 0.001$ Student's t-test.



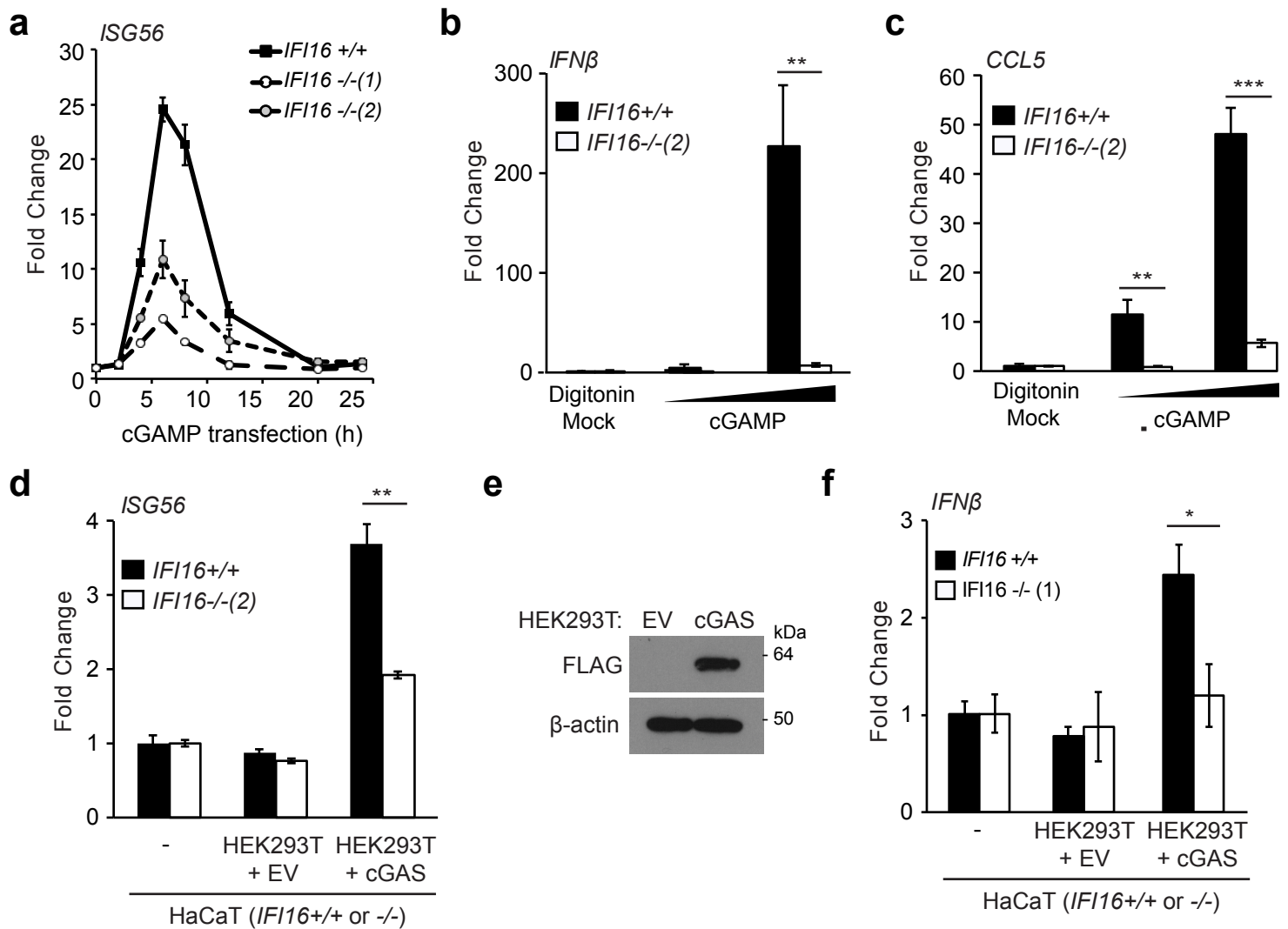
Supplementary Figure 3. IFI16 acts 'upstream' of STING, TBK1 and IRF3.

(a) Wild type or IFI16-deficient HaCaT cells were treated with 1 μ g/ml HT DNA, and STING clustering was observed by confocal microscopy. Cells were stained for STING (green) and IFI16 (red). (b) Cells as in (a) were scored for STING clustering. At least 200 cells were counted per sample. (c) *IFI16*^{+/+} or *IFI16*^{-/-} HaCaT cells were treated with Y-G3 DNA oligonucleotide for the times indicated. STING and IRF3 phosphorylation was assessed by Western blotting. (d) Cells were treated with 1 μ g/ml HT DNA or 100 ng/ml poly(I:C) for 4h. TBK1 and IRF3 phosphorylation was assessed by Western blotting. (e) Wild type or IFI16-deficient HaCaT cells were stimulated with 1 μ g/ml HT DNA for 4h. IRF3 translocation to the nucleus was observed by confocal microscopy. Cells were stained for IRF3 (green) and IFI16 (red), nuclear DNA is stained with DAPI (blue). (f) Cells as in (e) were scored for predominantly cytosolic (C), predominantly nuclear (N) or even nuclear and cytosolic distribution of IRF3. At least 200 cells were counted per sample. Scale bars: 20 μ m.



Supplementary Figure 4. IFI16 does not affect cGAMP production.

(a) HEK293 Trex FlpIn cells were induced to express IFI16-GFP or GFP alone by treatment with 1 μ g/ml tetracyclin for 18 h, prior to immunoprecipitation with anti-GFP antibody. cGAS and GFP fusion proteins were detected by immunoblotting. **(b)** Schematic representation of sample preparation for analysis by LC-MS. **(c)** Total and extracted ion chromatogram of 50 pg synthetic cGAMP and cyclic di-AMP standards. **(d)** Quantification of cGAMP by LC-MS in untreated wild type (*IFI16* +/+) or *IFI16* -/- HaCaT cells. **(e)** Production of endogenous cGAMP quantified by LC-MS 2 h post transfection of 1 μ g/ml HT DNA. Data are presented as mean values of triplicate samples; error bars represent standard deviations. **(f)** cGAMP extracted ion chromatogram of wild type HaCaT cells stimulated with 1 μ g/ml HT DNA for 4h (top) and from parallel lysates treated with 0.05 U snake venom phosphodiesterase



Supplementary Figure 5. IFI16 is required for the response to cGAMP.

(a) *IFI16* +/+ and two clones of *IFI16* -/- HaCaT cells were transfected with 20 µg/ml synthetic cGAMP, and *ISG56* mRNA induction was analysed by qRT-PCR at the time points indicated. (b, c) *IFI16* +/+ and *IFI16* -/- HaCaT cells were permeabilised with 5 µg/ml digitonin in the presence of 15 µM 2'3' cGAMP. *IFNβ* (b) and *CCL5* (c) mRNA levels were analysed after 6 h and normalised to *β-actin* mRNA levels and mock permeabilisation. (d) qRT-PCR analysis of *ISG56* mRNA induction in HaCaT cells grown in monoculture (-) or co-cultured with HEK293T cells transfected with a cGAS expression construct or empty vector (EV) as indicated. (e) *IFI16* +/+ or *IFI16* -/- (1) HaCaT cells were co-cultured with HEK293T cells expressing either cGAS-FLAG or empty vector (EV). cGAS protein expression was verified by Western blot. (f) qRT-PCR analysis of *IFN-β* mRNA expression from *IFI16* +/+ or *IFI16* -/- HaCaT cells cultured on their own (-) or co-cultured with HEK293T cells transfected with as cGAS expression construct or empty vector (EV) as indicated. Data are presented as mean values of biological triplicates. Error bars indicate standard deviation (sd). * p<0.05, ** p<0.01, *** p<0.001 Student's t-test.

Supplementary Figure 6. Uncropped immunoblots from Figures 1 - 7.

Fig. 1a

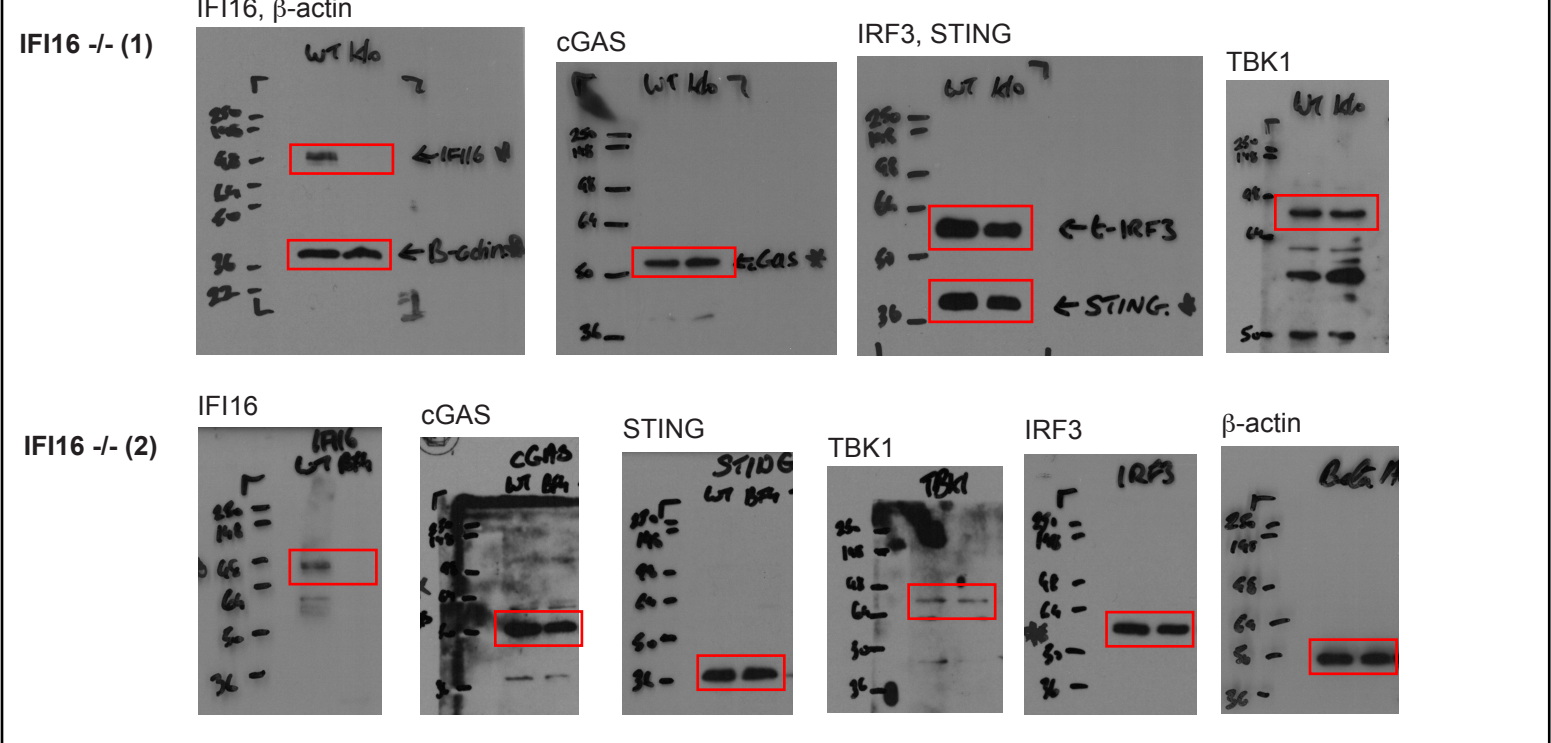


Fig. 2m

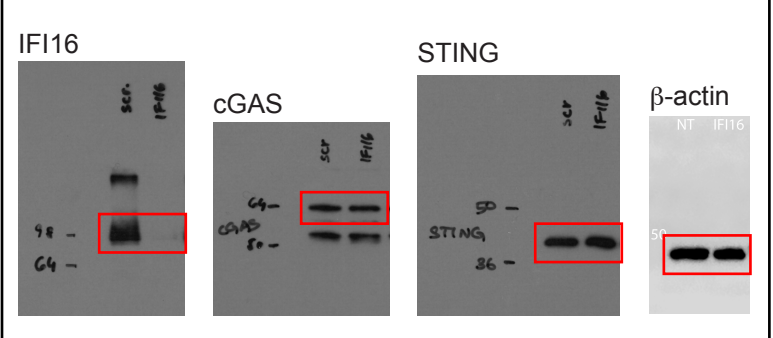


Fig. 3e

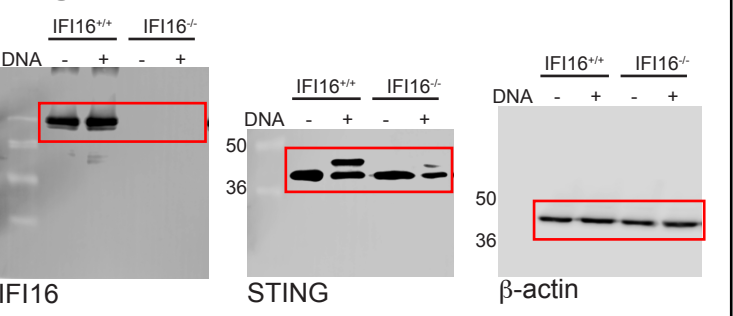


Fig. 3f

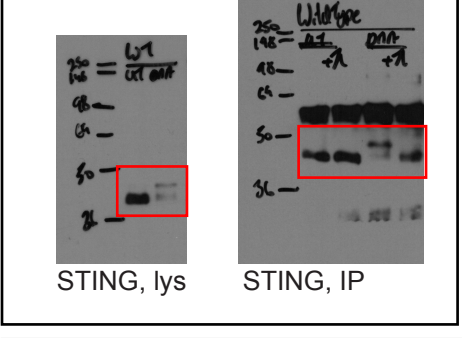


Fig. 3g

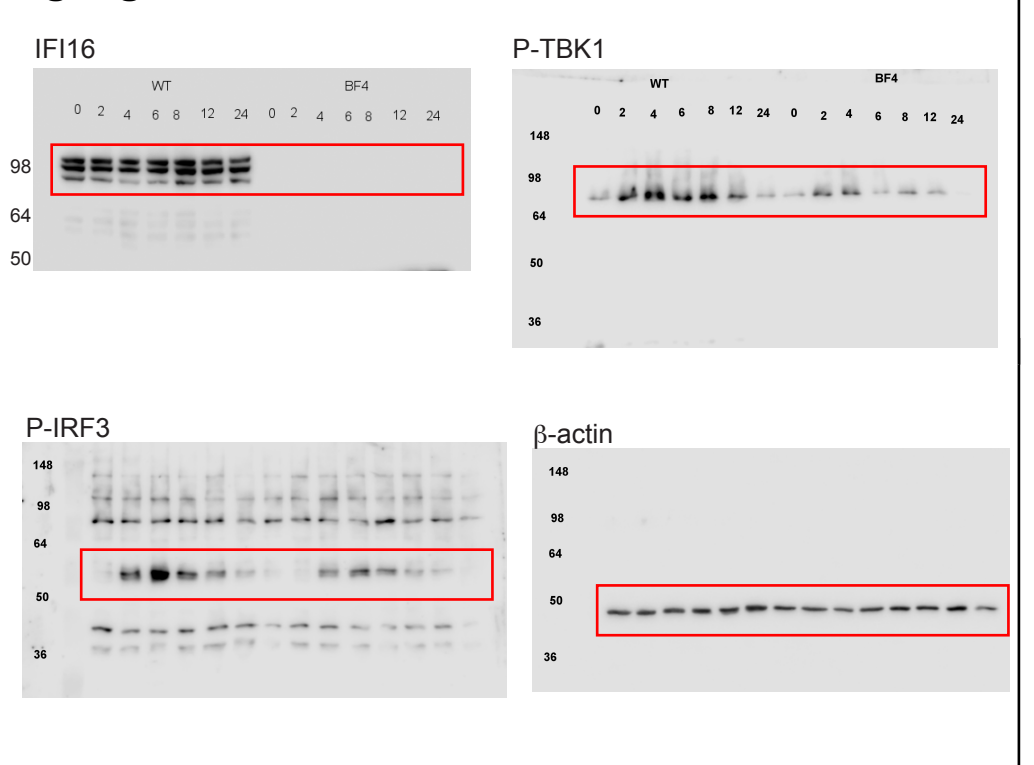


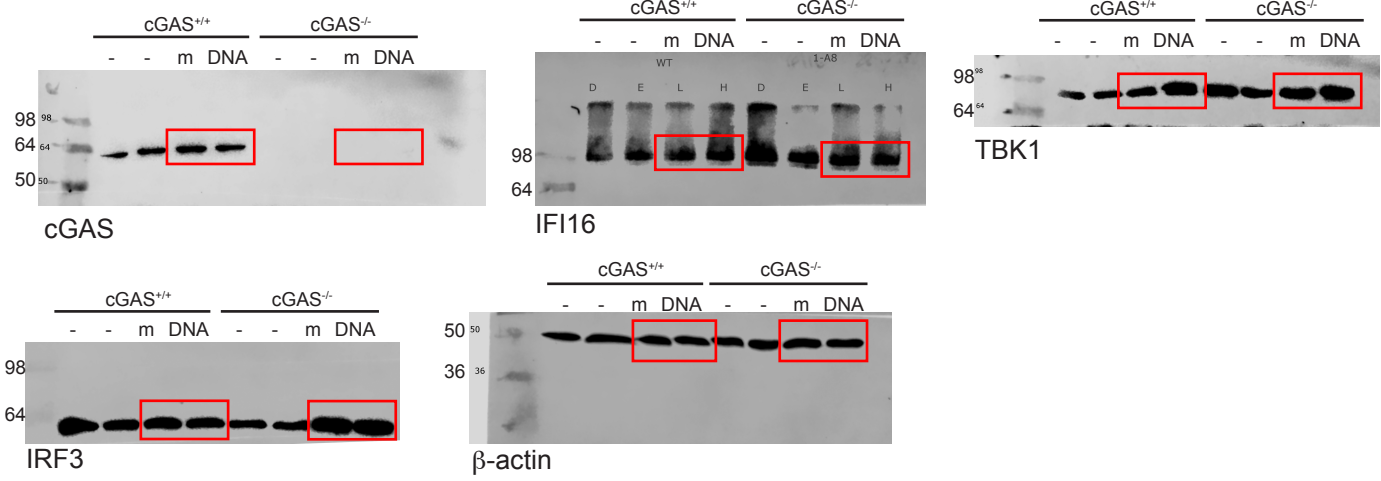
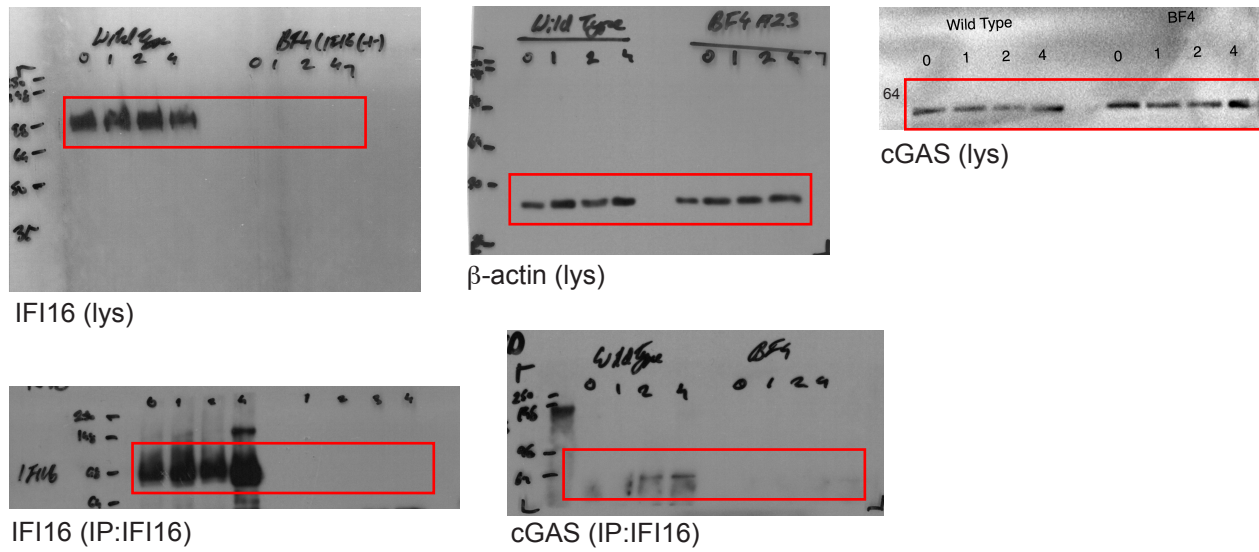
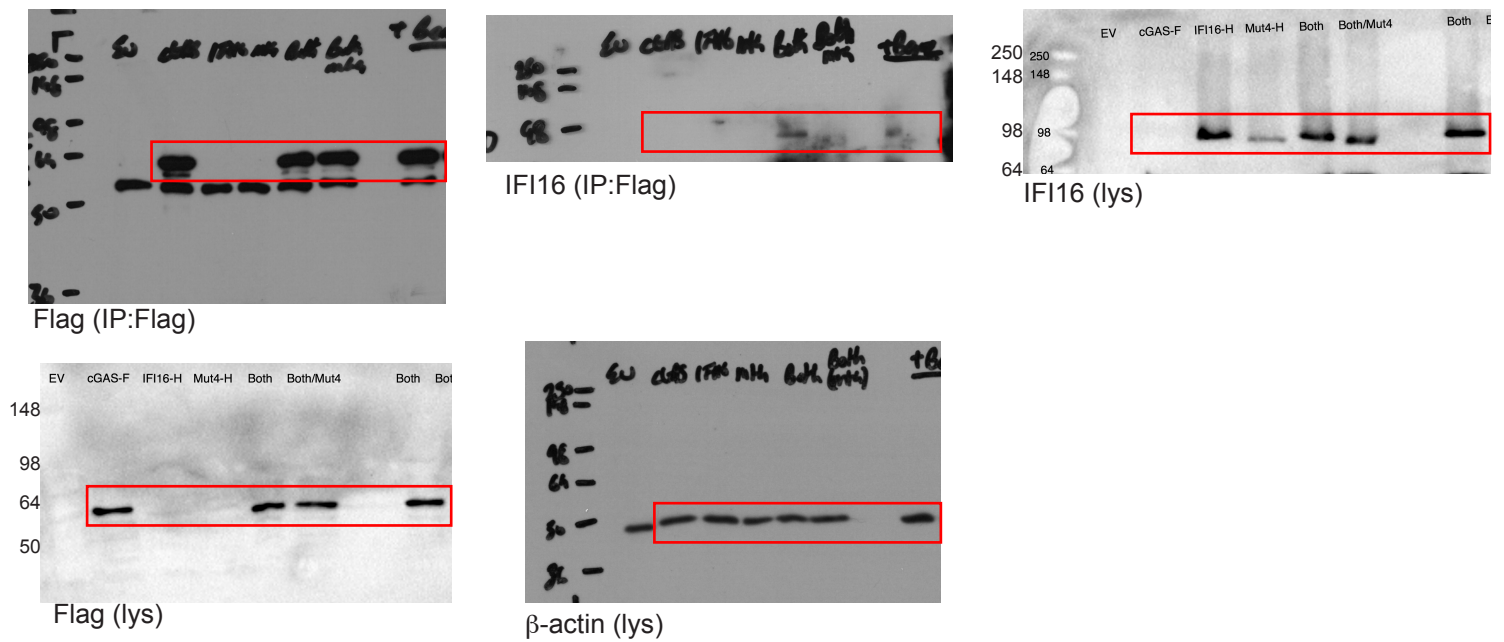
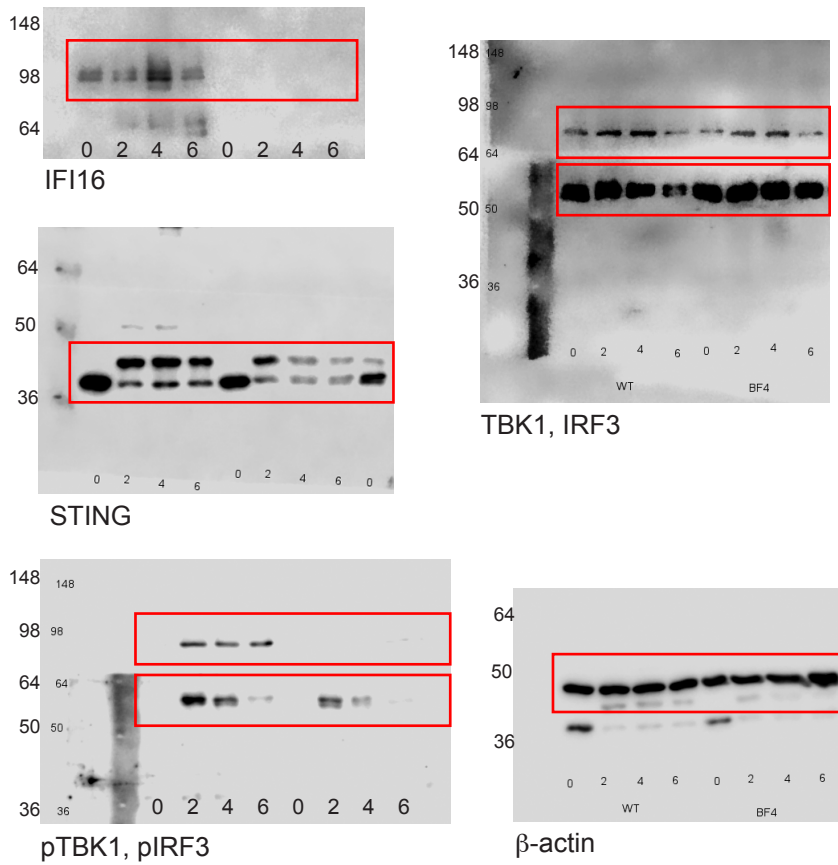
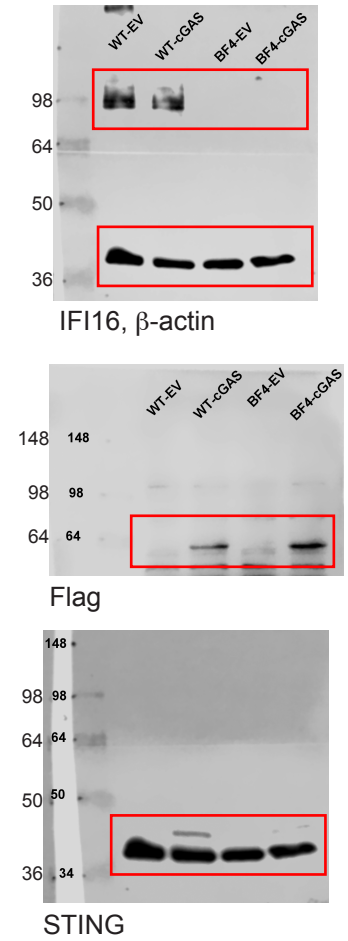
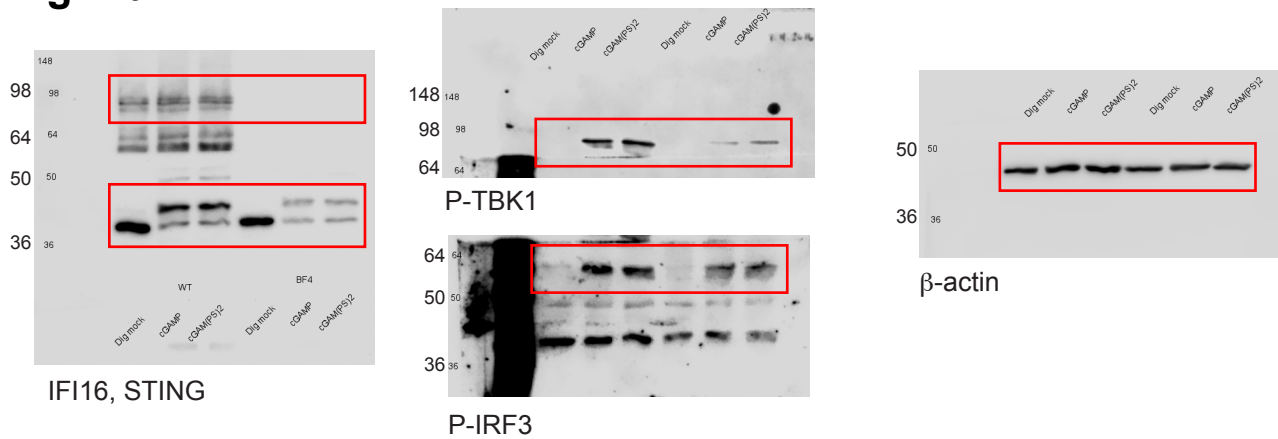
Fig. 4a**Fig. 5a****Fig. 5b**

Fig. 6c**Fig. 6g****Fig. 7b****Fig. 7d**